

## **INFORMATION TO USERS**

**This manuscript has been reproduced from the microfilm master. UMI films the text directly from the original or copy submitted. Thus, some thesis and dissertation copies are in typewriter face, while others may be from any type of computer printer.**

**The quality of this reproduction is dependent upon the quality of the copy submitted. Broken or indistinct print, colored or poor quality illustrations and photographs, print bleedthrough, substandard margins, and improper alignment can adversely affect reproduction.**

**In the unlikely event that the author did not send UMI a complete manuscript and there are missing pages, these will be noted. Also, if unauthorized copyright material had to be removed, a note will indicate the deletion.**

**Oversize materials (e.g., maps, drawings, charts) are reproduced by sectioning the original, beginning at the upper left-hand corner and continuing from left to right in equal sections with small overlaps. Each original is also photographed in one exposure and is included in reduced form at the back of the book.**

**Photographs included in the original manuscript have been reproduced xerographically in this copy. Higher quality 6" x 9" black and white photographic prints are available for any photographs or illustrations appearing in this copy for an additional charge. Contact UMI directly to order.**

# **UMI**

**A Bell & Howell Information Company  
300 North Zeeb Road, Ann Arbor MI 48106-1346 USA  
313/761-4700 800/521-0600**



University of Alberta

**Multivariate Statistical Methods For Control Loop  
Performance Assessment**

by

Biao Huang



A thesis  
submitted to the Faculty of Graduate Studies and Research  
in partial fulfillment of the requirements for the degree of

**Doctor of Philosophy**

in

**Process Control**

**Department of Chemical Engineering**

**Edmonton, Alberta**

**Spring 1997**



**National Library  
of Canada**

**Acquisitions and  
Bibliographic Services**

**385 Wellington Street  
Ottawa ON K1A 0N4  
Canada**

**Bibliothèque nationale  
du Canada**

**Acquisitions et  
services bibliographiques**

**385, rue Wellington  
Ottawa ON K1A 0N4  
Canada**

*Your file* *Votre référence*

*Our file* *Notre référence*

The author has granted a non-exclusive licence allowing the National Library of Canada to reproduce, loan, distribute or sell copies of his/her thesis by any means and in any form or format, making this thesis available to interested persons.

The author retains ownership of the copyright in his/her thesis. Neither the thesis nor substantial extracts from it may be printed or otherwise reproduced with the author's permission.

L'auteur a accordé une licence non exclusive permettant à la Bibliothèque nationale du Canada de reproduire, prêter, distribuer ou vendre des copies de sa thèse de quelque manière et sous quelque forme que ce soit pour mettre des exemplaires de cette thèse à la disposition des personnes intéressées.

L'auteur conserve la propriété du droit d'auteur qui protège sa thèse. Ni la thèse ni des extraits substantiels de celle-ci ne doivent être imprimés ou autrement reproduits sans son autorisation.

0-612-21580-6

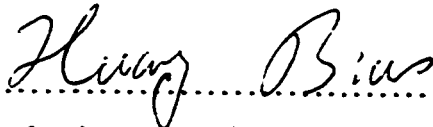


University of Alberta  
Library Release Form

Name of Author: **Biao Huang**  
Title of Thesis: **Multivariate Statistical Methods For Control Loop  
Performance Assessment**  
Degree: **Doctor of Philosophy**  
Year this degree granted: **1997**

Permission is hereby granted to the **University of Alberta Library** to reproduce single copies of this thesis and to lend or sell such copies for private, scholarly or scientific research purposes only.

The author reserves all other publication and other rights in association with the copyright in the thesis, and except as hereinbefore provided neither the thesis nor any substantial portion thereof may be printed or otherwise reproduced in any material form whatever without the author's prior written permission.

  
.....

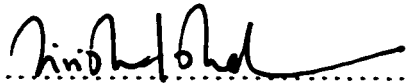
(Student's signature)

Biao Huang  
Department of Chemical Engineering  
University of Alberta  
Edmonton, Alberta  
Canada T6G 2G6

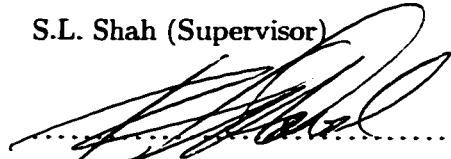
Date : *JAN. 24, 1997*

University of Alberta  
Faculty of Graduate Studies and Research

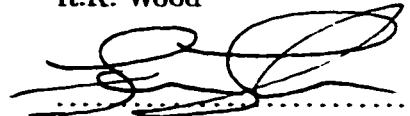
The undersigned certify that they have read, and recommend to the Faculty of Graduate Studies and Research for acceptance, a thesis entitled **Multivariate Statistical Methods For Control Loop Performance Assessment** submitted by **Biao Huang** in partial fulfillment of the requirements for the degree of **Doctor of Philosophy** in Process Control.



S.L. Shah (Supervisor)



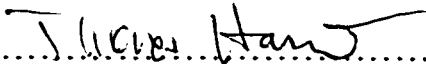
R.K. Wood



F. Forbes



H. Marquez



T. Harris (External examiner)

Date : 20 January 1997

**To Yali and Linda**

# Abstract

Performance assessment of univariate control loops is carried out by comparing the actual output variance with the minimum variance. The latter term is estimated by simple time series analysis of routine closed-loop operating data. This thesis extends these univariate performance assessment concepts to the multivariate case and develop new multivariate performance assessment techniques.

A key to performance assessment of multivariate processes using minimum variance control as a benchmark, is to estimate the benchmark performance from routine operating data with *a priori* knowledge of time-delays/interactor-matrices. An algorithm for estimation of the interactor matrix from closed-loop data is developed in this thesis. The expression for the feedback controller-invariant (minimum variance) term is then derived by using the unitary, weighted unitary and generalized unitary interactor matrices. It is shown that this term can be estimated from routine operating data. The same idea is extended to performance assessment of systems with non-invertible zeros and to performance assessment of multivariate feedback plus feedforward controllers. Although these methods are originally developed for stochastic systems, it is shown that the same methods can also be applied to deterministic systems by appropriate re-formulation of

the initial problem. Thus, a unified approach for control loop performance assessment is proposed. Efficient algorithms for performance assessment are developed and evaluated by simulations as well as applications on real industrial processes.

Minimum variance characterizes the most fundamental performance limitation of a system due to existence of time-delays/infinite-zeros. Practically there are many limitations on the achievable control loop performance. For example, a feedback controller that indicates poor performance relative to minimum variance control is not necessarily a poor controller. Further analysis of other performance limitations with more realistic benchmarks is usually required. Performance assessment in a more practical context such as a user-defined benchmark or control action constraints is therefore proposed and evaluated by applications in this thesis. Practical performance assessment generally requires complete knowledge of a plant model. An identification effort is usually required. As a complement to existing identification methods, a two-step closed-loop identification method is proposed and tested by simulated and experimental data from a computer-interfaced pilot-scale processes.

# Acknowledgments

**— Do not follow where the path may lead.**

**Go instead where there is no path and leave a trail...**

Chinese Proverb

The hallmark of good research is to tread the unknown and the uncharted and persevere especially under challenging circumstances. Through my frequent interactions with my supervisor, Dr. Sirish Shah, I have been inspired and encouraged to always seek this goal. I would like to thank him for challenging me with the multivariate control performance assessment problem and his enthusiastic guidance and support during the entire course of my Ph.D program. This support extended beyond technical guidance and at a more personal and collegial level has helped me “grow” tremendously.

It is a pleasure to be able to thank the many people who have contributed so generously in the conception and creation of this thesis. The Computer Process Control Group at the Department of Chemical and Materials Engineering “lives” in a highly stimulating environment where creativity and innovation are encouraged. The camaraderie and the cooperative spirit within the group has allowed me to debate and discuss my ideas freely. The broad range of talent within this group has also allowed cross-fertilization and nurturing of many different ideas that have invariably influenced the direction of this thesis. I am naturally indebted to all members, past and present, of the group. I would particularly like to thank Dr. D.G. Fisher for his valuable suggestions and help with my research work, and particularly for emphasizing the practical aspects of control. I thank him for adding the extra practical dimension to my life. I would also like to thank Dr. R.

K. Wood for leading me into process dynamics through his enthusiastic teaching and help in my graduate course ChE662.

I am indebted to thank Dr. E.K. Kwok, R. Miller, H. Fujii and J. Zurcher for cooperating so enthusiastically and providing me with an opportunity for industrial application and evaluation of my thesis results.

Thanks are also due to all my student colleagues in the process control group for many stimulating discussions. In particular, I have enjoyed many interesting discussions on robust control, and joint identification and control with Dr. Pranob Banerjee, on Kalman filtering with Dr. Ravindra Gudi, on statistical methods with S. Lakshminarayanan, on model predictive control with Dr. Kent Qi, on state space models with Dr. Lanre badmus, on linear matrix inequality and dynamic matrix control with Rohit Patwardhan, on real-time adaptive control with Dr. Dan Yang Liu, on generalized predictive control with Dr. Munawar Saudagar, on control loop performance assessment with Anand Vishnubhotla and Amy Yiu and many others. I would also like to thank Bob Barton and Kevin Dorma for their help with the computing facilities in the DACS center.

Special thanks to my parents on the other side of the Pacific for their encouragement and patience and especially for understanding why I have not been able to visit them for such a long time. My wife Yali Yu and my daughter Linda deserve special thanks for letting me spend many evenings and weekends on "work", a very precious time which was rightfully theirs. Thank you both for tolerating a husband and a father in absentia.

Financial support from the University of Alberta in the form of U of A Ph.D Scholarship, Dissertation Fellowship and the Andrew Steward Memorial Graduate Prize, and to Du Pont and Paprican in the form of the Du Pont/Paprican Scholarship are also gratefully acknowledged.

The publication of research results in first-rate, peer-reviewed journals is an important aspect of research. The task of dealing with paper reviews, many with excellent critiques but others completely off the mark, can be especially frustrating. We encountered such a case during the course of this research. Encouraging letters of support from Professors Harris, Seborg and MacGregor made a big difference. I wish to thank them for their help.

# Contents

## Chapter 1

<b>Introduction</b>	<b>1</b>
1.1 An overview of control loop performance assessment with objectives for this thesis . . . . .	1
1.2 Contributions of this thesis . . . . .	6
1.2.1 Contributions to the theory . . . . .	6
1.2.2 Contributions via industrial applications and evaluations . . . . .	7
1.2.3 Computational platform . . . . .	8
1.3 Organization of the thesis . . . . .	8

## Chapter 2

<b>Feedback Controller Performance Assessment of SISO Processes</b>	<b>10</b>
2.1 Introduction . . . . .	10
2.2 Feedback controller-invariance of minimum variance term and its separation from routine operating data . . . . .	12
2.3 The FCOR algorithm for SISO processes . . . . .	13
2.4 Evaluation via simulation and industrial application . . . . .	14
2.5 Conclusions . . . . .	16



## **Chapter 3**

<b>Multivariate Processes: Preliminaries</b>	<b>21</b>
3.1 Introduction . . . . .	21
3.2 Preliminaries of MIMO processes . . . . .	21
3.3 Conclusions . . . . .	25

## **Chapter 4**

<b>Unitary Interactor Matrices and Minimum Variance Control</b>	<b>26</b>
4.1 Introduction . . . . .	26
4.2 Unitary interactor matrices . . . . .	28
4.3 Unitary interactor matrices and the explicit solution of minimum variance control law . . . . .	30
4.4 Weighted unitary interactor matrices and singular LQ control . . . . .	35
4.5 Numerical Example . . . . .	40
4.6 Conclusions . . . . .	42

## **Chapter 5**

<b>Estimation of the Unitary Interactor Matrices</b>	<b>43</b>
5.1 Introduction . . . . .	43
5.2 Determination of the order of interactor matrices . . . . .	46
5.3 Factorization of unitary interactor matrices . . . . .	49
5.4 Estimation of the interactor matrix under closed-loop conditions . . . . .	51
5.5 Numerical rank . . . . .	54
5.6 Simulation and experimental evaluation on a pilot scale process . . . . .	56
5.7 Industrial application . . . . .	59
5.8 Conclusions . . . . .	64

## **Chapter 6**

<b>Feedback Controller Performance Assessment: Simple Interactor</b>	<b>66</b>
6.1 Introduction . . . . .	66
6.2 Feedback controller-invariance of minimum variance term and its separation from routine operating data . . . . .	67
6.3 The FCOR algorithm . . . . .	70
6.3.1 Multivariable performance index . . . . .	70
6.3.2 Filtering or whitening . . . . .	73
6.4 Simulation . . . . .	73
6.5 Conclusions . . . . .	75

## **Chapter 7**

<b>Feedback Controller Performance Assessment: Diagonal Interactor</b>	<b>77</b>
7.1 Introduction . . . . .	77
7.2 Feedback controller-invariance of minimum variance term and its separation from routine operating data . . . . .	78
7.3 Performance measures . . . . .	82
7.3.1 The FCOR algorithm . . . . .	82
7.3.2 The effect of sampling intervals . . . . .	83
7.4 Application to a headbox control system . . . . .	85
7.4.1 Process description . . . . .	85
7.4.2 Process control . . . . .	85
7.4.3 Problem description . . . . .	86
7.5 Performance assessment of the headbox control system . . . . .	87
7.5.1 Single loop performance assessment . . . . .	87

7.5.2	Multivariate performance assessment . . . . .	90
7.6	Conclusions . . . . .	93

## Chapter 8

<b>Feedback Controller Performance Assessment: General Interactor</b>		<b>97</b>
8.1	Introduction . . . . .	97
8.2	Feedback controller-invariance of minimum variance term and its separation from routine operating data . . . . .	98
8.2.1	Review of the unitary interactor matrix . . . . .	98
8.2.2	Feedback controller-invariance of minimum variance term and its separation from routine operating data . . . . .	99
8.3	The FCOR algorithm for general interactor matrices . . . . .	106
8.3.1	Multivariable performance measures . . . . .	106
8.4	Evaluation of the FCOR algorithm on a simulated example and an industrial application . . . . .	109
8.4.1	Simulated example . . . . .	109
8.4.2	Industrial application . . . . .	113
8.5	Conclusions . . . . .	114

## Chapter 9

<b>Feedforward &amp; Feedback Controller Performance Assessment</b>		<b>119</b>
9.1	Introduction . . . . .	119
9.2	Performance assessment of MIMO processes using minimum variance FF&FB control as the benchmark . . . . .	120
9.2.1	Minimum variance FF&FB control benchmark performance . . . . .	120
9.2.2	Feedback controller performance assessment of MIMO processes using minimum variance FF&FB control as the benchmark . . . . .	124

9.3	Numerical example and an industrial application . . . . .	125
9.3.1	Numerical example . . . . .	125
9.3.2	Industrial application . . . . .	127
9.4	Conclusions . . . . .	128

## Chapter 10

<b>Performance Assessment of Nonminimum Phase Systems</b>	<b>131</b>
10.1	Introduction . . . . . 131
10.2	Generalized unitary interactor matrices . . . . . 132
10.3	Feedback controller performance assessment of MIMO processes with non-invertible zeros . . . . . 136
10.3.1	Performance assessment with admissible minimum variance control as the benchmark . . . . . 136
10.3.2	Alternative proof of admissible minimum variance control . . . . . 140
10.4	Numerical example . . . . . 143
10.5	Conclusions . . . . . 147

## Chapter 11

<b>A Unified Approach to Performance Assessment</b>	<b>148</b>
11.1	Introduction . . . . . 148
11.2	Setpoint tracking problem . . . . . 149
11.3	Deterministic disturbances occurring at random time . . . . . 150
11.4	Performance assessment with both stochastic and deterministic disturbances 152
11.5	Performance assessment with pure deterministic disturbances . . . . . 154
11.6	Unified assessment of stochastic and deterministic systems . . . . . 155
11.7	Simulation . . . . . 157
11.8	Conclusions . . . . . 160

## Chapter 12

<b>Performance Assessment: User-defined Benchmark</b>	<b>161</b>
12.1 Introduction . . . . .	161
12.2 Preliminaries . . . . .	162
12.3 Performance assessment with desired closed-loop dynamics as the benchmark: minimum phase systems . . . . .	163
12.3.1 SISO case . . . . .	163
12.3.2 MIMO case . . . . .	170
12.4 Performance assessment with desired closed-loop dynamics as the benchmark: nonminimum phase systems . . . . .	177
12.5 Conclusions . . . . .	182

## Chapter 13

<b>Performance Assessment: LQG Benchmark</b>	<b>184</b>
13.1 Introduction . . . . .	184
13.2 Performance assessment with control action taken into account . . . . .	186
13.2.1 LQG solution via state space or input-output model . . . . .	186
13.2.2 LQG solution via GPC . . . . .	187
13.2.3 The tradeoff curve . . . . .	188
13.2.4 Performance assessment . . . . .	190
13.3 Pilot-scale experimental evaluation . . . . .	191
13.4 Case study on an industrial process . . . . .	195
13.5 Conclusions . . . . .	196

## Chapter 14

<b>Closed-loop Identification</b>	<b>204</b>
-----------------------------------	------------

14.1 Introduction . . . . .	204
14.2 Accuracy aspects of closed-loop identification . . . . .	207
14.3 Two-step closed-loop identification . . . . .	213
14.3.1 Estimation of the sensitivity function—Step 1 . . . . .	214
14.3.2 Estimation of the process model—step 2 . . . . .	215
14.3.3 Other practical considerations . . . . .	222
14.4 Extension to MIMO systems . . . . .	223
14.5 Simulation . . . . .	224
14.6 Experimental evaluation on a pilot-scale process . . . . .	234
14.7 Conclusions . . . . .	241

## **Chapter 15**

<b>Conclusions and Recommendations</b>	<b>242</b>
15.1 Concluding remarks . . . . .	242
15.2 Recommendations for future work . . . . .	244

<b>References</b>	<b>246</b>
-------------------	------------

## **Appendix A**

<b>The algorithm for the calculation of a unitary interactor matrix</b>	<b>255</b>
---	------------

## **Appendix B**

<b>Examples of the diagonal/general interactor matrices</b>	<b>258</b>
---	------------

# List of Tables

10.1 The procedure for calculation of the benchmark performance of MIMO processes with non-invertible zeros . . . . .	141
13.1 The procedure for calculation of the LQG tradeoff curve . . . . .	189
13.2 Controller tuning parameters . . . . .	192
14.1 Expressions of the asymptotic variance and bias errors . . . . .	212
14.2 Item to item correspondence between two equations . . . . .	214
14.3 The procedure for two-step identification . . . . .	219
14.4 The procedure for two-step identification plus shaping . . . . .	220

# List of Figures

2.1	Schematic diagram of SISO process under feedback control. . . . .	18
2.2	Schematic diagram of the FCOR algorithm . . . . .	18
2.3	Comparison of the ARMA, $R^2$ and FCOR approaches for control loop performance measures . . . . .	19
2.4	Schematic diagram of the industrial cascade reactor control loop . . . . .	19
2.5	Estimation of minimum variance and performance measure for the inner loop	20
2.6	Estimation of minimum variance and performance measure for the outer loop	20
5.1	A simplified process control loop diagram . . . . .	52
5.2	Schematic of the two-interacting tank pilot-scale process. . . . .	60
5.3	Open-loop (input and output) test data where $u = 0$ corresponds to 50% open of the valve, and the units of $h_1$ and $h_2$ are voltage. The time scale is in terms of sampling intervals. . . . .	60
5.4	Closed-loop (dither and output) test data where the units of $h_1$ and $h_2$ are voltage. The time scale is in terms of sampling intervals. . . . .	61
5.5	The industrial process flowsheet . . . . .	62
5.6	Setpoints for the closed-loop tests. The time scale is in terms of sampling intervals . . . . .	63
5.7	Predicted vs actual outputs; all data have been zero-mean centered. The time scale is in terms of sampling intervals . . . . .	64
6.1	Schematic diagram of white noise or innovation sequence estimation . . . . .	76
6.2	Simple interactor matrix MIMO performance assessment. Each asterisk represents an estimation based on 1000 data points using the FCOR algorithm. . . . .	76
7.1	Schematic of the headbox . . . . .	94



7.2	Schematic diagram of the control system . . . . .	94
7.3	Process data trajectory . . . . .	95
7.4	Performance assessment from the single-input and single-output approach. .	95
7.5	Performance assessment from the multivariate approach. . . . .	96
8.1	Performance assessment of a square MIMO process (with a general interactor matrix) under multiloop minimum variance control . . . . .	111
8.2	Performance assessment of a square MIMO process (with a general interactor matrix and output weighting) under multiloop minimum variance control . . . . .	116
8.3	Performance assessment of a non-square MIMO process (with a general interactor matrix) under multivariable control . . . . .	116
8.4	Schematic diagram of the industrial absorption process . . . . .	117
8.5	Absorption process data . . . . .	117
8.6	Multivariable performance assessment of absorption process . . . . .	118
9.1	Schematic diagram of the industrial process . . . . .	130
9.2	Process data trajectory. The time scale is in terms of sampling intervals. . .	130
11.1	Block diagram of closed-loop process . . . . .	150
11.2	Probability distribution of the shock . . . . .	151
11.3	Signal generated by passing the shock through filters . . . . .	152
11.4	Block diagram representation of the simulated process . . . . .	157
11.5	Process response and identification results (Dahlin controller) . . . . .	159
11.6	Predicted output response to a step disturbance (Dahlin controller) . . . . .	160
12.1	Control loop configuration under IMC framework . . . . .	171
12.2	Closed-loop impulse response coefficients for a simple integral controller. . .	171
12.3	Closed-loop impulse response coefficients for an integral plus filter controller.	172
12.4	Closed-loop impulse response coefficients for a detuned integral plus filter controller. . . . .	172
12.5	Block diagram of the closed-loop system. . . . .	183
13.1	a typical tradeoff curve . . . . .	198
13.2	Schematic diagram of the pilot-scale process. . . . .	198

13.3 Time domain validation of the open-loop model. The time scale is in terms of sampling intervals. . . . .	199
13.4 Closed-loop test for controller #1. The time scale is in terms of sampling intervals. . . . .	199
13.5 Closed-loop test for controller #2. The time scale is in terms of sampling intervals. . . . .	200
13.6 Closed-loop test for controller #3. The time scale is in terms of sampling intervals. . . . .	200
13.7 Closed-loop test for controller #4. The time scale is in terms of sampling intervals. . . . .	201
13.8 Tradeoff curve estimated from different set of data. Controller #3 (DMC#3) is not shown in the graph for clarity of the graph. . . . .	201
13.9 Time domain validation for controller #1. The time scale is in terms of sampling intervals. . . . .	202
13.10 Performance assessment of the four controllers. . . . .	202
13.11 Schematic diagram of the industrial cascade reactor control loop . . . . .	203
13.12 Performance assessment of the industrial cascade control loop (outer loop) .	203
14.1 Process model block diagram . . . . .	208
14.2 Feedback control loop block diagram . . . . .	210
14.3 Equivalent transformation of block diagrams. . . . .	223
14.4 Residual test for the model identified by using direct identification method (first-order plant and third-order noise). . . . .	227
14.5 Residual test for the model identified by using the $y$ -filtering method (first-order plant and third-order noise). . . . .	228
14.6 Comparison between direct identification and the $y$ -filtering methods. . . .	228
14.7 Residual test for the model identified by using the $y$ -filtering method (first-order plant and fifth-order noise). . . . .	229
14.8 Residual test for the model identified by using the $y$ -filtering method (second-order plant and second-order noise). . . . .	229
14.9 Variance of the estimate calculated from Monte-Carlo simulation (second-order plant and second-order noise). . . . .	230
14.10 Predicted $1\sigma$ bound of the Nyquist plot (second-order plant and second-order noise). . . . .	230
14.11 Comparison between $y$ -filtering and $w$ -filtering approaches. . . . .	232

14.12	Cross-correlation test for $w$ -filtering. . . . .	232
14.13	Cross-correlation test for $y$ -filtering. . . . .	232
14.14	Estimate of the sensitivity function . . . . .	233
14.15	The upper plot is the sensitivity function. The lower plot is the averaged Bode magnitude graph of $\hat{T}$ over 50 runs. . . . .	234
14.16	The averaged Nyquist plot of the estimate over 50 runs . . . . .	235
14.17	Schematic of the computer-interfaced pilot-scale process. . . . .	236
14.18	Block diagram for implementation of IMC control using the real-time Simulink Workshop. . . . .	236
14.19	Excitation signal and response. The physical units are voltage in the plot where $-2V$ to $+2V$ correspond to 0% to 100%. The time scale is in terms of sampling intervals. . . . .	237
14.20	Predicted versus actual data from another open-loop test. The time scale is the sampling intervals. . . . .	238
14.21	Excitation signal and response under the closed- loop condition. All physical units are voltage in the plot where $-2V$ to $+2V$ correspond to 0% to 100%. The time scale is in terms of sampling intervals. . . . .	239
14.22	Comparison of the identified process models using different methods when a second-order model is used. . . . .	239
14.23	Comparison of the identified process models using different methods when a first-order model is used. . . . .	240
14.24	Effect of the shaping filter for the first-order model. . . . .	240

# Nomenclature

$a_t, a_i$	white noise sequences, driving force of disturbances	(-)
$\hat{a}_t$	estimated white noise sequence	(-)
$b_t$	driving force of measurable disturbances	(-)
$c$	constant	(-)
$D$	interactor matrix	(-)
$D_w$	weighted unitary interactor matrix	(-)
$D_G$	generalized unitary interactor matrix	(-)
$\underline{D}$	algebraic form of the interactor matrix	(-)
$D_f$	interactor matrix that contains finite unstable zeros	(-)
$D_{inf}$	interactor matrix that contains infinite zeros	(-)
DMC	dynamic matrix control	(-)
$d$	order of interactor matrix (MIMO), time-delay (SISO)	(-)
$d_i$	time-delay in the $i^{th}$ output	(-)
$diag(.)$	diagonal matrix operator	(-)
$e_t$	process output under minimum variance control	(-)
$\tilde{e}_t$	interactor-filtered $e_t$	(-)
$E(.)$	expectation (mean) operator	(-)
$F, \tilde{F}$	matrix polynomials	(-)
$F_i, \tilde{F}_i$	constant matrices	(-)
FCOR	Filtering and Correlation analysis	(-)
$G_i$	Markov parameter matrix	(-)
$\underline{G}$	block-Toeplitz	(-)

$G_f, G_F$	filter transfer function (matrix)	(-)
$G_R$	desired closed-loop transfer function (matrix)	(-)
$GPC$	generalized predictive control	(-)
$I$	identity matrix	(-)
IMC	internal model control	(-)
$J$	index of linear quadratic objective function	(-)
$K$	full rank constant matrix	(-)
$K_t$	rush/drag ratio	(-)
$K^{sp}$	setpoint of rush/drag ratio	(-)
$L_i, \tilde{L}_i$	constant matrices	(-)
LQ	linear quadratic	(-)
$m$	column dimension of transfer function matrix $T$	(-)
$M$	number of data points	(-)
$M_F$	$= q^d F$ , polynomial matrix	(-)
MIMO	multi-input and multi-output	(-)
$n$	row dimension of transfer function matrix $T$	(-)
$N$	disturbance transfer function (matrix for MIMO system)	(-)
$\tilde{N}$	interactor-filtered disturbance transfer function matrix	(-)
$\hat{N}$	model used to identify disturbance dynamics	(-)
$N_{ij}, N'_{ij}$	disturbance transfer functions	(-)
$N_a$	transfer function matrix of unmeasurable disturbances	(-)
$N_b$	transfer function matrix of measurable disturbances	(-)
OEM	output error method	(-)
$p_t$	air pad pressure (deviation variable)	(Pa)
$p_t^{sp}$	setpoint of air pad pressure	(Pa)
$P_t$	air pad pressure (original variable)	(Pa)
PEM	prediction error method	(-)
$q^{-1}$	backshift operator	(-)
$Q$	feedback controller transfer function	(-)
$Q^*$	IMC controller transfer function (matrix)	(-)

$r$	number of infinite zeros	(–)
$R, \tilde{R}$	rational transfer function matrices	(–)
$R_{mp}$	stable polynomial transfer function (matrix)	(–)
$R_{nmp}$	unstable polynomial transfer function (matrix)	(–)
$S$	sensitivity function (matrix)	(–)
SISO	single-input and single-output	(–)
SSE	sum of square error	(–)
SVD	singular value decomposition	(–)
$t_d$	process time-delay	(s)
$t_c$	control interval	(s)
$t_s$	sampling interval	(s)
$tr(\cdot)$	trace of matrix	(–)
$T$	process transfer function (matrix for MIMO system)	(–)
$\tilde{T}$	delay-free transfer function matrix	(–)
$\hat{T}$	model used to identify plant dynamics	(–)
$T_{ij}, T'_{ij}$	transfer functions	(–)
$u_t, U_t$	manipulated variables	(–)
$u_1$	manipulated variable of air flow control valve	(–)
$u_2$	manipulated variable of fan pump speed	(–)
$V_t$	wire speed	(m/s)
$w_{t-d}, \tilde{w}_{t-d}$	portion of output due to non-optimal FB	(–)
$w$	dither signal	(–)
$W$	weighting matrix	(–)
$x$	process input	(–)
$y_i$	individual output	(–)
$\tilde{y}_i$	interactor-filtered individual output	(–)
$Y_t$	process output (vector)	(–)
$\tilde{Y}_t$	interactor-filtered process output (vector)	(–)
$Y_t^{sp}$	process setpoint (vector)	(–)
$Y_t _{mv}, \tilde{Y}_t _{mv}$	(filtered/output under MV control	(–)

$Z$	block matrix of correlation coefficient matrices	(-)
<i>Greek</i>		
$\eta(d), \eta'(d)$	performance indices (PI)	(-)
$\eta_{y_i}$	the $i^{th}$ individual performance index	(-)
$\eta_{min}$	PI with MV or opt. $H_2$ control as benchmark	(-)
$\eta_{admv}$	PI with admissible MV or opt. $H_2$ control as benchmark	(-)
$\eta_{user}$	PI with user-specified control as benchmark	(-)
$\omega$	frequency	(rad/s)
$\sigma_{mv}^2$	minimum variance	(-)
$\tilde{\sigma}_{mv}^2$	achievable minimum variance	(-)
$\Sigma_{mv}, \Sigma_{\tilde{mv}}$	minimum variance matrix	(-)
$\Sigma_a$	variance matrix of $a_t$	(-)
$\tilde{\Sigma}_a$	diagonal matrix of $\Sigma_a$	(-)
$\sigma_y^2$	output variance	(-)
$\Sigma_Y$	output variance matrix	(-)
$\Sigma_{\tilde{Y}}$	interactor-filtered output variance matrix	(-)
$\tilde{\Sigma}_Y$	diagonal matrix of $\Sigma_Y$	(-)
$\tilde{\Sigma}_{\tilde{Y}}$	diagonal matrix of $\Sigma_{\tilde{Y}}$	(-)
$\Sigma_{\tilde{Y}a}(i)$	covariance matrix between $\tilde{Y}_t$ and $a_{t-i}$	(-)
$\rho_a$	autocorrelation matrix of $a_t$	(-)
$\rho_{\tilde{Y}a}(i)$	cross correlation matrix between $\tilde{Y}_t$ and $a_{t-i}$	(-)
$\bar{\rho}_{\tilde{Y}a}(i)$	scaled cross correlation matrix	(-)
$\epsilon_t$	tracking error	(-)
$\nu_t$	white noise sequence	(-)
$\theta$	rational transfer function	(-)
$\xi_t$	measured disturbances	(-)

# Chapter 1

## Introduction

### 1.1 An overview of control loop performance assessment with objectives for this thesis

The design of advanced control algorithms has largely preoccupied the control practitioners' efforts. The rationale has been that systems which are difficult to control need advanced optimal, non-linear, adaptive or like control algorithms for better regulation. Although there are a variety of control design techniques such as  $l_1$ ,  $H_2$ ,  $H_\infty$ , etc, few techniques exist for objective measures of control loop performance or conversely measures of the level of difficulty in controlling a process variable from *routine operating industrial process data*. The control literature is relatively sparse on studies concerned with such proper or formal measures of control loop performance.

Astrom(1970), Harris(1989), and Stanfelj et al.(1993) have reported the use of minimum variance control as a benchmark standard against which to assess control loop performance. DeVries and Wu(1978) have applied the analysis of dispersion and spectral methods to multivariate performance assessment. The most notable work is that by Harris, who in a 1989 study showed how simple time series analysis techniques can be used to find a suitable expression for the feedback controller-invariant term from routine operating data of the SISO process and the subsequent use of this as a benchmark to assess control loop



performance. This contribution of Harris was significant in the sense that it marked a new direction and framework for the control loop performance monitoring area. More recently another related performance assessment statistic defined as the normalized performance index has been proposed by Desborough and Harris(1992). Kozub and Garcia(1993) have also reported yet another, but similar, measure of performance which they define as closed loop potential (or CLP). Lynch and Dumont(1993) have applied a similar idea to the monitoring of a pulp mill process. Tyler and Morari(1995) have extended the same idea to SISO processes with non-minimum phase and/or unstable poles. Eriksson and Isaksson(1994), Rhinehart(1995), Miao and Seborg(1995) , and Tyler and Morari(1995) have suggested alternative performance assessment and monitoring schemes for practical consideration. Huang et al.(1995a,1996a) and Harris et al.(1995,1996) have extended Harris' performance assessment concepts to performance assessment of MIMO feedback controllers.

The concept of a delay term is important in minimum variance control. This idea obviously carries over to the MIMO minimum variance control case as well. What is difficult to handle in the MIMO case is the concept of a time-delay matrix (defined elsewhere as the *interactor* matrix (Wolovich and Falb, 1976; Goodwin and Sin, 1984; Shah *et al.*, 1987; Tsiligiannis and Svoronos, 1988)) as an entity in itself, *i.e.*, one that can be factored out to design a MIMO minimum variance controller, if that is the objective. The interactor matrix, as originally proposed by Wolovich and Falb(1976), had a lower triangular form. With this form of the interactor matrix, the minimum variance control law(Goodwin and Sin, 1984; Dugard *et al.*, 1984) and minimum ISE control law(Tsiligiannis and Svoronos, 1988) are not unique and furthermore are output-order dependent, *i.e.* under minimum variance control,  $Var[y_1(t)]$  is minimized,  $Var[y_2(t)]$  is minimized subject to the constraint that  $Var[y_1(t)]$  is minimized, and so on. Therefore the importance of each output depends on the order it is stacked in the output vector, *i.e.* the first output variable is the most important for the design of minimum variance control, the last output variable is the least important. Re-arrangement of the output variables results in different optimal control law. Nevertheless, the lower triangular interactor matrix has played an important role in classic multivariable control design. Readers are referred to

Walgama (1986) and Sripada (1988) for interesting discussions on this issue. Shah et al.(1987) pointed out that selection of the form of an interactor matrix is application-dependent, *i.e.* it may take an upper triangular form or a full matrix form, and yet in LRPC schemes for a specific choice of tuning parameters, this requirement can be avoided. Rogozinski *et al.*(1987) proposed an algorithm for factorization of the nilpotent interactor matrix which has the full-matrix form. Peng and Kinnaert(1992) found the existence of the unitary interactor matrix, which is a special form of the nilpotent interactor matrix. Since the unitary interactor is an all-pass term, factorization of such unitary interactor matrix does not change the spectral property of the underlying system. This property of the unitary interactor matrix is desirable for minimum variance control or singular LQ control and multivariate control loop performance assessment using minimum variance control as the benchmark (Huang *et al.*, 1996b; Harris *et al.*, 1996). Here the term “singular LQ control” denotes LQ design without penalty on control action. The minimum variance control law as developed by Goodwin and Sin (1984) requires a simple design procedure, and is suitable for derivation of the feedback controller-invariant term which is the benchmark of multivariate performance assessment. The downside of this control law is that it is not unique and is input-output order dependent. By introducing the unitary and the weighted unitary interactor matrix into this design procedure, it can be shown that the minimum variance control law is unique, and is identical to the singular LQ control law as developed by Harris and MacGregor (1987) .

The algorithm for factoring the lower triangular interactor matrix as suggested by Wolovich and Falb (1976) and Goodwin and Sin (1984) generally requires a complete knowledge of the transfer function matrix. Shah et al. (1987) and Mutoh and Ortega (1993), however, have suggested a solution of the interactor matrix by solving a set of linear, algebraic equations of certain Markov parameter matrices (impulse response coefficient matrices). This latter approach directly connects the Markov parameter matrices to the interactor matrix without going through the transfer function and is numerically convenient and attractive for estimation of the interactor matrix of a MIMO process. For closed-loop control performance assessment, estimation of the interactor matrix under closed-loop conditions is desired. In this thesis, an algorithm for estimation

of the unitary interactor matrix is proposed. Using the proposed method, the interactor matrix can be estimated from closed-loop data without estimation of the open-loop transfer function matrix. With complete knowledge of process dynamics, many possible limitations on the achievable performance may be calculated via optimization procedures suggested by Boyd and Barratt (1991) and Dahleh and Diaz-Bobillo (1995) .

However, having to know the complete model of a process is not a very attractive approach to process performance monitoring, since a typical plant can have hundreds and even thousands of control loops, and identification of all loops is a very demanding requirement. Performance monitoring should be carried out in such a way that the normal production of a process is affected as less as possible. In addition, process dynamics and disturbances may drift from time to time, and the initially identified model may not represent the true dynamics. Thus on-line performance monitoring is necessary.

Different levels of constraints require different level of process knowledge. Some constraints require less *a priori* knowledge of processes than others. If one can break the constraints into different levels, then control loop performance may be assessed from the easiest to the hardest. Only those loops which indicate poor performance at the previous level need be examined at the next level performance assessment. Time-delays pose the most fundamental limitations but typically are relatively easy to obtain or estimate. Therefore, the performance limitation due to time-delays is assessed at the first level. The second level of performance limitation would be due to non-invertible zeros. Thus performance assessment of MIMO processes with non-invertible zeros is also discussed in this thesis.

Minimum variance control is the best possible control in the sense that no other controller can provide a lower output variance. However, its implementation is not recommended in practice due to its poor robustness and excessive control action. Nevertheless as a benchmark it does provide useful information. For example, if a process indicates poor performance relative to minimum variance control, then alternate controller tuning or redesigning of the control algorithm can be considered to improve control loop performance. However, if a process indicates good performance and yet its variance is not

within the desired limits, then alternate tuning or redesigning of the control algorithm will not be useful. In this case alternate control strategies such as feedforward control may be necessary in order to reduce the process variance. Desborough and Harris(1993) have discussed feedforward controller performance assessment of SISO processes. This idea is extended to the MIMO processes in this thesis.

Eriksson and Isaksson (1994) have shown that performance assessment using minimum variance control as a benchmark gives an inadequate measure of the performance if the aim is not stochastic control, but, for example, deterministic type step disturbance rejection or setpoint tracking. Tyler and Morari(1995) have a similar claim on this issue. These issues are also considered in this thesis. It is shown that many practical problems such as those posed by Eriksson and Isaksson and others can be readily solved under the same framework as proposed by Harris (1989) via appropriate formulation of the initial problem. It is also shown that performance assessment of both stochastic and deterministic systems can be unified under the  $H_2$  framework.

Minimum variance characterizes the most fundamental performance limitation of a system due to existence of time-delays. Practically there are many limitations on the achievable control loop performance. Minimum variance control performance requires minimum effort to estimate (routine operating data plus *a priori* knowledge of time-delays), and therefore serves as the most convenient first-level performance assessment benchmark. Only those loops that indicate poor first-level performance then need to be re-evaluated by higher-level performance assessment. A higher-level performance test usually requires more *a priori* knowledge than the knowledge of time-delays. This thesis also considers other practical benchmarks which are considered for the higher-level performance assessment.

However, all of the aforementioned methods are concerned with performance assessment which does not explicitly take into account the control effort. In general, tighter quality specifications result in smaller variation in the process output but typically require more control effort. One may therefore be more interested in knowing how far away is the control performance from the "best" achievable performance with the same

control effort. For example, the problem may be cast as follows: Given  $E[u_t^2] \leq \alpha$ , what is  $\min\{E[y_t^2]\}$ ? The solution to this problem is discussed by investigating the LQG design method and considering the classic LQG tradeoff curve.

A prerequisite for control loop performance assessment at a higher level is generally a model of the process. Ideally this model should be estimated under closed-loop conditions so that it does not upset normal process operation. A new two-step closed-loop identification algorithm is developed in this thesis. The estimated model is shown to have asymptotically identical expressions for the bias and variance terms regardless of how the identification run is conducted, *i.e.* irrespective of open-loop or closed-loop conditions. The estimated model can then be subsequently used for improving existing controller design, or controller re-design or for control-loop performance assessment or general analysis.

## 1.2 Contributions of this thesis

### 1.2.1 Contributions to the theory

The main theoretical contributions include:

1. Extension of the unitary interactor matrix to the weighted unitary interactor matrix and the generalized unitary interactor matrix.
2. Proof of equivalence between the minimum variance control law (Goodwin and Sin, 1984) and the singular LQ control law (a special solution in Harris and MacGregor(1987)), if a weighted unitary interactor matrix is used.
3. Factorization and estimation of the interactor matrix under both open and closed-loop conditions, which is a necessary prerequisite step for control loop performance assessment.
4. Proof of the *feedback controller invariance* of the output minimum variance performance for MIMO systems by using the unitary, weighted unitary or generalized unitary interactor matrices. This is the key to control loop performance assessment.

5. Development of an efficient algorithm for control loop performance assessment involving filtering and correlation analysis (the FCOR algorithm), which simplifies the calculations and allows the new technique to be easily applied to industrial processes.
6. Development of a performance assessment algorithm for MIMO processes with non-invertible zeros.
7. Development of a performance assessment algorithm for feedforward plus feedback control.
8. Proposal of a unified approach for control performance assessment under both stochastic and deterministic framework, and under regulatory and setpoint tracking framework.
9. Extension of performance assessment methodology to cover practical situations such as performance assessment with user-defined benchmarks.
10. Proposal of an LQG benchmark which can take control action constraints into account for performance assessment.
11. Development of an algorithm for *closed-loop identification of SISO/MIMO systems*. This is a spin-off from the work on control loop performance assessment and has strong industrial appeal.

### **1.2.2 Contributions via industrial applications and evaluations**

The methods and algorithms developed in this thesis have been applied and evaluated at several industrial complexes in the Alberta area and internationally:

1. Multivariable control system validation for distillation columns at two Mitsubishi Chemical Corporation locations: 1) Kurosaki Plant and 2) Mizushima Plant, Japan.
2. Multivariable control system validation for a heat exchanger, a reactor and a distillation column at Agrium Inc's (Sheritt Inc.) Redwater Fertilizer complex in Alberta.

3. Benefit analysis for upgrading the existing headbox control of a paper machine at Weyerhaeuser Canada's Grande Prairie operations in Alberta.

### **1.2.3 Computational platform**

Script and function ('.m' files) written using Matlab, Matlab/Simulink, Real-time Matlab/Simulink, and the associated toolboxes running under the Unix/PC platforms formed the main computational engine for all the calculations, demonstrations and applications performed in this thesis.

## **1.3 Organization of the thesis**

The thesis is organized as follows. In Chapter 2, the performance assessment algorithm is first introduced for SISO systems. The key to extend the SISO results to the MIMO system is the understanding of the concept of the time delay matrix or the interactor matrix. This concept is introduced in Chapter 3. In Chapter 4, the role of the unitary interactor matrix in minimum variance or singular LQ control design is discussed. The algorithm for estimation of the interactor matrix is established in Chapter 5. The methods for feedback controller performance assessment of MIMO systems are developed in Chapters 6, 7 and 8. This treatment is in an ascending degree of difficulty from the simple interactor, the diagonal interactor to the general interactor. When the feedback controller indicates good performance relative to minimum variance control, further improvement of performance may require a different control strategy such as feedforward plus feedback control. The benchmark of feedforward plus feedback control is therefore discussed in Chapter 9. Existence of non-invertible zeros affects the achievable performance of the feedback controller. This issue is addressed in Chapter 10. In Chapter 11, the methodology developed in the previous chapters is extended to performance assessment of deterministic disturbance and/or setpoint tracking. A practical performance assessment for a user-defined benchmark is proposed in Chapter 12. Performance assessment with control action taken into account is a relatively unexplored research area and one possible solution to

this problem is discussed in Chapter 13. Performance assessment with a benchmark other than minimum variance control usually requires an identification effort. A new approach to closed-loop identification is developed in Chapter 14.

This thesis has been written in a paper-format in accordance with the rules and regulations of the Faculty of Graduate Studies and Research, University of Alberta. Many of the chapters have appeared or are to appear in archival journals or conference proceedings. In order to link the different chapters, there is some overlap and redundancy of material. This has been done to ensure completeness and cohesiveness of the thesis material and help the reader understand the material easily.



## Chapter 2

# Feedback Controller Performance Assessment of SISO Processes

### 2.1 Introduction

A typical industrial process includes thousands of control loops. Instrumentation technicians generally maintain and service these loops, but rather infrequently. It is important for control engineers to have an efficient tool to monitor and assess control loop performance. Monitoring and assessment of control loop performance should not disturb routine operation of the processes or at least should be carried out under closed-loop conditions. As pointed by Eriksson and Isaksson (1994), *"in the short term, such a tool probably has to be a stand-alone unit with its own software that hooks on to and collects data straight from the input of the process computer; in the long term, such a function will be an integral part of any commercial control system"*.

The control literature has been relatively sparse on studies concerned with such proper or formal measures of control loop performance. Harris (1989) has developed an efficient technique for control loop performance assessment using only routine closed-loop operating data. The control objective is to minimize process variance, and minimum variance control is used as the benchmark standard against which to assess current control loop performance. It has been shown (Harris, 1989) that for a system with time delay  $d$ , a

portion of the output variance is feedback control invariant and can be estimated from routine operating data. This is the minimum variance portion. To separate this invariant term, one needs to model the closed-loop output data  $y_t$  by a moving average process such as

$$y_t = \underbrace{f_0 a_t + f_1 a_{t-1} + \cdots + f_{d-1} a_{t-(d-1)}}_{e_t} + f_d a_{t-d} + f_{d+1} a_{t-(d+1)} + \cdots$$

where  $a_t$  is a white noise sequence. Then  $e_t$  is the portion of the minimum variance control output. It is independent of feedback control (Harris, 1989). This portion of minimum variance can be estimated by time series analysis of routine closed-loop operating data, and can be subsequently used as a benchmark measure of theoretically achievable absolute lower bound of output variance to assess control loop performance. Using minimum variance control as the benchmark does not mean that one has to implement such a controller on the actual process. This benchmark control may or may not be achievable in practice depending on process invertibility and other physical constraints of the processes. However as a benchmark, it provides useful information such as how good the current controller performance is compared to the minimum variance controller and how much “potential” there is to further improve controller performance. If the controller indicates good performance measure relative to minimum variance control, further tuning or re-designing of the control algorithm is neither necessary nor helpful. In this case, if further reduction of process variation is desired, implementation of feedforward control or re-engineering of the process itself may be necessary. On the other hand, if the controller indicates a poor performance measure, further analysis such as process identification and controller re-design may be necessary since the poor performance measure may be due to constraints such as unstable or poorly damped zeros or control action limits.

As a general introduction to feedback control performance assessment of MIMO processes in this thesis, performance assessment of SISO processes is discussed in this chapter. This chapter is organized as follows. In Section 2.2 the feedback control invariant term is re-derived. The FCOR (Filtering and CORrelation analysis) algorithm for performance assessment of SISO processes is developed in Section 2.3. The proposed algorithm is then evaluated by simulation and actual processes in Section 2.4, followed by

concluding remarks in Section 2.5.

## 2.2 Feedback controller-invariance of minimum variance term and its separation from routine operating data

Consider a SISO process under regulatory control as shown in Figure 2.1, where  $d$  is the time-delay,  $\tilde{T}$  is the delay-free plant transfer function,  $N$  is the disturbance transfer function,  $a_t$  is a white noise sequence with zero mean, and  $Q$  is the controller transfer function.

It follows from Figure 2.1 that

$$y_t = \frac{N}{1 + q^{-d}\tilde{T}Q} a_t \quad (2.1)$$

where using the Diophantine identity:

$$N = \underbrace{f_0 + f_1 q^{-1} + \dots + f_{d-1} q^{-d+1}}_F + R q^{-d}$$

where  $f_i$  (for  $i = 1, \dots, d-1$ ) are constant coefficients, and  $R$  is the remaining rational, proper transfer function, equation 2.1 can be written as

$$\begin{aligned} y_t &= \frac{F + q^{-d}R}{1 + q^{-d}\tilde{T}Q} a_t \\ &= [F + \frac{R - F\tilde{T}Q}{1 + q^{-d}\tilde{T}Q} q^{-d}] a_t \\ &= F a_t + L a_{t-d} \end{aligned} \quad (2.2)$$

where  $L = \frac{R - F\tilde{T}Q}{1 + q^{-d}\tilde{T}Q}$  is a proper transfer function. Since  $F a_t = f_0 a_t + \dots + f_{d-1} a_{t-d+1}$ , the two terms on the left hand side of equation (2.2) are independent, and as a result,

$$\text{Var}(y_t) = \text{Var}(F a_t) + \text{Var}(L a_{t-d})$$

Therefore

$$\text{Var}(y_t) \geq \text{Var}(F a_t)$$

The equality holds when  $L = 0$ , i.e.

$$R - F\tilde{T}Q = 0$$

This yields the minimum variance control law:

$$Q = \frac{R}{\bar{T}F}$$

Since  $F$  is independent of the controller transfer function  $Q$ , the term  $Fa_t$ , which is the process output under minimum variance control, is feedback controller-invariant. Therefore, if a stable process output  $y_t$  is modelled by a infinite moving-average model, then its first  $d$  terms constitute an estimate of the minimum variance term  $Fa_t$ .

## 2.3 The FCOR algorithm for SISO processes

A stable closed-loop process can be written as an infinite-order moving-average (MA) process:

$$y_t = (f_0 + f_1q^{-1} + f_2q^{-2} + \dots + f_{d-1}q^{-(d-1)} + f_dq^{-d} + \dots)a_t \quad (2.3)$$

Multiplying equation (2.3) by  $a_t, a_{t-1}, \dots, a_{t-d+1}$  respectively and then taking the expectation of both sides of the equation yields

$$\begin{aligned} r_{ya}(0) &= E[y_t a_t] = f_0 \sigma_a^2 \\ r_{ya}(1) &= E[y_t a_{t-1}] = f_1 \sigma_a^2 \\ r_{ya}(2) &= E[y_t a_{t-2}] = f_2 \sigma_a^2 \\ &\vdots \\ r_{ya}(d-1) &= E[y_t a_{t-d+1}] = f_{d-1} \sigma_a^2 \end{aligned} \quad (2.4)$$

Therefore the minimum variance or the invariant portion of output variance is

$$\begin{aligned} \sigma_{mv}^2 &= (f_0^2 + f_1^2 + f_2^2 + \dots + f_{d-1}^2) \sigma_a^2 \\ &= \left[ \left( \frac{r_{ya}(0)}{\sigma_a^2} \right)^2 + \left( \frac{r_{ya}(1)}{\sigma_a^2} \right)^2 + \left( \frac{r_{ya}(2)}{\sigma_a^2} \right)^2 + \dots + \left( \frac{r_{ya}(d-1)}{\sigma_a^2} \right)^2 \right] \sigma_a^2 \\ &= [r_{ya}^2(0) + r_{ya}^2(1) + r_{ya}^2(2) + \dots + r_{ya}^2(d-1)] / \sigma_a^2 \end{aligned} \quad (2.5)$$

Let the controller performance index be defined as

$$\eta(d) \triangleq \sigma_{mv}^2 / \sigma_y^2 \quad (2.6)$$

This has been referred to as the closed-loop potential (CLP) by Kozub and Garcia (1993), and the inequality  $0 \leq \eta(d) \leq 1$  is held.

Substituting equation (2.5) into equation (2.6) yields

$$\eta(d) = [r_{ya}^2(0) + r_{ya}^2(1) + r_{ya}^2(2) + \cdots + r_{ya}^2(d-1)] / \sigma_y^2 \sigma_a^2 \quad (2.7)$$

$$= \rho_{ya}^2(0) + \rho_{ya}^2(1) + \rho_{ya}^2(2) + \cdots + \rho_{ya}^2(d-1) \quad (2.8)$$

$$\triangleq Z Z^T \quad (2.9)$$

where  $Z$  is the cross-correlation coefficient vector between  $y_t$  and  $a_t$  for lags 0 to  $d-1$  and is denoted as

$$Z \triangleq [\rho_{ya}(0), \rho_{ya}(1), \cdots, \rho_{ya}(d-1)] \quad (2.10)$$

The corresponding sampled version of the performance index is therefore written as

$$\hat{\eta}(d) = \hat{\rho}_{ya}^2(0) + \hat{\rho}_{ya}^2(1) + \hat{\rho}_{ya}^2(2) + \cdots + \hat{\rho}_{ya}^2(d-1) = \hat{Z} \hat{Z}^T \quad (2.11)$$

where

$$\hat{\rho}_{ya}(k) = \frac{\frac{1}{M} \sum_{t=1}^M y_t a_{t-k}}{\sqrt{\frac{1}{M} \sum_{t=1}^M y_t^2 \frac{1}{M} \sum_{t=1}^M a_t^2}} \quad (2.12)$$

Although  $a_t$  is unknown, it can be replaced by the estimated innovations sequence  $\hat{a}_t$ . The estimate  $\hat{a}_t$  is obtained by pre-whitening the process output variable  $y_t$  via time series analysis. This pre-whitening procedure will be further discussed in Chapter 6. This algorithm is denoted as the FCOR algorithm for Filtering and CORrelation analysis, and is schematically shown in Figure 2.2.

## 2.4 Evaluation via simulation and industrial application

**Example 1** *In order to compare the FCOR algorithm with other available SISO performance assessment algorithms, consider the following SISO process, as used by Desborough and Harris(1992), with time delay  $d = 2$ :*

$$y_t = u_{t-2} + \frac{1 - 0.2q^{-1}}{1 - q^{-1}} a_t \quad (2.13)$$

For a simple integral controller  $\Delta u_t = -Ky_t$ , it can be shown that the closed-loop response is given by

$$y_t = a_t + 0.8a_{t-1} + \frac{0.8(1 - K/0.8 - Kq^{-1})}{1 - q^{-1} + Kq^{-2}}a_{t-2} \quad (2.14)$$

Note that the first two terms are independent of  $K$  and represent the process output under minimum variance control.

The simulation results shown in Figure 2.3 show a comparison of the estimated control performance versus the theoretical performance as a function of  $K$ , and comparison with 1) the general approach proposed by Harris(1989) (denoted as the ARMA approach here), 2) normalized performance index or  $R^2$  approach (Desborough and Harris, 1992) and 3) the FCOR algorithm. Desborough and Harris(1992) have used the adjusted multiple coefficient of determination,  $R^2$ , as the performance index. This value is converted to the performance index used in this thesis via the relation,  $1 - R^2$ .

**Example 2** *The proposed performance assessment method was used to assess the performance of an important cascade control loop on a nitric acid ( $HNO_3$ ) production facility at a world-scale chemical plant in central Alberta, Canada.*

The schematic of the process is shown in Figure 2.4. The feed stocks are anhydrous ammonia ( $NH_3$ ) and air. The ammonia goes through a two-stage heating process before entering the catalytic reaction which contains a (gauze type) platinum-rhodium catalyst. Process air at over 400°F and 150 psig enters the reactor. The ammonia-air mixture reacts on the catalyst at over 1600°F and forms nitrogen dioxide with other by-products ( $NO_x$ ). In order to maximize the production of  $NO_2$  and minimize the by-products which are harmful to the environment, the gauze temperature is required to be kept as steady as possible even in the presence of disturbances in the ambient temperature air quality, ammonia feed temperature, and ammonia flow rate. The present control configuration is that the gauze temperature controller (outer loop) adjusts the setpoint of the ammonia flow rate (inner loop). In general, the inner loop is tightly tuned and is expected to have a good performance. The time delay of the outer loop from *a priori* analysis is known to be 15 seconds including the delay due to the zero-order-hold device. The sampling period

is 5 seconds; so the time delay is 3 sampling periods, *i.e.*,  $d = 3$ . The time delay of the inner loop is considered to be only one sampling interval caused by the zero order hold. A sample size of 35000 points taken over a two-day period is considered. Both loops use PID controllers. The available process data are the gauze temperature,  $y_1$ , the outer-loop controller output which is the setpoint of the inner loop, and the  $NH_3$  flow rate,  $y_2$ .

The performance measure of the inner loop by using the FCOR approach is shown in Figure 2.5. On the left part of this Figure, each point on the left graph represents the estimated minimum variance or the best achievable output variance based on the calculation of a window of 2000 data points. The right part of Figure 2.5 represents the corresponding performance index estimated using the FCOR approach. The 24 hour periodic trend of the disturbance magnitude is clearly seen from Figure 2.5. Despite this trend, the performance index is close to a constant value of 0.95, which is an indication of excellent performance or loop tuning, and further improvement in this loop by adjusting controller parameters may not be possible.

The estimated minimum variance of the outer loop is shown on the left part of Figure 2.6, and the corresponding performance measure is shown on the right part of this figure. Contrary to what would be expected, the performance index for this loop is not a constant. The trend of the index clearly shows a 24-hour cycling of the loop performance which is possibly due to the ambient temperature and air quality change over a 24-hour period. The average performance index of the outer loop is approximately 0.15, indicating relatively poor control. Clearly this loop performance may be improved significantly by re-tuning the existing controller or and/or providing feedforward control of ambient conditions.

## 2.5 Conclusions

A simple technique for evaluating univariate control loop performance has been proposed. This technique is based on filtering and correlation (FCOR) analysis of routine closed-loop operating data. Use of the proposed method is demonstrated by a

simulated and industrial application, and is shown to provide useful insight into control-loop performance analysis of univariate processes.



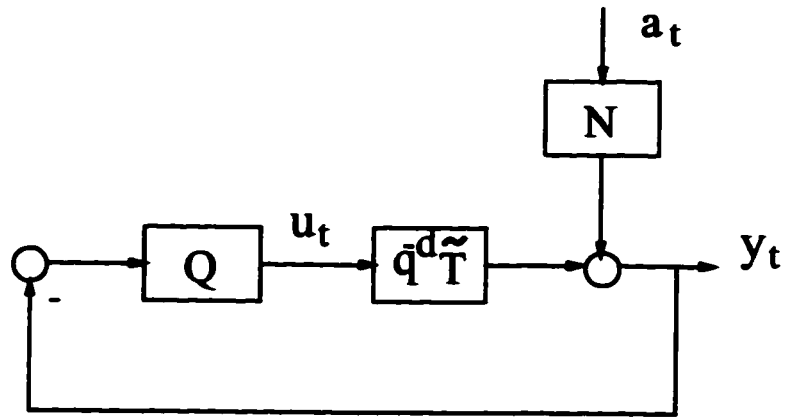


Figure 2.1: Schematic diagram of SISO process under feedback control.

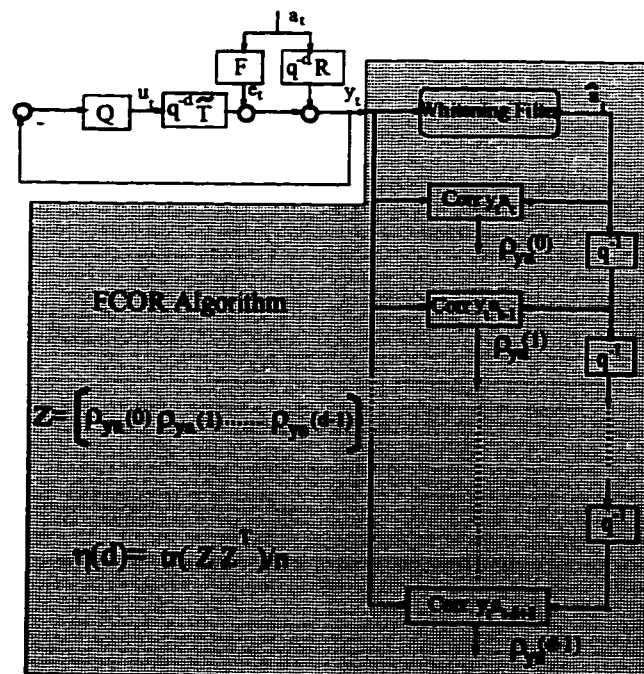


Figure 2.2: Schematic diagram of the FCOR algorithm

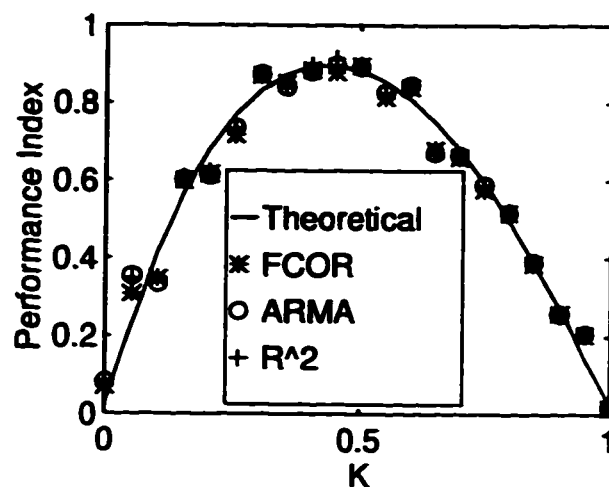


Figure 2.3: Comparison of the ARMA,  $R^2$  and FCOR approaches for control loop performance measures

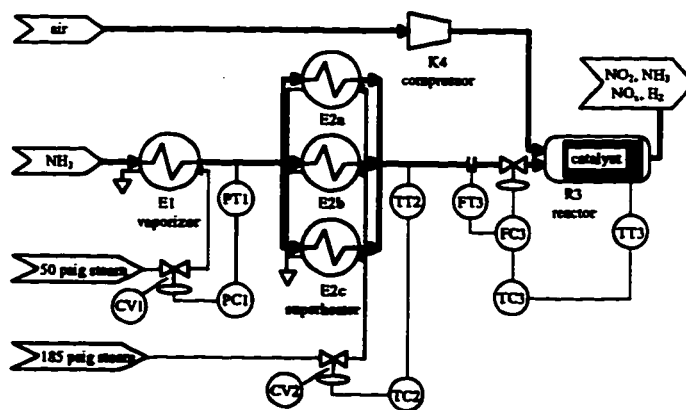


Figure 2.4: Schematic diagram of the industrial cascade reactor control loop

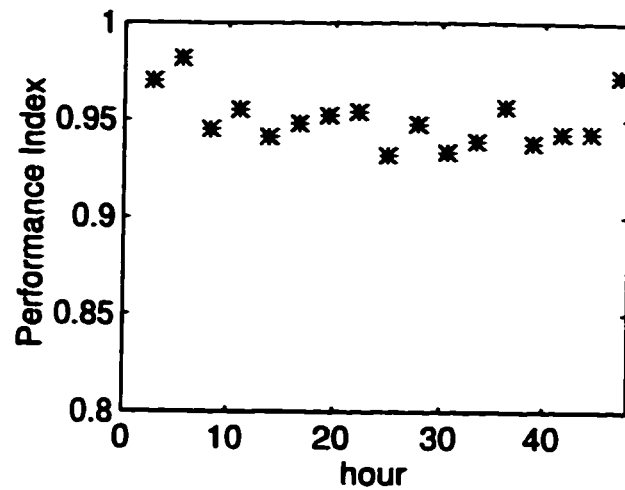
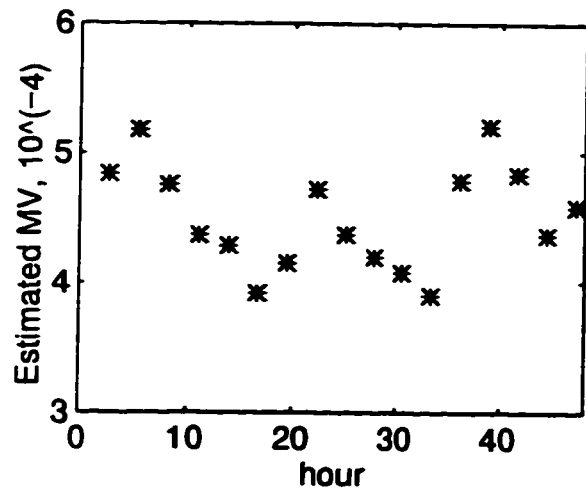


Figure 2.5: *Estimation of minimum variance and performance measure for the inner loop*

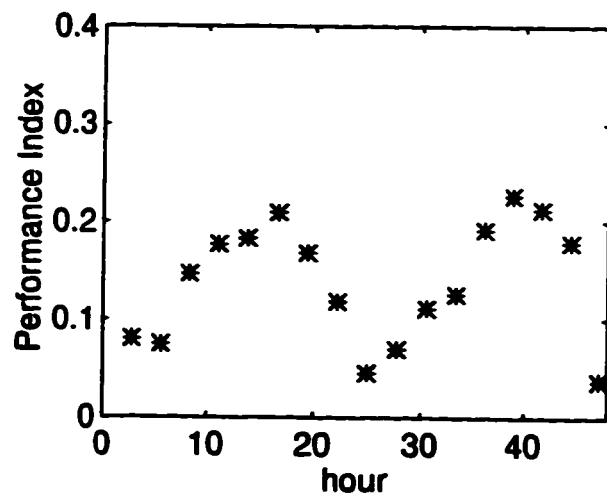
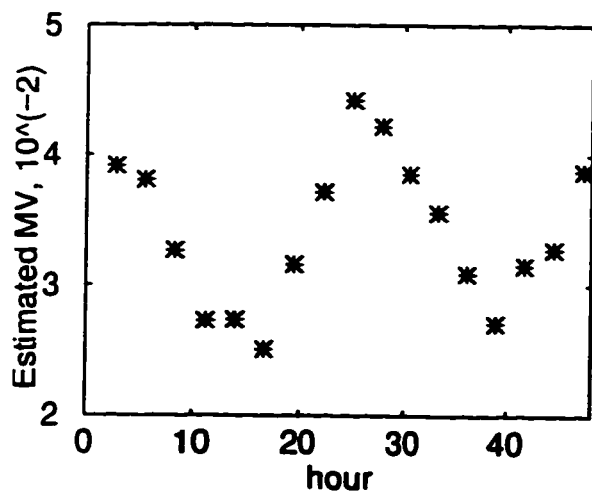


Figure 2.6: *Estimation of minimum variance and performance measure for the outer loop*

## Chapter 3

# Multivariate Processes: Preliminaries

### 3.1 Introduction

Time-delays are the most fundamental limitation on the achievable performance of any feedback controller. Performance assessment of SISO processes as introduced in Chapter 2 reflects this fundamental performance limitation in the stochastic framework. In the following chapters, we explore performance assessment of multivariable processes. The interactor matrix, a non-trivial extension of the SISO time-delay term, characterizes the most fundamental limitation on the achievable performance of any multivariable feedback controller.

### 3.2 Preliminaries of MIMO processes

For the sake of brevity and convenience, the backshift operator  $q^{-1}$  will be omitted throughout this thesis, unless circumstances necessitate its presence. For example, the transfer function matrix  $T(q^{-1})$  will be expressed simply as  $T$ . Unless otherwise illustrated, a standard MIMO process model

$$Y_t = TU_t + Na_t \tag{3.1}$$

is used throughout the thesis, where  $T$  and  $N$  are proper (causal), rational transfer function matrices in the backshift operator  $q^{-1}$ ;  $Y_t, U_t$ , and  $a_t$  are output, input and noise vectors of appropriate dimensions. For stochastic systems,  $a_t$  is further assumed to be white noise with zero mean and  $Var(a_t) = \Sigma_a$ .

To solve the multivariable deadbeat and minimum variance control problems, Wolovich and Falb (Wolovich and Falb, 1976), Wolovich and Elliott (Wolovich and Elliott, 1983), Goodwin and Sin (Goodwin and Sin, 1984) introduced the interactor matrix  $D$ , which is the generalization of the SISO time delay for the MIMO case.

**Theorem 1** *For every  $n \times m$  proper, rational polynomial transfer function matrix  $T$ , there is a unique, non-singular,  $n \times n$  lower left triangular polynomial matrix  $D$ , such that  $|D| = q^r$  and*

$$\lim_{q^{-1} \rightarrow 0} DT = \lim_{q^{-1} \rightarrow 0} \tilde{T} = K$$

where  $K$  is a full rank (full column rank or full row rank) constant matrix, the integer  $r$  is defined as the number of infinite zeros of  $T$ , and  $\tilde{T}$  is the delay-free transfer function matrix of  $T$  which contains only finite zeros. The matrix  $D$  is defined as the interactor matrix and can be written as

$$D = D_0 q^d + D_1 q^{d-1} + \cdots + D_{d-1} q$$

where  $d$  is denoted as the order of the interactor matrix and is unique for a given transfer function matrix (Shah et al., 1987; Mutoh and Ortega, 1993), and  $D_i$  (for  $i = 0, \dots, d-1$ ) are coefficient matrices.

The interactor matrix  $D$  can be one of the three forms described in the sequel. If  $D$  is of the form:  $D = q^d I$ , then the transfer function matrix  $T$  is regarded as having a *simple interactor matrix*. If  $D$  is a diagonal matrix, i.e.,  $D = \text{diag}(q^{d_1}, q^{d_2}, \dots, q^{d_n})$ , then  $T$  is regarded as having a *diagonal interactor matrix*. Otherwise  $T$  is considered to have a *general interactor matrix* (one realization of which is a triangular interactor matrix). However, the *general interactor matrix* also has forms other than the lower triangular form. It can be a full matrix or an upper triangular matrix (Shah et al., 1987; Huang

et al., 1996c). Rogozinski et al. (1987) have introduced an algorithm for the calculation of a *nilpotent interactor matrix*. Peng and Kinnaert (1992) have introduced the *unitary interactor matrix*.

**Definition 1** *Instead of taking the lower triangular form, if an interactor matrix as per Theorem 1 satisfies*

$$D^T(q^{-1})D(q) = I$$

*then this interactor matrix is denoted as the unitary interactor matrix.*

Existence of the unitary interactor matrix has been established by Peng and Kinnaert(1992) .

To illustrate the point, take a  $2 \times 2$  transfer function matrix as an example:

$$T = \begin{bmatrix} \frac{q^{-1}}{1+q^{-1}} & \frac{0.5q^{-1}}{1+2q^{-1}} \\ \frac{0.5q^{-1}}{1+3q^{-1}} & \frac{q^{-1}}{1+4q^{-1}} \end{bmatrix}$$

Since

$$\lim_{q^{-1} \rightarrow 0} qT = \begin{bmatrix} 1 & 0.5 \\ 0.5 & 1 \end{bmatrix}$$

is a full rank matrix,  $T$  has a simple interactor matrix with  $D = qI$ .

However, if  $T$  is changed to

$$T = \begin{bmatrix} \frac{q^{-2}}{1+q^{-1}} & \frac{0.5q^{-3}}{1+2q^{-1}} \\ \frac{0.5q^{-1}}{1+3q^{-1}} & \frac{q^{-1}}{1+4q^{-1}} \end{bmatrix}$$

then

$$\lim_{q^{-1} \rightarrow 0} \begin{bmatrix} q^2 & 0 \\ 0 & q \end{bmatrix} T = \begin{bmatrix} 1 & 0 \\ 0.5 & 1 \end{bmatrix}$$

is clearly full rank. Thus the interactor matrix

$$D = \begin{bmatrix} q^2 & 0 \\ 0 & q \end{bmatrix}$$

is a diagonal matrix.

Furthermore, if  $T$  is changed to

$$T = \begin{bmatrix} \frac{q^{-1}}{1+q^{-1}} & \frac{q^{-1}}{1+2q^{-1}} \\ \frac{q^{-1}}{1+3q^{-1}} & \frac{q^{-1}}{1+4q^{-1}} \end{bmatrix}$$

then it has a general interactor matrix. Goodwin and Sin(1984) have shown the lower triangular interactor matrix of this last transfer function matrix  $T$  as

$$D = \begin{bmatrix} q & 0 \\ -q^3 + 2q^2 & q^3 \end{bmatrix}$$

This can be easily checked by taking the  $\lim_{q^{-1} \rightarrow 0} DT = K$  and testing that  $K$  is full rank.

Now using the algorithm due to Rogozinski et al.(1987) , a unitary interactor matrix can be factored out as

$$D = \begin{bmatrix} 0.5q + 0.5q^2 & 0.5q - 0.5q^2 \\ 0.5q^2 - 0.5q^3 & 0.5q^2 + 0.5q^3 \end{bmatrix}$$

This matrix has the property:  $D^T(q^{-1})D(q) = I$ .

A clear explanation of the interactor matrix has been given by Shah et al.(1987) . For a SISO transfer function  $T = \frac{B}{A}q^{-d}$ , the time delay,  $q^{-d}$ , introduces  $d$  infinite zeros in the transfer function. The transfer function  $T$  is not invertible in the sense that the inversion of  $T$ ,  $T^{-1} = \frac{A}{B}q^d$ , is not proper. However, if we multiply the transfer function by the interactor matrix (it is a scalar in the SISO case),  $D = q^d$ , then the delay-free transfer function  $\tilde{T} = DT = \frac{B}{A}$  is invertible in the sense that the inversion is casual or proper. In the MIMO case, the interactor matrix  $D$  plays the same role as in the SISO case. Multiplication of the transfer function by the interactor matrix  $D$  removes the infinite zeros from the original transfer function matrix  $T$  and yields the delay-free transfer function matrix  $\tilde{T}$ , i.e.,  $\tilde{T} = DT$ .

The introduction of the interactor matrix is important not only because it solves the multivariable minimum variance control problem but it also provides a basic tool to seek the benchmark performance measure of the multivariable process as we will see in the following sections.

### **3.3 Conclusions**

Wolovich and Falb's lower-triangular interactor matrix and its extension to the unitary interactor matrix has been introduced in this chapter. Examples have been given to illustrate the concept. The unitary interactor matrix will play a fundamental role in the following chapters.



## Chapter 4

# Unitary Interactor Matrices and Minimum Variance Control

### 4.1 Introduction

There are many limitations to achievable control loop performance, for example time delays, existence of poorly damped or non-invertible zeros, constraints on control action, desired robustness characteristics, *etc.* Amongst all these constraints, the time delay is the most fundamental constraint that has attracted tremendous interest in the development and theory of process control. Wolovich and Falb(1976) have shown that the analog of the time-delay term for a SISO system, which is feedback control-invariant, is the interactor matrix for a MIMO system, which is also feedback control-invariant. Subsequently Wolovich and Elliott(1983) and Goodwin and Sin(1984) extended the concept of the interactor matrix to discrete systems. The interactor matrix characterizes the most fundamental performance limitation of a linear multivariable system.

The interactor matrix, as originally proposed by Wolovich and Falb(1976), had a lower triangular form. With this form of the interactor matrix, the minimum variance control law(Goodwin and Sin, 1984; Dugard *et al.*, 1984) and minimum ISE control

---

<sup>1</sup> A version of this chapter has been submitted to Automatica as a short paper.

law (Tsiligiannis and Svoronos, 1988) are output-order dependent, *i.e.* under minimum variance control,  $Var[y_1(t)]$  is minimized,  $Var[y_2(t)]$  is minimized subject to the constraint that  $Var[y_1(t)]$  is minimized, and so on. Therefore the importance of each output depends on the order it is stacked in the output vector, *i.e.* the first output variable is the most important for the design of minimum variance control, the last output variable is the least important. Re-arrangement of the output variables results in a different optimal control law. Shah *et al.* (1987) pointed out that selection of the form of an interactor matrix is application-dependent, *i.e.* it may take an upper triangular form or a full matrix form, and yet in LRPC schemes for a specific choice of tuning parameters, the controller is independent of the interactor matrix. Rogozinski *et al.* (1987) proposed an algorithm for factorization of the nilpotent interactor matrix which has the full-matrix form. Peng and Kinnaert (1992) found the existence of the unitary interactor matrix, which is a special form of the nilpotent interactor matrix. Since the unitary interactor is an all-pass term, factorization of such a unitary interactor matrix does not change the spectral property of the underlying system. This property of the unitary interactor matrix is desirable for minimum variance control or singular LQ control and multivariate control loop performance assessment using minimum variance control as the benchmark. Here the term “singular LQ control” denotes LQ design without penalty on the control action.

The main contributions in this chapter are 1) extension of the unitary interactor matrix into the weighted unitary interactor matrix; 2) an alternative derivation of the optimal singular LQ or minimum variance control law with respect to the minimum variance control law (Goodwin and Sin, 1984) and the singular LQ control law (Harris and MacGregor, 1987); 3) proof of equivalence of minimum variance control law (Goodwin and Sin, 1984) and the singular LQ control law (Harris and MacGregor, 1987), if a weighted unitary interactor matrix is used. This chapter is organized as follows. Section 4.2 introduces the unitary interactor matrix. In section 4.3 the unitary interactor matrix is applied to the explicit solution of the minimum variance control law. The unitary interactor matrix is then extended to the weighted unitary interactor matrix, and identity between the minimum variance control law and the singular LQ control law is established in section 4.4. This is followed by concluding remarks in section 4.6. Extension to the generalized unitary

interactor matrix, which factors out both unstable and infinite zeros and may be regarded as an alternative solution to the inner-outer factorization (Chu, 1985), is discussed in Chapter 10. For the sake of presentation, only the square transfer function matrix is considered in this chapter.

## 4.2 Unitary interactor matrices

The unitary interactor matrix has been defined in Chapter 3. Existence of the unitary interactor matrix is established in Peng and Kinnaert(1992) .

**Lemma 1** *For a full rank (in the field of  $q^{-1}$ ) rational, proper transfer function matrix  $T$ , there exists a non-unique unitary interactor matrix. However, any two unitary interactor matrices,  $D(q)$  and  $\bar{D}(q)$ , satisfy:*

$$\bar{D}(q) = \Gamma D(q)$$

where  $\Gamma$  is an  $n \times n$  unitary real matrix, i.e.  $\Gamma^T \Gamma = I$ .

**Proof:** See Peng and Kinnaert(1992) for the proof. ■

Readers are also referred to Peng and Kinnaert(1992) and Rogozinski *et al.*(1987) for the algorithm to factor the unitary interactor matrix from a transfer function matrix. For reader's convenience, the algorithm is summarized in Appendix A. In Chapter 5, this algorithm will be simplified by using QR decomposition of only the first few Markov parameter matrices or impulse response matrices. *A priori* knowledge of the interactor matrix is tantamount to knowing the entire transfer function matrix, which is often a demanding requirement. One alternative is to simply compute the interactor matrix by estimating the first few Markov parameters of the closed-loop process via dither signal excitation.

The non-uniqueness of the interactor matrix can also be due to different ordering of the output variables, i.e. the way to stack each output variable into the output vector. The relationship between differently-ordered unitary interactor matrices is established in the following lemma.

**Lemma 2** *If  $D(q)$  is the unitary interactor matrix of  $T$ , and  $\bar{D}(q)$  is the unitary interactor matrix of the output-reordered transfer function matrix  $\bar{T}(q^{-1}) = VT(q^{-1})$ , where  $V$  is row-exchanging operator (an orthogonal matrix), then*

$$\bar{D}(q) = \Gamma D(q) V^T$$

where  $\Gamma$  is an  $n \times n$  unitary real matrix.

**Proof:** From the definition of the unitary interactor matrix, we have

$$\lim_{q^{-1} \rightarrow 0} D(q)T(q^{-1}) = K_1 \quad (4.1)$$

$$\lim_{q^{-1} \rightarrow 0} \bar{D}(q)\bar{T}(q^{-1}) = \lim_{q^{-1} \rightarrow 0} \bar{D}(q)VT(q^{-1}) = K_2 \quad (4.2)$$

and  $(D(q))^{-1} = D^T(q^{-1})$ ,  $(\bar{D}(q))^{-1} = \bar{D}^T(q^{-1})$ ,  $V^{-1} = V^T$ .

From equation (4.1) and (4.2), one can obtain

$$\lim_{q^{-1} \rightarrow 0} D(q)V^T\bar{D}^T(q^{-1}) = K_1K_2^{-1} \triangleq \Gamma^{-1} \quad (4.3)$$

$$\lim_{q^{-1} \rightarrow 0} \bar{D}(q)VD^T(q^{-1}) = K_2K_1^{-1} = \Gamma \quad (4.4)$$

It is obvious from equations (4.3) and (4.4) that  $\Gamma^{-1} = \Gamma^T$ . Since  $D(q)V^T\bar{D}^T(q^{-1})$  is a finite-order matrix polynomial, *i.e.*

$$\begin{aligned} D(q)V^T\bar{D}^T(q^{-1}) &\triangleq E(q, q^{-1}) \\ &= q^{-d+1}E_{-d+1} + \cdots + q^{-2}E_{-2} + q^{-1}E_{-1} + E_0 + qE_1 + q^2E_2 + \cdots + q^{d-1}E_{d-1} \end{aligned}$$

equation (4.3) implies that  $D(q)V^T\bar{D}^T(q^{-1})$  has no positive power of  $q$ . One may therefore write it as  $D(q)V^T\bar{D}^T(q^{-1}) = E(q^{-1})$ . On the other hand, equation (4.4) also implies that  $\bar{D}(q)VD^T(q^{-1}) = E^T(q)$  has no positive power of  $q$  or equivalently  $E(q^{-1})$  has no negative power of  $q$ . Thus the matrix polynomial  $E(q, q^{-1})$  is neither a function of  $q$  nor  $q^{-1}$ . It follows then from (4.3) and (4.4) that

$$D(q)V^T\bar{D}^T(q^{-1}) = \Gamma^T$$

$$\bar{D}(q)VD^T(q^{-1}) = \Gamma$$

which yields

$$\bar{D}(q) = \Gamma D(q) V^T$$

Bittanti *et al.*(1994) have also defined a *spectral interactor matrix*, which has the same property as the right unitary interactor matrix defined by Panlinski and Rogozinski(1990) . The unitary interactor matrix is an all-pass factor, as a delay-term should be, and retains the spectral property of the underlying system after infinite zeros are removed and is an ideal factorization of time-delays for the design of minimum variance or singular LQ control. The advantage of factorizing a unitary interactor matrix as an all-pass factor is its computational simplicity compared to the spectral interactor factorization or the inner-outer factorization.

### 4.3 Unitary interactor matrices and the explicit solution of minimum variance control law

Goodwin and Sin(1984) have extended the deadbeat deterministic control strategy to minimum variance control of systems with stable zeros. Consider a multivariable system

$$Y_t = TU_t + Na_t$$

where  $T$  is the system transfer function matrix and  $N$  is the disturbance transfer function matrix. The minimum variance control law can be designed to make the variance of the interactor-filtered output  $DY_t$  or equivalently  $\tilde{Y}_t = q^{-d}DY_t$  minimum, where the positive integer  $d$  is the order of the interactor matrix or the minimum integer which makes  $q^{-d}D$  proper. This yields a simple multivariable control design strategy.

**Theorem 2** *For a multivariable process*

$$Y_t = TU_t + Na_t \tag{4.5}$$

*with the linear quadratic objective function (singular LQ objective function) defined by*

$$J = E(\tilde{Y}_t^T \tilde{Y}_t) \tag{4.6}$$

where  $\tilde{Y}_t = q^{-d}DY_t$ , an explicit optimal control law is given by

$$U_t = -\tilde{T}^{-1}RM_F^{-1}DY_t = -\tilde{T}^{-1}RF^{-1}(q^{-d}D)Y_t \quad (4.7)$$

where  $\tilde{T} = DT$ ,  $M_F = q^dF$ ,  $F$  and  $R$  satisfy the identity:

$$q^{-d}DN = \underbrace{F_0 + \dots + F_{d-1}q^{-d+1}}_F + q^{-d}R \quad (4.8)$$

and  $R$  is a rational proper transfer function matrix.

**Proof:** Consider the process with a general interactor matrix:

$$Y_t = TU_t + Na_t = D^{-1}\tilde{T}U_t + Na_t \quad (4.9)$$

Multiplying both sides of (4.9) by  $q^{-d}D$  yields

$$\begin{aligned} q^{-d}DY_t &= q^{-d}\tilde{T}U_t + q^{-d}DNa_t \\ &= q^{-d}\tilde{T}U_t + \tilde{N}a_t \end{aligned} \quad (4.10)$$

where  $\tilde{N}$  is a proper transfer function matrix. By defining  $\tilde{Y}_t = q^{-d}DY_t$ , equation (4.10) has been transformed to a process with a simple interactor matrix i.e.

$$\tilde{Y}_t = q^{-d}\tilde{T}U_t + \tilde{N}a_t \quad (4.11)$$

Substituting equation (4.8) into (4.11) yields

$$\tilde{Y}_t = \tilde{T}U_{t-d} + Ra_{t-d} + Fa_t \quad (4.12)$$

The last term in this equation cannot be affected by the control action, i.e.

$$\text{Var}(\tilde{Y}_t) = E(\tilde{Y}_t\tilde{Y}_t^T) \geq \text{Var}(Fa_t)$$

Therefore

$$E(\tilde{Y}_t^T\tilde{Y}_t) \geq \text{tr}(\text{Var}(Fa_t))$$

The minimum variance control is achieved when the sum of the first two terms on the right hand side of equation (4.12) is set to zero, i.e.

$$\tilde{T}U_{t-d} + Ra_{t-d} = 0$$

This yields

$$U_t = -\tilde{T}^{-1} R a_t \quad (4.13)$$

Substituting equation (4.13) into (4.12) yields

$$\tilde{Y}_t = F a_t \quad (4.14)$$

Therefore

$$a_t = F^{-1} \tilde{Y}_t \quad (4.15)$$

Substituting equation (4.15) into (4.13) gives the minimum variance control law

$$U_t = -\tilde{T}^{-1} R F^{-1} \tilde{Y}_t = -\tilde{T}^{-1} R F^{-1} (q^{-d} D) Y_t \quad (4.16)$$

By defining  $M_F = q^d F$ , Equation (4.16) can be written as

$$U_t = -\tilde{T}^{-1} R M_F^{-1} D Y_t$$

where  $F$  and  $R$  are defined by

$$q^{-d} D N = \underbrace{F_0 + \dots + F_{d-1} q^{-d+1}}_F + q^{-d} R$$

or

$$D N = M_F + R$$

■

However this minimum variance control law is only able to minimize variance of the interactor-filtered variable  $\tilde{Y}_t$ . If  $D$  is a lower triangular interactor matrix as used by Goodwin and Sin(1984), then the minimum variance control law of  $\tilde{Y}_t$  has the property that  $\text{Var}[y_1(t)]$  is minimized,  $\text{Var}[y_2(t)]$  is minimized subject to the constraint that  $\text{Var}[y_1(t)]$  is minimized, and so on. Therefore the control law is output-order dependent (Dugard *et al.*, 1984). On the other hand, if  $D$  is a unitary interactor matrix, we have the following result:

**Lemma 3** *If  $D$  is a unitary interactor matrix, then a proper optimal control law which minimizes the LQ objective function of the interactor-filtered output  $\tilde{Y}_t$*

$$J_1 = E(\tilde{Y}_t^T \tilde{Y}_t) \quad (4.17)$$

also minimizes the LQ objective function of the original output  $Y_t$

$$J_2 = E(Y_t^T Y_t) \quad (4.18)$$

and  $J_1 = J_2$ . Thus the singular LQ control law of the original variable  $Y_t$  can be obtained via the singular LQ control law of the unitary interactor-filtered variable  $\tilde{Y}_t$ .

**Proof:** Since  $a_t$  is random white noise with zero mean, we have

$$E(\tilde{Y}_t^T \tilde{Y}_t) = \text{tr}[\text{Var}(\tilde{Y}_t)]$$

Using Parseval's theorem and noticing the property of the unitary interactor matrix, i.e.

$$D^T(q^{-1})D(q) = I \quad \text{or} \quad D^T(e^{-j\omega})D(e^{j\omega}) = I \quad (\text{for all } \omega)$$

we have

$$\begin{aligned} \text{tr}[\text{Var}(\tilde{Y}_t)] &= \frac{1}{2\pi} \int_{-\pi}^{\pi} \text{tr}[D(e^{j\omega})\phi_Y(\omega)D^T(e^{-j\omega})]d\omega \\ &= \frac{1}{2\pi} \int_{-\pi}^{\pi} \text{tr}[D^T(e^{-j\omega})D(e^{j\omega})\phi_Y(\omega)]d\omega \\ &= \frac{1}{2\pi} \int_{-\pi}^{\pi} \text{tr}[\phi_Y(\omega)]d\omega \\ &= \text{tr}[\text{Var}(Y_t)] = E(Y_t)^T(Y_t) \end{aligned}$$

where  $\phi_Y(\omega)$  is the power spectrum density of  $Y_t$ , and the notation of the power spectrum density is given by (Ljung, 1987):  $\phi_Y(\omega) = \sum_{\tau=-\infty}^{\infty} R_Y(\tau)e^{-j\tau\omega}$  and  $R_Y(\tau) = E(Y_t Y_{t-\tau}^T)$ . Therefore  $J_1 = J_2$ , and minimization of  $J_1$  is equivalent to minimization of  $J_2$ . ■

Another important property of the unitary interactor matrix for minimum variance control is that the control law is output-order independent.

**Lemma 4** *If  $D$  is a unitary interactor matrix, then the minimum variance control law as solved by Theorem 2 is output-order invariant.*

**Proof:** It follows from Theorem 2 that for the original system

$$Y_t = TU_t + Na_t$$



the minimum variance control law is

$$U_t = -\tilde{T}^{-1} R M_F^{-1} D$$

and for the output re-ordered system

$$\bar{Y}_t = V Y_t = V T U_t + V N a_t = \bar{T} U_t + \bar{N} a_t$$

the minimum variance control law is

$$\bar{U}_t = -\bar{\tilde{T}}^{-1} \bar{R} \bar{M}_F^{-1} \bar{D} \bar{Y}_t \quad (4.19)$$

where  $\bar{D} \bar{N} = \bar{M}_F + \bar{R}$  and  $\bar{\tilde{T}} = \bar{D} \bar{T}$ . From Lemma 2, we have

$$\bar{D} = \Gamma D V^T$$

Therefore

$$\bar{\tilde{T}} = \bar{D} \bar{T} = \Gamma D V^T V T = \Gamma D T = \Gamma \tilde{T}$$

and

$$\bar{M}_F + \bar{R} = \bar{D} \bar{N} = \Gamma D V^T V N = \Gamma D N = \Gamma (M_F + R)$$

Thus  $\bar{M}_F = \Gamma M_F$  and  $\bar{R} = \Gamma R$ . Substituting  $\bar{\tilde{T}}$ ,  $\bar{R}$ ,  $\bar{M}_F$ ,  $\bar{D}$  and  $\bar{Y}_t = V Y_t$  into equation (4.19) yields

$$\bar{U}_t = -\bar{\tilde{T}}^{-1} \Gamma^T \Gamma R M_F^{-1} \Gamma^T \Gamma D V^T V Y_t = -\tilde{T}^{-1} R M_F^{-1} D Y_t = U_t$$

■

**Lemma 5** *The minimum variance control law as given in Theorem 2 is scaling independent, i.e. if a interactor matrix  $D$  is pre-multiplied by an invertible constant matrix  $P$  ( $\bar{D} = P D$ ), then using  $\bar{D}$  as the interactor matrix results in the same control law as using  $D$  as the interactor matrix.*

**Proof:** For two interactor matrices,  $D$  and  $\bar{D}$ , with

$$\bar{D} = P D \quad (4.20)$$

we have

$$\tilde{\tilde{T}} = \bar{D}T = \bar{D}D^{-1}\tilde{T} = PDD^{-1}\tilde{T} = P\tilde{T} \quad (4.21)$$

and

$$\bar{M}_F + \bar{R} = \bar{D}N = PDN = P(M_F + R) = PM_F + PR$$

Therefore

$$\bar{M}_F = PM_F \quad (4.22)$$

$$\bar{R} = PR \quad (4.23)$$

The minimum variance controller (with  $\bar{D}$  as its interactor matrix) is

$$\bar{U}_t = -\tilde{\tilde{T}}^{-1} \bar{R} \bar{M}_F^{-1} \bar{D} Y_t \quad (4.24)$$

Substituting equations (4.20), (4.21), (4.22) and (4.23) into (4.24) yields

$$\bar{U}_t = -\tilde{\tilde{T}}^{-1} P^{-1} P R M_F^{-1} P^{-1} P D Y_t = -\tilde{\tilde{T}}^{-1} R M_F^{-1} D Y_t = U_t$$

■

**Theorem 3** *If  $D$  is a unitary interactor matrix, the minimum variance control law as given in Theorem 2 is unique.*

**Proof:** Non-uniqueness of the unitary interactor matrix is due to 1) output ordering and/or 2) scaling, i.e.  $\bar{D} = \Gamma D$ . It has been shown in Lemma 4 that the minimum variance control law is output order invariant. From Lemma 5, it follows that the unitary scaling matrix  $\Gamma$  does not affect the control law. Therefore the minimum variance control law with the unitary interactor matrix is unique. ■

#### 4.4 Weighted unitary interactor matrices and singular LQ control

**Definition 2** *Instead of taking the lower triangular form or unitary interactor matrix form, if an interactor matrix as per Theorem 1 satisfies*

$$D_w^T(q^{-1}) D_w(q) = W \quad (4.25)$$

where  $W > 0$  is a symmetric weighting matrix, then this interactor matrix is regarded as the weighted unitary interactor matrix.

The weighted unitary interactor matrix has similar properties as the unitary interactor matrix. Existence of the weighted unitary interactor matrix is established in the following theorem.

**Theorem 4** For a full rank (in the field of  $q^{-1}$ ) rational, proper transfer function matrix  $T$ , there exists a non-unique weighted unitary interactor matrix. However, any two weighted unitary interactor matrices,  $D_w(q)$  and  $\bar{D}_w(q)$ , satisfy

$$\bar{D}_w(q) = \Gamma D_w(q)$$

where  $\Gamma$  is a  $n \times n$  unitary real matrix, i.e.  $\Gamma^T \Gamma = I$ .

**Proof:** From the definition of the weighted unitary interactor matrix, we have

$$\lim_{q^{-1} \rightarrow 0} D_w(q)T(q^{-1}) = K_1 \quad (4.26)$$

$$\lim_{q^{-1} \rightarrow 0} \bar{D}_w(q)T(q^{-1}) = K_2 \quad (4.27)$$

From equation (4.26) and (4.27), one can obtain

$$\lim_{q^{-1} \rightarrow 0} D_w(q)(\bar{D}_w(q))^{-1} = K_1 K_2^{-1} = \Gamma^{-1} \quad (4.28)$$

$$\lim_{q^{-1} \rightarrow 0} \bar{D}_w(q)(D_w(q))^{-1} = K_2 K_1^{-1} = \Gamma \quad (4.29)$$

From the definition (equation (4.25)), the following equations follow:

$$(D_w(q))^{-1} = W^{-1} D_w^T(q^{-1}) \quad (4.30)$$

$$(\bar{D}_w(q))^{-1} = W^{-1} \bar{D}_w^T(q^{-1}) \quad (4.31)$$

Substituting (4.31) and (4.30) into (4.28) and (4.29) respectively yields

$$\lim_{q^{-1} \rightarrow 0} D_w(q)W^{-1} \bar{D}_w^T(q^{-1}) = K_1 K_2^{-1} = \Gamma^{-1} \quad (4.32)$$

$$\lim_{q^{-1} \rightarrow 0} \bar{D}_w(q)W^{-1} D_w^T(q^{-1}) = K_2 K_1^{-1} = \Gamma \quad (4.33)$$

It follows from equations (4.32) and (4.33) that  $\Gamma$  is a unitary real matrix, i.e.  $\Gamma^{-1} = \Gamma^T$ . Equations (4.32) and (4.33) imply that  $D_w(q)W^{-1}\bar{D}_w^T(q^{-1})$  and  $\bar{D}_w(q)W^{-1}D_w^T(q^{-1})$  have neither a positive nor negative power of  $q$ . Therefore

$$\begin{aligned} D_w(q)W^{-1}\bar{D}_w^T(q^{-1}) &= \Gamma^T \\ \bar{D}_w(q)W^{-1}D_w^T(q^{-1}) &= \Gamma \end{aligned}$$

It follows that

$$\bar{D}_w(q) = \Gamma D_w^{-T}(q^{-1})W \quad (4.34)$$

Substituting (4.30) into (4.34) yields

$$\bar{D}_w(q) = \Gamma D_w(q)$$

Existence of the weighted unitary interactor matrix is given by Corollary 1. ■

**Corollary 1** *One of the solutions for the weighted unitary interactor matrix is given by*

$$D_w(q) = D(q)W^{1/2}$$

where  $D(q)$  is a unitary interactor matrix of the weighted transfer matrix  $W^{1/2}T(q^{-1})$ . In general, any weighted unitary interactor matrix  $D_w(q)$  can be written as

$$D_w(q) = \Gamma D(q)W^{1/2}$$

**Proof:** Since  $D(q)$  is the unitary interactor matrix of  $W^{1/2}T(q^{-1})$ ,  $D_w(q) = D(q)W^{1/2}$  must be an interactor matrix of  $T(q^{-1})$ . Furthermore, from  $D_w^T(q^{-1})D_w(q) = W^{1/2}D^T(q^{-1})D(q)W^{1/2} = W$ , one can conclude that  $D_w(q)$  is a weighted unitary interactor matrix. From Theorem 4, the general solution of the weighted unitary interactor matrix can be written as  $D_w(q) = \Gamma D(q)W^{1/2}$ . ■

**Corollary 2** *If the interactor matrix is a weighted unitary interactor matrix  $D_w$ , the result obtained in Theorem 2 is equivalent to the solution of the weighted singular LQ control problem:*

$$J = E(Y_t^T W Y_t)$$

where  $W$  is the weighting matrix.

**Proof:** It follows from the same procedure as the proof of Lemma 3. Thus minimization of the variance of the interactor-filtered variable  $\tilde{Y}_t$  by a proper optimal control law is equivalent to minimization of the weighted variance of the original variable  $Y_t$ . ■

The unitary interactor matrix or weighted unitary interact matrix can be used for the design of singular LQ output feedback control law.

**Theorem 5** *If a weighted unitary interactor is used for a process without non-invertible zeros, then its minimum variance control law as solved in Corollary 2 via Theorem 2 is the same as the singular LQ output feedback control law solved via spectral factorization (Harris and MacGregor, 1987; Harris et al., 1996).*

**Proof:** For a MIMO process

$$Y_t = TU_t + Na_t$$

where  $N$  can be represented by an ARIMA model as  $N = \Theta\Phi^{-1}$ . Harris and MacGregor(1987) and Harris *et al.*(1996) have shown that the singular LQ control law (when input penalty matrix  $Q_2 = 0$ ) is solved as

$$U_t = -H_1(Y_t - L\Lambda^{-1}U_t) = -H_1Na_t = -H_1\Theta\Phi^{-1}a_t \quad (4.35)$$

where  $L\Lambda^{-1} = T$  is a matrix fraction representation of the transfer matrix  $T$ ,  $H_1$  is a filter transfer matrix with

$$H_1 = \tilde{T}^{-1}F_1 \quad (4.36)$$

where  $\tilde{T}^{-1} = \Lambda\Gamma^{-1}$  is the optimal inverse of  $T$  (a proper inverse).  $\Gamma$  is solved from spectral factorization

$$\Gamma^H\Gamma = L^HWL \quad (4.37)$$

where  $W$  is the output weighting matrix <sup>2</sup>.  $F_1$  is solved via

$$F_1 = \tau\Theta^{-1} \quad (4.38)$$

where  $\tau$  is solved from the Diophantine equation

$$L^HW\Theta = \Gamma^H\tau + qP(q)\Phi \quad (4.39)$$

---

<sup>2</sup>In Harris and MacGregor (1987),  $W$  is denoted as  $Q_1$ .

Notice that here we use the notation  $\Gamma^H(q^{-1}) = \Gamma^T(q)$  and  $L^H(q^{-1}) = L^T(q)$ .

Left-multiplying both sides of (4.37) by  $\Lambda^{-H}$  and right-multiplying by  $\Lambda^{-1}$ , and using the fact that  $\tilde{T} = \Gamma\Lambda^{-1}$  and  $T = L\Lambda^{-1}$ , we have

$$\tilde{T}^H \tilde{T} = T^H W T \quad (4.40)$$

If a weighted unitary interactor is used as a factorization of time delays, then  $\tilde{T} = D_w T$  does not contain any infinite zeros(time-delays), and equation (4.40) or (4.37) is also satisfied, i.e.  $\tilde{T}$  ( $\tilde{T} = D_w T$ ) is the proper optimal inverse of  $T$ . Now left-multiplying (4.39) by  $\Lambda^{-H}$  yields

$$T^H W \Theta = \tilde{T}^H \tau + \Lambda^{-H} [qP(q)] \Phi \quad (4.41)$$

Right-multiplying both sides of (4.41) by  $\Phi^{-1}$  yields

$$T^H W N = \tilde{T}^H \tau \Phi^{-1} + \Lambda^{-H} [qP(q)] \quad (4.42)$$

From the definition of the weighted unitary interactor, we have

$$T^H = (D_w^{-1} \tilde{T})^H = \tilde{T}^H D_w^{-H} = \tilde{T}^H D_w W^{-1}$$

Substituting this into (4.42) yields

$$\tilde{T}^H D_w N = \tilde{T}^H \tau \Phi^{-1} + \Lambda^{-H} [qP(q)] \quad (4.43)$$

Multiplying (4.43) by  $\tilde{T}^{-H}$  results in

$$D_w N = \tau \Phi^{-1} + \tilde{T}^{-H} \Lambda^{-H} [qP(q)] = \tau \Phi^{-1} + \Gamma^{-H} [qP(q)] = R + M_F \quad (4.44)$$

The first term  $R = \tau \Phi^{-1}$  is simply a proper matrix and involves only negative power terms of  $q^{-1}$ . The second term  $M_F = \Gamma^{-H} [qP(q)] = \Gamma^{-T}(q) [qP(q)]$  involves only positive power terms of  $q$ . This has the same representation as in Theorem 2, and therefore  $M_F$  must be a finite order matrix polynomial.

Combining (4.44), (4.38), (4.36) and (4.35) yields

$$U_t = -\tilde{T}^{-1} \tau \Phi^{-1} a_t = -\tilde{T}^{-1} R a_t \quad (4.45)$$

Under this control law, the closed-loop response can be written as

$$\begin{aligned}
 Y_t &= TU_t + Na_t \\
 &= -D_w^{-1}\tilde{T}\tilde{T}^{-1}Ra_t + D_w^{-1}D_wNa_t \\
 &= -D_w^{-1}Ra_t + D_w^{-1}[M_F + R]a_t \\
 &= D_w^{-1}M_Fa_t
 \end{aligned} \tag{4.46}$$

Therefore

$$a_t = M_F^{-1}D_wY_t$$

Substituting this into (4.45) yields

$$U_t = -\tilde{T}^{-1}RM_F^{-1}D_wY_t \tag{4.47}$$

This yields the same control law as Theorem 2 with the weighted unitary interactor matrix,  $D_w$ . ■

## 4.5 Numerical Example

Consider a  $2 \times 2$  multivariable process, with the open-loop transfer function matrix  $T$  and disturbance transfer function matrix  $N$  given by

$$\begin{aligned}
 T &= \begin{bmatrix} \frac{q^{-1}}{1-0.4q^{-1}} & \frac{K_{12}q^{-2}}{1-0.1q^{-1}} \\ \frac{0.3q^{-1}}{1-0.1q^{-1}} & \frac{q^{-2}}{1-0.8q^{-1}} \end{bmatrix} \\
 N &= \begin{bmatrix} \frac{1}{1-0.5q^{-1}} & \frac{-0.6}{1-0.5q^{-1}} \\ \frac{0.5}{1-0.5q^{-1}} & \frac{1.0}{1-0.5q^{-1}} \end{bmatrix}
 \end{aligned}$$

Suppose that the LQ objective function is given by

$$J = E[Y_t^T Y_t]$$

Then, a unitary interactor matrix is required for the design of the optimal control law.

Following the procedure in Appendix A, a unitary interactor matrix  $D$  can be factored as:

$$D = \begin{bmatrix} -0.9578q & -0.2873q \\ -0.2873q^2 & 0.9578q^2 \end{bmatrix}$$

and the order of the interactor matrix  $d = 2$ . Thus,  $DN$  can be calculated as

$$DN = \begin{bmatrix} \frac{-1.1014q}{(1-0.5q^{-1})} & \frac{0.2874q}{(1-0.5q^{-1})} \\ \frac{0.1916q^2}{(1-0.5q^{-1})} & \frac{1.1302q^2}{(1-0.5q^{-1})} \end{bmatrix}$$

From  $q^{-d}DN = F + q^{-d}R$ , one can calculate  $F$  and  $R$  as

$$F = \begin{bmatrix} -1.1014q^{-1} & 0.2874q^{-1} \\ 0.1916 + 0.0958q^{-1} & 1.1302 + 0.5651q^{-1} \end{bmatrix}$$

$$R = \begin{bmatrix} \frac{-0.5507}{1-0.5q^{-1}} & \frac{0.1437}{1-0.5q^{-1}} \\ \frac{0.0479}{1-0.5q^{-1}} & \frac{0.2826}{1-0.5q^{-1}} \end{bmatrix}$$

The optimal (minimum variance) control law can then be calculated from equation (4.7). The interactor-filter output ( $\tilde{Y}_t = q^{-d}DY_t$ ) under optimal control is given by equation (4.14):

$$\tilde{Y}_t|_{mv} = Fa_t = \begin{bmatrix} -1.1014q^{-1} & 0.2874q^{-1} \\ 0.1916 + 0.0958q^{-1} & 1.1302 + 0.5651q^{-1} \end{bmatrix} a_t$$

Now consider a weighted LQ objective

$$J = E[Y_t^T W Y_t]$$

Suppose the weighting matrix is given by

$$W = \begin{bmatrix} 1 & 0 \\ 0 & 4 \end{bmatrix}$$

It follows from Corollary 1 that the weighted interactor matrix is given by

$$D_w = DW^{1/2}$$

where  $D$  is a unitary interactor matrix of the weighted transfer function matrix  $W^{1/2}T$ . Following the procedure in Appendix A, the unitary interactor matrix  $D$  is calculated as

$$D = \begin{bmatrix} -0.8575q & -0.5145q \\ 0.5145q^2 & -0.8575q^2 \end{bmatrix} \quad (4.48)$$



Thus, the weighted unitary interactor matrix is

$$D_w = \begin{bmatrix} -0.8575q & -1.029q \\ 0.5145q^2 & -1.715q^2 \end{bmatrix}$$

The matrices  $F$  and  $R$  can be calculated from  $q^{-d}D_wN = F + q^{-d}R$  as

$$F = \begin{bmatrix} -1.3720q^{-1} & -0.5145q^{-1} \\ -0.3430 - 0.1715q^{-1} & -2.0240 - 1.0120q^{-1} \end{bmatrix}$$

$$R = \begin{bmatrix} \frac{-0.6860}{1-0.5q^{-1}} & \frac{-0.2572}{1-0.5q^{-1}} \\ \frac{-0.0858}{1-0.5q^{-1}} & \frac{-0.5060}{1-0.5q^{-1}} \end{bmatrix}$$

The optimal (minimum variance) control law can then be calculated from equation (4.7) with the interactor matrix  $D$  substituted by the weighted unitary interactor matrix  $D_w$ , i.e.

$$U_t = -\bar{T}^{-1}RM_F^{-1}D_wY_t = -(D_wT)^{-1}RF^{-1}(q^{-d}D_w)Y_t$$

The interactor-filtered output ( $\tilde{Y}_t = q^{-d}D_wY_t$ ) under optimal control is given by equation (4.14) as

$$\tilde{Y}_t|_{mv} = Fa_t = \begin{bmatrix} -1.3720q^{-1} & -0.5145q^{-1} \\ -0.3430 - 0.1715q^{-1} & -2.0240 - 1.0120q^{-1} \end{bmatrix} a_t$$

## 4.6 Conclusions

This chapter has shown that the unitary/weighted-unitary interactor matrix is an “ideal” factorization of the time-delays of multivariable systems for the design of minimum variance control or singular LQ control. Using the unitary/weighted-unitary interactor matrix, the simple multivariable minimum variance control strategy as proposed by Goodwin and Sin(1984) gives a unique solution which is identical to the singular LQ output feedback control law (Harris and MacGregor, 1987). This result is particularly useful for multivariable control loop performance assessment and for the design of singular LQ control of a minimum phase MIMO process.

## Chapter 5

# Estimation of the Unitary Interactor Matrices

### 5.1 Introduction

The notion of an interactor matrix (Wolovich and Falb, 1976) for a multivariate system can be best understood by relating it to the meaning of the time delay for a univariate process. In the case of a univariate process, the time delay in terms of the sampling time is equal to the number of zero or almost-zero impulse response coefficients, and corresponds to the time that elapses between the moment a change in the input occurs to the moment it takes for this input to have an effect on the output; or it is the result of the first *nonsingular* or non-zero impulse response coefficient having an effect on the output. From a systems theoretic viewpoint the delay corresponds to the number of infinite zeros of a discrete-time process.

This idea is easily generalized to the multivariate case also in terms of the impulse response coefficient or the Markov parameter matrices. In the multivariate case, the notion of a delay corresponds to the fewest number of impulse response or Markov parameter matrices whose linear combination is *nonsingular*. This means that a set of inputs acting

---

<sup>1</sup> A version of this chapter is to appear in the Journal of Process Control (in press), and a shorter version is also in the Proceedings of 1996 IFAC World Congress.

via this specific linear combination of Markov parameter matrices can have a desired effect on the output. This linear combination of impulse response matrices can be expressed in a polynomial matrix form. The determinant of this polynomial matrix has as its roots the number of infinite zeros of the discrete time multivariate system. Simple examples to illustrate these concepts are considered in Shah et al.(1987). The knowledge of the interactor matrix is an important prerequisite to high performance control strategies such as minimum variance control. However, until recently a knowledge of the delay or the interactor matrix was tantamount to the knowledge of the entire process transfer function matrix. As per the above definition, it should appear that relatively simple tests can be performed to determine if a linear combination of the first few Markov or impulse response matrices is singular or not. This is precisely the purpose of this chapter in which we propose the use of a SVD-based procedure to determine if a linear combination of a set of matrices has full rank. The proposed procedure allows us to compute the time delay matrix with minimum effort using routine closed or open-loop data with dither excitation and its subsequent use in multivariate control loop performance assessment or control law design.

The algorithm for factoring the lower triangular interactor matrix as suggested by Wolovich and Falb (1976) and Goodwin and Sin (1984) generally requires a complete knowledge of the transfer function matrix. Shah et al. (1987) and Mutoh and Ortega (1993), however, have suggested a solution of the interactor matrix by solving a set of linear, algebraic equations of certain Markov parameter matrices (impulse response coefficient matrices). This latter approach directly connects the Markov parameter matrices to the interactor matrix without going through the transfer function and is numerically convenient and attractive for estimation of the interactor matrix of a MIMO process. The lower triangular interactor matrix has played an important role in classic multivariable control. Readers are referred to Walgama (1986) and Sripada (1988) for interesting discussions on this issue. Shah et al. (1987) and Rogozinski et al. (1987) have also pointed out that the interactor matrix need not necessarily take the lower-triangular form in application. For example, an interactor matrix with a unit-DC gain or other useful features may be more important in practice, and therefore the interactor matrix

(as proposed by Wolovich and Falb) is not necessarily unique in the sense that it can have forms other than the lower triangular form. However, the “optimal” form of the interactor matrix is application dependent. For a deterministic system, optimal control design based on the lower triangular interactor matrix yields a conditional minimum-time or minimum-ISE control in the sense that the optimization is input-output pairing or ordering dependent (Tsiligiannis and Svoronos, 1988). For a stochastic system, optimal control design based on the lower triangular interactor matrix yields a conditional minimum variance control (Dugard *et al.*, 1984). Peng and Kinnaert (1992) and Bittanti *et al.* (1994) have introduced the *unitary* or *spectrum* interactor matrix for the design of singular LQ state feedback control and optimal filter. Design of multivariable (singular) LQ control for processes with time delays usually involves spectral factorization (Harris and MacGregor, 1987). The unitary interactor matrix simplifies such a procedure. It gives an alternative derivation (with respect to Harris and MacGregor(1987)) of the LQ controller for processes without finite unstable zeros and with output penalty matrix  $Q_1 = I$  and control weighting  $Q_2 = 0$ , i.e.  $J = E[Y^T Y]$ . The unitary interactor matrix can be easily extended to *weighted unitary interactor*. This weighted unitary interactor matrix can then be used for the design of the weighted singular LQ controller, i.e. a controller which minimizes  $J = E[Y^T Q_1 Y]$ . The unitary interactor matrix is in fact a special case of the nilpotent interactor matrix as defined by Rogozinski and co-workers (1987,1990), and plays an important role in multivariate control loop performance assessment theory.

For closed-loop control performance assessment, estimation of the interactor matrix under closed-loop conditions is desired. In this chapter, an algorithm for estimation of the unitary interactor matrix is proposed. Using the proposed method, the interactor matrix can be estimated from closed-loop data without estimation of the open-loop transfer function matrix.

The main contributions of this chapter are: 1) development of a new method for determination of the order of the interactor matrix by using the singular value decomposition technique; 2) extension of the results in Rogozinski *et al.* (1987) and Peng and Kinnaert (1992) for factorization of the unitary interactor by using the first few Markov parameters of a transfer function matrix; 3) use of closed-loop data for the

estimation of the Markov parameters of the transfer function matrix; and 4) experimental evaluation and industrial application of the proposed algorithm. Unlike other interactor factorization methods which generally require complete knowledge of the entire transfer function matrix, this algorithm only requires the first few Markov parameter matrices.

This chapter is organized as follows. The method for determination of the order of the interactor matrix is developed in Section 5.2. The algorithm for the calculation of the unitary interactor matrix is then introduced in Section 5.3. The estimation of the unitary interactor matrix under closed-loop conditions is given a detailed treatment in Section 5.4. The determination of a numerical rank is discussed in Section 5.5. The chapter ends with illustration on a simulated example and a pilot-scale experiment in Section 5.6, and an industrial application in Section 5.7.

## 5.2 Determination of the order of interactor matrices

The interactor matrix has been given in Theorem 1. Wolovich and Falb (1976), and Goodwin and Sin (1984) have suggested factoring a lower triangular interactor matrix from the transfer function matrix. To do this, *a priori* knowledge of the entire transfer matrix is generally required. This is a fairly strong requirement. Shah et al. (1987) have suggested factoring the interactor matrix directly from Markov parameters of the process. This idea is further explored for the determination of the order of the interactor matrix.

The Markov parameter representation of a transfer function matrix can be written as

$$T = \sum_{i=0}^{\infty} G_i q^{-i-1} \quad (5.1)$$

and the interactor matrix is written as

$$D = D_0 q^d + D_1 q^{d-1} + \cdots + D_{d-1} q \quad (5.2)$$

From Theorem 1:

$$\lim_{q^{-1} \rightarrow 0} DT = \lim_{q^{-1} \rightarrow 0} [D_0 q^d + D_1 q^{d-1} + \cdots + D_{d-1} q][G_0 q^{-1} + G_1 q^{-2} + \cdots] = K$$

where  $K$  is a full rank matrix (i.e.  $\text{rank}(K)=\min(n,m)$ ), we have

$$\begin{aligned} D_0 G_0 &= 0 \\ D_1 G_0 + D_0 G_1 &= 0 \\ &\vdots \\ D_{d-1} G_0 + \cdots + D_1 G_{d-2} + D_0 G_{d-1} &= K \end{aligned}$$

Solving the above algebraic equations yields the general solution of the interactor matrix.

The above algebraic equations can be further written in a matrix form as

$$[D_{d-1}, \dots, D_0] \begin{bmatrix} G_0 & 0 & 0 & \cdots & 0 \\ G_1 & G_0 & 0 & \cdots & 0 \\ \vdots & \vdots & \ddots & \ddots & \vdots \\ G_{d-2} & G_{d-3} & \cdots & \ddots & 0 \\ G_{d-1} & G_{d-2} & \cdots & \cdots & G_0 \end{bmatrix} = [K, 0, \dots, 0] \quad (5.3)$$

or for simplicity

$$\underline{D} \underline{G} = \underline{K} \quad (5.4)$$

where  $\underline{G}$  is a block-Toeplitz matrix.  $\underline{D}$  denotes the algebraic matrix form of the interactor, while  $D$  is the matrix polynomial form of the interactor. If  $G_0$  is not full rank, then in addition to the infinite zeros due to the zero-order-hold, at least one more infinite zero exists in the transfer function matrix. Direct inversion for solving equation (5.4) is impossible due to  $\underline{G}$  being rank defective. Existence of the solution for equation (5.4) also depends on the order of the interactor matrix  $d$ , i.e., the “size” of  $\underline{G}$  such that there is at least an exact solution of  $\underline{D}$ . For determining the order of the interactor matrix, the singular value decomposition technique can be used.

Consider the singular value decomposition<sup>2</sup> of the block-Toeplitz matrix as:

$$\underline{G} = U \Sigma V^T = [U_1, U_2] \begin{bmatrix} \Sigma_r & 0 \\ 0 & 0 \end{bmatrix} \begin{bmatrix} V_1^T \\ V_2^T \end{bmatrix} \quad (5.5)$$

---

<sup>2</sup>Note here that the linear matrix equation is in the form of  $XA = B$ , instead of  $AX = B$ , where  $X$  is the unknown vector or matrix. The definitions of the null space and the image space of  $A$  for the two equations are consequently different.

where  $[U_1, U_2]$  and  $[V_1, V_2]^T$  are orthogonal matrices, the columns of  $U_2$  span the null space of  $\underline{G}$  (in the sense that  $U_2^T \underline{G} = 0$ ),  $\Sigma_r$  is a full rank diagonal matrix, and the rows of  $V_1^T$  span the row space of  $\underline{G}$ .

Existence of the exact solution for equation (5.4) requires that 1)  $\text{rank}(\underline{G}) \geq \text{rank}(\underline{K}) = \text{rank}(K) = \min(n, m)$ , and 2) each row of  $\underline{K}$  must be within the row space spanned by  $V_1^T$  or orthogonal to the row space spanned by  $V_2^T$ , i.e.,

$$\underline{K}V_2 = 0 \quad (5.6)$$

This can be simplified by writing

$$\underline{K}V_2 = [K, 0, \dots, 0] \begin{bmatrix} V_{21} \\ V_{22} \\ \vdots \\ V_{2d} \end{bmatrix} = KV_{21} \quad (5.7)$$

where  $V_{21}$  is the upper partition of  $V_2$  with its row dimension same as the column dimension of  $T$ . Thus, the condition expressed by equation (5.6) is equivalent to

$$KV_{21} = 0 \quad (5.8)$$

If  $K$  (or  $T$ ) is a square matrix or is an  $n \times m$  non-square matrix with  $n > m$ , equation (5.8) is further simplified to

$$V_{21} = 0 \quad (5.9)$$

If, however, these conditions are not satisfied, the block-Toeplitz matrix must be expanded by adding more Markov parameters until they are satisfied. Thus, the order of the interactor matrix  $d$  can be determined from Equation (5.8) or (5.9).

If  $T$  is a square transfer function matrix, then the *nullity increasing property* of the block-Toeplitz matrix (see Remark 1) can also be conveniently used to determine the order of the interactor matrix.

**Remark 1** *Mutoh and Ortega (1999) have suggested using the nullity increasing property of Markov parameters for determination of the order of the interactor matrix,  $d$ , of a square*

*transfer function matrix. According to the nullity increasing property, the dimension of null space of  $\underline{G}$  increases with expansion of  $\underline{G}$  until all  $d$  Markov parameters are included in Matrix  $\underline{G}$ .*

In summary, the result presented in this section is not only useful for factorization of the interactor matrix as discussed in the following sections, but also useful in the design of multivariate adaptive control without a complete knowledge of the interactor matrix (Shah *et al.*, 1987).

### 5.3 Factorization of unitary interactor matrices

The solution of equation (5.4) is not unique. The “optimal” solution depends on the application. The unitary interactor matrix discussed in this section is one of several such “optimal” solutions for the application in minimum variance control and multivariable control loop performance assessment. Rogozinski *et al.* (1987) have introduced the *nilpotent interactor matrix*. For a class of interactor matrices which are more suitable for LQ design, Peng and Kinnaert (1992) have further considered the *unitary interactor matrix* which is a *special case* of the nilpotent interactor matrix. Bittanti *et al.* (1994) have also defined a *spectral interactor matrix*, which has essentially the same property as the *right unitary interactor matrix* discussed in a separate paper by Panlinski and Rogozinski (1990). In Chapter 4, the unitary interactor matrix has been shown to be a suitable factorization of the time delay for minimum variance or singular LQ control. It maintains the spectral property of underlying system unchanged after infinite zeros of the transfer matrix are removed. The “Inner-Outer” factorization as introduced in (Chu, 1985) factors out an “all-pass” transfer matrix which also maintains the spectral property. However, it requires the solution of an algebraic Riccati equation. Significant additional effort and process information are then required to factor out the infinite zeros from the Inner-Outer factorization.

The algorithm for the calculation of the unitary interactor matrix proposed by Rogozinski *et al.* requires right matrix fraction (RMF) of the transfer matrix. This is



tantamount to knowing the entire transfer function matrix. In the present chapter, if the Markov parameter representation is used, the algorithm can be simplified.

**Assumption 1** :  $T$  is of a full rank  $n \times m$  rational polynomial transfer function matrix, i.e.,  $\text{rank}[T(q^{-1})] = \min(n, m)$

**Assumption 2** :  $T$  is proper, i.e.,  $\lim_{q^{-1} \rightarrow 0} T(q^{-1}) < \infty$ .

A block matrix of the first  $d$  Markov parameters is expressed in a block matrix form as

$$\Lambda = [G_0^T, G_1^T, \dots, G_d^T]^T$$

Once this block matrix  $\Lambda$  is formed, the unitary interactor matrix  $D(q)$  can be factored out from this block matrix following the procedure in Rogozinski et al. (1987) and Peng and Kinnaert (1992). However, the numerator matrix coefficients of the right matrix fraction (RMF) of  $T$  would be replaced by the first  $d$  Markov parameter matrices. Note that even without the knowledge of the order of the interactor matrix  $d$ , the algorithm can also factor the unitary interactor matrix but must include enough Markov parameter matrices into  $\Lambda$  by, e.g. trial and error.

**Example 3** A numerical example is given to illustrate the proposed algorithm

Consider a  $2 \times 2$  transfer function matrix:

$$T = \begin{bmatrix} \frac{q^{-1}}{1-0.1q^{-1}} & \frac{q^{-1}}{1-0.1q^{-1}} \\ \frac{2q^{-1}}{1-0.3q^{-1}} & \frac{2q^{-1}}{1-0.4q^{-1}} \end{bmatrix} \quad (5.10)$$

To determine the order of the interactor matrix, using the SVD method (skipping the first step  $\underline{G} = G_0$  which is obviously rank defective) gives

$$\underline{G} = \begin{bmatrix} G_0 & 0 \\ G_1 & G_0 \end{bmatrix} = \begin{bmatrix} 1 & 1 & 0 & 0 \\ 2 & 2 & 0 & 0 \\ 0.1 & 0.1 & 1 & 1 \\ 0.6 & 0.8 & 2 & 2 \end{bmatrix} \quad (5.11)$$

Using the SVD decomposition ( $\underline{G} = U\Sigma V^T$ ) and Equation (5.5) gives

$$U_2 = \begin{bmatrix} 0.8944 \\ -0.4472 \\ 0 \\ 0 \end{bmatrix} \quad V_2 = \begin{bmatrix} 0 \\ 0 \\ -0.7071 \\ 0.7071 \end{bmatrix} \quad \Sigma_r = \begin{bmatrix} 3.6812 & 0 & 0 \\ 0 & 2.7322 & 0 \\ 0 & 0 & 0.0629 \end{bmatrix}$$

The column dimension of  $T$  is 2, thus the upper partition of  $V_2$  can be written as

$$V_{21} = \begin{bmatrix} 0 \\ 0 \end{bmatrix}$$

and  $\text{rank}(\underline{G}) > \text{rank}(K) = \min(n, m) = 2$ . The conditions for existence of the interactor matrix are therefore satisfied, and consequently the order of the interactor matrix  $d = 2$  is selected. The block matrix of the first two Markov parameters can be formed as

$$\Lambda = \begin{bmatrix} 1 & 2 & 0.1 & 0.6 \\ 1 & 2 & 0.1 & 0.8 \end{bmatrix}^T$$

Following the algorithm in Rogozinski et al. (1987) (see also Appendix A), a unitary interactor matrix can be factored as

$$D = \begin{bmatrix} -0.4472q & -0.8944q \\ -0.8944q^2 & 0.4472q^2 \end{bmatrix} \quad (5.12)$$

It can be easily verified that  $D^T(q^{-1})D(q) = I$ .

## 5.4 Estimation of the interactor matrix under closed-loop conditions

The proposed factorization algorithm requires only the first  $d$  Markov parameter matrices (or impulse response coefficient matrices), i.e., the first several steps of the initial responses of a system. Since the first few Markov parameter matrices contribute to the initial transient response of the process, these parameters characterize the high frequency dynamics of the process. Thus the interactor matrix, which consists of a linear combination

of the first few Markov parameters, typically represents the high-frequency gain (Shah *et al.*, 1987) of a system. An identification strategy which can yield good estimates in the high frequency range is more desired. A relatively high-frequency dither signal may be used for such purpose. Computationally a correlation analysis generally provides a relatively good estimate of these first few Markov parameters, since  $Var(\hat{G}_k) \propto 1/(N - k)$  (Box and Jenkins, 1976), where  $\hat{G}_k$  is the estimated Markov parameters via cross correlation analysis, and  $N$  is total number of data points used for the estimation. Alternatively, an FIR or a parametric model can also be fitted from input-output data, which can also yield Markov parameters. By utilizing the following lemma, correlation analysis or parametric model fitting can be performed directly from closed-loop data.

**Lemma 6** *For a multivariable process as shown in Figure 5.1, the interactor matrix ( $D_d$ ) of the closed-loop transfer function matrix from  $W_t$  to  $Y_t$  ( $T_d = (I + TQ)^{-1}T$ ) is the same as the interactor matrix ( $D$ ) of the open-loop transfer function matrix ( $T$ )*

**Proof:** It follows from the matrix inversion lemma (Soderstrom and Stoica, 1989) that

$$\begin{aligned} T_d &= (I + TQ)^{-1}T \\ &= [I - T(QT + I)^{-1}Q]T \\ &= T(I + QT)^{-1} \end{aligned}$$

Thus, if  $D$  is the interactor matrix of  $T$ , then  $\lim_{q^{-1} \rightarrow 0} DT = K$  and

$$\lim_{q^{-1} \rightarrow 0} DT_d = \lim_{q^{-1} \rightarrow 0} DT(I + QT)^{-1}$$

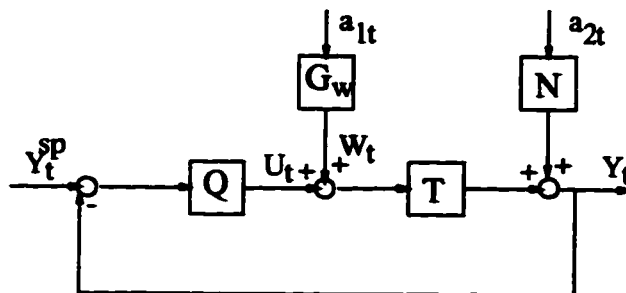


Figure 5.1: A simplified process control loop diagram

$$\begin{aligned}
&= \lim_{q^{-1} \rightarrow 0} DT(I+0)^{-1} \text{ (due to the zero-order-hold)} \\
&= K
\end{aligned}$$

On the other hand, if  $D_d$  is the interactor matrix of  $T_d$ , then  $\lim_{q^{-1} \rightarrow 0} D_d T_d = K_d$ , or

$$\lim_{q^{-1} \rightarrow 0} D_d T(I + QT)^{-1} = K_d$$

Thus

$$\lim_{q^{-1} \rightarrow 0} D_d T = K_d$$

and therefore  $D_d$  is also the interactor matrix of the open-loop transfer function matrix  $T$ . ■

If the dither signal is inserted from the setpoint, the same conclusion holds for the closed-loop transfer function matrix from  $Y_t^{sp}$  to  $Y_t$  following the same procedure of the proof, provided that the controller transfer function matrix does not introduce new infinite zeros to the process.

**Remark 2** This lemma provides a well-known fact that the delay structure or the interactor matrix is “feedback invariant” (Wolovich and Falb, 1976), i.e. the Markov parameters of the open and closed-loop transfer function matrix are different but their linear combination yields the same interactor matrix. With this result, the interactor matrix of an open-loop transfer function can be estimated directly from the closed-loop data.

Whenever the dither signal is “white” or can be whitened by time series analysis, simple correlation analysis can be performed. For actual plants, a random dither signal may not be allowed. For such case simple step changes of the setpoint may be conducted instead. However, such simple setpoint signals may not be sufficiently modelled by a time series model, and therefore a correlation analysis is not appropriate. In this case, a parametric model (including FIR) should be considered. As mentioned earlier, one must keep in mind that a low-frequency dither signal may yield a poorer estimate of the interactor matrix than a relatively high-frequency dither signal.

Our purpose is to identify the interactor matrix from closed-loop data via the dither signal or the setpoint to the output. A MISO identification procedure can be used if the dither signals or setpoint changes of all loops are conducted simultaneously. If, however, the dither signal or setpoint change of each loop is conducted separately, a SISO identification procedure can be used.

**Remark 3** A typical industrial process could be very high order and subject to non-linearity. A process under regulatory control usually operates around a nominal point. Identification of the interactor matrix under closed-loop conditions therefore provides a more realistic estimate than under open-loop conditions in the sense that it gives the interactor matrix of the process around the current operating point. This property is particularly useful for adaptive control and control loop performance monitoring. Similarly, a good estimate of the first few Markov parameters or initial transient responses is more important than a “good” estimate of the overall transfer function matrix which often compromises a fit over a wider frequency range. Computationally, a direct identification of the first few Markov parameters is also more desirable than identification of the full transfer function matrix first and then transferring it to Markov parameters. Therefore, factorization of the interactor matrix from the first few Markov parameters is preferred to factorization of the interactor matrix from the transfer function matrix.

## 5.5 Numerical rank

The estimated Markov parameter matrices are not exact due to disturbances, and this makes numerical determination of the rank of the block-Toeplitz matrix  $\underline{G}$  somewhat arbitrary. To cope with the difficulty, a result from Aoki (1987) (see also Paige (1981)) is used:

Let  $H$  be a theoretical matrix with its theoretically exact singular value decomposition,  $U\Sigma V^T$ . Suppose that a numerically constructed approximation to  $H$  is available as  $\hat{H} = H + \Delta H$ , where it is known that  $\|H - \hat{H}\| \leq a\|\hat{H}\|$ . Here the constant  $a$  represents a measure of data accuracy. If the computer round-off error is omitted, then in terms of

the singular values of  $H$  and  $\hat{H}$ , this inequality can be stated as

$$|\sigma_i - \hat{\sigma}_i| \leq a\hat{\sigma}_1$$

where  $\sigma_i, \hat{\sigma}_i$  denote the  $i^{th}$  theoretical singular and calculated singular values respectively. If  $\hat{\sigma}_r$  is greater than  $a\hat{\sigma}_1$ , but  $\hat{\sigma}_{r+1}$  is less than this number then clearly  $\sigma_r$  is positive. Hence the rank of the matrix is at least  $r$ . The next singular value,  $\sigma_{r+1}$  may be possibly zero. Such an  $r$  may then be chosen as the numerical rank of the true but unknown matrix  $H$ .

Golub and van Loan(1989) have another useful result that the difference of the singular value of  $H + E$  and  $H$  is bounded by the largest singular value of  $E$ , where  $E$  is considered as a perturbation matrix. We will regard this largest singular value as the threshold value.

The above results can be applied to find the rank of  $G_i$  and  $\underline{G}$ . The Aoki approach requires *a priori* knowledge of  $a$ . To find the value  $a$ , we may use an empirical value or a statistical value. As an example, Tiao and Box (1981) use  $2/\sqrt{M}$  (where  $M$  is the sample size) as the relative error,  $a$ .

The threshold value approach is also useful if some pre-knowledge of perturbation is available. The correlation analysis or FIR model fitting often provides such knowledge. In addition to the Markov parameter matrices expressed by equation (5.1), the Markov parameter matrix corresponding to the zero order of  $q$ , written as  $G_{-1}$  in accordance with equation (5.1), is also obtained simultaneously in the correlation analysis. Due to the zero-order-hold,  $G_{-1}$  is theoretically zero, and therefore it does not appear in equation (5.1). However its estimation is not zero due to disturbance. Thus, the estimated value of  $G_{-1}$  provides an approximation of the perturbation matrix,  $E$ , and can be used to determine the rank of the estimated Markov parameters. Once the order of the interactor matrix is determined, the column block matrix of the Markov parameters can be formed, and the factorization of the unitary interactor matrix can proceed.

## 5.6 Simulation and experimental evaluation on a pilot scale process

**Example 4** *A closed-loop multivariable process, represented by the block diagram shown in Figure 5.1, is simulated. The interactor factorization algorithm based on correlation analysis is used to find the closed-loop interactor matrix, and the results are compared to the open-loop interactor matrix. To keep routine operation of process and to show the asymptotic property of correlation analysis, the magnitude of the dither signal is chosen such that it has a very weak effect on the process output relative to the existing process disturbances.*

For the sake of comparison, we use the same open-loop transfer function  $T$  as that of example 3. The remaining transfer function matrices of Figure 5.1 take the following values:

$$Q = \begin{bmatrix} 0.4 & 0 \\ 0 & 0.3 \end{bmatrix} \quad N = \begin{bmatrix} 1 & 2 \\ 3 & 4 \end{bmatrix} \quad G_w = \begin{bmatrix} 1 & 0 \\ 0 & 1 \end{bmatrix}$$

The setpoint is assumed to be zero.  $a_{1t}$  and  $a_{2t}$  are white noise random processes with  $\Sigma_{a1} = 0.07^2 I$  and  $\Sigma_{a2} = 0.1^2 I$ . In this simulation, the existing variance of the output without the dither signal has a magnitude of

$$\Sigma_Y = \begin{bmatrix} 0.2203 & 0.3958 \\ 0.3958 & 0.7402 \end{bmatrix} \quad (5.13)$$

With injection of the dither signal, variance of the process output becomes

$$\Sigma_Y = \begin{bmatrix} 0.2381 & 0.4268 \\ 0.4268 & 0.7956 \end{bmatrix}$$

Thus the dither signal has a negligible effect on the process. Since the dither signal is weak, a relatively large sample size of 5000 points is used<sup>3</sup>. Applying the cross-correlation analysis, the first three Markov parameter matrices (including  $G_{-1}$ ) are calculated as

$$\hat{G}_{-1} = \begin{bmatrix} -0.0223 & 0.0135 \\ -0.0268 & -0.0182 \end{bmatrix} \quad \hat{G}_0 = \begin{bmatrix} 1.0161 & 0.9824 \\ 2.0435 & 1.9626 \end{bmatrix} \quad \hat{G}_1 = \begin{bmatrix} -0.9321 & -0.8885 \\ -1.4394 & -1.1543 \end{bmatrix}$$

<sup>3</sup>The sample size can certainly be reduced if the magnitude of the dither signal is increased.

The SVD decomposition of  $\hat{G}_{-1}$  yields the largest singular value as 0.0355. Thus, the value of 0.0355 can be taken as the threshold to decide if a singular value is significantly different from zero. We can also use the relative error  $a = 2/\sqrt{N} = 2/\sqrt{5000} = 0.0283$  to test the rank.

Form the matrix  $\underline{G}$  as  $\underline{G} = \hat{G}_0$ . The SVD decomposition of  $\underline{G}$  yields

$$U = \begin{bmatrix} 0.4464 & 0.8948 \\ 0.8948 & -0.4464 \end{bmatrix} \quad \Sigma = \begin{bmatrix} 3.1663 & 0 \\ 0 & 0.0043 \end{bmatrix} \quad V = \begin{bmatrix} 0.7208 & -0.6932 \\ 0.6932 & 0.7208 \end{bmatrix}$$

Compared to either the threshold value or the relative error, it is clearly reasonable to assume that  $\text{rank}(\underline{G}) = 1$ , and no exact solution of the matrix  $\underline{D}$  exists. Thus, the dimension of  $\underline{G}$  must be increased by adding more Markov parameter matrices. Before collecting more Markov parameters, It is convenient for further analysis to modify  $\hat{G}_0$  by setting its smallest singular value to zero, i.e.,

$$\begin{aligned} \hat{G}'_0 &= U\Sigma'V \\ &= \begin{bmatrix} 0.4464 & 0.8948 \\ 0.8948 & -0.4464 \end{bmatrix} \begin{bmatrix} 3.1663 & 0 \\ 0 & 0 \end{bmatrix} \begin{bmatrix} 0.7208 & -0.6932 \\ 0.6932 & 0.7208 \end{bmatrix} = \begin{bmatrix} 1.0187 & 0.9797 \\ 2.0422 & 1.9640 \end{bmatrix} \end{aligned}$$

This is a reasonable approximation when a singular value is significantly smaller than other singular values and the matrix has been tested to be rank defective. If fact, it is recommended to test the rank of each Markov parameter matrix and modify them accordingly before one forms the block-Toeplitz matrix  $\underline{G}$  and the block matrix  $\Lambda$ . Now increase the dimension of  $\underline{G}$  by

$$\underline{G} = \begin{bmatrix} \hat{G}'_0 & 0 \\ \hat{G}_1 & \hat{G}'_0 \end{bmatrix} \quad (5.14)$$

The SVD decomposition yields

$$\Sigma = \begin{bmatrix} 4.4745 & 0 & 0 & 0 \\ 0 & 2.2556 & 0 & 0 \\ 0 & 0 & 0.0687 & 0 \\ 0 & 0 & 0 & 0 \end{bmatrix} \quad V = \begin{bmatrix} 0.6074 & -0.3866 & 0.6940 & 0 \\ 0.5474 & -0.4294 & -0.7183 & 0 \\ -0.4150 & -0.5883 & 0.0355 & -0.6932 \\ -0.3991 & -0.5657 & 0.0341 & 0.7208 \end{bmatrix}$$

Clearly  $\text{rank}(\underline{G}) \geq 2$  and

$$V_{21} = \begin{bmatrix} 0 \\ 0 \end{bmatrix}$$



An exact solution of  $\underline{D}$  exists and the order of the interactor matrix  $d = 2$  is selected.

The block matrix is formed as

$$\hat{\Lambda} = \begin{bmatrix} 1.0187 & 2.0422 & -0.9321 & -1.4394 \\ 0.9797 & 1.9604 & -0.8885 & -1.1543 \end{bmatrix}^T$$

Following the algorithm in (Rogozinski *et al.*, 1987) (see Appendix A also), the estimated unitary interactor matrix can be factored as

$$\hat{D} = \begin{bmatrix} -0.4464q & -0.8948q \\ -0.8948q^2 & 0.4464q^2 \end{bmatrix}$$

This result agrees well with the theoretical open-loop interactor matrix shown in Equation (5.12).

**Example 5** *To evaluate the proposed algorithm on a physical process, both open-loop and closed-loop experiments have been conducted on a two-interacting tank pilot-scale process. Each tank is a double-walled glass tank 50 cm high with an inside diameter of 14.5 cm. The levels ( $h_1, h_2$ ) of the two tanks are the two controlled variables. The signals to the two valves ( $u_1, u_2$ ) are manipulated to control the levels. The process is shown in figure 5.2. The sampling interval is taken as  $T_s = 20\text{sec}$ . A two-step delay (including zero-order-hold) is introduced in front of the first valve, and a three-step delay (including zero-order-hold) is introduced in front of the second valve. Two sets of multiloop P/PI controllers are implemented in the experiments. Open-loop and closed-loop interactor matrices are estimated from open-loop and closed-loop data respectively. The estimated open-loop and closed-loop interactor matrices are then compared.*

An open-loop multivariable test was conducted with the result shown in figure 5.3. The two manipulated signals,  $u_1$  and  $u_2$ , are applied simultaneously. The multivariate prediction error method (Ljung, 1987) is used for identification of this multivariate process, which yields the following Markov parameters:

$$T_{open} = \begin{bmatrix} 0.1632 & 0 \\ 0.0169 & 0 \end{bmatrix} q^{-2} + \begin{bmatrix} 0.1462 & 0.0185 \\ 0.0355 & 0.1249 \end{bmatrix} q^{-3} + \dots$$

Following the procedure as introduced in the foregoing sections, a unitary interactor matrix can be calculated as

$$D_{open} = \begin{bmatrix} -0.9947q^2 & -0.1030q^2 \\ -0.1030q^3 & 0.9947q^3 \end{bmatrix} \quad (5.15)$$

The interactor matrix depends on the first few steps of the initial responses. Since the initial responses of the interaction terms between the two tanks are relatively weak, the interactor matrix is dominated by the diagonal terms.

Closed-loop tests with a P-controller (Proportional only) and with a PI-controller are conducted respectively, which yield results shown in figure 5.4. Dither signals,  $w_1$  and  $w_2$ , are applied to the process simultaneously. The following Markov parameters of the closed-loop process are obtained from the closed-loop data:

$$T_P = \begin{bmatrix} 0.1910 & 0 \\ 0.0192 & 0 \end{bmatrix} q^{-2} + \begin{bmatrix} 0.1600 & 0.0090 \\ 0.0414 & 0.1260 \end{bmatrix} q^{-3} + \dots$$

and

$$T_{PI} = \begin{bmatrix} 0.1704 & 0 \\ 0.0177 & 0 \end{bmatrix} q^{-2} + \begin{bmatrix} 0.1451 & 0.0132 \\ 0.0369 & 0.1290 \end{bmatrix} q^{-3} + \dots$$

These yield the closed-loop interactor matrices as

$$D_P = \begin{bmatrix} -0.9950q^2 & -0.1000q^2 \\ -0.1000q^3 & 0.9950q^3 \end{bmatrix} \quad (5.16)$$

and

$$D_{PI} = \begin{bmatrix} -0.9946q^2 & -0.1033q^2 \\ -0.1033q^3 & 0.9946q^3 \end{bmatrix} \quad (5.17)$$

The similarity between equation (5.15) and equations (5.16) and (5.17) clearly demonstrates that the interactor matrix is “feedback-invariant”, and can be estimated from closed-loop data. The small differences between these three interactor matrices may be attributed to disturbances.

## 5.7 Industrial application

**Example 6** *A multivariate industrial distillation process is studied in this example. A*

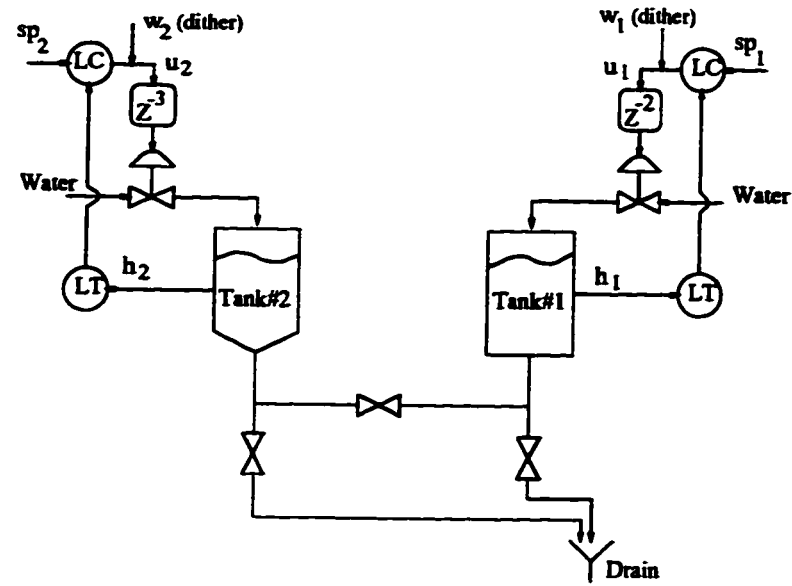


Figure 5.2: *Schematic of the two-interacting tank pilot-scale process.*

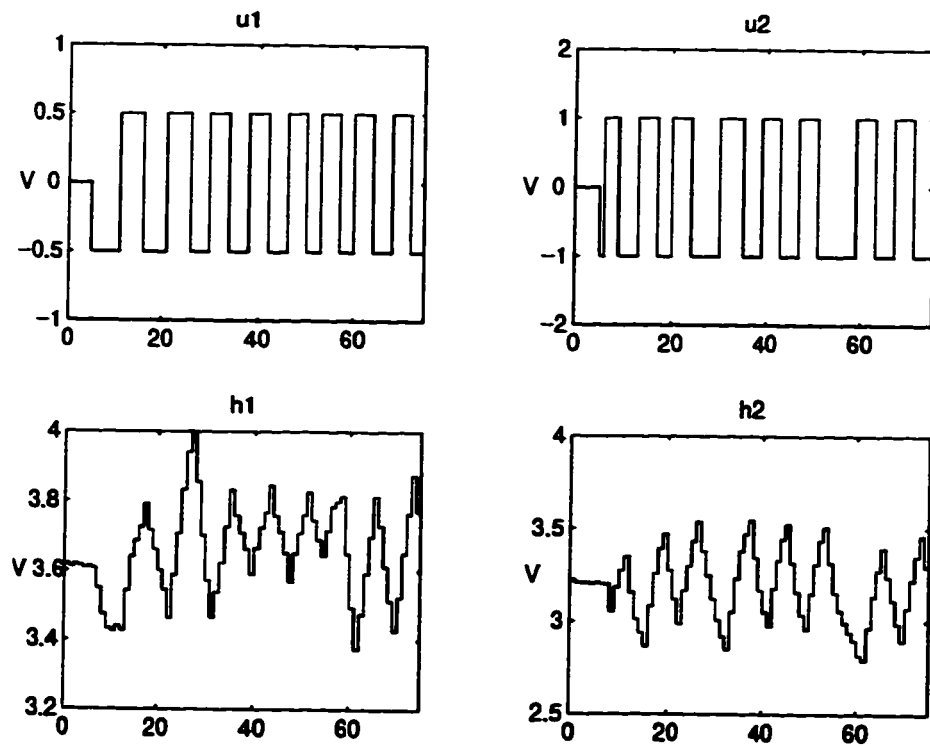


Figure 5.3: *Open-loop (input and output) test data where  $u = 0$  corresponds to 50% open of the valve, and the units of  $h_1$  and  $h_2$  are voltage. The time scale is in terms of sampling intervals.*

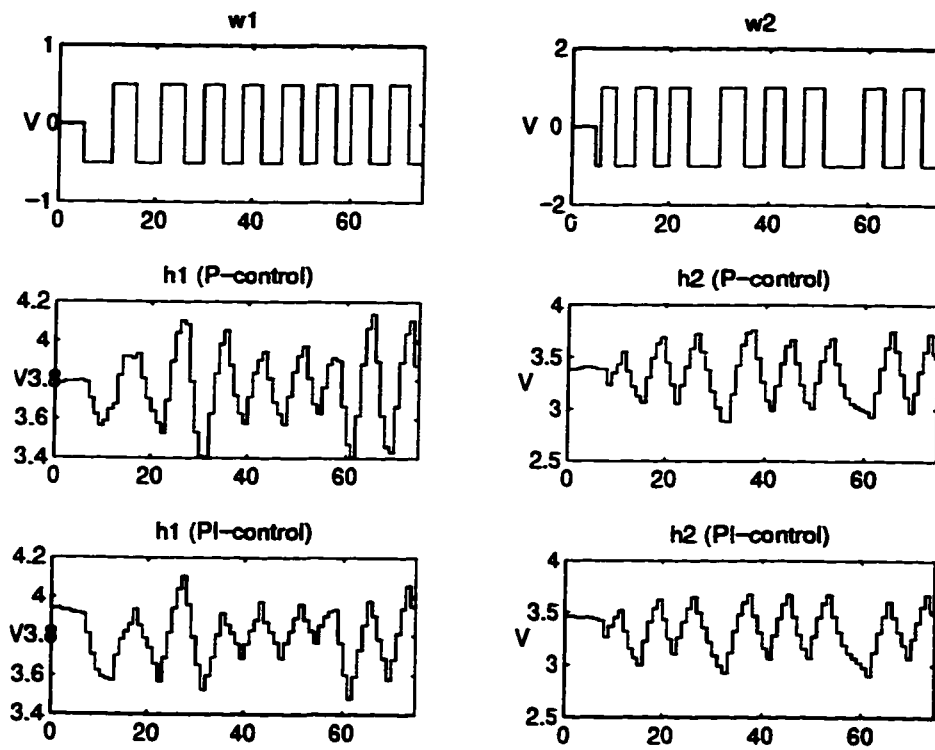


Figure 5.4: *Closed-loop (dither and output) test data where the units of  $h_1$  and  $h_2$  are voltage. The time scale is in terms of sampling intervals.*

*unitary interactor matrix is estimated from industrial closed-loop data.*

The process consists of 3 distillation towers as shown in figure 5.5. The bottom product of the last tower is the main product and the distillates or the top products of the remaining two towers are recycled to the upstream process. The problem encountered for the multiloop controller design of this process is the strong interaction between levels of the first two towers and between the temperature and the level of the second tower.

Since the last tower is relatively small, temperature variation in the second tower can significantly disturb the temperature of the last tower. Regulating the temperature of the last tower at a constant value is important for regulating the quality of the final product. Due to the strong interaction between the temperature and the level loops in the second tower, a multivariable controller is clearly desirable. Therefore, the control objective in this study is the temperature and level control of the second tower in order to reduce disturbances to the last tower. To design a high performance multivariable controller, it is in the interest of control engineers to know the interactor matrix.

Simple closed-loop setpoint changes were conducted on this process. To simplify the test, setpoint changes of the level and temperature were conducted separately. Identification of the closed-loop Markov parameters or transfer function matrix can therefore be cast as four separate open-loop identification problems of SISO impulse response parameters or transfer functions. Figure 5.7 shows the four SISO identification results. The corresponding setpoints are shown in figure 5.6. To identify closed-loop

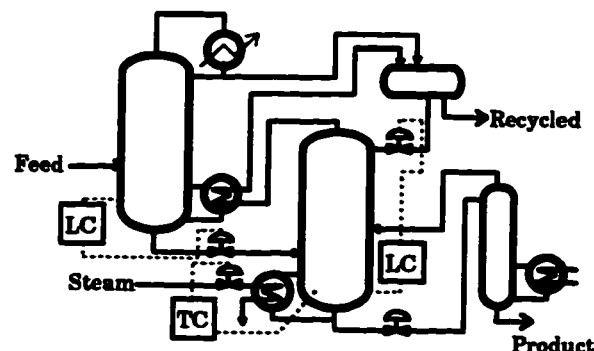


Figure 5.5: *The industrial process flowsheet*

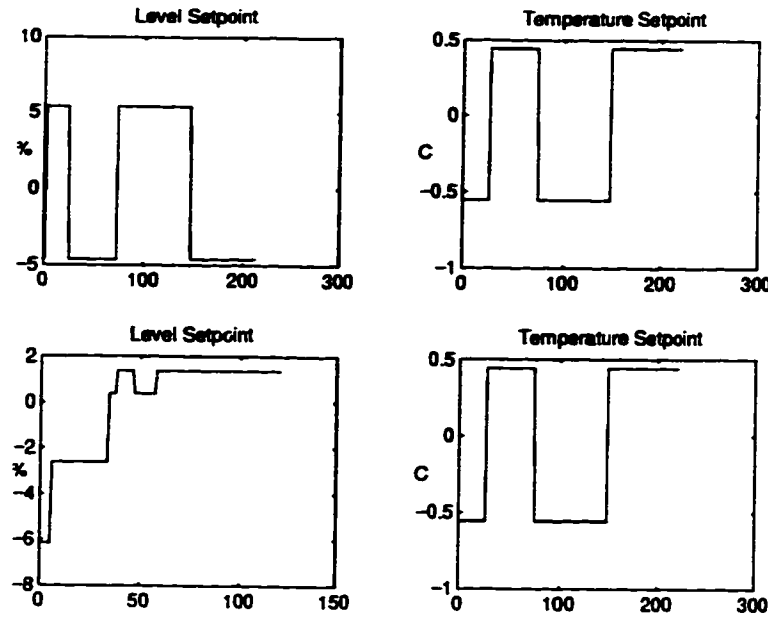


Figure 5.6: *Setpoints for the closed-loop tests. The time scale is in terms of sampling intervals*

transfer function matrices of the temperature and level, only two experiments are required. One is for the level setpoint test, and the other one is for the temperature setpoint test. However, in this example the level setpoint tests were conducted twice with different excitation signals due to saturated data record of the temperature response when the first set of level setpoint test was conducted. Note that in figure 5.7, the solid line denotes the estimated-model prediction based only on the past inputs, and the dash-dotted line denotes actual outputs.

The four identified SISO models form the closed-loop transfer function matrix and yield the following Markov parameters.

$$\begin{aligned} \hat{G} = & \begin{bmatrix} 0 & 0 \\ 0 & 0.1513 \end{bmatrix} q^{-1} + \begin{bmatrix} 0 & -0.6629 \\ 0.0130 & 0.1267 \end{bmatrix} q^{-2} + \\ & + \begin{bmatrix} 0.0713 & -0.5022 \\ 0.0118 & 0.1062 \end{bmatrix} q^{-3} + \dots \end{aligned}$$

Since time-delays of each SISO model can be easily determined through SISO identification procedure (Soderstrom and Stoica, 1989), zeros which appear in the above Markov

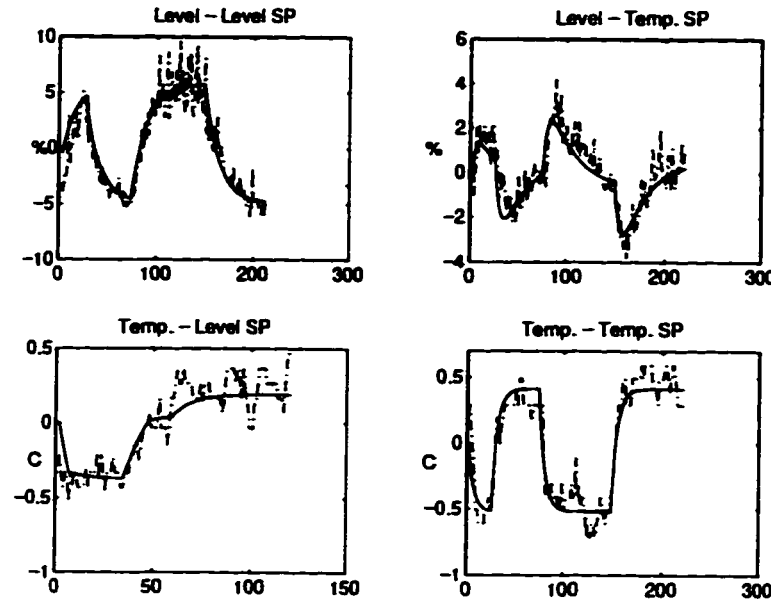


Figure 5.7: *Predicted vs actual outputs; all data have been zero-mean centered. The time scale is in terms of sampling intervals*

parameter matrices are exact zeros and correspond to time-delays in the SISO models.

Following the same procedure as introduced earlier, an order of the interactor matrix  $d = 3$  is obtained. The block matrix of the first three Markov parameters is formed as

$$\hat{\Lambda} = \begin{bmatrix} 0 & 0 & 0 & 0.0130 & 0.0713 & 0.0118 \\ 0 & 0.1513 & -0.6629 & 0.1267 & -0.5022 & 0.1062 \end{bmatrix}^T$$

The unitary interactor matrix is calculated as

$$D = \begin{bmatrix} 0.9749q^2 & -0.2225q \\ 0.2225q^3 & 0.9749q^2 \end{bmatrix}$$

## 5.8 Conclusions

In this chapter, an algorithm has been developed for estimating interactor matrices and in particular the unitary interactor matrices under closed-loop as well as open-loop conditions. The singular value decomposition method has been used to determine the order of the interactor matrix. The algorithm for factorization of the unitary interactor matrix

has been simplified by using only first few Markov parameter matrices. The proposed algorithm has been evaluated by simulated example, pilot-scale experiment and industrial processes. The results presented in this chapter are useful for the design of minimum variance or singular LQ control, optimal  $H_2$ -control, optimal filtering, and particularly multivariable control loop performance assessment methods.



## Chapter 6

# Feedback Controller Performance Assessment: Simple Interactor

### 6.1 Introduction

The interactor matrix  $D$  can be one of the three forms as discussed in Chapter 3. If  $D$  is of the form:  $D = q^d I$ , then the transfer function matrix  $T$  is regarded as having a *simple interactor matrix*. This is the simplest form of the interactor matrices. Although it is usually unlikely to encounter a real process with a simple interactor matrix, the result presented in this chapter provides a basis for solutions to processes with diagonal and general interactor matrices that follow later in this thesis.

This chapter is organized as follows. The feedback controller-invariance property of the minimum variance control term is discussed in Section 6.2. The FCOR (for Filtering and CORrelation analysis) algorithm is presented in Section 6.3. The proposed algorithm is illustrated by a simulated example in Section 6.4, followed by concluding remarks in Section 6.5

---

<sup>1</sup>A version of this chapter is in the Proceedings of 1995 American Control Conference and a part of material will also appear in *Automatica* (in press).

## 6.2 Feedback controller-invariance of minimum variance term and its separation from routine operating data

The simplest form of a multivariable process has a square process transfer function matrix with a simple interactor matrix. Keviczky (Keviczky and Hetthessy, 1977) and Borison (Borison, 1979) have given the minimum variance control law for processes with simple interactor matrices. The purpose of this section is to show that the minimum variance term is feedback control invariant and can be estimated from routine operating data.

**Theorem 6** *For the multivariable process with a simple interactor matrix:*

$$Y_t = TU_t + Na_t \quad (6.1)$$

*the minimum variance control is obtained by minimizing*

$$J = E[Y_t^T Y_t]$$

*or equivalently (for the simple interactor matrix) minimizing*

$$J = E[Y_t Y_t^T]$$

*The performance measure is given by the following steps:*

1. *The quadratic measure of minimum variance is given by*

$$E[Y_t^T Y_t]_{\min} = E(e_t^T)(e_t) = \text{tr}(\text{Var}(Fa_t))$$

*and the minimum variance itself is given by*

$$\text{Var}(Y_t)|_{\min} = \text{Var}(e_t) = \text{Var}(Fa_t)$$

*where  $e_t = Fa_t$ , the polynomial matrix  $F$  depends only on the time-delay  $d$  and the noise model, and satisfies the identity:*

$$q^{-d}DN = \underbrace{F_0 + \cdots + F_{d-1}q^{-(d-1)}}_F + q^{-d}R$$

*where  $R$  is a proper rational transfer function matrix; and furthermore*

2. if one models closed-loop routine operating data under feedback control by the following multivariate moving-average process:

$$Y_t - E(Y_t) = \underbrace{F_0 a_t + F_1 a_{t-1} + \dots + F_{d-1} a_{t-d+1}}_{e_t} + \underbrace{L_0 a_{t-d} + L_1 a_{t-d-1} + \dots}_{w_{t-d}}$$

then the minimum variance term,  $e_t = Fa_t$ , consists of the first  $d$  terms of this moving-average model, and therefore can be separated using time series analysis of routine operating data and be used as a benchmark measure of multivariate minimum variance control.

**Proof:** For this case of the simple interactor matrix, the transfer function matrix can be written as

$$T = q^{-d} \tilde{T} \quad (6.2)$$

where  $\tilde{T}$  is the delay-free transfer function matrix of  $T$ . Substituting equation (6.2) into equation (6.1) yields

$$Y_t = q^{-d} \tilde{T} U_t + N a_t$$

Consider the feedback control law given by  $U_t = -Q Y_t$ . The closed-loop transfer function is then given by

$$Y_t = -q^{-d} \tilde{T} Q Y_t + N a_t \quad (6.3)$$

Now consider the Diophantine identity:

$$N = F + q^{-d} R \quad (6.4)$$

where

$$F = F_0 + F_1 q^{-1} + \dots + F_{d-1} q^{-(d-1)}$$

and  $R$  is the remaining proper and rational transfer function matrix. Substituting equation (6.4) into equation (6.3) gives

$$Y_t = (q^d I + \tilde{T} Q)^{-1} q^d (F + q^{-d} R) a_t$$

Applying the matrix inverse lemma yields

$$\begin{aligned}
 Y_t &= [q^{-d}I - q^{-d}\tilde{T}(I + q^{-d}Q\tilde{T})^{-1}Qq^{-d}]q^d[F + q^{-d}R]a_t \\
 &= Fa_t - q^{-d}\tilde{T}(I + q^{-d}Q\tilde{T})^{-1}QFa_t + q^{-d}Ra_t - \\
 &\quad - q^{-2d}\tilde{T}(I + q^{-d}Q\tilde{T})^{-1}QRa_t \\
 &= Fa_t + q^{-d}Ra_t - q^{-d}\tilde{T}(I + q^{-d}Q\tilde{T})^{-1}QNa_t \\
 &\triangleq Fa_t + La_{t-d}
 \end{aligned} \tag{6.5}$$

where

$$L = R - \tilde{T}(I + q^{-d}Q\tilde{T})^{-1}QN \tag{6.6}$$

is a proper rational transfer function matrix. The two terms on the right hand side of equation (6.5) are therefore independent.

Define  $e_t = Fa_t$  and  $w_{t-d} = La_{t-d}$ . Then

$$\text{Var}(Y_t) \geq \text{Var}(e_t) = \text{Var}(Fa_t)$$

and

$$E[Y_t^T Y_t] \geq E[e_t^T e_t] = \text{tr}(\text{Var}(Fa_t))$$

The equality holds under minimum variance control when  $L = 0$ . The minimum variance control law is therefore obtained by simply setting  $L = 0$  in equation (6.6). The resulting controller transfer function,  $U_t = -QY_t$  is given by

$$Q = -\tilde{T}^{-1}(q^{-d}I - NR^{-1})^{-1}$$

Combining this with equation (6.4) yields

$$\begin{aligned}
 Q &= -\tilde{T}^{-1}[q^{-d}I - (F + q^{-d}R)R^{-1}]^{-1} \\
 &= \tilde{T}^{-1}RF^{-1}
 \end{aligned} \tag{6.7}$$

which is the minimum variance control law. Notice that in equation (6.5), the controller has no influence on the first term, which is minimum variance term of the process output,

$$Y_t|_{mv} = e_t = Fa_t = (F_0 + F_1q^{-1} + \dots + F_{d-1}q^{-(d-1)})a_t \tag{6.8}$$

Therefore if a closed-loop response under feedback control is modelled by a multivariate moving-average process as

$$\tilde{Y}_t - E(\tilde{Y}_t) = \underbrace{F_0 a_t + F_1 a_{t-1} + \dots + F_{d-1} a_{t-d+1}}_{e_t} + \underbrace{L_0 a_{t-d} + L_1 a_{t-d-1} + \dots}_{w_{t-d}} \quad (6.9)$$

It follows that the feedback control invariant term,  $e_t$ , can be separated out from other feedback control relevant terms. The minimum variance performance is subsequently estimated from  $e_t$ . ■

## 6.3 The FCOR algorithm

### 6.3.1 Multivariable performance index

As proved in the last section,  $e_t \triangleq F a_t$  is the feedback control invariant minimum variance term. This minimum variance term can be used as a benchmark for the multivariable performance measure. By using equation (6.8), one can write the minimum variance term  $e_t$  as

$$e_t = (F_0 + q^{-1} F_1 + \dots + q^{-d+1} F_{d-1}) a_t$$

Thus

$$\begin{aligned} \Sigma_{mv} &= E[e_t e_t^T] \\ &= F_0 \Sigma_a F_0^T + \dots + F_{d-1} \Sigma_a F_{d-1}^T \end{aligned} \quad (6.10)$$

where

$$\Sigma_a = E(a_t a_t^T)$$

On the other hand, the closed-loop output vector  $Y_t$  under feedback control can be represented by an infinite multivariate moving average process, i.e.,

$$Y_t = F_0 a_t + F_1 a_{t-1} + \dots + F_{d-1} a_{t-d+1} + F_d a_{t-d} + \dots \quad (6.11)$$

So the covariance of the output and the noise at lag  $i$  is given by

$$\Sigma_{Y_a}(i) = E[Y_t a_{t-i}^T] = F_i \Sigma_a \quad (6.12)$$

Now consider the definition of the performance index as

$$\eta(d) \triangleq \text{tr}(\Sigma_{mv} \tilde{\Sigma}_Y^{-1})/n \quad (6.13)$$

where  $n$  is the dimension of  $Y_t$ ,  $\tilde{\Sigma}_Y = \text{diag}(\Sigma_Y)$  and  $\Sigma_Y = \text{Var}(Y_t)$ . When a process is under minimum variance control, we have  $\Sigma_Y = \Sigma_{mv}$ ; thus it can be shown that  $\eta(d) = 1$ . If control is poor relative to the minimum variance control, then we should expect  $0 < \eta(d) < 1$ . Applying equation (6.13) to a SISO process where  $n = 1$  gives

$$\eta(d) = \text{tr}\left(\frac{\sigma_{mv}^2}{\sigma_y^2}\right) = \frac{\sigma_{mv}^2}{\sigma_y^2}$$

which is the performance measure of a SISO process. A correlation analysis yields a computationally simple procedure for calculating  $\eta(d)$  as follows.

Equation (6.13) can be written as

$$\begin{aligned} n \times \eta(d) &= \text{tr}(\Sigma_{mv} \tilde{\Sigma}_Y^{-1}) \\ &= \text{tr}(\tilde{\Sigma}_Y^{-1/2} \Sigma_{mv} \tilde{\Sigma}_Y^{-1/2}) \end{aligned} \quad (6.14)$$

Substituting equations (6.10) into equation (6.14) and using the relation established in equation (6.12) yields

$$\begin{aligned} n \times \eta(d) &= \text{tr}[\tilde{\Sigma}_Y^{-1/2} \Sigma_{Y_a}(0) \Sigma_a^{-1} \Sigma_{aY}(0) \tilde{\Sigma}_Y^{-1/2} + \\ &\quad + \tilde{\Sigma}_Y^{-1/2} \Sigma_{Y_a}(1) \Sigma_a^{-1} \Sigma_{aY}(1) \tilde{\Sigma}_Y^{-1/2} + \\ &\quad + \cdots + \tilde{\Sigma}_Y^{-1/2} \Sigma_{Y_a}(d-1) \Sigma_a^{-1} \Sigma_{aY}(d-1) \tilde{\Sigma}_Y^{-1/2}] \\ &= \text{tr}(\rho_{Y_a}(0) \rho_a^{-1} \rho_{aY}(0) + \rho_{Y_a}(1) \rho_a^{-1} \rho_{aY}(1) + \cdots + \\ &\quad + \rho_{Y_a}(d-1) \rho_a^{-1} \rho_{aY}(d-1)) \end{aligned}$$

where  $\rho_{Y_a}(i) = \tilde{\Sigma}_Y^{-1/2} \Sigma_{Y_a}(i) \tilde{\Sigma}_a^{-1/2}$ , ( $\tilde{\Sigma}_a \triangleq \text{diag}(\Sigma_a)$ ), is the multivariate cross correlation between  $Y_t$  and  $a_{t-i}$ ;  $\rho_a = \tilde{\Sigma}_a^{-1/2} \Sigma_a \tilde{\Sigma}_a^{-1/2}$ , is the multivariate autocorrelation of  $a_t$ . If a scaled cross correlation is defined as  $\bar{\rho}_{Y_a}(i) \triangleq \rho_{Y_a}(i) \rho_a^{-1/2}$  and

$$Z \triangleq \begin{bmatrix} \bar{\rho}_{Y_a}(0) & \bar{\rho}_{Y_a}(1) & \cdots & \bar{\rho}_{Y_a}(d-1) \end{bmatrix}$$

then we have

$$\eta(d) = \text{tr} Z Z^T / n \quad (6.15)$$

Note from equation (6.14) and equation (6.15) that

$$ZZ^T = \tilde{\Sigma}_Y^{-1/2} \Sigma_{mv} \tilde{\Sigma}_Y^{-1/2}$$

The above multivariable performance thus has a clear physical interpretation which is stated as follows. The diagonal elements of matrix  $ZZ^T$  are the performance measures of each single output  $\eta_{Y1}(d), \dots, \eta_{Yn}(d)$ , and therefore

$$\begin{aligned} \eta(d) &= \text{tr}(ZZ^T)/n = \frac{\eta_{Y1}(d) + \dots + \eta_{Yn}(d)}{n} \\ &= (\text{the average performance of } n \text{ outputs}) \end{aligned}$$

where the individual performance,  $\eta_{Yi}(d)$ , is the ratio of the minimum variance (under multivariable minimum variance control) and the actual variance in the  $i^{\text{th}}$  output. The performance measure is therefore a comparison between the variance of each single output and that of the corresponding minimum variance output achieved under **multivariable minimum variance control**. Thus, one can simultaneously obtain the single output performance index from the diagonal elements of the matrix  $ZZ^T$ , when we calculate the overall multivariable performance index  $\eta(d)$ . Furthermore, if we take the process offset into account, the modified performance index can be written as

$$\eta'(d) = \text{tr}(\Sigma_{mv} \tilde{\Sigma}_{mse}^{-1})/n \quad (6.16)$$

where  $\tilde{\Sigma}_{mse}$  is the diagonal matrix of  $\Sigma_{mse}$ , and  $\Sigma_{mse} = \Sigma_Y + \delta\delta^T$  is the mean square error. The expression for  $\eta'(d)$  can also be simplified by following the analogous procedure for  $\eta(d)$  that results in expression (6.15) from equation (6.14).

Although  $a_t$  is unknown, it can be replaced by the estimated white noise  $\hat{a}_t$  as introduced in the next section. The FCOR approach provides a relatively easy way to calculate the performance measure of a multivariable process with a simple interactor matrix. However, the algorithm is not limited to the simple interactor matrix process. In the following chapters it will be shown that, via interactor filtering of the outputs, multivariable processes with diagonal or triangular interactor matrices can eventually be transferred to the simple interactor matrix form for the sake of minimum variance control and performance assessment.

### 6.3.2 Filtering or whitening

The original source of variation in a regulatory closed-loop process may be traced back to a white noise excitation,  $a_t$ , as shown in Figure 6.1. The relationship between  $Y_t$  and  $a_t$  is established by the closed-loop transfer function  $G_{Y_a} = (I + TQ)^{-1}N$ . Thus the variation of  $Y_t$  is due to the excitation of  $a_t$  through  $G_{Y_a}$ . The estimation of this noise sequence is important for performance assessment. By reversing the process, the white noise sequence can be viewed as an output from a filter whose input is the process output  $Y_t$ . Many methods have been developed to fit the filter model and obtain estimates of the white noise sequence from output data, and in some literature the estimation of  $a_t$  is known as “whitening” or “prewhitening” (Box and MacGregor, 1974; Soderstrom and Stoica, 1989; Goodwin and Sin, 1984). Such a whitened noise sequence can also be denoted as the “innovation sequence” (Goodwin and Sin, 1984). The process of obtaining such a “whitening” filter is analogous to time-series modeling, where the final test of the adequacy of the model consists of checking if the residuals are “white”; these residuals are the estimated white noise sequence. In contrast to time-series modeling where the estimation of the model is of interest, the residual or the innovation sequence is the main item of interest in this “whitening” process. Depending on data, an AR or ARMA (alternatively a Kalman Filter based innovation model in state space representation) can be used for estimating  $a_t$ . The identification of these MIMO innovation models (i.e., “whitening” filters) has attracted some interest (Reinsel, 1993; Aoki, 1987). Many efficient algorithms have been developed such as *arz*, *armaz*, etc. in Matlab (The Math Works, Inc.).

## 6.4 Simulation

**Example 7** *This example illustrates the performance assessment of a multivariable process with a simple interactor matrix.*

Consider a multivariable process:  $Y_t = TU_t + Na_t$ , where

$$T = q^{-2} \begin{bmatrix} \frac{1}{1-0.4q^{-1}} & \frac{2}{1-0.5q^{-1}} \\ \frac{1}{1-0.1q^{-1}} & \frac{1}{1-0.2q^{-1}} \end{bmatrix}$$



$$N = \begin{bmatrix} \frac{2}{1-0.9q^{-1}} & \frac{1}{1-0.3q^{-1}} \\ \frac{1}{1-0.4q^{-1}} & \frac{2}{1-0.5q^{-1}} \end{bmatrix}$$

Because

$$\lim_{q^{-1} \rightarrow 0} q^2 T = \begin{bmatrix} 1 & 2 \\ 1 & 1 \end{bmatrix}$$

is of full rank, we conclude that  $d = 2$ . Using equation (6.4),  $N$  is separated to

$$\begin{aligned} N &= \begin{bmatrix} 2 + 1.8q^{-1} & 1 + 0.3q^{-1} \\ 1 + 0.4q^{-1} & 2 + q^{-1} \end{bmatrix} + \begin{bmatrix} \frac{1.62q^{-2}}{1-0.9q^{-1}} & \frac{0.09q^{-2}}{1-0.3q^{-1}} \\ \frac{0.16q^{-2}}{1-0.4q^{-1}} & \frac{0.5q^{-2}}{1-0.5q^{-1}} \end{bmatrix} \\ &\triangleq F + q^{-2}R \end{aligned} \quad (6.17)$$

Under minimum variance control, the process output is written as  $e_t = Fa_t$ , and this part of the output is invariant under feedback control and can be used as a benchmark to access controller performance of this process.

For the sake of illustration, consider a simple proportional control of the form

$$U_t = -QY_t = - \begin{bmatrix} K & 0 \\ 0 & K \end{bmatrix} Y_t$$

Applying the FCOR algorithm to the output vector  $Y_t$  yields the results shown in Figure 6.2. The solid line and the dashed line denote the theoretical value of the performance indices with and without considering the offset respectively, while the asterisk and circle denote the corresponding estimated performance indices. The abscissa in this graph corresponds to the value of the proportional gain. It can be seen that for this form of proportional, diagonal control, if the offset is not considered in the performance measure, the maximum performance measure is 0.7 when the proportional gain  $K$  takes the value of 0.1. The performance measure under open-loop condition (when  $K = 0$ ) appears to be acceptable compared to the maximum performance measure (0.7). If the offset of a process output is also considered in the measure of performance, a deteriorated performance would be expected. As shown by the dashed line (the setpoint is taken as  $Y_t^{sp} = [3, 3]^T$  in the simulation), the overall performance index is now lower than the performance measure without considering the offset. The open loop process ( $K = 0$ ) no

longer demonstrates good performance. The best performance is obtained when  $K = 0.2$  instead of  $K = 0.1$ . Increasing the proportional gain decreases the offset and therefore improves the performance when the offset dominates the output. This is the reason that the best performance shifts toward the right from  $K = 0.1$  to  $K = 0.2$ . However, with gain greater than 0.2, the process becomes more oscillatory and eventually becomes unstable. When the variation caused by the oscillation dominates the output, the performance goes down rapidly. The offset no longer dominates the performance measure and the measure now approaches the same performance as that without considering the offset.

## 6.5 Conclusions

The multivariable performance measure has been defined, and the computationally simple algorithm (the FCOR algorithm) to estimate multivariate performance indices has been established in this chapter. The results can be applied to multivariable processes with simple interactor matrices and provide a basis for the following chapters. The application of the proposed algorithm has been demonstrated by a simulated example.

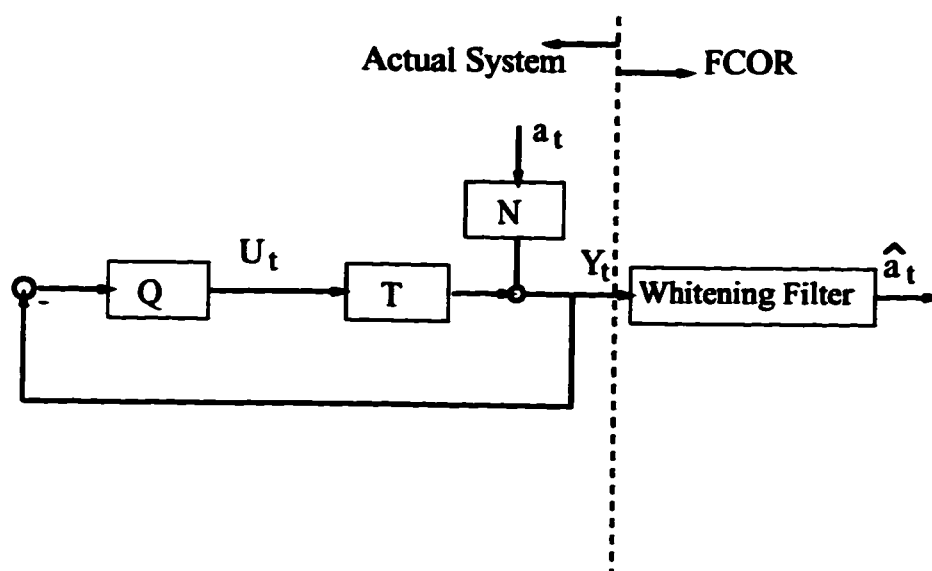


Figure 6.1: Schematic diagram of white noise or innovation sequence estimation

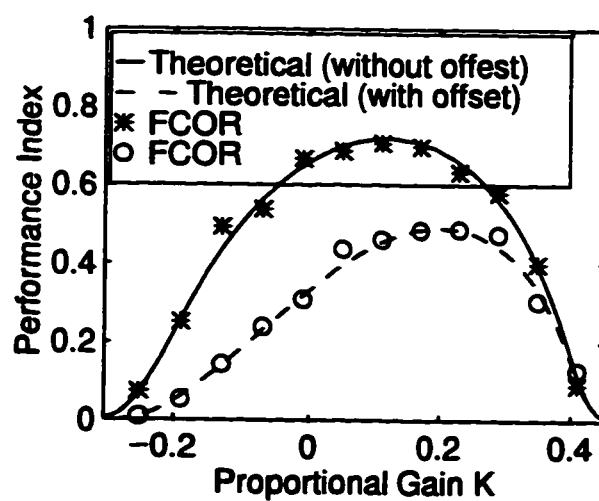


Figure 6.2: Simple interactor matrix MIMO performance assessment. Each asterisk represents an estimation based on 1000 data points using the FCOR algorithm.

## Chapter 7

# Feedback Controller Performance Assessment: Diagonal Interactor

### 7.1 Introduction

Although minimum variance control is not practically desirable due to its poor robustness and/or excessive control effort requirement, it does provide an absolute lower bound on the process variance. This lower bound naturally serves as a useful benchmark to evaluate current control loop performance if reduction of process variation is the control objective. Such a control loop performance measure provides guidelines and useful information for control engineers when they design, tune or upgrade controllers or control strategies. If the best performance cannot satisfy the requirement, alternative control strategies such as implementing feedforward control and/or reducing dead time may be necessary. For a number of industrial processes (particularly pulp/paper processes), reduction of process variation is the main objective in controller design. Performance assessment with minimum variance control as the benchmark is therefore particularly useful for such processes. In fact, the first application of the performance assessment technique was on a paper machine (Astrom, 1967). However, most industrial processes

---

<sup>1</sup>A version of this chapter is to appear in the Canadian Journal of Chemical Engineering, February, 1997.

are inherently multivariate in nature. Performance assessment with multivariate minimum variance control as the benchmark is therefore more desirable. This chapter is an extension of Chapter 6 considering closed-loop performance assessment of multivariate processes with the diagonal interactor matrix.

In this chapter, feedback invariance of multivariable processes with diagonal interactor matrix is discussed in Section 7.2, followed by a brief extension of the FCOR algorithm in Section 7.3. The chapter also considers a detailed evaluation of an industrial headbox control system using routine operating data in Sections 7.4 and 7.5.

## 7.2 Feedback controller-invariance of minimum variance term and its separation from routine operating data

Chapter 2 has shown that the measure of minimum variance control performance of SISO processes can be estimated from routine operating data. The key to this property is that the minimum variance term is feedback control invariant. This idea has been extended to MIMO processes with the simple interactor matrix in Chapter 6.

For MIMO processes with a general interactor matrix (neither simple nor diagonal), the feedback invariance property of minimum variance control (minimizing  $J = E(Y_t - Y_t^{sp})^T(Y_t - Y_t^{sp})$  or  $J = E(Y_t - Y_t^{sp})^T W(Y_t - Y_t^{sp})$ ) can also be solved by using the unitary or weighted unitary interactor matrix as will be discussed in Chapter 8. Just as *a priori* knowledge of the time delay is required for SISO applications, performance assessment of MIMO processes with general interactor matrices requires that the interactor matrix must be known from *a priori* knowledge. This is tantamount to knowing the entire transfer function matrix (Goodwin and Sin, 1984) or at least the first few Markov parameters or impulse response coefficients of the transfer function matrix as discussed in Chapter 5.

However, some well-designed multivariable processes have the structure of the diagonal interactor. Like the SISO case, the diagonal interactor matrix only depends on the pure time delays of the transfer function and is easier to obtain from *a priori* knowledge of processes. This diagonal structure is therefore elaborated in the present chapter. The

treatment of the general interactor matrix is discussed in Chapter 8.

In Chapter 6, we have shown that for the process with a simple interactor matrix:

$$Y_t = q^{-d}\tilde{T}U_t + Na_t \quad (7.1)$$

where  $d$  is the time delay and  $\tilde{T}$  is the delay-free transfer function matrix, the following inequality holds:

$$\text{Var}(Y_t) \geq E(e_t)(e_t)^T = \text{Var}(Fa_t)$$

where  $e_t = Fa_t$ ,  $F$  is defined by the identity:

$$N = \underbrace{F_0 + F_1q^{-1} + \dots + F_{d-1}q^{-(d-1)}}_F + q^{-d}R$$

$F_i$  (for  $i = 0, \dots, d-1$ ) are also constant coefficient matrices, and  $R$  is a proper rational transfer function matrix. If closed-loop, routine operating data under feedback control is modelled by a multivariate moving-average process:

$$Y_t - E(Y_t) = \underbrace{F_0a_t + F_1a_{t-1} + \dots + F_{d-1}a_{t-d+1}}_{e_t} + \underbrace{L_0a_{t-d} + L_1a_{t-d-1} + \dots}_{w_{t-d}} \quad (7.2)$$

where  $L_i$  (for  $i = 0, 1, \dots$ ) are constant coefficient matrices, then the term  $w_{t-d}$  is feedback control dependent, and the term  $e_t$  consisting of the first  $d$  terms of the moving-average model is independent of feedback control. Under minimum variance control,  $w_{t-d}$  vanishes, and therefore  $e_t$  represents the process under minimum variance control and can be estimated from routine operating data.

Now consider a process with a diagonal interactor matrix,  $D = \text{diag}(q^{d_1}, q^{d_2}, \dots, q^{d_n})$ :

$$Y_t = TU_t + Na_t = D^{-1}\tilde{T}U_t + Na_t \quad (7.3)$$

Multiplying both sides of equation (7.3) by  $q^{-d}D$ , where  $d = \max(d_1, \dots, d_n)$ , yields

$$\begin{aligned} q^{-d}DY_t &= q^{-d}\tilde{T}U_t + q^{-d}DNa_t \\ &= q^{-d}\tilde{T}U_t + \tilde{N}a_t \end{aligned} \quad (7.4)$$

where  $\tilde{N}$  is a proper transfer function matrix between the disturbance  $a_t$  and the interactor-filtered output  $q^{-d}DY_t$ . By defining  $\tilde{Y}_t = q^{-d}DY_t$ , equation (7.4) has been transferred to

the same form as equation (7.1), i.e.,

$$\tilde{Y}_t = q^{-d}\tilde{T}U_t + \tilde{N}a_t \quad (7.5)$$

This is a process with a simple interactor matrix. It follows that

$$\text{Var}(\tilde{Y}_t) \geq E(\tilde{e}_t)(\tilde{e}_t)^T = \text{Var}(\tilde{F}a_t)$$

where  $\tilde{e}_t = \tilde{F}a_t$ , and  $\tilde{F}$  is defined by the identity:

$$\tilde{N} = \underbrace{\tilde{F}_0 + \tilde{F}_1 q^{-1} + \dots + \tilde{F}_{d-1} q^{-(d-1)}}_{\tilde{F}} + q^{-d} \tilde{R}$$

Thus if the interactor-filtered, routine operating data under feedback closed-loop control is modelled by a multivariate moving-average process:

$$\tilde{Y}_t - E(\tilde{Y}_t) = \underbrace{\tilde{F}_0 a_t + \tilde{F}_1 a_{t-1} + \dots + \tilde{F}_{d-1} a_{t-d+1}}_{\tilde{e}_t} + \underbrace{\tilde{L}_0 a_{t-d} + \tilde{L}_1 a_{t-d-1} + \dots}_{\tilde{w}_{t-d}} \quad (7.6)$$

then the minimum variance term  $\tilde{e}_t$  is independent of feedback control and can therefore be estimated from routine operating data.

Although the feedback invariance term  $\tilde{e}_t$  represents the minimum variance term of the interactor-filtered variable  $\tilde{Y}_t$ , it also represents the minimum variance term of the original variable  $Y_t$ . Dugard et al.(1984) have shown that for the case of the diagonal interactor matrix, the control law which minimizes variance of the interactor-filtered variable  $\tilde{Y}_t$  also minimizes variance of each element of the original variable  $Y_t$  (i.e.,  $y_i(t)$ , for  $i = 1, \dots, n$ ). Thus the diagonal elements of  $\text{Var}(\tilde{e}_t)$  also provide absolute lower bounds of variance for each original output under multivariable feedback control. Furthermore note that  $\tilde{y}_i = q^{-d+d_i} y_i$ , and therefore

$$\begin{aligned} \text{Var}(y_1(t)) &= \text{Var}(\tilde{y}_1(t)) \\ &\vdots \\ \text{Var}(y_n(t)) &= \text{Var}(\tilde{y}_n(t)) \end{aligned}$$

i.e., the diagonal elements of variance (covariance) matrix of the original variable  $Y_t$  are the same as that of the interactor-filtered variable  $\tilde{Y}_t$ . As shown in Chapter 6, the diagonal

elements of the variance (covariance) matrix are the variance of each output and are the terms required in performance assessment. Thus performance assessment of the original variable  $Y_t$  is equivalent to performance assessment of the interactor-filtered variable  $\tilde{Y}_t$ .

One natural question that arises is: how does one do performance evaluation of processes that have non-minimum phase zeros? Desborough and Harris (1992) and Huang et al. (1996b) have pointed out that this does not affect its application. Performance assessment simply provides an absolute lower bound of process variance, although the lower bound may or may not be practically realizable or admissible depending on the zero location of the process. This information of the absolute lower bound is particularly useful for the design, tuning, monitoring and upgrading of control loops. For loops which indicate high performance measures, further tuning of controllers is neither necessary nor useful. For loops which indicate poor performance measures, further analysis such as process identification and/or re-design of the control algorithm may be necessary. Existence of non-minimum phase zeros implies that the actual or achievable lower bound is larger than the absolute lower bound. Consequently the performance measure underestimates the actual or achievable performance. Take the performance measure of a SISO process as an example. This performance measure or index is defined as  $\eta(d) = \sigma_{mv}^2 / \sigma_y^2$ , where  $\sigma_{mv}^2$  is the absolute lower bound of process variance, and  $\sigma_y^2$  is the variance of the process output. If a process has non-minimum phase zeros, then its achievable minimum variance is  $\tilde{\sigma}_{mv}^2$  with  $\tilde{\sigma}_{mv}^2 > \sigma_{mv}^2$ . Consequently

$$\eta(d) = \sigma_{mv}^2 / \sigma_y^2 < \tilde{\sigma}_{mv}^2 / \sigma_y^2 = \eta'(d)$$

where  $\eta'(d)$  is the achievable performance measure. Therefore the performance measure  $\eta(d)$  underestimates the achievable performance  $\eta'(d)$ . However, this does not affect its application. For example, if a process has an acceptable performance measure (e.g.  $\eta(d) > 0.5$ ), design considerations due to the existence of non-minimum phase zeros should in fact bolster its acceptability since its achievable performance measure is likely to be even higher than its absolute performance measure (i.e.  $\eta'(d) > \eta(d) > 0.5$ ). On the other hand, if a process has an unacceptable performance measure, it falls into the category of processes which may require further analysis, e.g. identification or controller re-design. Therefore



existence of non-minimum phase zeros does not matter since these non-minimum phase zeros can be detected via identification and the achievable performance measure  $\eta'(d)$  can be subsequently obtained anyway. Once again, it must be emphasized that the techniques proposed in this chapter and other literature, e.g. Harris(1989), only require routine operating data and *a priori* knowledge of time delays.

### 7.3 Performance measures

#### 7.3.1 The FCOR algorithm

The multivariable performance index is defined in Chapter 6 as:

$$\eta(d) \triangleq \text{tr}(\Sigma_{mv} \tilde{\Sigma}_Y^{-1})/n \quad (7.7)$$

and performance indices of individual outputs or the individual performance indices are defined as:

$$[\eta_{y_1}, \dots, \eta_{y_n}]^T \triangleq \text{diag}(\Sigma_{mv} \tilde{\Sigma}_Y^{-1}) \quad (7.8)$$

where  $\tilde{\Sigma}_Y = \text{diag}(\Sigma_Y)$ ,  $\Sigma_Y = \text{Var}(Y_t)$ , and  $\Sigma_{mv}$  is the lower bound of  $\Sigma_Y$ . These indices indicate the comparison of variance between the diagonal elements of the actual variance matrix and the corresponding diagonal elements of the minimum variance matrix.

For the process with a diagonal interactor matrix, these performance indices are equivalent to performance indices of the interactor-filtered variable. Therefore performance assessment of the original variable can be obtained from performance assessment of the interactor-filtered variable, i.e.,

$$\eta(d) = \text{tr}(\Sigma_{\tilde{m}v} \tilde{\Sigma}_{\tilde{Y}}^{-1})/n \quad (7.9)$$

and

$$[\eta_{y_1}, \dots, \eta_{y_n}]^T = \text{diag}(\Sigma_{\tilde{m}v} \tilde{\Sigma}_{\tilde{Y}}^{-1}) \quad (7.10)$$

where  $\tilde{\Sigma}_{\tilde{Y}} = \text{diag}(\Sigma_{\tilde{Y}})$ ,  $\Sigma_{\tilde{Y}} = \text{Var}(\tilde{Y}_t)$ , and  $\Sigma_{\tilde{m}v}$  is the lower bound of  $\Sigma_{\tilde{Y}}$ .

Chapter 6 has shown that multivariate correlation analysis yields a computationally simple procedure for calculating these performance indices as follows.

Define a scaled cross correlation as

$$\bar{\rho}_{\tilde{Y}_a}(i) \triangleq \rho_{\tilde{Y}_a}(i) \rho_a^{-1/2}$$

and a block matrix as

$$Z \triangleq [\bar{\rho}_{\tilde{Y}_a}(0), \bar{\rho}_{\tilde{Y}_a}(1), \dots, \bar{\rho}_{\tilde{Y}_a}(d-1)]$$

where  $\rho_{\tilde{Y}_a}(i) = \tilde{\Sigma}_{\tilde{Y}}^{-1/2} \Sigma_{\tilde{Y}_a}(i) \tilde{\Sigma}_a^{-1/2}$  is the multivariate cross correlation between  $\tilde{Y}_t$  and  $a_{t-i}$  (note  $\tilde{\Sigma}_a = \text{diag}(\Sigma_a)$  and  $\tilde{\Sigma}_{\tilde{Y}} = \text{diag}(\Sigma_{\tilde{Y}})$ ); and  $\rho_a = \tilde{\Sigma}_a^{-1/2} \Sigma_a \tilde{\Sigma}_a^{-1/2}$  is the multivariate autocorrelation of  $a_t$ . Then

$$\eta(d) = \text{tr}(ZZ^T)/n \quad (7.11)$$

and

$$[\eta_{y_1}, \dots, \eta_{y_n}]^T = \text{diag}\{ZZ^T\} \quad (7.12)$$

where  $\eta(d)$  is in fact the average of the individual performance indices. Although  $a_t$  is unknown, it can be replaced by the estimated white noise  $\hat{a}_t$  from a filtering process as shown in Chapter 6. This filtering procedure is equivalent to fitting  $Y_t$  by a multivariate time series (ARI or ARIMA). The residual after fitting is the “whitened” noise  $\hat{a}_t$ . This procedure based on Filtering and CORrelation analysis is labelled as the FCOR algorithm. Thus the FCOR approach provides a relatively easy way to calculate the performance measure of a multivariable process with a diagonal interactor matrix, which avoids solving the multivariate Diophantine identity. However, the algorithm is not limited to processes with the diagonal interactor matrix. It will be extended to processes with the general interactor matrix in Chapter 8.

### 7.3.2 The effect of sampling intervals

To apply the FCOR algorithm, a representative set of routine operating data should be sampled. Theoretically, the data sampling frequency is assumed to be the same as the controller sampling frequency. However, this sampling frequency may not be always desirable in practice due to the following reasons: 1) the quality measure of many industrial process is based on the outputs sampled at other frequencies which can be higher or lower than the controller sampling frequency, and a different sampling frequency of a stochastic

signal may result in a different measure of the variance (MacGregor, 1976); 2) controller sampling rate can be very fast or even continuous on some control loops such as PID loops, and minimum variance control using such fast controller sampling frequency usually requires an excessive control action and gives an unrealistic benchmark performance; 3) different control loops may have different controller sampling frequencies, i.e. no unique sampling frequency may be available for multivariate performance assessment; and 4) many available industrial data are sampled typically at a lower frequency than the controller sampling frequency. In such cases, one has to use a data sampling frequency which is different from the controller sampling frequency. Since the feedback-invariance property holds for any causal linear feedback controller within the time-delay period, the FCOR algorithm is generally valid for any sampling frequency as well. It calculates a performance index relative to a minimum variance controller whose control sampling frequency is the same as the data sampling frequency. However, a controller sampling frequency different from the data sampling frequency means that actual performance assessment should consider the different effect of an extra time delay in addition to the actual physical delay in the process. This additional time delay corresponds to the presence of a zero-order-hold device. To illustrate the point, we assume that the process time delay is  $t_d$ , the control interval of the existing controller is  $t_c$ , and the data sampling interval or the control interval of the assumed benchmark (minimum variance) control is  $t_s$ . Then the actual time-delay in the process is  $t_d + t_c$ , and the time-delay for the assumed benchmark (minimum variance) control is  $t_d + t_s$ . In order to separate the minimum variance portion from routine operating data, feedback-invariance property must hold within the time-delay period from 0 to  $t_d + t_s$  in the existing control loops. Since feedback-invariance does hold within the actual time-delay period from 0 to  $t_d + t_c$ , the FCOR algorithm estimates a theoretically exact result if  $t_d + t_s \leq t_d + t_c$ , i.e. if the data sampling frequency is higher than the controller sampling frequency. However, if  $t_d + t_s > t_d + t_c$ , i.e. the data sampling frequency is lower than the controller sampling frequency, then the feedback-invariance property holds within the actual time-delay period from 0 to  $t_d + t_c$ , but does not hold from  $t_d + t_c$  to  $t_d + t_s$ . Therefore  $t_d + t_c$  (instead of  $t_d + t_s$ ) is recommended as the approximate time-delay in the calculation of the performance index when the data sampling frequency

is lower than the controller sampling frequency. This underestimates the time-delay by the portion  $t_s - t_c$  and consequently may underestimate the performance index. However, as illustrated in the last section, slight underestimation of the performance index does not affect its application.

## 7.4 Application to a headbox control system

The headbox is the soul of the entire pulp/paper machine (Newcombe, 1991). Its purpose is to transform a pipe flow of pulp stock into a homogeneous, uniform flow across the width of a machine wire running at high speed. Weyerhaeuser's Grande Prairie NSK pulp mill utilizes a Fourdrinier machine commissioned in the early 1970's. The process description, control objectives and problem description are discussed in the following.

### 7.4.1 Process description

The headbox is a unit operation within the pulp/paper-making process which takes stock (pulp and water mixture) flowing in a pipe and transforms it into a uniform, rectangular flow equal in width to the machine wire and at a uniform velocity in the machine direction. Good headbox operation results in uniform basis weight, little or no flocculation, and excellent retention on the wire. The schematic of the Fourdrinier machine employed by the mill at Grande Prairie is shown in Figure 7.1. The pressure/vacuum-air-pad headbox is used to produce a sheet of approximately 149.7 kg/278.7 m<sup>2</sup> (330 lb/3000 ft<sup>2</sup>). White water mixed with thick stock is delivered to the bottom of the headbox by a high-speed fan pump. A rotating rectifier near the slice lip keeps the pulp evenly distributed across the machine. A vacuum pump is used to reduce the air pad pressure below atmospheric.

### 7.4.2 Process control

The primary control objective in headbox control is to obtain a uniform basis weight, moisture, and caliper on the sheet. These properties are important for both the operability

of the machine and the pulp's final quality. In keeping with common practice (Nordstrom and Norman, 1994), sheet formation is maintained by continuous jet/wire ratio, headbox consistency and pond level control. The plant experiences poor operability when these control parameters deviate from their optimum values. Headbox consistency is controlled through thick stock (basis mass) valve adjustments, although slice opening will impact consistency as well (Rice, 1972). Pond level is controlled by changing the fan pump speed. The jet/wire ratio is a function of total head and wire speed. The total head at the slice lip is indirectly controlled by adjusting the air pad pressure which is directly controlled by adjusting the air flow valve on the high pressure side of the air re-circulation pump. Wire speed (in conjunction with the basis mass valve) is manually adjusted by the operator to control production rate.

### **7.4.3 Problem description**

Unlike consistency control, which has been trouble-free over the years, jet/wire and pond level control have been the source of many operational problems. These problems stem from the pressure and level loops complexity in dynamics, a high degree of coupling between the two loops, significant noise in the measured values; and the dependence of the loops on external variables that change with time such as production rate or grade changes.

Man-power limitation is also a major cause of poorly tuned control loops. For instance, the duties of control engineers usually include maintenance of the control system, maintenance of existing computer applications, development of new control applications, and other day-to-day "fire-fighting" assignments. Therefore, the largest problem in achieving or maintaining "healthy" control loops is the time-consuming testing required to analyze and monitor each individual control loop. From a time allocation perspective, manual loop analysis results usually fall into one of three categories: 1) A preponderance of tests achieves very good performance for hundreds of control loops, but occupies most of the control engineer's time. 2) A large number of negative results indicates that testing is insufficient, but no control engineer is available to mitigate the problems. 3) A series

of time-consuming and labour-intensive tests shows very good tuning results, but process drifts or changes quickly nullify the results and re-tuning is required all over again. Because of other time commitments, insufficient testing is the norm and, as a result, costly sheet breaks are often the first indication of poor control performance.

The objective of this research into loop performance is to provide the plant control engineers with an on-line measure of control loop performance obviating the time-consuming manual test. This measure can be monitored on a regular basis and performance statistics used to schedule loop re-tuning. The result of a proactive re-tuning schedule that requires less control engineer and technician effort will maintain better overall loop performance and reduce plant downtime.

## **7.5 Performance assessment of the headbox control system**

### **7.5.1 Single loop performance assessment**

The schematic diagram of the current control system is shown in figure 7.2. The present control strategy is to regulate the total head (pressure plus level) by adjusting the air pad pressure and the pond level via multiloop PID controllers. To assess control performance, we first applied the SISO loop performance assessment technique to individual loops, which may answer the following questions: 1) If the current level loop cannot be further tuned due to some constraints, is it possible to further reduce variation of the total head by adjusting the pressure loop controller? 2) If the pressure loop is well tuned and cannot be adjusted, is it possible to further reduce variation of the level by adjusting the level loop controller?

Feedback control performance assessment of SISO processes has been discussed by Harris (1989), and Desborough and Harris (1992) . The FCOR algorithm can also be directly applied to SISO processes. However, the setpoint of the pressure loop is randomly adjusted in this application, which requires a special treatment.

The process of the pressure loop can be written in a standard form as

$$p_t = q^{-d} T u_t + N a_t$$

where  $T$  and  $N$  are (SISO) rational transfer functions. Under feedback control  $u_t = -Q(p_t - p_t^{sp})$ ,

$$p_t = -q^{-d} T Q (p_t - p_t^{sp}) + N a_t$$

This is equivalent to

$$p_t - p_t^{sp} = -q^{-d} T Q (p_t - p_t^{sp}) - p_t^{sp} + N a_t$$

The random adjusted setpoint can be modelled by  $p_t^{sp} = M b_t$ , where  $M$  is a rational transfer function and  $b_t$  is white noise. By defining  $\epsilon_t = p_t - p_t^{sp}$ , we have

$$\epsilon_t = -q^{-d} T Q \epsilon_t - M b_t + N a_t$$

The last two terms on the right hand side of the equation may be lumped as  $\theta \nu_t$  via, e.g. the spectral factorization, where  $\theta$  is a rational transfer function and  $\nu_t$  is white noise. Therefore

$$\epsilon_t = -q^{-d} T Q \epsilon_t + \theta \nu_t \quad (7.13)$$

Equation (7.13) is a standard form as used in performance assessment of SISO processes with a zero setpoint. Thus the algorithm in Chapter 2 can be applied to assess performance of the variable  $\epsilon_t$  without restriction. The only question is whether it is appropriate to replace  $p_t$  with  $\epsilon_t$  as the monitored variable.

The rush/drag ratio is defined by

$$K_t \triangleq \frac{\sqrt{P_t + H_t}}{c V_t}$$

where  $K_t$  is the rush/drag ratio,  $V_t$  is the wire speed,  $P_t$  is the pressure,  $H_t$  is the level and  $c$  is a unit conversion coefficient. Here we use the notation that  $P_t$  and  $H_t$  are the original variables (actual measurements) of the pressure and the level respectively, while  $p_t$  and  $h_t$  are their deviation variables.

Ideally, the rush/drag ratio should be kept constant so that the fibre suspension can be distributed uniformly on the wire. In practice, the operator always monitors the rush/drag ratio which is an indication of how well the total head is being controlled.

It follows from Figure 7.2 that

$$P_t^{sp} = (cK^{sp}V_t)^2 - H_t \quad (7.14)$$

The setpoint of rush/drag ratio  $K^{sp}$  is set by the operator and is a constant.  $V_t$  is kept constant by the motor driving the wire. Using deviation variables, equation (7.14) can be written as

$$p_t^{sp} = -h_t$$

Thus

$$\epsilon_t = p_t - p_t^{sp} = p_t + h_t$$

which is a variable representing the total head variation and is indicative of the rush/drag ratio variation. This is indeed the most important variable for the operator to monitor continually.

Presently, the performance measure of the headbox by the operating personnel is the variance of pressure and level data being sampled with the sampling interval 15 seconds. The same sampling interval is therefore used for performance assessment here. It is known from previous step tests that both the pressure and level loops have time delays of approximately 3 sampling intervals each. Figure 7.3 shows a typical set of data which was collected over 50 hours at a 15 seconds sampling interval. Note that both the level and the pressure are measured by using the pressure unit, Pa. The process was under multiloop PID control with a control interval of 1 second. Applying the FCOR algorithm to variables  $\epsilon_t$  and  $h_t$  respectively yields results shown in Figure 7.4, where each performance index is calculated from 1000 data points, i.e. 4.2 hours for calculation of each performance index.

By definition, the performance index should be in-between '0' and '1'. While '1' means the best performance, '0' means the worst performance including unstable control. For example, a performance index of 0.5 implies that current variance can be reduced (potentially) by a factor of 0.5 if an optimal tuning is implemented. Depending on the application, the loop performance measure can be classified as optimal/good/bad or acceptable/unacceptable or others. Single loop performance assessment results shown in Figure 7.4 clearly indicate an 'optimal' performance of current single loop tunings



of both loops. Note that the benchmark performance is minimum variance control of the individual loop. Therefore there is little potential for further reduction in process variance by adjusting or re-designing the controller individually. It should be noted that the performance index is cycling periodically due to differences between day-and-night ambient conditions. Although the headbox process is housed inside a building, ambient conditions do affect the pulp quality before it enters the headbox.

### 7.5.2 Multivariate performance assessment

SISO performance assessment can only indicate the potential of performance improvement by adjusting individual loops. Since the level and the pressure loops are coupled, a multivariate control strategy can further reduce process variations. Multivariate performance assessment can provide the measure of such potential.

Previous tests provided the following *a priori* knowledge of the process: 1) the time delay from a change of the air flow control valve to both the pressure and level responses is approximately 3 sampling intervals; 2) the time delay from the fan pump speed change to the level response is approximately 3 sampling intervals, and the time delay from the fan pump speed change to the pressure response is approximately 2 sampling intervals. It follows from Tsiligiannis and Svoronos (1988) that this process has a diagonal interactor matrix, i.e., by examining each row of the transfer function matrix, it can be shown that each output can be paired to an input with the minimum delay in that row. For detailed discussion of the occurrence of diagonal interactor matrix in practice, readers are referred to Appendix B.

Since the pressure loop has a randomly adjusted setpoint and the variable of interest of this assessment is the total head ( $p + h$ ), the problem should be reformulated as it was done in the SISO case. The multivariable model with the outputs  $p_t$  and  $h_t$  can be written as

$$p_t = T_{11}u_1 + T_{12}u_2 + N_{11}a_1 + N_{12}a_2 \quad (7.15)$$

$$h_t = T_{21}u_1 + T_{22}u_2 + N_{21}a_1 + N_{22}a_2 \quad (7.16)$$

where  $u_1$  is the manipulated variable of the air flow control valve;  $u_2$  is the manipulated variable of the fan pump speed;  $T_{11}$ ,  $T_{21}$  and  $T_{22}$  are approximately first-order transfer functions, while  $T_{12}$  can be approximated by a second order transfer function;  $N_{ij}$  (for  $i = 1, 2, j = 1, 2$ ) are disturbance transfer functions and can be modelled by autoregressive moving average processes. The pressure,  $p_t$ , is measured by a low range differential pressure transmitter with the low side of the transmitter vented to atmosphere. The level,  $h_t$ , is measured by a flange mounted transmitter. The air flow control valve on the suction of the vacuum pump is a Fisher V100 segmented ball valve. The fan pump speed is controlled by a variable speed DC drive. Multiloop PID controllers are implemented in the process. The pressure loop is controlled by manipulating the air flow control valve, and the level loop is controlled by manipulating the fan pump speed. Note that except for *a priori* knowledge of the time-delays in  $T_{ij}$ , other information about  $T_{ij}$ ,  $N_{ij}$  and controller transfer functions is not required for performance assessment.

It follows from the analysis in the SISO case that (in the deviation variable sense):

$$p_t^{sp} = -h_t \quad (7.17)$$

Substituting equation (7.16) into equation (7.17) yields

$$p_t^{sp} = -T_{21}u_1 - T_{22}u_2 - N_{21}a_1 - N_{22}a_2 \quad (7.18)$$

Subtracting equation (7.18) from equation (7.15) yields

$$p_t - p_t^{sp} = (T_{11} + T_{21})u_1 + (T_{12} + T_{22})u_2 + (N_{11} + N_{21})a_1 + (N_{12} + N_{22})a_2 \quad (7.19)$$

For simplicity, equation (7.19) can be written as

$$\epsilon_t = T'_{11}u_1 + T'_{12}u_2 + N'_{11}a_1 + N'_{12}a_2 \quad (7.20)$$

It follows from equation (7.17) that  $\epsilon_t = p_t - p_t^{sp} = p_t + h_t =$  “total head” which conveniently is the variable of interest that we would like to monitor. More importantly, equation (7.20) represents the pressure equation, which transfers the random setpoint to a constant (zero) setpoint. Therefore equation (7.20) together with (7.16) represents a  $2 \times 2$  multivariable process with constant setpoints for both variables  $\epsilon_t$  and  $h_t$ . In this

case, it can be easily verified that the time delay structure of the multivariable process with process variables  $\epsilon_t$  and  $h_t$  is the same as that of the multivariable process with process variables  $p_t$  and  $h_t$ . Therefore, performance assessment methods as introduced in the foregoing sections can be readily applied and their results are shown in Figure 7.5.

In Figure 7.5, '+' represents the performance index of the total head, and '\*' represents the performance index of the level output. The average performance index of the total head is 0.85 and the average performance index of the level is 0.22. Note that the benchmark is multivariable minimum variance control. Compared to the SISO assessment which yields the performance index of the total head as an almost perfect '1', multivariate assessment does indicate that, if desired, there is a potential to reduce the variation of the total head very slightly by implementing multivariable control. However, the improvement may not be significant to justify implementation of the multivariable control or an interaction compensator in practice. There is clearly a potential to reduce level variation by implementing multivariate control. However, reduction of level variation is not the objective. Therefore in order to reduce the variance of the total head, alternative control strategies such as feedforward control or reduction of the dead time may be necessary if further improvement in performance is desired.

Since the current total head variance is  $260.6 \text{ Pa}^2$  ( $0.0042 [\text{in. H}_2\text{O}]^2$ ) and level variance is  $387 \text{ Pa}^2$  ( $0.0062 [\text{in. H}_2\text{O}]^2$ ), the multivariable performance indices also imply that within the present control framework the total head variance is never less than  $0.85 \times 260.6 = 221.5 \text{ Pa}^2$  ( $0.0036 [\text{in. H}_2\text{O}]^2$ ) and the level variance is never less than  $0.22 \times 387.7 = 85.3 \text{ Pa}^2$  ( $0.0014 [\text{in. H}_2\text{O}]^2$ ).

The assessment results thus indicate that:

1. the overall control performance is subject to periodic changes due to the difference between day and night ambient conditions;
2. within the framework of the single-loop controller tuning, there is little potential to reduce the total-head variance by tuning the pressure controller or reduce the level variance by tuning the level controller;

3. within the current control structure, total-head variance is no less than  $221.5 \text{ Pa}^2$  ( $0.0036 [\text{in. H}_2\text{O}]^2$ ) under any linear (SISO or MIMO) feedback control;
4. the present controllers have been well tuned, and it may be unnecessary to further adjust controller tunings or implement a multivariable control algorithm;
5. since any possible deduction in the total-head variance is no more than 15% by tuning or re-designing the feedback control, it may be necessary to implement feedforward control or reduce dead times or change the current control structure in order to significantly reduce the variance of the total head.

Since the selected data sampling frequency is lower than the controller sampling frequency in this example, as stated in the previous sections, a possible underestimation of the performance indices may be expected. However, any possible underestimation error only implies that the actual performance is even better than the estimated performance or the actual lower bound is larger than the estimated lower bound, and therefore it does not affect any of the above conclusions.

## 7.6 Conclusions

Control-loop performance assessment of multivariate processes with diagonal interactor matrices has been introduced. Both single loop performance and multivariable performance of the headbox control loops have been estimated from actual industrial data. The results have shown that the present controllers have been well tuned, and it is unnecessary to further adjust controller tunings or implement multivariate control under current control structure. In order to further improve control performance, implementation of feedforward control or reduction of dead times or re-design of the control structure may be necessary. These results therefore provide guidelines for control loop tuning and provide an insight for the potential benefits of exploring multivariable control strategy.

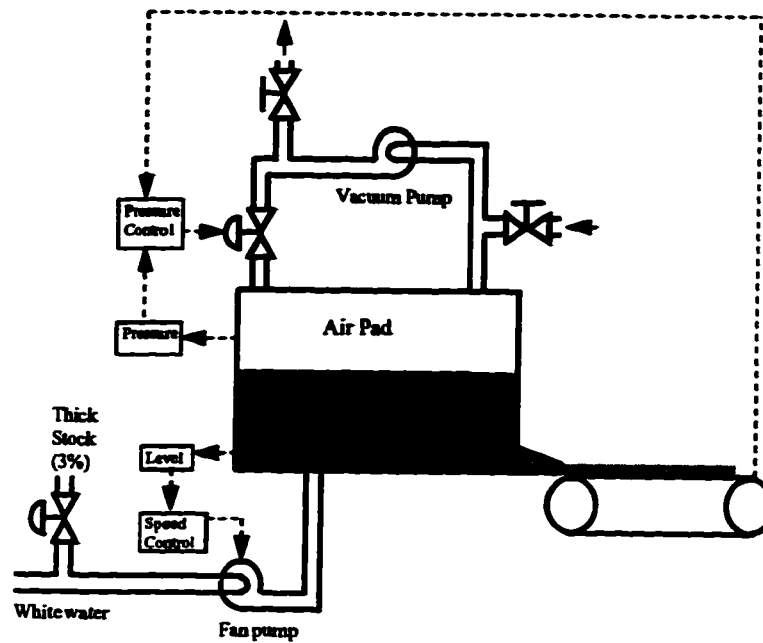


Figure 7.1: Schematic of the headbox

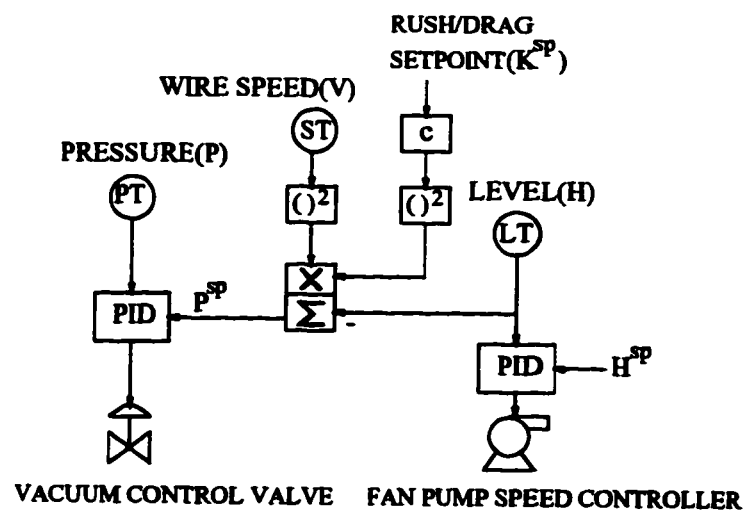


Figure 7.2: Schematic diagram of the control system

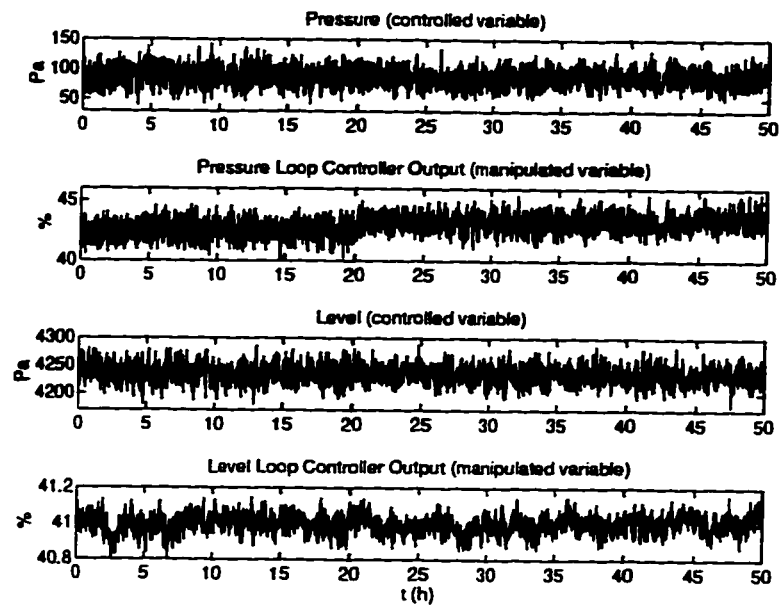


Figure 7.3: *Process data trajectory*

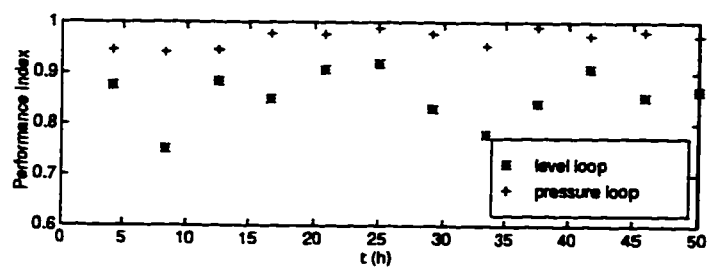


Figure 7.4: *Performance assessment from the single-input and single-output approach.*

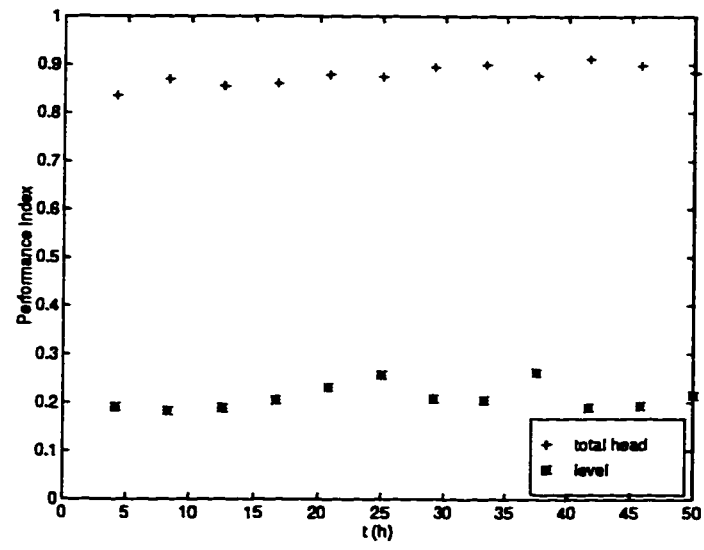


Figure 7.5: *Performance assessment from the multivariate approach.*

## Chapter 8

# Feedback Controller Performance Assessment: General Interactor

### 8.1 Introduction

Factorization of a simple or diagonal interactor matrix only requires *a priori* knowledge of the pure time-delays of each element in a transfer function matrix. Factorization of a general interactor matrix, however, requires a complete knowledge or at least the first few Markov parameter matrices of a MIMO process. The *unitary interactor matrix* as introduced by Peng and Kinnaert(1992) plays an important role in feedback controller performance assessment of processes with general interactor matrices. Estimation of the unitary interactor matrix using closed-loop data from simple closed-loop tests has been discussed in Chapter 5.

The main contribution of this chapter is to obtain the feedback controller-invariant term for MIMO processes with general interactor matrices and proposal of a control loop performance measure that is conceptually simple and computationally efficient. The algorithm is valid for performance assessment of all class of multivariable (square or *non-square*) systems. Although the method introduced in this chapter can be applied to

---

<sup>1</sup>A version of this chapter is to appear in *Automatica* (in press), and a shorter version is also in the Proceedings of the 1996 IFAC World Congress.



simple or diagonal interactor matrices as well, it is not recommended since the algorithms introduced in Chapters 6 and 7 are more efficient in handling these special class of processes.

This chapter is organized as follows. The interactor matrix is first reviewed, and a suitable expression for the MIMO feedback controller-invariant, minimum variance control loop performance measure, is derived, all in section 8.2. The key ingredient of this scheme is filtering and subsequent correlation analysis (FCOR). The FCOR algorithm is used to estimate the achievable multivariate minimum variance performance from routine operating data. Its derivation for the general interactor matrix is considered in section 8.3. The application of the FCOR algorithm to a simulated square and a non-square MIMO process, and an industrial absorption unit is considered in section 8.4, followed by concluding remarks in section 8.5.

## 8.2 Feedback controller-invariance of minimum variance term and its separation from routine operating data

### 8.2.1 Review of the unitary interactor matrix

Consider the MIMO process with a general interactor matrix:

$$Y_t = TU_t + Na_t \quad (8.1)$$

where  $T$  and  $N$  are proper (causal), rational transfer function matrices in the backshift operator  $q^{-1}$ ;  $Y_t$ ,  $U_t$ , and  $a_t$  are output, input and white-noise vectors of appropriate dimensions.

Wolovich and Falb(1976) and Goodwin and Sin(1984) have shown existence of a unique lower triangular form of the general interactor matrix. However, the interactor matrix can also take other forms. It can be a full matrix or an upper triangular matrix (Shah *et al.*, 1987). Rogozinski *et al.*(1987) have introduced an algorithm for the calculation of a *nilpotent interactor matrix*. Peng and Kinnaert(1992) have introduced the *unitary interactor matrix*, which is a special case of the nilpotent interactor matrix. The unitary

interactor matrix has been discussed in Chapter 3. Some important properties of the unitary interactor matrix in minimum variance or singular LQ control have been discussed in Chapter 4.

Existence of the unitary interactor matrix is established in Peng and Kinnaert(1992). The unitary interactor matrix has been shown to be an “ideal” factorization of the time delay matrix for minimum variance or singular LQ type control in Chapter 4. A simple algorithm exists for the calculation of the unitary interactor matrix (Rogozinski *et al.*, 1987; Peng and Kinnaert, 1992) (see also Appendix A). The traditional procedure for factorization of the general interactor matrix does require complete knowledge of the transfer function matrix (Wolovich and Falb, 1976; Goodwin and Sin, 1984; Rogozinski *et al.*, 1987; Peng and Kinnaert, 1992). In Chapter 5, it has been shown that factorization of the interactor matrix can be achieved from the first few Markov parameter or impulse response coefficient matrices of the process. Consequently, estimation of the unitary interactor matrix is simplified and can be estimated by using closed-loop data from simple closed-loop tests. The two special interactor matrices, the *simple* interactor matrix,  $D = q^{-d}I$ , and the *diagonal* interactor matrix,  $D = \text{diag}(q^{-d_1}, \dots, q^{-d_n})$ , are also unitary interactor matrices. Performance assessment for the simple interactor and the diagonal interactor has been discussed in Chapter 6 and Chapter 7 respectively.

### 8.2.2 Feedback controller-invariance of minimum variance term and its separation from routine operating data

Minimum variance control (or the benchmark control) is defined by a feedback control law which minimizes the output LQ objective function without penalty on the control action:

$$J = E(Y_t - Y_t^{sp})^T(Y_t - Y_t^{sp})$$

or the weighted LQ objective function:

$$J = E(Y_t - Y_t^{sp})^T W(Y_t - Y_t^{sp})$$

This is also regarded as *Singular LQ* control (Peng and Kinnaert, 1992). For simplicity in the following proof we shall first assume that the setpoint,  $Y_t^{sp}$ , is zero and the weighting

function  $W = I$ . Then the singular LQ objective function is reduced to

$$J = E[Y_t^T Y_t]$$

The general case is discussed in Remark 5 when the setpoint is not zero, and in Remark 7 when  $W \neq I$ .

Consider the multivariable process

$$Y_t = TU_t + Na_t$$

Using the notation of multivariable minimum variance control due to Goodwin and Sin(1984), the minimum variance control law can be designed to make the variance of the output  $DY_t$  or equivalently  $\tilde{Y}_t = q^{-d}DY_t$  minimum, where the positive integer  $d$  is the maximum order (highest power of  $q$ ) of all the elements of the interactor matrix,  $D$ . The filter,  $q^{-d}D$ , removes infinite zeros from the transfer function matrix. Since  $D$  is a unitary interactor matrix, the singular LQ or minimum variance control laws for  $\tilde{Y}_t$  and  $Y_t$  are the same. This important property of the unitary interactor matrix is discussed in Remark 6. Unlike previous work on the design of multivariable minimum variance control by Goodwin and Sin(1984) and many others in the literature (Tsiligiannis and Svoronos, 1988; Harris and MacGregor, 1987), the main focus of this study is the derivation of a *suitable* expression for the feedback controller-invariant, minimum variance term, from *routine operating data*.

**Theorem 7** *For a multivariable process*

$$Y_t = TU_t + Na_t \tag{8.2}$$

*the minimum variance control is obtained by minimizing*

$$J = E[\tilde{Y}_t^T \tilde{Y}_t] \tag{8.3}$$

*where  $\tilde{Y}_t = q^{-d}DY_t$  is the interactor-filtered output. The performance measure is then given by the following steps:*

1. The quadratic measure of minimum variance is given by

$$E[\tilde{Y}_t^T \tilde{Y}_t]_{\min} = E(e_t^T)(e_t) = \text{tr}(\text{Var}(Fa_t))$$

where  $e_t = Fa_t$ , the polynomial matrix  $F$  depends only on the interactor matrix and the noise model, and satisfies the identity:

$$q^{-d}DN = \underbrace{F_0 + \cdots + F_{d-1}q^{-(d-1)}}_F + q^{-d}R \quad (8.4)$$

where  $R$  is a proper rational transfer function matrix;

2. If one models closed-loop routine operating data under feedback control by the following multivariate moving-average process:

$$\begin{aligned} \tilde{Y}_t - E(\tilde{Y}_t) &= \underbrace{F_0a_t + F_1a_{t-1} + \cdots + F_{d-1}a_{t-d+1}}_{e_t} \\ &\quad + \underbrace{L_0a_{t-d} + L_1a_{t-d-1} + \cdots}_{w_{t-d}} \end{aligned} \quad (8.5)$$

then the minimum variance term,  $e_t = Fa_t$ , consists of the first  $d$  terms of this moving-average model, and therefore can be separated from time series analysis of routine operating data and be used as a benchmark measure of multivariate minimum variance control.

**Proof:** As shown in Chapter 6, for a process with a simple interactor matrix, i.e.  $D = q^{-d}I$ ,

$$Y_t = q^{-d}\tilde{T}U_t + Na_t \quad (8.6)$$

where  $\tilde{T}$  is the delay-free transfer function matrix, the following inequality holds:

$$E[Y_t^T Y_t] \geq E(e_t^T)(e_t) = \text{tr}(\text{Var}(Fa_t))$$

where  $e_t = Fa_t$ , and  $F$  is defined by the identity:

$$N = \underbrace{F_0 + F_1q^{-1} + \cdots + F_{d-1}q^{-(d-1)}}_F + q^{-d}R$$

where  $F_i$ , for  $i = 0, \dots, d-1$ , are constant coefficient matrices, and  $R$  is a proper rational transfer function matrix. The equality holds when the minimum variance control law is implemented on the process.

If routine closed-loop operating data under feedback control is modelled by a multivariate moving-average process:

$$Y_t - E(Y_t) = \underbrace{F_0 a_t + F_1 a_{t-1} + \cdots + F_{d-1} a_{t-d+1}}_{e_t} + \underbrace{L_0 a_{t-d} + L_1 a_{t-d-1} + \cdots}_{w_{t-d}} \quad (8.7)$$

then the term  $w_{t-d}$  is feedback controller-dependent, and the term  $e_t$  consisting of the first  $d$  terms of the moving-average model is independent of feedback control. Under minimum variance control,  $w_{t-d}$  vanishes, and therefore  $e_t$  represents the minimum variance term and can be separated from time series analysis of routine operating data.

Now consider the process with a general *unitary interactor matrix* i.e.  $D \neq q^{-d}I$ :

$$Y_t = TU_t + Na_t = D^{-1}\tilde{T}U_t + Na_t \quad (8.8)$$

Multiplying both sides of (8.8) by  $q^{-d}D$  yields

$$\begin{aligned} q^{-d}DY_t &= q^{-d}\tilde{T}U_t + q^{-d}DNa_t \\ &= q^{-d}\tilde{T}U_t + \tilde{N}a_t \end{aligned} \quad (8.9)$$

where  $\tilde{N}$  is a proper transfer function matrix. By defining  $\tilde{Y}_t = q^{-d}DY_t$ , equation (8.9) is now transformed to the same form as (8.6), i.e.

$$\tilde{Y}_t = q^{-d}\tilde{T}U_t + \tilde{N}a_t \quad (8.10)$$

This is a process with a *simple interactor matrix*. It follows that

$$E[\tilde{Y}_t^T \tilde{Y}_t] \geq E(\tilde{e}_t^T)(\tilde{e}_t) = \text{tr}(\text{Var}(\tilde{F}a_t))$$

where  $\tilde{e}_t = \tilde{F}a_t$ ,  $\tilde{F}$  is defined by the identity:

$$\tilde{N} = q^{-d}DN = \underbrace{\tilde{F}_0 + \tilde{F}_1 q^{-1} + \cdots + \tilde{F}_{d-1} q^{-(d-1)}}_{\tilde{F}} + q^{-d}\tilde{R} \quad (8.11)$$

Thus if the interactor-filtered, routine operating data under feedback control is modelled by a multivariate moving-average process:

$$\tilde{Y}_t - E(\tilde{Y}_t) = \underbrace{\tilde{F}_0 a_t + \tilde{F}_1 a_{t-1} + \cdots + \tilde{F}_{d-1} a_{t-d+1}}_{\tilde{e}_t} + \underbrace{\tilde{L}_0 a_{t-d} + \tilde{L}_1 a_{t-d-1} + \cdots}_{\tilde{w}_{t-d}} \quad (8.12)$$

then the lower bound term  $\tilde{e}_t$  is independent of feedback control and can therefore be estimated from routine operating data. To simplify notation, the tilde signs,  $\sim$ , on the right hand side of equation (8.12) and (8.11) have been dropped in the statement of Theorem 7. ■

**Remark 4** The feedback controller-invariant property of the minimum variance term is valid for both square and non-square transfer function matrices. When the transfer function is of full rank with the row dimension smaller than the column dimension, then the minimum variance is achievable. This is clear from the proof in Chapter 4 and Chapter 6, where the inverse of  $\tilde{T}$ ,  $\tilde{T}^{-1}$ , is replaced by its pseudoinverse,  $\tilde{T}^\dagger$ . On the other hand, when the transfer function matrix is a non-square matrix with the row dimension larger than the column dimension, then the feedback controller-invariant term may not be achievable. Since a unitary interactor matrix can always be factored irrespective of whether the transfer function matrix is a square or non-square matrix (Rogozinski *et al.*, 1987), the methodology for performance assessment as proposed in this chapter is valid for both square and non-square transfer function matrices.

**Remark 5** If the setpoint is not zero, then we define

$$\epsilon_t \triangleq Y_t^{sp} - Y_t$$

The interactor-filtered singular LQ objective is now written as

$$J = E(\tilde{Y}_t - \tilde{Y}_t^{sp})^T (\tilde{Y}_t - \tilde{Y}_t^{sp}) = E[\tilde{\epsilon}_t^T \tilde{\epsilon}_t]$$

where  $\tilde{Y}_t = q^{-d}DY_t$ ,  $\tilde{Y}_t^{sp} = q^{-d}DY_t^{sp}$  and  $\tilde{\epsilon}_t = q^{-d}D\epsilon_t$ . Chapter 11 will show that in this case, instead of using  $\tilde{Y}_t$  for the time series analysis as shown in Theorem 7,  $\tilde{\epsilon}_t$  should be used for the analysis. Then the first  $d$  terms of the moving-average model of  $\tilde{\epsilon}_t$  constitute the feedback controller-invariant minimum variance term.

**Remark 6** It has been shown in Chapter 4 that if  $D$  is a unitary interactor matrix, then the minimum variance control law which minimizes the following objective function of the interactor-filtered variable  $\tilde{Y}_t$ :

$$J_1 = E(\tilde{Y}_t - \tilde{Y}_t^{sp})^T (\tilde{Y}_t - \tilde{Y}_t^{sp}) \quad (8.13)$$

also minimizes the objective function of the original variable  $Y_t$

$$J_2 = E(Y_t - Y_t^{sp})^T (Y_t - Y_t^{sp}) \quad (8.14)$$

and  $J_1 = J_2$ .

Thus the performance measure of the original variable  $Y_t$  can be obtained via the performance measure of the interactor-filtered variable  $\tilde{Y}_t$ .

**Remark 7** In Remark 6, if the unitary interactor matrix is replaced by a weighted unitary interactor matrix,  $D_w$ , then

$$E(\tilde{Y}_t - \tilde{Y}_t^{sp})^T (\tilde{Y}_t - \tilde{Y}_t^{sp}) = E(Y_t - Y_t^{sp})^T W (Y_t - Y_t^{sp})$$

where  $D_w$  satisfies  $D_w^T D_w = W$ . Existence and factorization of such weighted unitary interactor matrix can be found in Chapter 4. With such an interactor matrix, the minimum variance control law for the interactor-filtered variable,  $\tilde{Y}$ , is identical to the weighted minimum variance control law for the original variable,  $Y_t$ . In fact, in Chapter 4 it has been shown that the minimum variance control law is identical to the singular LQ control law solved via the spectral factorization method (Harris and MacGregor, 1987).

To summarize Theorem 7 and Remarks 4 to 7, the following general result is presented:

For a multivariable (square/non-square) process

$$Y_t = T U_t + N a_t$$

the minimum variance control is obtained by minimizing

$$J = E[(Y_t - Y_t^{sp})^T W (Y_t - Y_t^{sp})] = E(\epsilon_t^T W \epsilon_t)$$

If one models closed-loop routine operating data under feedback control by the following multivariate moving-average process:

$$\begin{aligned} \tilde{\epsilon}_t - E(\tilde{\epsilon}_t) &= \underbrace{F_0 a_t + F_1 a_{t-1} + \cdots + F_{d-1} a_{t-d+1}}_{e_t} \\ &\quad + \underbrace{L_0 a_{t-d} + L_1 a_{t-d-1} + \cdots}_{w_{t-d}} \end{aligned}$$

where  $\tilde{\epsilon}_t = q^{-d} D_w \epsilon_t$ , then the minimum variance term,  $\tilde{\epsilon}_t|_{mv} = e_t = F a_t$ , consists of the first  $d$  terms of this moving-average model, and therefore can be separated from time series analysis of routine operating data. The quadratic benchmark performance measure,  $E(\epsilon_t^T W \epsilon_t)|_{mv}$  can then be calculated from  $E(e_t^T e_t)$ .

**Remark 8** Deduction of the minimum variance control benchmark performance as in this chapter requires knowledge of only the time-delays (or infinite zeros) of the transfer function matrix. No other information is required. In practice there are many limitations in reducing output variance through feedback control. Control action constraints, existence of poorly damped or unstable (NMP) zeros, desired robustness characteristics etc., are examples of such limitations. Time-delays or the interactor matrices are the most fundamental level of limitation in reducing variance, and is the only possible performance limitation that can be estimated from routine operating data. Identification of such benchmark performance does not imply implementation of such a control law. However, this benchmark performance provides an *absolute* lower bound or *global* minimum (Astrom and Wittenmark, 1990) of process variance and “so can be used much like the Cramer-Rao lower bound on variance in statistical parameter estimation (Harris *et al.*, 1996)”. Even for minimum phase systems, implementation of minimum variance control is usually not recommended (Desborough and Harris, 1992; Eriksson and Isaksson, 1994) due to its poor robustness and need for excessive control action. Certainly for non-minimum phase systems, it would be imprudent to implement such a benchmark control law. Nevertheless, minimum variance control does serve as a useful “global minimum” reference point and provides a first-level benchmark against which to assess current control performance. This first-level performance measure is obtained with minimum effort—from routine operating data together with *a priori* knowledge of the time delay matrix. This *a priori* knowledge can be obtained from simple tests of the MIMO process under closed-loop conditions and subsequent SVD analysis of the data as discussed in Chapter 5. Using this SVD method, entire knowledge of the model of the process is not a necessary prerequisite for estimating the interactor. The proposed method thus provides an efficient tool to comprehensively monitor modern processing facilities which can have hundreds and possibly thousands of control loops. For those loops which indicate good first-level performance measures,



no further adjustment or testing is necessary. For loops which indicate poor performance measures, a second-level study which may require process identification and/or redesign or retuning of control loops, may be necessary. Thus the second-level performance assessment need only be conducted on a limited number of loops and this saves valuable personnel time. The benchmark performance (*local* minimum) subject to constraints such as non-minimum phase and control action constraints can then be studied at this second-level performance assessment; other performance measures such as regulation of step-type disturbances (Eriksson and Isaksson, 1994) are also studied at this level; these issues will be discussed in the following chapters.

### 8.3 The FCOR algorithm for general interactor matrices

#### 8.3.1 Multivariable performance measures

As proved in the previous sections, performance assessment of multivariable processes can be reduced to finding the minimum variance term,  $e_t$ , from a multivariate moving average process, which has the general form shown in equation (8.5). From equation (8.5), the covariance between the output and the white noise sequence at lag  $i$  (for  $i < d$ ) is given by

$$E[\tilde{Y}_t a_{t-i}^T] = F_i \Sigma_a \triangleq \Sigma_{\tilde{Y}_a}(i) \quad (8.15)$$

where  $\Sigma_a = E(a_t a_t^T)$ . From

$$q^{-d} D Y_t|_{mv} \triangleq \tilde{Y}_t|_{mv} = e_t = F_0 a_t + \cdots + F_{d-1} a_{t-d+1}$$

one can solve for  $Y_t|_{mv}$  as

$$Y_t|_{mv} = q^d D^{-1} (F_0 a_t + F_1 a_{t-1} + \cdots + F_{d-1} a_{t-d+1})$$

where  $\tilde{Y}_t|_{mv}$  is the interactor-filtered output under minimum variance control, and  $Y_t|_{mv}$  is the original output under the same control law. Note that from Remark 6 the minimum variance control laws of  $Y_t$  and  $\tilde{Y}_t$  are identical. For the unitary interactor matrix, we have  $(D^{-1}(q) = D^T(q^{-1}))$ , i.e.

$$\begin{aligned}
D^{-1} &= (D_0 q^d + \dots + D_{d-1} q)^{-1} \\
&= D_0^T q^{-d} + \dots + D_{d-1}^T q^{-1}
\end{aligned} \tag{8.16}$$

Therefore

$$\begin{aligned}
Y_t|_{mv} &= (D_0^T + \dots + D_{d-1}^T q^{d-1})(F_0 + \dots + F_{d-1} q^{-d+1})a_t \\
&\triangleq (E_0 + E_1 q^{-1} + \dots + E_{d-1} q^{-d+1})a_t
\end{aligned} \tag{8.17}$$

(Note that for a weighted unitary interactor matrix,  $D_w^{-1}(q) \neq D_w^T(q^{-1})$ , but  $D_w = D_{uni} W^{1/2}$  and  $D_{uni}$  is a unitary interactor. Thus,  $D_w^{-1} = W^{-1/2} D_{uni}^T(q^{-1})$  and equation (8.16) has to be modified accordingly.)

Due to causality, any term with positive power of  $q$  in equation (8.17) must be zero. Equation (8.17) can be written as a compact matrix form:

$$\begin{aligned}
&[E_0, E_1, \dots, E_{d-1}] = \\
&[D_0^T, D_1^T, \dots, D_{d-1}^T] \begin{bmatrix} F_0 & F_1 & \dots & F_{d-1} \\ F_1 & F_2 & \dots & \\ \vdots & \vdots & & \\ \vdots & F_{d-1} & & \\ F_{d-1} & & & \end{bmatrix}
\end{aligned} \tag{8.18}$$

From equation (8.17), variance of  $Y_t$  under minimum variance control can be written as

$$\begin{aligned}
\Sigma_{mv} &= \text{Var}(Y_t|_{mv}) = E_0 \Sigma_a E_0^T + \dots + E_{d-1} \Sigma_a E_{d-1}^T \\
&\triangleq X X^T
\end{aligned} \tag{8.19}$$

$$\text{where } X \triangleq [E_0 \Sigma_a^{1/2}, E_1 \Sigma_a^{1/2}, \dots, E_{d-1} \Sigma_a^{1/2}] \tag{8.20}$$

$$\text{From equation (8.15), we have } F_i = \Sigma_{\hat{Y}_a}(i) \Sigma_a^{-1} \tag{8.21}$$

Substituting equation (8.21) into (8.18), and then substituting the result into (8.20) yields

$$X = [D_0^T, D_1^T, \dots, D_{d-1}^T] \begin{bmatrix} \Sigma_{\hat{Y}_a}(0) \Sigma_a^{-1/2} & \Sigma_{\hat{Y}_a}(1) \Sigma_a^{-1/2} & \dots & \Sigma_{\hat{Y}_a}(d-1) \Sigma_a^{-1/2} \\ \Sigma_{\hat{Y}_a}(1) \Sigma_a^{-1/2} & \Sigma_{\hat{Y}_a}(2) \Sigma_a^{-1/2} & \dots & \\ \vdots & \vdots & & \\ \vdots & \Sigma_{\hat{Y}_a}(d-1) \Sigma_a^{-1/2} & & \\ \Sigma_{\hat{Y}_a}(d-1) \Sigma_a^{-1/2} & & & \end{bmatrix}$$

Since variance of  $Y_t$  under minimum variance control can be calculated from equation (8.19), the objective function based performance measure (denoted as MIMO performance measure) can be calculated as

$$\begin{aligned}\eta(d) &= \frac{\text{minimum variance}}{\text{actual variance}} = \frac{E[Y_t^T Y_t]_{\min}}{E[Y_t^T Y_t]} \\ &= \frac{\text{tr} \Sigma_{mv}}{\text{tr}(E[Y_t Y_t^T])} \\ &= \frac{\text{tr}(X X^T)}{\text{tr} \Sigma_Y}\end{aligned}$$

It is often desired to compare the variance-covariance matrix of the actual output with the variance-covariance matrix of ideal output under minimum variance control. The performance indices of individual outputs are obtained from the diagonal elements of such comparison:

$$[\eta_{y_1}, \dots, \eta_{y_n}]^T = \text{diag}\{\Sigma_{mv} \tilde{\Sigma}_Y^{-1}\} = \text{diag}\{X X^T \tilde{\Sigma}_Y^{-1}\}$$

where  $\tilde{\Sigma}_Y = \text{diag}(\Sigma_Y)$ . The individual output performance indices represent the performance of each output with respect to the ideal output under multivariable minimum variance control. If an offset exists in the process output, then the output variance,  $\Sigma_Y$ , should be replaced by the output mean square error in the above calculation of the performance indices.

Although  $a_t$  is unknown in this calculation, it can be replaced by the estimated “white” noise sequence,  $\hat{a}_t$ , or the innovation term via time series analysis as introduced in the filtering or whitening section in Chapter 6. This whole procedure of obtaining the multivariable performance index is the FCOR algorithm. The FCOR approach provides a relatively easy way to calculate the performance measure of a multivariable process.

Harris *et al.*(1996) have proposed another approach to assess performance of multivariable systems using spectral factorization to normalize the lower triangular interactor matrix and subsequently using the Diophantine identity to calculate the benchmark performance. Readers are referred to Harris *et al.*(1996) for detailed discussion.

## 8.4 Evaluation of the FCOR algorithm on a simulated example and an industrial application

### 8.4.1 Simulated example

**Example 8** *This simulation example demonstrates application of the FCOR algorithm to both square and non-square multivariable systems with the general interactor matrix.*

Consider a  $2 \times 2$  multivariable process, with the open-loop transfer function matrix  $T$  and disturbance transfer function matrix  $N$  given by

$$T = \begin{bmatrix} \frac{q^{-1}}{1-0.4q^{-1}} & \frac{K_{12}q^{-2}}{1-0.1q^{-1}} \\ \frac{0.3q^{-1}}{1-0.1q^{-1}} & \frac{q^{-2}}{1-0.8q^{-1}} \end{bmatrix}$$

$$N = \begin{bmatrix} \frac{1}{1-0.5q^{-1}} & \frac{-0.6}{1-0.5q^{-1}} \\ \frac{0.5}{1-0.5q^{-1}} & \frac{1.0}{1-0.5q^{-1}} \end{bmatrix}$$

The white noise excitation,  $a_t$ , is a two-dimensional normally-distributed white noise sequence, with  $\Sigma_a = I$ . The output quality is measured by  $J = E[Y_t^T Y_t]$ . A unitary interactor matrix  $D$  can then be factored out as:

$$D = \begin{bmatrix} -0.9578q & -0.2873q \\ -0.2873q^2 & 0.9578q^2 \end{bmatrix} \quad (8.22)$$

Then  $DN$  is given by

$$DN = \begin{bmatrix} \frac{-1.1014q}{(1-0.5q^{-1})} & \frac{0.2874q}{(1-0.5q^{-1})} \\ \frac{0.1916q^2}{(1-0.5q^{-1})} & \frac{1.1302q^2}{(1-0.5q^{-1})} \end{bmatrix}$$

$q^{-d}DN$  ( $d = 2$ ) can be separated in the form of equation (8.4), where  $F$  and  $R$  matrices are obtained as

$$F = \begin{bmatrix} -1.1014q^{-1} & 0.2874q^{-1} \\ 0.1916 + 0.0958q^{-1} & 1.1302 + 0.5651q^{-1} \end{bmatrix} \quad (8.23)$$

$$R = \begin{bmatrix} \frac{-0.5507}{1-0.5q^{-1}} & \frac{0.1437}{1-0.5q^{-1}} \\ \frac{0.0479}{1-0.5q^{-1}} & \frac{0.2826}{1-0.5q^{-1}} \end{bmatrix} \quad (8.24)$$

The feedback controller-invariant term is therefore

$$e_t = Fa_t = \begin{bmatrix} -1.1014q^{-1} & 0.2874q^{-1} \\ 0.1916 + 0.0958q^{-1} & 1.1302 + 0.5651q^{-1} \end{bmatrix} a_t$$

The theoretical minimum variance matrix under the minimum variance control can be calculated from  $Y_t|_{mv} = q^d D^{-1} Fa_t$  as

$$Y_t|_{mv} = \begin{bmatrix} 1 - 0.02752q^{-1} & -0.6 - 0.1623q^{-1} \\ 0.5 + 0.09176q^{-1} & 1 + 0.5412q^{-1} \end{bmatrix} a_t$$

This will be the theoretical benchmark to assess performance of the feedback controller. The FCOR algorithm will estimate this benchmark from routine operating data.

Suppose a multiloop minimum variance controller based on the two single loops without interaction compensation:

$$Q = \begin{bmatrix} \frac{0.5 - 0.20q^{-1}}{1 - 0.5q^{-1}} & 0 \\ 0 & \frac{0.25 - 0.200q^{-1}}{(1 - 0.5q^{-1})(1 + 0.5q^{-1})} \end{bmatrix}$$

is implemented on this process. The *a priori* knowledge of the interactor matrix can be estimated either from previous open-loop tests or from simple closed-loop tests. One can then apply the FCOR algorithm to the interactor-filtered variable  $\tilde{Y}_t$ , and the MIMO performance index of the original variable  $Y_t$  can be estimated. The result is shown in figure 8.1, where performance indices include objective function based performance index (denoted as MIMO) and individual output performance indices (denoted as  $y_1$  and  $y_2$  respectively). In this example, when  $K_{12} \rightarrow 0$  ( $K_{12}$  is the numerator gain of element (1,2) of the process transfer function matrix  $T$ ), the performance measure of both outputs reaches the optimal value due to weak interaction. However, with increasing interaction (i.e. as  $K_{12}$  increases) the performance deteriorates, and eventually the performance index of  $y_1$  approaches zero. Performance of  $y_1$  is more sensitive to the change in  $K_{12}$ . It appears that the objective function based MIMO performance index is influenced significantly by  $y_1$  in this example. This plot also shows a good agreement of the estimated performance indices with the theoretical ones.

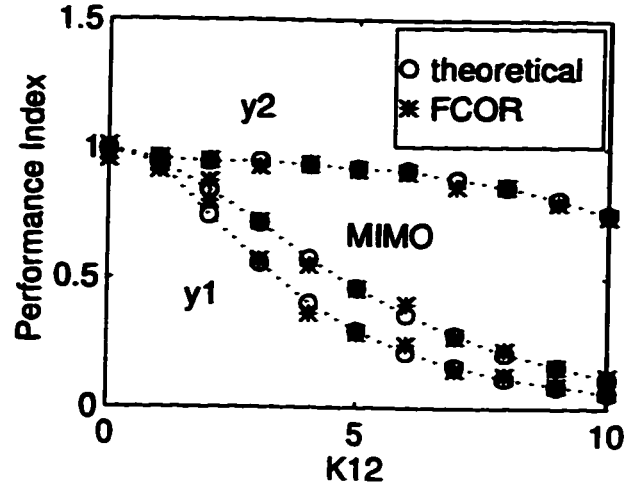


Figure 8.1: *Performance assessment of a square MIMO process (with a general interactor matrix) under multiloop minimum variance control*

To see the effect of output weighting, a weighting matrix

$$W = \begin{bmatrix} 1 & 0 \\ 0 & 4 \end{bmatrix}$$

is assumed, i.e.  $y_2$  is regarded as a more important output variable than  $y_1$ . Following the procedure in Chapter 4, a weighted unitary interactor matrix is formed as

$$D_w = \begin{bmatrix} -0.8575q & -1.029q \\ 0.5145q^2 & -1.715q^2 \end{bmatrix}$$

The feedback control invariant polynomial matrix  $F$  can be calculated from  $q^{-d}D_wN = F + q^{-d}R$  as

$$F = \begin{bmatrix} -1.3720q^{-1} & -0.5145q^{-1} \\ -0.3430 - 0.1715q^{-1} & -2.0240 - 1.0120q^{-1} \end{bmatrix}$$

The theoretical minimum variance matrix under the weighted minimum variance control can be calculated from  $Y_{t|mv} = q^d D_w^{-1} F a_t$  as

$$Y_{t|mv} = \begin{bmatrix} 1 - 0.08824q^{-1} & -0.6 - 0.5207q^{-1} \\ 0.5 + 0.07354q^{-1} & 1 + 0.4339q^{-1} \end{bmatrix} a_t$$

This will be the theoretical benchmark to assess performance of the feedback controller. The FCOR algorithm will estimate this benchmark from routine operating data. The

results are shown in Figure 8.2. Since  $y_2$  becomes the more important output variable, the benchmark variance of  $y_2$  should be reduced and the benchmark variance of  $y_1$  is expected to increase. Consequently, the performance indices of  $y_2$  should decrease and the performance indices of  $y_1$  is expected to increase. The objective function based MIMO performance indices should somehow move toward the performance index of  $y_2$ . All these are confirmed by Figure 8.2. This figure also shows good agreement between the theoretical indices and estimated from the FCOR algorithm. Notice that while individual performance indices can be larger than 1, the objective function based MIMO performance indices are always less than 1.

The FCOR algorithm can also handle non-square systems. Consider the input-output transfer function in example 8 replaced by a  $2 \times 3$  transfer function matrix:

$$T = \begin{bmatrix} \frac{q^{-1}}{1-0.4q^{-1}} & \frac{K_{12}q^{-2}}{1-0.1q^{-1}} & \frac{0.2q^{-2}}{1-0.5q^{-1}} \\ \frac{0.7q^{-1}}{1-0.2q^{-1}} & \frac{q^{-2}}{1-0.8q^{-1}} & \frac{0.8q^{-2}}{1-0.7q^{-1}} \end{bmatrix}$$

This non-square transfer function matrix has the following unitary interactor matrix:

$$D = \begin{bmatrix} -0.8192q & -0.5735q \\ -0.5735q^2 & 0.8192q^2 \end{bmatrix}$$

Suppose a multivariable controller:

$$Q = \begin{bmatrix} \frac{0.5-0.20q^{-1}}{1-0.5q^{-1}} & 0 \\ 0 & \frac{0.25-0.200q^{-1}}{(1-0.5q^{-1})(1+0.5q^{-1})} \\ \frac{0.6-0.1q^{-1}}{1-q^{-1}} & \frac{0.6-0.1q^{-1}}{1-q^{-1}} \end{bmatrix}$$

is designed for this system. With the multivariable controller operating on this 2-output and 3-input system, the performance can be estimated by using the FCOR algorithm on routine operating data. The results are shown in figure 8.3. For this example, the performance index of  $y_1$  steadily deteriorates with increasing interaction, while the performance index of  $y_2$  shows a more complicated pattern of performance change with increasing interaction.

### 8.4.2 Industrial application

An industrial absorption process is shown in figure 8.4. The process is designed for the removal of  $CO_2$  from the feed gas that is a mixture of  $CO_2$ ,  $H_2$ , and  $N_2$ . The solution contains a combination of potassium carbonate and a catalyst additive. It absorbs  $CO_2$  from the  $CO_2$  absorber on the right and is regenerated in the  $CO_2$  stripper on the left by reboiling and steam-stripping the  $CO_2$  from the solution. The term "lean solution" refers to stripper bottom flow which is mostly free of  $CO_2$  whereas the "semi-lean solution" coming from the first-stage stripping still contains some  $CO_2$ . Since the solution is circulated continuously between the two towers, an extremely strong interaction exists between the two PID-controlled level loops of both towers. The objective of this analysis is performance assessment of the two level controllers. For this process, the output quality is measured by  $J = E(Y_t - Y_t^{sp})^T W (Y_t - Y_t^{sp})$  with the weighting matrix  $W = I$  (defined as weighting #1) and the setpoint being constant. Different weighting matrices are also studied in this example. A representative set of routine operating data was sampled over 15 hours with sampling time  $T_s = 5\text{sec}$  as shown in Figure 8.5. The time delay of the loop  $u_1 - y_1$  is known to be 19 sampling periods, and the time delay of the loop  $u_2 - y_2$  is known to be 23 sampling periods. The interactor matrix has the diagonal structure, which is a special unitary interactor matrix. According to plant engineers, the  $u_1 - y_1$  loop is supposed to be tightly tuned.

The left graph in Figure 8.6 shows the estimated multivariable performance indices (weighting #1), where each point represents the performance measure based on the last 750 data points, i.e one hour of data. The performance indices can be seen to be fairly stable over 14 hours with an average multivariable performance index (objective function based) of 0.5. To further investigate this process, the individual output performance is studied. The performance indices of output  $y_1$  and  $y_2$  are also shown in the left graph of Figure 8.6. The performance measure of  $y_1$  is close to minimum variance control ( $\approx 1$ ). However, the performance measure of  $y_2$  ( $\approx 0.2$ ) indicates rather poor control of this output. Thus these two loop tunings are fairly "unbalanced". Further study shows that a strong negative correlation exists between the variations of  $y_1$  and  $y_2$ . Therefore



this assessment suggests that 1) in order to improve the overall performance, the loop 1 controller (for  $y_1$ ) needs to be detuned so that the loop 2 controller (for  $y_2$ ) can be more tightly tuned; 2) there may be little or no incentive to further improve the performance of  $y_1$  since it is performing at almost minimum variance levels; and 3) the performance of  $y_2$  may be significantly improved by simply adjusting current control parameters or redesigning the control algorithm, e.g., by detuning the loop 1 controller and tightly tuning the loop 2 controller. In summary, this assessment justifies further analysis of this process, and indicates the potential for improving regulatory performance, particularly the performance of  $y_2$ .

Now suppose that the level of the first column is a much more important variable to regulate than the level of the second column. A weighting matrix  $W = \text{diag}(100, 1)$  (defined as weighting #2) is assumed. Then, one would expect this process to indicate good performance in terms of objective function based MIMO performance index. On the other hand, if a weighting matrix  $W = \text{diag}(1, 100)$  (defined as weighting #3) is assumed, i.e. the level of the second column is much more important than the first column, then one should expect that this process has very poor performance. All these are confirmed in the right side graph in Figure 8.6.

## 8.5 Conclusions

The main contributions of this chapter are:

- Development of a computationally simple algorithm to estimate control loop performance measure of a general class (square and non-square) of MIMO processes. The use of this measure for preliminary process diagnosis and monitoring of multivariable processes under multiloop control has been illustrated by application to an industrial process. This later topic is bound to be the subject of considerable industrial interest for pre- and post-audit of advanced control applications.
- The derivation of this algorithm is based on the idea of a minimum variance benchmark standard that has been extended from the SISO to the MIMO case.

- The derived algorithm is simple and has been successfully evaluated by simulated and actual industrial application.
- The proposed performance assessment together with the analysis of dispersion and spectral analysis as introduced by DeVries and Wu(1978) can result in a powerful tool for multivariable performance monitoring and diagnosis.

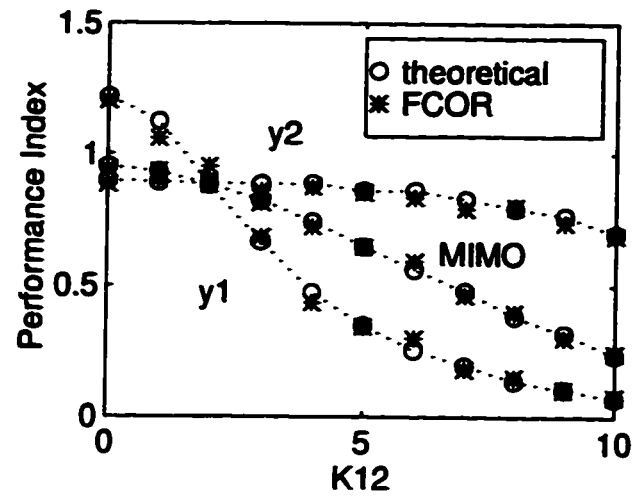


Figure 8.2: *Performance assessment of a square MIMO process (with a general interactor matrix and output weighting) under multiloop minimum variance control*

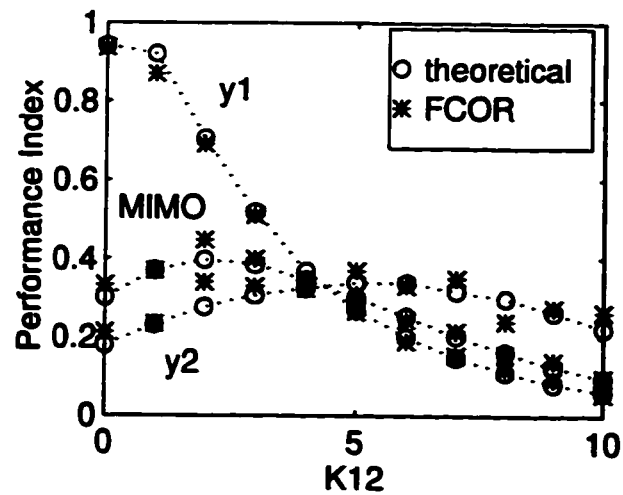


Figure 8.3: *Performance assessment of a non-square MIMO process (with a general interactor matrix) under multivariable control*

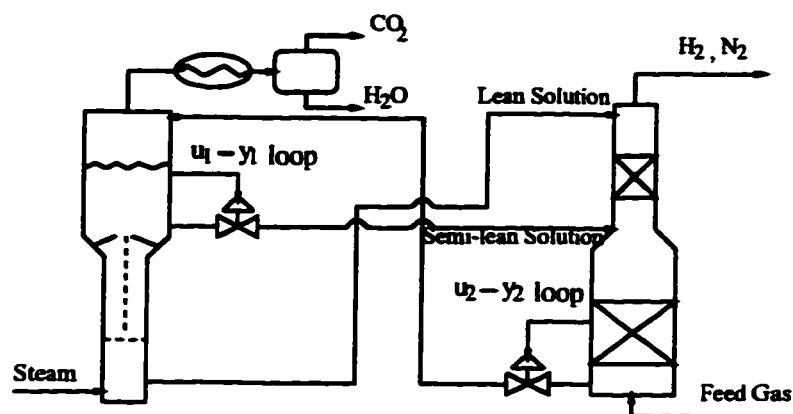


Figure 8.4: *Schematic diagram of the industrial absorption process*

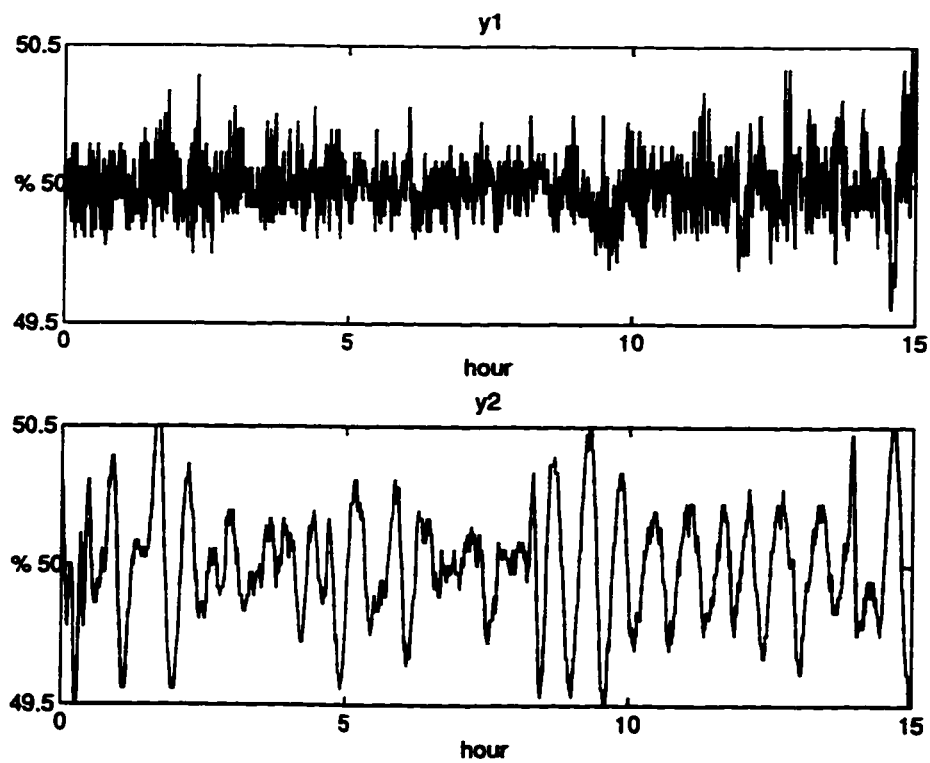


Figure 8.5: *Absorption process data*

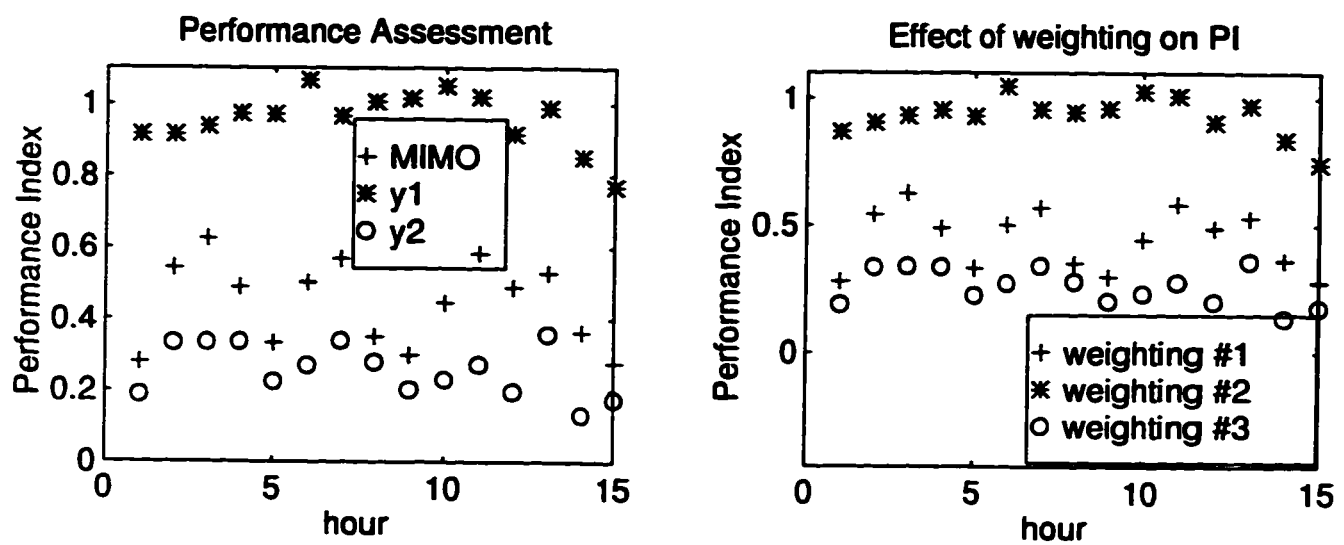


Figure 8.6: *Multivariable performance assessment of absorption process*

## **Chapter 9**

# **Feedforward & Feedback Controller Performance Assessment**

### **9.1 Introduction**

Minimum variance feedback control is the best possible feedback control in the sense that no other controllers can give lower process variance than it. If a process indicates a good performance measure relative to minimum variance control, further tuning of the existing feedback controller is neither useful nor helpful. If further reduction of process variance is required, then one may have to implement feedforward control.

Design of minimum variance feedforward & feedback control can be found in Box and Jenkins(1976), Sternad and Soderstrom(1988). Desborough and Harris(1993) have discussed feedforward controller performance assessment of SISO processes. The main contribution of this chapter is to extend the MIMO feedback controller performance assessment technique to feedforward plus feedback case. If feedforward controllers have not been actually implemented on the process, then this analysis gives a measure of the potential benefit of implementing feedforward controllers. This chapter is organized as

follows. In section 9.2, the theoretical background and calculation procedure for FF&FB control performance assessment is established. The proposed method is then illustrated by a numerical example and an industrial application in section 9.3, followed by concluding remarks in section 9.4.

## 9.2 Performance assessment of MIMO processes using minimum variance FF&FB control as the benchmark

### 9.2.1 Minimum variance FF&FB control benchmark performance

Consider a MIMO process:

$$Y_t = TU_t + N_a a_t + N_b b_t \quad (9.1)$$

where  $T$  ( $n \times n$ ) is the input-output transfer function matrix,  $N_a$  ( $n \times n_a$ ) and  $N_b$  ( $n \times n_b$ ) are disturbance transfer function matrices,  $a_t$  ( $n_a \times 1$ ) is the “driving force (white noise)” for realization of the unmeasurable disturbances, and  $b_t$  ( $n_b \times 1$ ) is the “driving force” for realization of the measurable disturbances and is independent of  $a_t$ . The “driving force”,  $b_t$ , can be indirectly measured through time series analysis (data prewhitening):

$$\xi_t = G_m b_t \quad (9.2)$$

where  $\xi_t$  ( $n_b \times 1$ ) is directly measured disturbances,  $G_m$  ( $n_b \times n_b$ ) is the transfer function matrix obtained from time series analysis of  $\xi_t$ .

By factoring  $T$  as  $T = D^{-1}\tilde{T}$  where  $D^{-1}$  is the delay matrix or the inverse interactor matrix, equation(9.1) can be written as

$$Y_t = D^{-1}\tilde{T}U_t + N_a a_t + N_b b_t \quad (9.3)$$

Multiplying both sides of equation(9.3) by  $q^{-d}D$  where  $d$  is the order of the interactor matrix (the smallest integer that makes  $q^{-d}D$  casual or the largest power of  $q$  in  $D$ ), yields

$$\tilde{Y}_t = q^{-d}\tilde{T}U_t + \tilde{N}_a a_t + \tilde{N}_b b_t \quad (9.4)$$

where

$$\begin{aligned}\tilde{Y}_t &= q^{-d}DY_t \\ \tilde{N}_a &= q^{-d}DN_a \\ \tilde{N}_b &= q^{-d}DN_b\end{aligned}$$

Using the Diophantine identity

$$\begin{aligned}\tilde{N}_a &= F_a + q^{-d}R_a \\ \tilde{N}_b &= F_b + q^{-d}R_b\end{aligned}$$

where

$$\begin{aligned}F_a &= F_0^{(a)} + F_1^{(a)}q^{-1} + \dots + F_{d-1}^{(a)}q^{-(d-1)} \\ F_b &= F_0^{(b)} + F_1^{(b)}q^{-1} + \dots + F_{d-1}^{(b)}q^{-(d-1)}\end{aligned}$$

are matrix polynomials, and  $R_a$  and  $R_b$  are proper rational transfer function matrices.

Using these Diophantine identities, equation(9.4) can be written as

$$\tilde{Y}_t = F_a a_t + F_b b_t + \tilde{T}U_{t-d} + R_a a_{t-d} + R_b b_{t-d} \quad (9.5)$$

Due to causality of the control law,  $U_{t-d}$  must be independent of  $F_a a_t$  and  $F_b b_t$ , since these two terms occur after the time  $t - d$ . Therefore, the first two terms on the right hand side of equation(9.4) are control independent. In other words,

$$Var(\tilde{Y}_t) \geq Var(F_a a_t + F_b b_t)$$

or in LQ form (total variance):

$$E(\tilde{Y}_t^T \tilde{Y}_t) \geq tr(Var(F_a a_t)) + tr(Var(F_b b_t))$$

Equality holds when the remaining terms on the left hand side of equation(9.5) are equal to zero, i.e.

$$\tilde{T}U_{t-d} + R_a a_{t-d} + R_b b_{t-d} = 0$$

which gives the following control law:

$$U_t = -\tilde{T}^{-1}(R_a a_t + R_b b_t) \quad (9.6)$$



Substituting equation(9.6) into equation(9.5) yields

$$\tilde{Y}_t = F_a a_t + F_b b_t$$

This gives

$$a_t = F_a^{-1}(\tilde{Y}_t - F_b b_t) \quad (9.7)$$

Substituting equation(9.7) into equation(9.6) results in the feedback plus feedforward control law:

$$U_t = -\tilde{T}^{-1} R_a F_a^{-1} (q^{-d} D) Y_t + \tilde{T}^{-1} (R_a F_a^{-1} F_b - R_b) b_t \quad (9.8)$$

By using equation(9.2), equation(9.8) can be written as

$$U_t = -\tilde{T}^{-1} R_a F_a^{-1} (q^{-d} D) Y_t + \tilde{T}^{-1} (R_a F_a^{-1} F_b - R_b) G_m^{-1} \xi_t \quad (9.9)$$

The first term on the right hand side of equation(9.9) reflects the feedback part of the minimum variance feedforward and feedback control law, and the second term reflects the feedforward part of the minimum variance feedforward and feedback control law. This minimum variance control law may or may not be practically implementable depending on the invertibility of process zeros. In practice, there are many limitations on achievable performance in addition to time-delays and non-invertible zeros. Constraints on control action, existence of poorly damped zeros, and desired robustness characteristics are examples of such limitations on the achievable performance as discussed in Chapter 8. Nevertheless, this minimum variance control provides the absolute lower bound on the process variation and serves as a convenient benchmark for the first-level performance assessment.

This minimum variance feedback & feedforward control law apparently only minimizes the total variance (LQ objective function) of the interactor-filtered variable  $\tilde{Y}_t$ . However, if  $D$  is a unitary interactor matrix, then the minimum variance control law which minimizes the following LQ objective function (total variance) of the interactor-filtered variable  $\tilde{Y}_t$ :

$$J_1 = E[\tilde{Y}_t^T \tilde{Y}_t] \quad (9.10)$$

also minimizes the LQ objective function of the original variable  $Y_t$ :

$$J_2 = E[Y_t^T Y_t] \quad (9.11)$$

and  $J_1 = J_2$  (for proof see Lemma 3). In the sequel, this LQ objective function or total variance will be used for the scalar performance measure of the MIMO system, and we will no longer distinguish the performance measures between the original variable,  $Y_t$ , and the interactor-filtered variable,  $\tilde{Y}_t$ .

In summary, under minimum variance FF&FB control, the closed-loop response can be denoted by

$$e_t \triangleq \tilde{Y}_t|_{\min} = F_a a_t + F_b b_t \quad (9.12)$$

where  $e_t$  is the FF&FB controller-invariant term, i.e. no feedforward and feedback controllers can change this term, and therefore it can be estimated from routine closed-loop operating data under any linear FF&FB controllers. This yields the following theorem.

**Theorem 8** *The minimum variance of the interactor-filtered output  $\tilde{Y}_t$  is FF&FB control invariant, and can be estimated from routine operating data  $Y_t$ . The estimation is via multivariate moving-average time series analysis of  $\tilde{Y}_t$ , i.e. if write  $\tilde{Y}_t$  as*

$$\tilde{Y}_t = \underbrace{F_0^{(a)} a_t + \dots + F_{d-1}^{(a)} a_{t-d+1} + F_d^{(a)} a_{t-d} + \dots}_{e_t^u = F_a a_t} + \underbrace{F_0^{(b)} b_t + \dots + F_{d-1}^{(b)} b_{t-d+1} + F_d^{(b)} b_{t-d} + \dots}_{e_t^m = F_b b_t}$$

then

$$e_t = e_t^u + e_t^m$$

constitutes the minimum FF&FB variance, where  $e_t^u = F_a a_t$  is the contribution of the unmeasurable disturbances to the minimum variance sequence  $e_t$ , and  $e_t^m = F_b b_t$  is the contribution of the measurable disturbances to the minimum variance sequence  $e_t$ .

Note that this minimum FF&FB variance may not be achieved by minimum variance feedback control only, and the lower bound achieved by feedback control is no less than the lower bound achieved by feedforward plus feedback control (Pierce, 1975). Estimation of the lower bound achieved by feedback control (minimum FB variance) has been established in Chapter 8, i.e. if one models the interactor-filtered output,  $\tilde{Y}_t$ , by the following moving-average model:

$$\tilde{Y}_t = \underbrace{F_0 \nu_t + \dots + F_{d-1} \nu_{t-d+1} + F_d \nu_{t-d} + \dots}_{e_t^{FB}}$$

then  $e_t^{FB}$  is feedback controller-invariant, and  $E[(e_t^{FB})^T(e_t^{FB})]$  constitutes the total minimum FB variance. Here  $\nu_t$  is actually a lumped disturbance from both unmeasurable and measurable disturbances. The benefit of implementing feedforward & feedback control is therefore

$$\Delta J = J_{FB} - J_{FF\&FB} = E[(e_t^{FB})^T(e_t^{FB})] - E(e_t^T e_t) \quad (9.13)$$

or the benefit relative to the present process variance

$$\Delta J\% = \frac{E[(e_t^{FB})^T(e_t^{FB})] - E(e_t^T e_t)}{E(Y_t^T Y_t)}$$

or the benefit relative to minimum FB variance

$$\Delta J\% = \frac{E[(e_t^{FB})^T(e_t^{FB})] - E(e_t^T e_t)}{E[(e_t^{FB})^T(e_t^{FB})]}$$

### 9.2.2 Feedback controller performance assessment of MIMO processes using minimum variance FF&FB control as the benchmark

A closed-loop response to both unmeasurable and measurable disturbances can be written as

$$Y_t = G_a a_t + G_\xi \xi_t \quad (9.14)$$

where  $G_a$  and  $G_\xi$  are rational, proper transfer function matrices. Equation (9.14) can be estimated via any standard system identification tools with  $\xi_t$  as the known input and  $Y_t$  as the output. Substituting  $\xi_t = G_m b_t$  into equation(9.14) yields

$$Y_t = G_a a_t + G_\xi G_m b_t \quad (9.15)$$

where the transfer function matrix  $G_m$  can be estimated from multivariate time series analysis of  $\xi_t$  via system identification tools. Multiplying equation(9.15) by  $q^{-d}D$  yields

$$q^{-d}DY_t = \tilde{Y}_t = q^{-d}DG_a a_t + q^{-d}DG_\xi G_m b_t \quad (9.16)$$

Equation (9.16) can be further written as the Markov parameter form (impulse response form):

$$\tilde{Y}_t = \underbrace{F_0^{(a)} a_t + \cdots + F_{d-1}^{(a)} a_{t-(d-1)}}_{\tilde{e}_t^a} + \underbrace{F_d^{(a)} a_{t-d} + \cdots}_{\tilde{e}_t^a} + \underbrace{F_0^{(b)} b_t + \cdots + F_{d-1}^{(b)} b_{t-(d-1)}}_{\tilde{e}_t^m} + \underbrace{F_d^{(b)} b_{t-d} + \cdots}_{\tilde{e}_t^m} \quad (9.17)$$

where  $F_i^{(a)}$  and  $F_i^{(b)}$  are the Markov parameter matrices (impulse response coefficient matrices);  $\hat{e}_t^u$  is the inflation in  $e_t^u$  due to non-optimal FB control to the unmeasurable disturbances;  $\hat{e}_t^m$  is the inflation in  $e_t^m$  due to non-optimal FF/FB control to the measurable disturbances. From equation(9.17), we have

$$\begin{aligned} Var(e_t^u) &= F_0^{(a)} \Sigma_a (F_0^{(a)})^T + \dots + F_{d-1}^{(a)} \Sigma_a (F_{d-1}^{(a)})^T \\ Var(e_t^m) &= F_0^{(b)} \Sigma_b (F_0^{(b)})^T + \dots + F_{d-1}^{(b)} \Sigma_b (F_{d-1}^{(b)})^T \end{aligned}$$

where  $\Sigma_a = E(a_t a_t^T)$  and  $\Sigma_b = E(b_t b_t^T)$ . Thus the quadratic measure (total variance) of minimum FF&FB variance control,

$$J_{FF\&FB} = E(e_t^T e_t) = E(e_t^u)^T (e_t^u) + E(e_t^m)^T (e_t^m)$$

can be calculated following the above procedure and can then be used as the benchmark against which to assess performance of feedforward & feedback controllers. The quadratic measure of minimum FB-only control  $J_{FB} = E[(e_t^{FB})^T (e_t^{FB})]$  may be estimated via the FCOR algorithm. Then the benefit of implementing optimal FF&FB control can be calculated from equation (9.13).

## 9.3 Numerical example and an industrial application

### 9.3.1 Numerical example

Performance assessment of feedback control for a  $2 \times 2$  process has been studied in Chapter 8. In this example, the benefit of implementing feedforward & feedback control to the same process will be discussed. The process has the following transfer function matrices:

$$\begin{aligned} T &= \begin{bmatrix} \frac{q^{-1}}{1-0.4q^{-1}} & \frac{q^{-2}}{1-0.1q^{-1}} \\ \frac{0.3q^{-1}}{1-0.1q^{-1}} & \frac{q^{-2}}{1-0.8q^{-1}} \end{bmatrix} \\ N_a &= \begin{bmatrix} \frac{1}{1-0.5q^{-1}} & \frac{-0.6}{1-0.5q^{-1}} \\ \frac{0.5}{1-0.5q^{-1}} & \frac{1.0}{1-0.5q^{-1}} \end{bmatrix} \quad N_b = \begin{bmatrix} \frac{0.1q^{-2}}{1-0.4q^{-1}} & \frac{-0.2q^{-1}}{1-0.3q^{-1}} \\ \frac{0.3q^{-2}}{1-0.2q^{-1}} & \frac{0.4q^{-1}}{1-0.1q^{-1}} \end{bmatrix} \end{aligned}$$

A unitary interactor matrix  $D$  can be factored as:

$$D = \begin{bmatrix} -0.9578q & -0.2873q \\ -0.2873q^2 & 0.9578q^2 \end{bmatrix}$$

Then  $\tilde{N}_a = q^{-d}DN_a$  is given by

$$\tilde{N}_a = \underbrace{\begin{bmatrix} -1.1014q^{-1} & 0.2874q^{-1} \\ 0.1916 + 0.0958q^{-1} & 1.1302 + 0.5651q^{-1} \end{bmatrix}}_{F_a} + q^{-2} \underbrace{\begin{bmatrix} \frac{-0.5507}{1-0.5q^{-1}} & \frac{0.1437}{1-0.5q^{-1}} \\ \frac{0.0479}{1-0.5q^{-1}} & \frac{0.2826}{1-0.5q^{-1}} \end{bmatrix}}_{R_a}$$

and  $\tilde{N}_b = q^{-d}DN_b$  is given by

$$\tilde{N}_b = \underbrace{\begin{bmatrix} 0 & 0 \\ 0 & 0.3256q^{-1} \end{bmatrix}}_{F_b} + q^{-2} \underbrace{\begin{bmatrix} \frac{-4.55q^{-1}+1.341q^{-2}}{(5-q^{-1})(5-2q^{-1})} & \frac{-30.65+5.363q^{-1}}{(10-q^{-1})(10-3q^{-1})} \\ \frac{6.465-2.73q^{-1}}{(5-q^{-1})(5-2q^{-1})} & \frac{2.104-0.9768q^{-1}}{(10-q^{-1})(10-3q^{-1})} \end{bmatrix}}_{R_b}$$

The minimum FF&FB variance term can then be written as

$$e_t = F_a a_t + F_b b_t = \begin{bmatrix} -1.1014q^{-1} & 0.2874q^{-1} \\ 0.1916 + 0.0958q^{-1} & 1.1302 + 0.5651q^{-1} \end{bmatrix} a_t + \begin{bmatrix} 0 & 0 \\ 0 & 0.3256q^{-1} \end{bmatrix} b_t$$

Assuming  $\Sigma_a = E a_t a_t^T = I$  and  $\Sigma_b = E b_t b_t^T = 4I$ , the quadratic measure (total variance) of minimum variance FF&FB control can be calculated as

$$J_{FF\&FB} = E e_t^T e_t = 3.3626$$

If, on the other hand, only minimum variance feedback control law is implemented, the feedback controller-invariant minimum variance term can be estimated by applying a FB performance assessment algorithm such as the FCOR algorithm to process data. This gives the quadratic measure (total variance) of minimum feedback control as

$$J_{FB} = 4.1873$$

The benefit of adding optimal feedforward control relative to minimum FB variance is then:

$$\Delta J\% = \frac{4.1873 - 3.3626}{4.1873} = 19.6\%$$

In summary, the achievable total variance by implementing any feedback control is no less than 4.1873; the achievable total variance by implementing any feedback and feedforward control is no less than 3.3626. The benefit of adding feedforward control is about 20% relative to minimum variance FB control. The optimal values may or may not be achievable depending on practical constraints.

### 9.3.2 Industrial application

The proposed performance assessment methods were applied to a Mitsubishi Chemical Corporation industrial process at Mizushima, Japan. As depicted in Figure 9.1, the process consists of an integrated cracking unit and a separation unit. In the current operation, oscillatory behavior in both TC2 and TC3 occurs frequently which causes the composition of the distillate and bottoms to fluctuate. Clearly, the cracking furnaces are highly integrated with the distillation column and therefore when tuning all of the single loop controllers, interactions and the multivariable plant performance must be considered. The main objective of this study is to assess the current control performance of TC2 and TC3, identify their primary source of variation and analyze the benefit of implementing feedforward control. Based on this analysis, recommendations regarding control structure, controller tuning and process modification can be made that will reduce variation of TC2 and TC3. Expected benefits of a reduction in the variance of TC2 and TC3 are improved operability and yields of subsequent processes and lower reboiler and condenser energy requirements for the distillation column.

It is known from a previous plant test that the process has a diagonal interactor matrix as

$$D^{-1} = \begin{bmatrix} q^{-3} & 0 \\ 0 & q^{-35} \end{bmatrix}$$

This interactor matrix clearly satisfies  $D^T(q^{-1})D(q) = I$ , which is a unitary interactor matrix. The number of data points used for this analysis is 7000 with sampling interval  $T_s = 1min$ . There are more than 20 measured disturbances. Three measured disturbances were selected from a screening test as candidates for feedforward control.

They are the flow rate measurement  $FM2$ , the temperature measurement  $TM1$  and the pressure measurement  $PM3$ . In this case, feedforward controllers have not been actually implemented. This study will analyze the benefit of implementing feedforward controllers. A representative set of data for the two outputs and the three measured disturbances is shown in Figure 9.2. Following the procedure as proposed in this chapter, the total minimum FF&FB variance is estimated as

$$J_{FF\&FB} = E(e_t^u)^T(e_t^u) + E(e_t^m)^T(e_t^m) = 0.0356 + 0.0683 = 0.1039$$

The total minimum FB variance (if only minimum variance feedback control is implemented) is estimated from the FCOR algorithm as

$$J_{FB} = E[(e_t^{FB})^T(e_t^{FB})] = 0.1386$$

The total current process variance is calculated as

$$J_{act} = E(Y_t - Y_t^{sp})^T(Y_t - Y_t^{sp}) = 0.2366$$

Based on these results, the total variance of the process variables may be reduced from the current value of 0.2366 to a minimum of about 0.14 or 42% reduction in the variance by implementing a multivariate minimum variance feedback control only. The minimum value itself may or may not be achievable depending on invertibility of the process zeros. On the other hand, a multivariate minimum variance feedforward plus feedback control strategy may bring the total variance down by  $1 - 0.1039/0.2366 = 56\%$ . The improvement relative to the actual variance due to applying feedforward control is therefore

$$\Delta J\% = \frac{0.1386 - 0.1039}{0.2366} = 15\%$$

These results lead to the recommendations that both feedforward control and multivariate feedback may be beneficial and worthwhile for further analysis.

## 9.4 Conclusions

This chapter has extended the MIMO performance assessment of feedback controllers to feedforward plus feedback controllers. It has been shown that the minimum FF&FB

variance is feedforward and feedback controller-invariant and can be estimated from routine operating data via time series analysis. The proposed performance assessment method has been illustrated by a numerical example and applied to an industrial application.



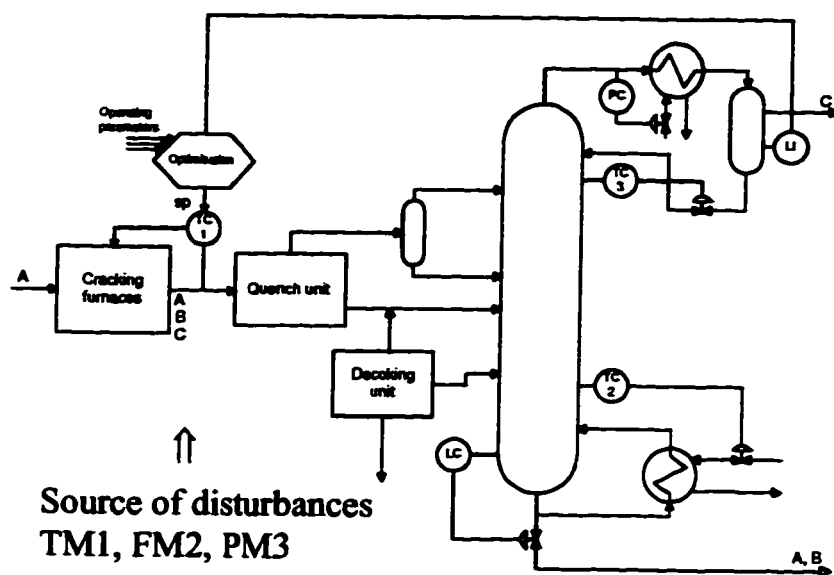


Figure 9.1: Schematic diagram of the industrial process

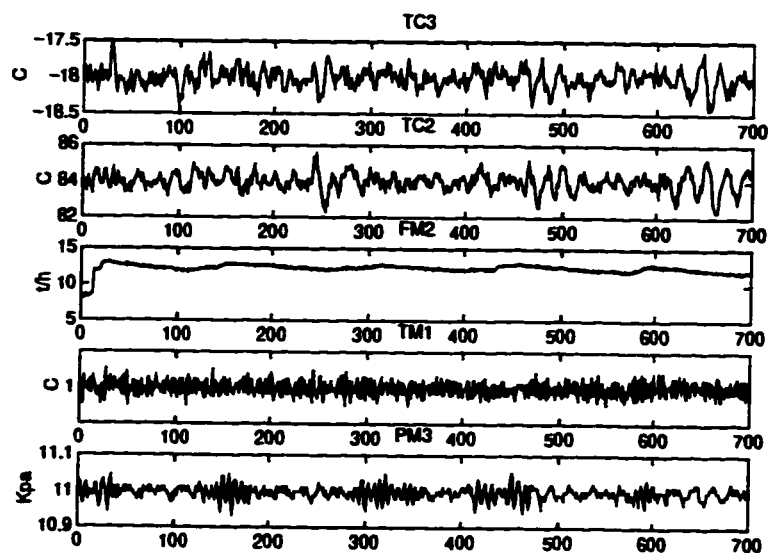


Figure 9.2: Process data trajectory. The time scale is in terms of sampling intervals.

## Chapter 10

# Performance Assessment of Nonminimum Phase Systems

### 10.1 Introduction

With complete knowledge of process dynamics, any possible limitations on the achievable performance may be calculated via procedures such as convex optimization and linear programming (Boyd and Barratt, 1991; Dahleh and Diaz-Bobillo, 1995). This is generally not a very attractive approach to process performance monitoring, since a typical plant can have hundreds and thousands of control loops, and identification of all loops, to obtain process models, is a very demanding requirement. Performance monitoring should be carried out in such a way that the normal operation of a process is affected as less as possible. In addition, process dynamics and disturbances may drift from time to time, and the initially identified model may not represent the true dynamics. Thus on-line performance monitoring is necessary.

Different types of constraints require different levels of process knowledge. Some constraints require less *a priori* knowledge of processes than others. If one can separate the constraints into different levels, then control loop performance may be assessed from the simplest to the hardest constraints with progressively more information required about the process at each stage. Only those loops which indicate poor performance at the first

level then need to be examined at the next level of performance assessment. Time-delays pose the first level of performance limitations. However, time-delays are easiest to obtain or estimate. Therefore, performance limitations due to time-delays is assessed at the first level. The second level of performance limitation would be due to non-invertible zeros.

Tyler and Morari(1995) have considered performance assessment of SISO systems with non-invertible zeros. In Chapter 6, 7 and 8, performance assessment of MIMO processes with time delays or infinite zeros has been considered. This chapter is an extension to the previous results in which we can consider performance limitations and assessment in the presence of unstable process zeros. Throughout this chapter, we shall assume that the process is open-loop stable, i.e. no poles lie outside the unit circle.

This chapter is organized as follows. The generalized unitary interactor matrix, an all-pass factor, is introduced in Section 10.2. Performance assessment of processes with non-invertible zeros is discussed in Section 10.3, followed by a numerical example in Section 10.4. Concluding remarks are addressed in Section 10.5.

## 10.2 Generalized unitary interactor matrices

For multivariable processes with non-invertible zeros, an interactor matrix which can also factorize the non-invertible zeros in addition to the infinite zeros is desirable. The optimal control law corresponding to the admissible minimum variance and minimum ISE control requires such an interactor matrix (Tsiligiannis and Svoronos, 1989).

**Definition 3** *An interactor matrix,  $D_G$ , satisfying the following four conditions, is defined as the generalized unitary interactor matrix of  $T$ .*

1. *The unitary condition is held:  $D_G^T(q^{-1})D_G(q) = I$ .*
2. *There exists a non-singular constant matrix  $K_{inf} \in R^{n \times m}$  such that*

$$\lim_{q^{-1} \rightarrow 0} D_G T = K_{inf} \quad (10.1)$$

3. There exist non-singular matrices  $K_i \in R^{n \times m}$  such that

$$\lim_{q^{-1} \rightarrow 1/\sigma_i} D_G T = K_{f_i} \quad (i = 1, \dots, s) \quad (10.2)$$

where  $\sigma_i$ , ( $i = 1, \dots, s$ ) are the non-invertible zeros of  $T$ , i.e.  $|\sigma_i| > 1$ .

4. The poles of  $D_G$  in terms of  $q$  are  $\{\sigma_1, \dots, \sigma_s\}$  (including the multiplicities).

The algorithm for factorization of the unitary interactor matrix as discussed in Chapter 4 extracts infinite zeros from the transfer function matrix. To extract finite non-invertible zeros, a bilinear transformation as introduced by Tsiligiannis and Svoronos(1989) can be used:

$$q^{-1} = \frac{1 + p^{-1}\sigma}{p^{-1} + \sigma}$$

and therefore

$$p^{-1} = \frac{1 - \sigma q^{-1}}{q^{-1} - \sigma}$$

where  $\sigma$  is an unstable zero, and  $p^{-1}$  is a map of  $q^{-1}$ . For any non-minimum phase zero  $q^{-1} = 1/\sigma$ , this mapping transforms the finite zero in the  $q$ -domain to an infinite zero in the  $p$ -domain, i.e. from  $q^{-1} = 1/\sigma$  to  $p^{-1} = 0$ . Therefore existing methods for extraction of the infinite zeros can be applied. This also proves existence of the generalized unitary interactor matrix.

The generalized unitary interactor can therefore be factored as

$$D_G = D_f D_{inf}$$

where  $D_{inf}$  is a unitary interactor matrix representing infinite zeros of  $T$ , and  $D_f$  is a unitary interactor matrix representing non-invertible zeros of  $T$ . The order ( $d$ ) of the interactor matrix  $D_G$  is defined as the order of  $D_{inf}$ . According to this procedure, each p-q transformation factors out one unstable zero. To factor out all  $\{\sigma_1, \dots, \sigma_s\}$  non-invertible zeros,  $s$  steps of such transformation are required. Each step involves a simple algebraic manipulation.  $D_f$  can therefore be written as

$$D_f = D_{f_s} D_{f_{s-1}} \cdots D_{f_1}$$

The “Inner-Outer” factorization (Chu, 1985) can also factor the unstable and infinite zeros. It involves solution of an algebraic Riccati equation in the state space framework. The generalized unitary interactor matrix provides an alternative solution to the inner-outer factorization.

**Example 9** Consider the following system from Tsiligiannis and Svoronos(1989):

$$T = \begin{bmatrix} \frac{0.6q^{-1}}{1-0.4q^{-1}} & \frac{0.5q^{-1}}{1-0.5q^{-1}} \\ \frac{0.6q^{-1}}{1-0.5q^{-1}} & \frac{0.6q^{-1}}{1-0.4q^{-1}} \end{bmatrix}$$

Tsiligiannis and Svoronos(1989) have shown that a lower triangular generalized interactor matrix can be factored as

$$\begin{bmatrix} q & 0 \\ -1.0954q \frac{1-1.5477q}{q-1.5477} & q \frac{1-1.5477q}{q-1.5477} \end{bmatrix}$$

The optimal control law based on such lower triangular interactor matrix results in optimal (minimum variance) control of the first variable, and conditional optimal control of the remaining variables (Tsiligiannis and Svoronos, 1989). Therefore, importance of each variable depends on the order it is stacked in the output vector. Different ordering of the output vector results in the different optimal control laws. On the other hand, as shown in the next section a generalized unitary interactor matrix gives an optimal control law which minimizes the LQ objective function or  $H_2$  norm and therefore the resulting optimal control law is unique.

Now we show a procedure for factoring a generalized unitary interactor matrix from this process. The transfer function matrix has a simple time-delay structure or a simple interactor matrix  $D_{inf} = qI$  (therefore  $d = 1$ ), and an unstable zero at  $1 + \sqrt{0.3} = 1.5477$ . If the infinite zeros are factored out, then the transfer function matrix with finite (stable and unstable) zeros is obtained as

$$\begin{bmatrix} \frac{0.6q^{-1}}{1-0.4} & \frac{0.5}{1-0.5q^{-1}} \\ \frac{0.6}{1-0.5q^{-1}} & \frac{0.6}{1-0.4q^{-1}} \end{bmatrix}$$

Mapping from q-domain to p-domain using the bilinear transformation

$$q^{-1} = \frac{1 + 1.5477p^{-1}}{1.5477 + p^{-1}}$$

yields the transfer function matrix ( $\tilde{T}_f$ ) in the  $p$ -domain as

$$T = \begin{bmatrix} \frac{0.6(1.5477+p^{-1})}{1.1477+0.3809p^{-1}} & \frac{0.5(1.5477+p^{-1})}{1.0477+0.2262p^{-1}} \\ \frac{0.6(1.5477+p^{-1})}{1.0477+0.2262p^{-1}} & \frac{0.6(1.5477+p^{-1})}{1.1477+0.3809p^{-1}} \end{bmatrix}$$

This can be further written in the Markov parameter form as:

$$T = \begin{bmatrix} 0.8091 & 0.7386 \\ 0.8863 & 0.8091 \end{bmatrix} + \begin{bmatrix} 0.2542 & 0.3178 \\ 0.3814 & 0.2542 \end{bmatrix} p^{-1} + \dots$$

The first Markov parameter matrix is rank defective, therefore there is at least one infinite zero in  $T$  in the  $p$ -domain. Using the first two Markov parameter matrices to form a block Markov parameter matrix yields

$$\Lambda^{(0)} = \begin{bmatrix} 0.8091 & 0.7386 \\ 0.8863 & 0.8091 \\ 0.2542 & 0.3178 \\ 0.3814 & 0.2542 \end{bmatrix}$$

Applying the algorithm given by equations (A.4) to (A.7) to  $\Lambda^{(0)}$ , one can then proceed as follows:

For  $i = 1$  (iteration #1):  $r_1 = 1, k_1 = 1,$

$$Q^{(1)} = \begin{bmatrix} -0.7385 & 0.6742 \\ -0.6742 & -0.7385 \end{bmatrix}$$

$$U^{(1)} = \begin{bmatrix} 0 & 0 \\ 1 & 0 \\ 0 & 1 \\ 0 & 0 \end{bmatrix}$$

$$U^{(1)}(q) = \begin{bmatrix} 0 & 1 \\ p & 0 \end{bmatrix}$$

$$\Lambda^{(1)} = \begin{bmatrix} -1.2001 & -1.0955 \\ 0.0694 & -0.0633 \\ -0.4531 & -0.4020 \\ 0 & 0 \end{bmatrix}$$

Because  $\text{rank}(\Lambda^{(1)}) = 2 = \min(n, m)$ , the algorithm terminates and the unitary interactor matrix given by equations (A.2) and (A.3) is calculated as

$$D_f(p) = \begin{bmatrix} -0.6742 & -0.7385 \\ -0.7385p & 0.6742p \end{bmatrix}$$

Substituting the bilinear transformation

$$p^{-1} = \frac{1 - 1.5477q^{-1}}{q^{-1} - \sigma}$$

back into  $D_f(p)$  yields the unitary interactor matrix in  $q$ -domain which contains the unstable zero of  $T$ :

$$D_f = \begin{bmatrix} -0.6742 & -0.7385 \\ \frac{-0.7385(1-1.5477q)}{q-1.5477} & \frac{0.6742(1-1.5477q)}{q-1.5477} \end{bmatrix}$$

A generalized unitary interactor matrix, containing both infinite and finite non-invertible zeros, can therefore be calculated as

$$D_G = D_f D_{inf} = \begin{bmatrix} -0.6742q & -0.7385q \\ \frac{-0.7385(1-1.5477q)q}{q-1.5477} & \frac{0.6742(1-1.5477q)q}{q-1.5477} \end{bmatrix}$$

## 10.3 Feedback controller performance assessment of MIMO processes with non-invertible zeros

### 10.3.1 Performance assessment with admissible minimum variance control as the benchmark

For MIMO systems with non-invertible zeros, the LQ problem can be solved via spectral factorization (Youla and Bongiorno, 1985; Harris and MacGregor, 1987; Peng and Kinnaert, 1992), via optimal  $H_2$  control (Morari and Zafiriou, 1989; Dahleh and Diaz-Bobillo, 1995) or via the state space approach (Kwakernaak and Sivan, 1972). Alternatively, one may solve it through a simple and intuitive approach as discussed in Astrom and Wittenmark(1990) . This last approach provides an explicit expression for the feedback controller invariant terms, and is the most suitable approach for seeking

the feedback control invariant term (benchmark control performance) for control loop performance assessment. Astrom and Wittenmark(1990) have shown that this admissible minimum variance control problem for SISO systems can be solved by minimizing the filtered variable  $y_t^f$ . The filter is an all-pass factor, which removes all zeros that are outside the unit circle from the input-output transfer function while keeping the spectrum unchanged. The spectrum of  $y_t^f$  is therefore the same as that of  $y_t$ . Minimization of  $Var(y_t^f)$  is equivalent to minimization of  $Var(y_t)$ . The generalized unitary interactor matrix is also an all-pass factor and can serve as such a filter for the MIMO system as well. Thus the methodology used in the SISO case can be extended to the MIMO case in an intuitive way. The following theorem is an extension to Astrom and Wittenmark(1990), or to Goodwin and Sin(1984) to consider the generalized unitary interactor matrix for the solution of the admissible minimum variance control law. The admissible minimum variance control law can also be derived from the optimal  $H_2$  control law. This is discussed in Section 10.3.2.

**Theorem 9** *Consider a MIMO process with unstable zeros*

$$Y_t = TU_t + Na_t \quad (10.3)$$

*The control objective is to minimize the LQ objective function defined by*

$$J = E(Y_t^T Y_t) \quad (10.4)$$

*Then the admissible minimum variance control law is given by*

$$U_t = -\tilde{T}^{-1} R_{mp} (F + q^{-d} R_{nmp})^{-1} (q^{-d} D_G) Y_t \quad (10.5)$$

where  $\tilde{T} = D_G T$ ;  $d$  is the order of the interactor matrix;  $D_G$  is the generalized unitary interactor;  $F$ ,  $R_{mp}$  and  $R_{nmp}$  are derived from the Diophantine identity:

$$q^{-d} D_G N = \underbrace{F_0 + F_1 q^{-1} + \dots + F_{d-1} q^{-d+1}}_F + q^{-d} \underbrace{(R_{nmp} + R_{mp})}_R \quad (10.6)$$

where  $F_i$  (for  $i = 0, 1, \dots, d-1$ ) are constant coefficient matrices,  $R$  is the remaining proper transfer matrix,  $R_{nmp}$  contains all unstable poles of  $R$  after partial fraction expansion, and  $R_{mp}$  is the remaining term of  $R$  after the partial fraction expansion.



**Proof:** Multiplying both sides of equation (10.3) by  $q^{-d}D_G$  yields

$$q^{-d}D_G Y_t = \tilde{T}U_{t-d} + q^{-d}D_G N a_t \quad (10.7)$$

Substituting equation (10.6) into equation (10.7) yields

$$q^{-d}D_G Y_t = \tilde{T}U_{t-d} + F a_t + q^{-d}R_{nmp}a_t + q^{-d}R_{mp}a_t \quad (10.8)$$

Since  $G_G^T(q^{-1})G_G(q) = I$  by the definition of the generalized unitary interactor, minimization of  $E[(q^{-d}D_G Y_t)^T(q^{-d}D_G Y_t)]$  is equivalent to minimization of  $E[Y_t^T Y_t]$  for any admissible feedback control.

The following interpretation of the unstable operator follows from Astrom and Wittenmark(1990) (see also Wiener(1949)). Consider the operator  $1/(1 + aq^{-1})$  where  $|a| > 1$ . This operator is normally interpreted as a causal unstable operator. Because  $|a| > 1$ , and the shift operator has the norm  $|q| = 1$ , the series expansion

$$\frac{1}{1 + aq^{-1}} = \frac{1}{a} \frac{q}{1 + q/a} = \frac{q}{a} [1 - \frac{1}{a}q + \frac{1}{a^2}q^2 - \dots]$$

converges. Thus the operator  $1/(1 + aq^{-1})$  can be interpreted as a noncausal stable operator. Therefore the term,  $q^{-d}R_{nmp}$ , in equation (10.8) can be expanded in terms of the 'q' operator. For example, consider  $R_{nmp} = 1/(1 + aq^{-1})$ . Then the expansion

$$\frac{q^{-d}}{1 + aq^{-1}} = \frac{1}{a} \frac{q^{-d+1}}{1 + q/a} = \frac{1}{a} [q^{-d+1} - \frac{1}{a}q^{-d+2} + \frac{1}{a^2}q^{-d+3} - \dots]$$

converges, and the most recent term in this expansion is  $\frac{1}{a}q^{-d+1}$  that cannot be controlled by the control action,  $U_{t-d} = U_t q^{-d}$ , which is one step earlier. Clearly the term  $F a_t$  is also independent of  $U_{t-d}$ . Therefore the optimal control law is obtained by letting the sum of the remaining terms in equation (10.8) to zero. This yields

$$U_{t-d} = -\tilde{T}^{-1}R_{mp}a_{t-d} \quad (10.9)$$

or

$$U_t = -\tilde{T}^{-1}R_{mp}a_t \quad (10.10)$$

Substituting equation (10.10) into equation (10.8) yields

$$q^{-d}D_G Y_t = (F + q^{-d}R_{nmp})a_t \quad (10.11)$$

Thus

$$a_t = (F + q^{-d}R_{nmp})^{-1}(q^{-d}D_G)Y_t \quad (10.12)$$

Substituting equation (10.12) into equation (10.10) yields the admissible minimum variance control law:

$$U_t = -\tilde{T}^{-1}R_{mp}(F + q^{-d}R_{nmp})^{-1}(q^{-d}D_G)Y_t \quad (10.13)$$

■

From equation (10.11), the closed-loop response under the admissible minimum variance control is given by

$$Y_t = (q^{-d}D_G)^{-1}(F + q^{-d}R_{nmp})a_t \triangleq G_{min}a_t \quad (10.14)$$

Now we are in the position to show an approach to estimate the admissible minimum variance control variance from closed-loop data using the results in Theorem 9. It is clear from the proof of Theorem 9 that for such a purpose, one needs to estimate the terms  $F$  and  $R_{nmp}$  from closed-loop data in order to obtain equation (10.11) or equation (10.14).

If  $D_G$  contains only infinite zeros, then equation (10.11) reduces to

$$q^{-d}D_G Y_t = F a_t$$

Any non-optimal feedback control will inflate the process by adding an extra term to this equation as discussed in Chapter 8, i.e.

$$q^{-d}D_G Y_t = F a_t + L a_{t-d}$$

where  $L$  is a proper rational transfer function matrix and is feedback control dependent. The correlation analysis between the interactor-filtered variable  $q^{-d}D_G Y_t$  and  $a_t$  yields the feedback controller-invariant term  $F$ . Thus a simple FCOR based correlation analysis yields the benchmark performance. However, if  $D_G$  contains unstable poles (non-invertible zeros of  $T$ ), then equation (10.11) is the closed-loop response under admissible minimum variance control. It is evident from the proof of Theorem 9 that the terms  $F$  and  $R_{nmp}$

are feedback control invariant, and any non-optimal feedback control will add an extra term to equation (10.11) as

$$q^{-d}D_G Y_t = F a_t + R_{nmp} a_{t-d} + L a_{t-d}$$

where  $L$  is feedback control dependent.

To estimate the terms  $F$  and  $R_{nmp}$ , we shall fit  $Y_t$  by a time series model as

$$Y_t = G_d a_t$$

Then multiply  $G_d$  by  $q^{-d}D_G$  to obtain the interactor-filtered closed-loop transfer function matrix  $G'_d$ , i.e.

$$G'_d = q^{-d}D_G G_d$$

Let  $G'_d$  be expanded to

$$G'_d = F a_t + \Phi a_{t-d}$$

where  $F = F_0 + F_1 q^{-1} + \dots + F_{d-1} q^{-d+1}$ , and  $\Phi$  is the remaining rational proper transfer function matrix of  $G'_d$ . Finally, from  $\Phi$  one can obtain  $R_{nmp}$  as

$$R_{nmp} = \{\Phi\}_+$$

where  $\{\cdot\}_+$  denotes that after a partial fraction expansion of the operand, only the terms corresponding to unstable poles are retained. With the knowledge of  $F$  and  $R_{nmp}$ , the closed-loop response under the admissible minimum variance control can be calculated from equation (10.14).

The algorithm to calculate the admissible minimum variance control response for feedback control performance assessment of nonminimum phase processes is summarized in Table 10.1

### 10.3.2 Alternative proof of admissible minimum variance control

To justify the proof and also the interpretation of causal unstable operators adopted in Theorem 9, we compare the control law obtained in Theorem 9 with the optimal  $H_2$  control law. Morari and Zafiriou(1989) have solved minimum  $H_2$ -norm control for the

Table 10.1: The procedure for calculation of the benchmark performance of MIMO processes with non-invertible zeros

1. estimate or factorize the generalized unitary interactor matrix from  $T$  as  $D_G$ ;
2. fit routine operating data  $Y_t$  by a time series model to obtain  $G_d$ ;
3. multiply  $G_d$  by  $q^{-d}D_G$  to obtain  $G'_d = q^{-d}D_G G_d$ , where  $d$  is the order of the interactor matrix;
4. expand  $G'_d$  into

$$G'_d = \underbrace{F_0 + F_1 q^{-1} + \cdots + F_{d-1} q^{-(d-1)}}_F + q^{-d} \phi$$

where  $F_i$  for  $(i = 1, 2, \dots, d-1)$  are constant coefficient matrices, and  $\phi$  is the remaining term after the expansion;

5. using partial fraction expansion,  $\phi$  can be expanded into

$$\phi = R_{nmp} + L$$

where  $R_{nmp}$  contains all unstable poles which are the non-invertible zeros of  $T$ , and  $L$  is the remaining term after the partial fraction expansion. Then the process under admissible minimum variance control can be written as

$$Y_t = q^d D_G^{-1} (F + q^{-d} R_{nmp}) a_t \quad (10.15)$$

MIMO system with non-invertible zeros. In this section, we show that the admissible minimum variance control law given in Theorem 9 is the same as the optimal  $H_2$  control law given by Morari and Zafiriou(1989) for stochastic systems.

**Theorem 10 (Morari and Zafiriou, 1989):** *Consider the MIMO process with non-invertible zeros,*

$$Y_t = TU_t + Na_t$$

*Factor  $T$  into all-pass portion and minimum-phase portion*

$$T = D_G^{-1}\tilde{T}$$

*where  $D_G^{-1}$  or  $D_G$  is an all-pass factor. Similarly factor  $N$  into*

$$N = \tilde{N}N_p$$

*where  $N_p$  is an all-pass factor. Then, the  $H_2$  optimal control is given by*

$$Q^* = q\tilde{T}^{-1}\{q^{-1}D_G\tilde{N}\}_* \tilde{N}^{-1}$$

*where  $Q^*$  is the controller transfer function matrix in the IMC framework. Its relation with the conventional feedback control  $Q$  ( $U_t = -QY_t$ ) is given by*

$$Q = Q^*(I - TQ^*)^{-1}$$

*The operator  $\{.\}_*$  denotes that after a partial fraction expansion of the operand, only the strictly proper terms are retained except those corresponding to the poles of  $D_G$ .*

Assume  $N$  has no zeros outside unit the circle. This is a general assumption for the stochastic system (Astrom and Wittenmark, 1990; Goodwin and Sin, 1984), since any unstable zeros in  $N$  can be replaced by their image (reciprocal) without changing the disturbance spectrum. With this assumption, the control law under conventional feedback control framework can be written as

$$Q = Q^*(I - TQ^*)^{-1} \quad (10.16)$$

$$\begin{aligned} &= q\tilde{T}^{-1}\{q^{-1}D_GN\}_* N^{-1}(I - qT\tilde{T}^{-1}\{q^{-1}D_GN\}_* N^{-1})^{-1} \\ &= q\tilde{T}^{-1}\{q^{-1}D_GN\}_* (N - qD_G^{-1}\{q^{-1}D_GN\}_*)^{-1} \\ &= q\tilde{T}^{-1}\{q^{-1}D_GN\}_* (D_GN - q\{q^{-1}D_GN\}_*)^{-1} D_G \end{aligned} \quad (10.17)$$

With use of the Diophantine identity:

$$q^{-d}D_G N = \underbrace{F_0 + F_1 q^{-1} + \dots + F_{d-1} q^{-d+1}}_F + q^{-d} \underbrace{(R_{nmp} + R_{mp})}_R$$

we have

$$\begin{aligned} q^{-1}D_G N &= q^{d-1}(q^{-d}D_G N) \\ &= q^{d-1}F + q^{-1}R_{nmp} + q^{-1}R_{mp} \end{aligned} \quad (10.18)$$

In equation (10.18), only the term  $q^{-1}R_{mp}$  is strictly proper without containing poles of  $D_G$ . Note that poles of  $D_G$  are the non-invertible zeros of  $T$ . Therefore

$$\{q^{-1}D_G N\}_* = q^{-1}R_{mp} \quad (10.19)$$

and consequently

$$D_G N - q\{q^{-1}D_G N\}_* = q^d F + R_{nmp} \quad (10.20)$$

Substituting equations (10.19) and (10.20) into equation (10.17) yields

$$\begin{aligned} Q &= q\tilde{T}^{-1}q^{-1}R_{mp}(q^d F + R_{nmp})^{-1}D_G \\ &= \tilde{T}^{-1}R_{mp}(F + q^{-d}R_{nmp})^{-1}(q^{-d}D_G) \end{aligned}$$

Thus the optimal  $H_2$  control law expressed in the conventional feedback control framework can be written as

$$U_t = -\tilde{T}^{-1}R_{mp}(F + q^{-d}R_{nmp})^{-1}(q^{-d}D_G)Y_t$$

which is the same as the admissible minimum variance control law in equation (10.13).

## 10.4 Numerical example

**Example 10** Consider the same system as in Example 9 with the disturbance transfer function matrix as:

$$N = \begin{bmatrix} \frac{1}{1-0.5q^{-1}} & \frac{-0.6}{1-0.5q^{-1}} \\ \frac{0.5}{1-0.5q^{-1}} & \frac{1}{1-0.5q^{-1}} \end{bmatrix}$$

A generalized unitary interactor matrix has been factored in Example 9 as

$$D_G = D_f D_{inf} = \begin{bmatrix} -0.6742q & -0.7385q \\ \frac{-0.7385(1-1.5477q)q}{q-1.5477} & \frac{0.6742(1-1.5477q)q}{q-1.5477} \end{bmatrix}$$

With the order of the interactor matrix  $d = 1$ , we have the Diophantine identity

$$\begin{aligned} q^{-d} D_G N &= q^{-1} D_G N \\ &= \underbrace{\begin{bmatrix} -1.0434 & -0.3340 \\ 0.6213 & -1.7293 \end{bmatrix}}_F + q^{-1} \underbrace{\begin{bmatrix} \frac{-0.5217}{1-0.5q^{-1}} & \frac{-0.167}{1-0.5q^{-1}} \\ \frac{0.8708-0.4808q^{-1}}{(1-0.5q^{-1})(1-1.5477q^{-1})} & \frac{-2.4238+1.3383q^{-1}}{(1-0.5q^{-1})(1-1.5477q^{-1})} \end{bmatrix}}_R \\ &= \underbrace{\begin{bmatrix} -1.0434 & -0.3340 \\ 0.6213 & -1.7293 \end{bmatrix}}_F + q^{-1} \underbrace{\begin{bmatrix} 0 & 0 \\ \frac{0.8275}{1-1.5477q^{-1}} & \frac{-2.3032}{1-1.5477q^{-1}} \end{bmatrix}}_{R_{nmp}} + q^{-1} \underbrace{\begin{bmatrix} \frac{-0.5217}{1-0.5q^{-1}} & \frac{-0.167}{1-0.5q^{-1}} \\ \frac{0.0433}{1-0.5q^{-1}} & \frac{-0.1206}{1-0.5q^{-1}} \end{bmatrix}}_{R_{mp}} \\ &= \underbrace{\begin{bmatrix} -1.0434 & -0.3340 \\ \frac{0.6213-0.1340q^{-1}}{1-1.5477q^{-1}} & \frac{-1.7293+0.3731q^{-1}}{1-1.5477q^{-1}} \end{bmatrix}}_{F+q^{-d}R_{nmp}} + q^{-1} \underbrace{\begin{bmatrix} \frac{-0.5217}{1-0.5q^{-1}} & \frac{-0.1670}{1-0.5q^{-1}} \\ \frac{0.0433}{1-0.5q^{-1}} & \frac{-0.1206}{1-0.5q^{-1}} \end{bmatrix}}_{R_{mp}} \end{aligned} \quad (10.21)$$

The closed-loop response under admissible minimum variance control is therefore

$$q^{-d} D_G Y_t = (F + q^{-d} R_{nmp}) a_t$$

Substituting numerical values, we have

$$\begin{bmatrix} -0.6742 & -0.7385 \\ \frac{-0.7385(q^{-1}-1.5477)}{1-1.5477q^{-1}} & \frac{0.6472(q^{-1}-1.5477)}{1-1.5477q^{-1}} \end{bmatrix} Y_t = \begin{bmatrix} -1.0434 & -0.3340 \\ \frac{0.6213-0.1340q^{-1}}{1-1.5477q^{-1}} & \frac{-1.7293+0.3731q^{-1}}{1-1.5477q^{-1}} \end{bmatrix} a_t$$

This can be simplified as

$$\begin{aligned} &\begin{bmatrix} -0.6742 & -0.7385 \\ -0.7385(q^{-1}-1.5477) & 0.6472(q^{-1}-1.5477) \end{bmatrix} Y_t \\ &= \begin{bmatrix} -1.0434 & -0.3340 \\ 0.6213-0.1340q^{-1} & -1.7293+0.3731q^{-1} \end{bmatrix} a_t \end{aligned} \quad (10.22)$$

Equation (10.22) represents the theoretical closed-loop response under admissible minimum variance control. Assume, for simplicity, that  $\text{Var}(a_t) = I$ , then the achievable

minimum variance can be calculated from equation (10.22) as

$$\text{Var}(Y_t)|_{mv} = \begin{bmatrix} 1.6137 & -0.3521 \\ -0.3521 & 1.4988 \end{bmatrix} \triangleq \Sigma_{ach} \quad (10.23)$$

Define the individual output variance under the admissible minimum variance control as

$$[\sigma_{1,ach}^2, \sigma_{2,ach}^2] \triangleq \text{diag}\{\Sigma_{ach}\} \quad (10.24)$$

Now consider calculation of this achievable minimum variance from the closed-loop transfer function under feedback control. An IMC controller (Tsiligiannis and Svoronos, 1989) given by

$$Q^* = \frac{(1 - 0.4q^{-1})(1 - 0.5q^{-1})}{(1 - 0.452q^{-1})(q^{-1} - 1.5477)} \begin{bmatrix} 7.78(1 - 0.357q^{-1}) & -8.333(1 - 0.4q^{-1}) \\ -12.432(1 - 0.517q^{-1}) & 10(1 - 0.5q^{-1}) \end{bmatrix}$$

is implemented on the process. The controller transfer function matrix  $Q^*$  denotes the control under IMC framework. Under IMC control, the closed-loop transfer function, which can be estimated via time series analysis in practice, is written as

$$\begin{aligned} G_d &= (I - TQ^*)N \\ &= \begin{bmatrix} 1 - q^{-1} & 0 \\ \frac{-2.7908(1-q^{-1})q^{-1}}{1.5477-q^{-1}} & \frac{1.5477(1-q^{-2})}{1.5477-q^{-1}} \end{bmatrix} \begin{bmatrix} \frac{1}{1-0.5q^{-1}} & \frac{-0.6}{1-0.5q^{-1}} \\ \frac{0.5}{1-0.5q^{-1}} & \frac{1}{1-0.5q^{-1}} \end{bmatrix} \end{aligned} \quad (10.25)$$

The interactor-filtered closed-loop transfer function matrix can be written as

$$\begin{aligned} G'_d &= q^{-d} D_G G_d = q^{-1} D_G G_d \\ &= \begin{bmatrix} \frac{-1.6150+3.7787q^{-1}-2.1637q^{-2}}{(1-0.5q^{-1})(1.5477-q^{-1})} & \frac{-0.5169-2.2672q^{-1}+2.7841q^{-2}}{(1-0.5q^{-1})(1.5477-q^{-1})} \\ \frac{0.6213-0.6213q^{-2}}{(1-0.5q^{-1})(1-1.5477q^{-1})} & \frac{-1.7293+1.7293q^{-2}}{(1-0.5q^{-1})(1-1.5477q^{-1})} \end{bmatrix} \\ &= \underbrace{\begin{bmatrix} -1.0434 & -0.3340 \\ 0.6213 & -1.7293 \end{bmatrix}}_F + q^{-1} \underbrace{\begin{bmatrix} \frac{1.9277-1.6420q^{-1}}{(1-0.5q^{-1})(1.5477-q^{-1})} & \frac{-2.8596+2.9511q^{-1}}{(1-0.5q^{-1})(1.5477-q^{-1})} \\ \frac{1.2722-1.1021q^{-1}}{(1-0.5q^{-1})(1-1.5477q^{-1})} & \frac{-3.5411+3.0676q^{-1}}{(1-0.5q^{-1})(1-1.5477q^{-1})} \end{bmatrix}}_R \\ &= \underbrace{\begin{bmatrix} -1.0434 & -0.3340 \\ 0.6213 & -1.7293 \end{bmatrix}}_F + q^{-1} \underbrace{\begin{bmatrix} 0 & 0 \\ \frac{0.8275}{1-1.5477q^{-1}} & \frac{-2.3032}{1-1.5477q^{-1}} \end{bmatrix}}_{R_{nmp}} + q^{-1} \underbrace{\begin{bmatrix} \frac{-0.5217}{1-0.5q^{-1}} & \frac{-0.167}{1-0.5q^{-1}} \\ \frac{0.0433}{1-0.5q^{-1}} & \frac{-0.1206}{1-0.5q^{-1}} \end{bmatrix}}_L \end{aligned}$$



$$\begin{aligned}
&= \underbrace{\begin{bmatrix} -1.0434 & -0.3340 \\ \frac{0.6213-0.1340q^{-1}}{1-1.5477q^{-1}} & \frac{-1.7293+0.3731q^{-1}}{1-1.5477q^{-1}} \end{bmatrix}}_{F+q^{-d}R_{nmp}} + \\
&\quad + q^{-1} \underbrace{\begin{bmatrix} \frac{1.9277-1.6420q^{-1}}{(1-0.5q^{-1})(1.5477-q^{-1})} & \frac{-2.8596+2.9511q^{-1}}{(1-0.5q^{-1})(1.5477-q^{-1})} \\ \frac{0.4448}{1-0.5q^{-1}} & \frac{-1.2380}{1-0.5q^{-1}} \end{bmatrix}}_L
\end{aligned}$$

The first term on the left hand side of the last equation is the same as that given in equation (10.21). Therefore, one can see that the achievable minimum variance term  $F + q^{-d}R_{nmp}$  can indeed be estimated from closed-loop data. In practice, estimation of this term requires time series analysis of closed-loop data  $Y_t$  and the *a priori* knowledge of the generalized unitary interactor matrix  $D_G$ .

By the assumption that  $Var(a_t) = I$ , the closed-loop output variance can be calculated from equation (10.25) as

$$Var(Y_t) = \begin{bmatrix} 1.8133 & -1.1546 \\ -1.1546 & 9.5164 \end{bmatrix} \triangleq \Sigma_Y \quad (10.26)$$

Comparing equation (10.26) to equation (10.23), allows one to compare the actual variance with the achievable minimum variance. The objective function based performance index as defined in Chapter 8 can be calculated as

$$\eta \triangleq \frac{\min(E[Y_t^T Y_t])}{E[Y_t^T Y_t]} = \frac{tr \Sigma_{ach}}{tr \Sigma_Y} = 0.27$$

which indicates an overall MIMO feedback control performance. With the maximum performance index as 1 and poorest performance index as 0, this index indicates relatively poor performance. The reason is: in Tsiligiannis and Svoronos (1989), the controller is actually designed for setpoint tracking of a step change but not for regulating the disturbances as assumed in this example. Nevertheless, output #1 is close to its lower bound with the individual performance index as

$$\eta_1 \triangleq \frac{\sigma_{1,ach}^2}{\sigma_{y_1}^2} = \frac{1.6137}{1.8133} = 0.89$$

where  $\sigma_{y_1}^2$  is the individual output variance defined by

$$[\sigma_{y_1}^2, \sigma_{y_2}^2] \triangleq diag(\Sigma_Y)$$

Output #2, on the other hand, is far away from its lower bound with the individual performance index as

$$\eta_2 \triangleq \frac{\sigma_{2,ach}^2}{\sigma_{y_2}^2} = \frac{1.4988}{9.5164} = 0.16$$

Thus, the controller has good performance in regulating output #1 but poor performance in regulating output #2. The reason is, as shown in Tsiligiannis and Svoronos (1989), a lower triangular interactor matrix was used for the control design, and therefore good performance of the first output should be expected.

## 10.5 Conclusions

A generalized unitary interactor matrix has been introduced in this chapter. The admissible minimum variance control law derived by using the generalized unitary has been shown to be identical to the optimal  $H_2$  control. With *a priori* knowledge of the generalized unitary interactor matrix, the admissible minimum variance control performance can be estimated from routine operating data, and subsequently used for control loop performance assessment. A numerical example demonstrates the applicability of the proposed method.

## Chapter 11

# A Unified Approach to Performance Assessment

### 11.1 Introduction

Feedback control performance assessment with minimum variance control as the benchmark has been discussed in the earlier chapters. It has been shown that this technique is an efficient and also the most convenient tool to monitor industrial processes which can have hundreds and even thousands of control loops.

However, Eriksson and Isaksson (1994) have shown that the aforementioned technique gives an inadequate measure of the performance if the aim is not stochastic control, but, for example, step disturbance rejection or setpoint tracking. Tyler and Morari(1995) have a similar claim on this issue. One objective of this chapter is to discuss this issue and extend Harris' idea of control loop performance assessment to cover practical issues such as deterministic disturbances and setpoint changes. It is shown that many practical problems such as those posed by Eriksson and Isaksson and others can be readily solved under the same framework as proposed by Harris (1989) via appropriate formulation of the initial problem. Another objective of this chapter is to unify the performance assessment of

---

<sup>1</sup> A part of this chapter has been accepted for presentation at the 1997 IFAC Advanced Chemical Process Control Symposium.

both stochastic and deterministic systems under the  $H_2$  norm framework. Therefore, the results developed in the earlier chapters can be extended to more general cases.

This chapter is organized as follows. Assessment of setpoint tracking performance is discussed in Section 11.2. In Section 11.3, deterministic disturbances are explained under the stochastic framework. Performance assessment of feedback controllers for regulating both stochastic and deterministic disturbances is discussed in Section 11.4, and the treatment on pure deterministic disturbances is discussed in Section 11.5. In Section 11.6, a unified approach for performance assessment is proposed. Simulation example is given in Section 11.7, followed by concluding remarks in Section 11.8.

## 11.2 Setpoint tracking problem

As discussed in the previous chapters, the standard formulation of performance assessment using minimum variance control as the benchmark is shown in Figure 11.1 by assuming  $Y_t^{sp} = 0$  or  $\xi_t = 0$ , where  $N$ ,  $Q$ ,  $T$  and  $M$  are disturbance, controller, plant and setpoint transfer function matrices respectively;  $a_t$  is white noise with zero mean; For this assumption it follows from figure 11.1 that

$$Y_t = -TQY_t + Na_t \quad (11.1)$$

Under this formulation, routine operating data  $Y_t$  can be used for performance assessment. However, this formulation is of interest only when applied for performance assessment of the regulatory controller. In some cases the setpoint tracking performance may also be of interest.

Define  $\epsilon_t = Y_t^{sp} - Y_t$  as the setpoint tracking error. Assuming  $a_t = 0$  for consideration of pure setpoint tracking problem<sup>2</sup>, it follows from figure 11.1 that

$$\epsilon_t = -TQ\epsilon_t + M\xi_t \quad (11.2)$$

where the setpoint,  $Y_t^{sp}$ , can be regarded as the realization of a white noise sequence,  $\xi_t$ , as input into a rational transfer function matrix,  $M$ . It will be shown that a “deterministic”

---

<sup>2</sup>If  $a_t \neq 0$ , the setpoint signal needs to be considered with other disturbances. This issue will be discussed in the following sections.

setpoint can also be produced by filtering a white noise input. One may note that equation (11.2) has the same form as equation (11.1), i.e. the setpoint tracking problem can be formulated as a regulatory control problem by a simple change of variables. The only difference is the data used for analysis. For the setpoint tracking problem, one uses  $\epsilon_t = Y_t^{sp} - Y_t$ , while either  $\epsilon_t$  or  $Y_t$  can be used for the performance assessment of the regulatory control problem. In the sequel, we will focus on the regulatory control problem, i.e. we consider performance assessment of  $Y_t$  with  $Y_t^{sp} = 0$ . If setpoint tracking is also considered, then  $Y_t$  simply needs to be replaced by the tracking error  $\epsilon_t = Y_t^{sp} - Y_t$ , and the results developed in the previous chapters can be used.

### 11.3 Deterministic disturbances occurring at random time

MacGregor et al.(1984) have shown that many deterministic disturbances such as the step, ramp and exponential changes can be modeled as autoregressive-integrated-moving-average (ARIMA) processes. The only difference between deterministic and stochastic disturbances is the probability distribution of the *shocks* or the white-noise sequence. This point is illustrated by using the following example.

Three (ARIMA) filters are studied in this example, i.e. the integral filter  $1/(1 - q^{-1})$ , the double integral filter  $1/(1 - q^{-1})^2$  and the sinusoidal filter  $\sin(\omega)q^{-1}/(1 - 2q^{-1}\cos(\omega) + q^{-2})$ . Figure 11.2 shows probability density function of the shock in a special case. It is symmetric but not normal-distributed. The shock takes only three values,  $-1, 0$  and  $1$  with 99.98% probability density concentrated at the point 0. Figure 11.3 shows the realization

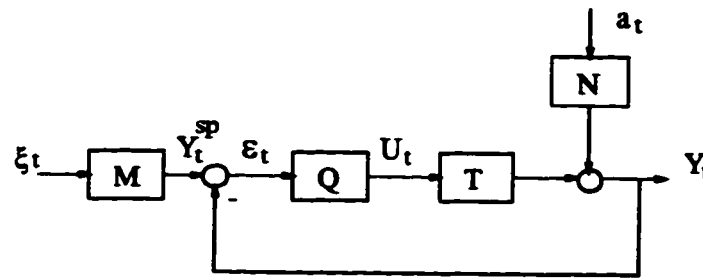


Figure 11.1: Block diagram of closed-loop process

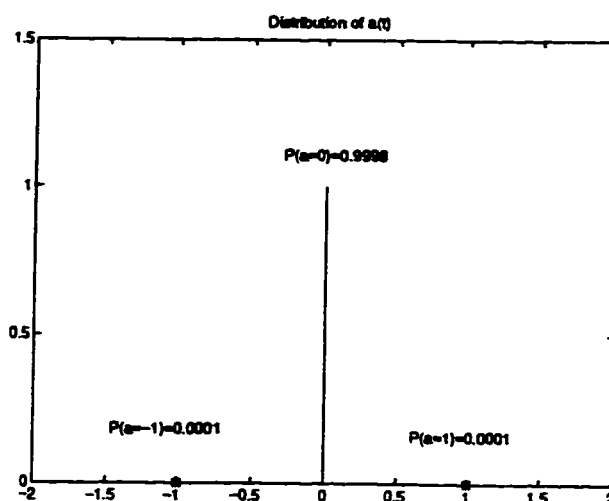


Figure 11.2: *Probability distribution of the shock*

of the signal by passing the shock through the three filters respectively. Clearly these graphs represent a deterministic step, ramp or sinusoidal signal with possible magnitude, slope or phase changes occurring at random times. The magnitude change of the sinusoidal signal in Figure 11.3 is due to the non-zero initial value when the second shock occurs. The true deterministic signal (occurring at random time) is obtained in the limiting case. Readers can also refer to (Ljung, 1987) for discussion of such deterministic signals for identification problems.

Optimal stochastic control laws, such as MVC, GPC and LQG, are independent of the probability distribution of the shock as long as the shock has zero mean and finite variance (MacGregor *et al.*, 1984). Instead, how to formulate the disturbance model is important for control design irrespective of the deterministic or stochastic nature of the disturbances. The minimum variance control law generally yields a minimum SSE control law<sup>3</sup> for deterministic disturbances (MacGregor *et al.*, 1984). For example, if the disturbance model is  $N = 1/(1 - q^{-1})$ , then the minimum variance control law will be a minimum SSE control law to step-type disturbances. Similarly, if the disturbance model is of the sinusoidal structure, then the minimum variance control law yields a minimum SSE control law to sinusoidal disturbances. These issues become more evident in the  $H_2$  control

<sup>3</sup>SSE = Sum of Square Error, i.e.  $J = \frac{1}{M} \sum_{i=1}^M \epsilon_i^2$ .

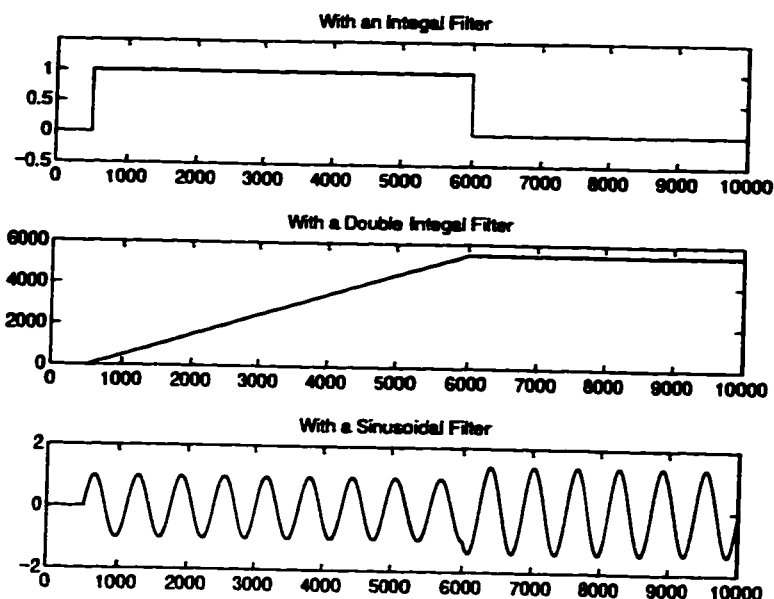


Figure 11.3: *Signal generated by passing the shock through filters*

framework in Section 11.6. Since the setpoint tracking problem can be re-formulated as a regulatory control problem, minimum variance control can naturally handle stochastic or deterministic setpoint tracking problems. Consequently, the methodology of performance assessment for stochastic regulatory control can be generalized to performance assessment of deterministic disturbance rejection as well as setpoint tracking property of the controller. However, estimation of the performance index must be given a special treatment when disturbances are deterministic in nature. This is illustrated in the following section.

## 11.4 Performance assessment with both stochastic and deterministic disturbances

We begin with an example to show difficulties in performance assessment when both stochastic and deterministic disturbances are concerned. Eriksson and Isaksson (1994) have a numerical example showing an unreasonable performance measure if minimum variance control is used as the benchmark. In the example, the transfer functions, in our

notation, have the following values

$$\begin{aligned} q^{-d}\tilde{T} &= q^{-4} \frac{0.33}{1 - 0.67q^{-1}} \\ N &= \frac{1 - 0.4q^{-1}}{1 - 0.67q^{-1}} \\ Q &= \frac{0.7 - 0.47q^{-1}}{0.33 - 0.10q^{-1} - 0.23q^{-4}} \end{aligned}$$

The white noise sequence  $a_t$  has variance  $\sigma_a^2 = 0.36$ . The controller is a well-designed Dahlin controller. The minimum variance can be calculated as  $\sigma_{mv}^2 = 0.4033$ , and the output variance with the Dahlin controller acting on the process is given as  $\sigma_y^2 = 0.6115$ . Hence the performance index (in our notation) is

$$\eta_{min} \triangleq \frac{\sigma_{mv}^2}{\sigma_y^2} = \frac{0.4033}{0.6115} = 0.66$$

where  $\eta_{min}$ <sup>4</sup> is the performance index with minimum variance control as the benchmark with  $0 < \eta_{min} \leq 1$ . If the controller is changed to a P-only controller with a gain of 0.1745, the output variance becomes  $\sigma_y^2 = 0.4037$ . This yields the performance index as

$$\eta_{min} = \frac{0.4033}{0.4037} = 0.999$$

This indicates that the performance of the P-controller is better than the Dahlin controller, and seems an unacceptable conclusion. It is, however, a correct result.

Performance assessment techniques as proposed by Harris(1989) provide assessment of control loop performance under *routine operating conditions*. In this example, step-type disturbances or setpoint changes do not affect the process. An integral control is clearly not necessary in this situation. Therefore a P-controller gives a better performance measure than the Dahlin controller which has integral action. However, integral action is practically desired in order to handle random-walk type stochastic disturbances or step-type deterministic disturbances or setpoint changes. It is therefore necessary to sample the data carefully before carrying out the performance evaluation. For example, one should ask if the set of sampled routine operating data contains effects of all disturbances that

---

<sup>4</sup>In this chapter, the subscript "min" stands for minimum variance or optimal  $H_2$  control. For example,  $\eta_{min}$  represents the performance index with minimum variance or optimal  $H_2$  control as a benchmark.



truly affect the process, i.e. if the set of data is representative. Performance assessment will then estimate the benchmark which optimally regulates the disturbances occurring during the data-sampling period.

Since all disturbances can be regarded as shocks (with different probability distributions) filtered by different disturbance filters, all of the disturbances can be theoretically lumped together via spectral factorization. Practically, the dynamics of the lumped disturbances can also be estimated via time series analysis. The benchmark control (one-degree-of-freedom control) would be a controller which minimizes the effect of the lumped disturbances.

### 11.5 Performance assessment with pure deterministic disturbances

If deterministic disturbances occur rather infrequently (e.g. only one step-change occurs in the collected data), time series modeling of the closed-loop process cannot depict the nature (e.g. step-type) of the disturbances. Performance assessment then may not be carried out under the stochastic framework. Under these circumstances, direct identification of the closed-loop transfer function from the disturbances to the process output is desired. There is no difficulty in identifying such a model if the deterministic disturbances are measurable (e.g. setpoint change) since it is equivalent to an open-loop identification problem.

Take the MIMO case with the simple interactor matrix (i.e.  $D = q^d I$ ) as an example. The closed-loop transfer function from  $a_t$  to  $Y_t$  can be written as

$$Y_t = (I + q^{-d} \tilde{T} Q)^{-1} N a_t \quad (11.3)$$

$$= \underbrace{(F_0 + F_1 q^{-1} + \dots + F_{d-1} q^{-(d-1)})}_F a_t + F_d a_{t-d} + \dots \quad (11.4)$$

where  $F_i$ 's correspond to impulse response coefficient matrices of the transfer function matrix from  $a_t$  to  $Y_t$ , and  $e_t = F a_t$  is feedback invariant irrespective of the probability distribution of  $a_t$ . If  $a_t$  is a random stochastic shock, then the closed-loop transfer

function matrix from  $a_t$  to  $Y_t$  can be estimated via time series analysis. If  $a_t$  is a single shock (deterministic disturbances), then the closed-loop transfer function matrix can be identified via identification tools. In both cases the term of  $e_t = Fa_t$  can then be separated from the closed-loop transfer function matrix, and subsequently used as a benchmark to assess control loop performance.

The performance measure for stochastic disturbances can be directly applied to performance assessment for deterministic disturbances. For stochastic disturbances, one can always normalize  $a_t$  such that  $Var(a_t) = I$  by adjusting  $N$ . According to the definition of the objective-based performance index for the stochastic disturbances as defined in Chapter 8, we have

$$\begin{aligned}\eta_{min} &= \frac{\min(E[Y_t^T Y_t])}{E[Y_t^T Y_t]} \\ &= \frac{\text{tr}(F_0^T F_0 + F_1^T F_1 + \dots + F_{d-1}^T F_{d-1})}{\text{tr}(F_0^T F_0 + F_1^T F_1 + \dots + F_{d-1}^T F_{d-1} + F_d^T F_d + F_{d+1}^T F_{d+1} + \dots)} \quad (11.5)\end{aligned}$$

Equation (11.5) defines an  $H_2$  norm measure (Dahleh and Diaz-Bobillo, 1995) of the system. The denominator in equation (11.5) represents the  $H_2$  norm of the closed-loop system, and the numerator represents the  $H_2$  norm of the feedback controller-invariant part. If  $a_t$  in equation (11.4) is a scalar impulse or shock, then equation (11.5) defines a measure of SSE performance, i.e.

$$\begin{aligned}\eta_{min} &= \frac{(F_0^T F_0 + F_1^T F_1 + \dots + F_{d-1}^T F_{d-1})}{F_0^T F_0 + F_1^T F_1 + \dots + F_{d-1}^T F_{d-1} + F_d^T F_d + F_{d+1}^T F_{d+1} + \dots} \\ &= \frac{\min(SSE)}{SSE}\end{aligned}$$

## 11.6 Unified assessment of stochastic and deterministic systems

Whether disturbances are stochastic or deterministic in nature, they require the two-step procedure for control loop performance assessment. The first step involves filtering (i.e. time series analysis using only output data to obtain closed-loop transfer function from  $a_t$  to  $Y_t$ ) in the stochastic case, and identification of the same closed-loop

transfer function in the deterministic case. The second step involves calculation of the performance index which is basically the ratio of the sum of square terms of the impulse response coefficients (matrices) of the closed-loop transfer function for both stochastic and deterministic disturbances. The sum of square terms of the impulse response coefficients (matrices) is in fact the  $H_2$  norm of the system. Thus performance assessment for both deterministic and stochastic systems may be unified under the  $H_2$  framework.

The  $H_2$  norm of a transfer function (matrix)  $G$  is defined as (Dahleh and Diaz-Bobillo, 1995):

$$\begin{aligned}\|G\|_2^2 &= \frac{1}{2\pi} \int_{-\pi}^{\pi} \text{tr}[G(e^{j\omega})G^T(e^{-j\omega})]d\omega \\ &= \sum_{t=0}^{\infty} \text{tr}[F_t F_t^T]\end{aligned}$$

where  $F_t$  is the impulse response coefficients (or Markov parameter matrices) of  $G$ . Consider the closed-loop response to disturbances  $a_t$  as shown in Figure 11.1 (with  $Y_t^{sp} = 0$ ), which is

$$Y_t = (I + TQ)^{-1} N a_t$$

The corresponding closed-loop transfer function matrix is therefore

$$G_d = (I + TQ)^{-1} N$$

If  $a_t$  is a single 'shock', then  $Y_t$  represents closed-loop response to a deterministic disturbance, and the  $H_2$  norm of  $G_d$  defines the sum of square of the errors (SSE) of the closed-loop system. However, if  $a_t$  is a white-noise sequence with  $\text{Var}(a_t) = I$ , then according to Parseval's Theorem,

$$E(Y_t^T Y_t) = \text{tr}[\text{Var}(Y_t)] = \frac{1}{2\pi} \int_{-\pi}^{\pi} \text{tr}(G_d(e^{j\omega})G_d^T(e^{-j\omega}))d\omega = \|G_d\|_2^2$$

which is the quadratic measure of variance of the closed-loop output. The variance matrix of the white noise sequence,  $a_t$ , can always be normalized to an identity matrix by adjusting the disturbance transfer function matrix  $N$ .

Therefore the  $H_2$  norm applies to both stochastic and deterministic systems. Consequently, the optimal  $H_2$  control law is an optimal control law for both deterministic

and stochastic disturbances. In the sequel, we simply consider the optimal or desired  $H_2$  control as the benchmark for control loop performance assessment of both stochastic and deterministic systems. For example, the unified scalar performance index with optimal  $H_2$  control as the benchmark is

$$\eta_{min} = \frac{\min(\|G_d\|_2^2)}{\|G_d\|_2^2}$$

Then for stochastic disturbances, this index is precisely the objective function based index defined in Chapter 8 for performance assessment of stochastic systems.

## 11.7 Simulation

For the same process as used in (Eriksson and Isaksson, 1994), performance of the Dahlin-controller and the simple P-controller is re-assessed. In addition to the “routine” disturbances from the shock  $a_t$  (Normal-distributed with  $Var(a_t) = 0.36$ ), deterministic step-type disturbances are added to the system as shown in Figure 11.4.  $b_t$  is the shock with the most of its probability density concentrated on  $b_t = 0$ . Therefore disturbance  $\delta_t$  is a randomly occurring step-type deterministic disturbance.

Simulation results of the process with the Dahlin-controller are shown in Figures 11.5 and 11.6. The FIR model or impulse response (using 20 coefficients) of closed-loop transfer

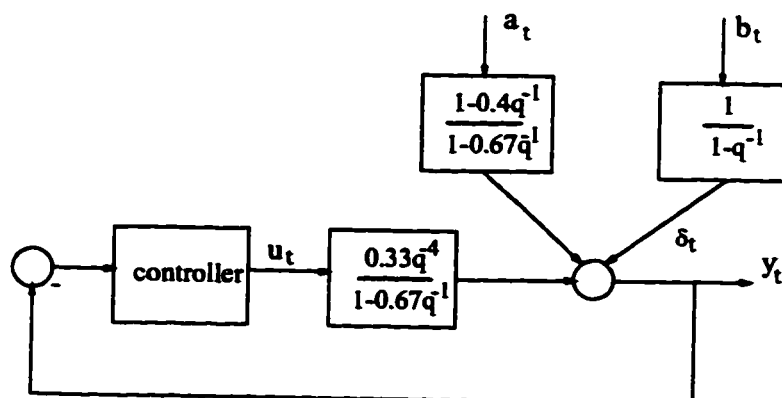


Figure 11.4: *Block diagram representation of the simulated process*

function from  $\delta_t$  to  $y_t$  is identified as

$$G_{y\delta} = 0.9798 - 0.0040q^{-1} + 0.0566q^{-2} - 0.0608q^{-3} - 0.7350q^{-4} - 0.1207q^{-5} - 0.0899q^{-6} + \dots$$

Due to time delay  $d = 4$ , the first four terms of  $G_{y\delta}$  are feedback invariant for impulse disturbances, i.e. for the disturbance model  $N = 1$ . For a step disturbance (i.e. for  $N = 1/(1 + q^{-1})$ ), one can either integrate impulse response coefficients or directly use the output and the differenced input data (i.e. filtering input data  $\delta_t$  by  $(1 - q^{-1})$ ) to obtain the step response coefficients. Direct identification (using 20 coefficients) yields the step response

$$s_t \triangleq y_t|_{step} = 0.9807 + 0.9775q^{-1} + 1.0341q^{-2} + 0.9732q^{-3} + 0.2383q^{-4} + 0.1174q^{-5} + \dots$$

The first four terms are feedback control invariant for this step-type disturbance (i.e. for  $N = 1/(1 - q^{-1})$ ). This also implies that the peak error due to a unit step disturbance is no less than 1 for any linear feedback controller. A comparison between theoretical step response and predicted step response and 95% error bounds (95% confidence interval) is shown in Figure 11.6. Clearly the Dahlin controller has performance very close to minimum SSE or optimal  $H_2$  controller for the step disturbance in this example since the first four points are feedback control invariant. The performance index for the step disturbance can be calculated as

$$\begin{aligned} \eta_{min} &= \frac{\min(\|s_t\|_2^2)}{\|s_t\|_2^2} \\ &\approx \frac{0.9807^2 + 0.9775^2 + 1.0341^2 + 0.9732^2}{0.9807^2 + 0.9775^2 + 1.0341^2 + 0.9732^2 + 0.2383^2 + 0.1174^2} \\ &= 0.9824 \end{aligned}$$

This is very close to the theoretically calculated index which is 0.976. The residuals from Figure 11.5 can be used to assess performance of the controller for rejection of "routine" stochastic disturbances. Applying the FCOR algorithm to the residuals yields the performance index for stochastic disturbances as

$$\eta_{min} \approx 0.69$$

This result agrees well with previous analysis for the same process with only stochastic disturbances in Section 11.4. Therefore, in this example the Dahlin controller has

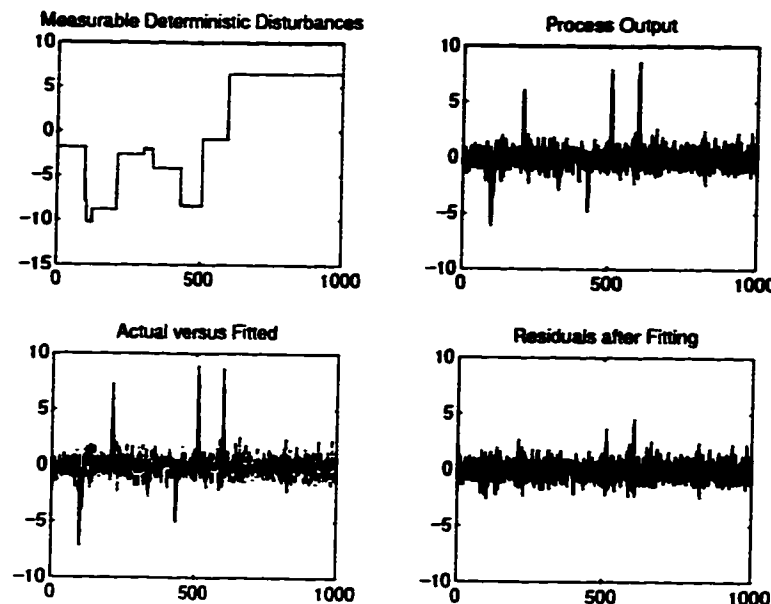


Figure 11.5: *Process response and identification results (Dahlin controller)*

“optimal” performance for rejection of step-type disturbances, but has relatively “low” performance for rejection of stochastic disturbances.

For the simple P-controller, using the same deterministic and stochastic disturbances as those used for the simulation of the Dahlin controller, the following polynomial transfer function is identified.

$$G_{y\delta} = \frac{0.9883 - 0.7674q^{-1}}{1 - 0.7382q^{-1}}$$

The predicted step response is

$$s_t \triangleq y_t|_{step} = \frac{0.9883 - 0.7674q^{-1}}{(1 - 0.7382q^{-1})(1 - q^{-1})}$$

This step response has an offset. Therefore the SSE or  $H_2$  norm of  $y_t$  is infinite, and the performance index of the P-controller to step disturbance is

$$\eta_{min} = \frac{\min(\|s_t\|_2^2)}{\|s_t\|_2^2} = 0$$

Similarly the residuals after fitting can be used to assess performance of the P-controller for rejection of the “routine” stochastic disturbances. Applying the FCOR algorithm yields the performance index for stochastic disturbances as

$$\eta = 0.97$$

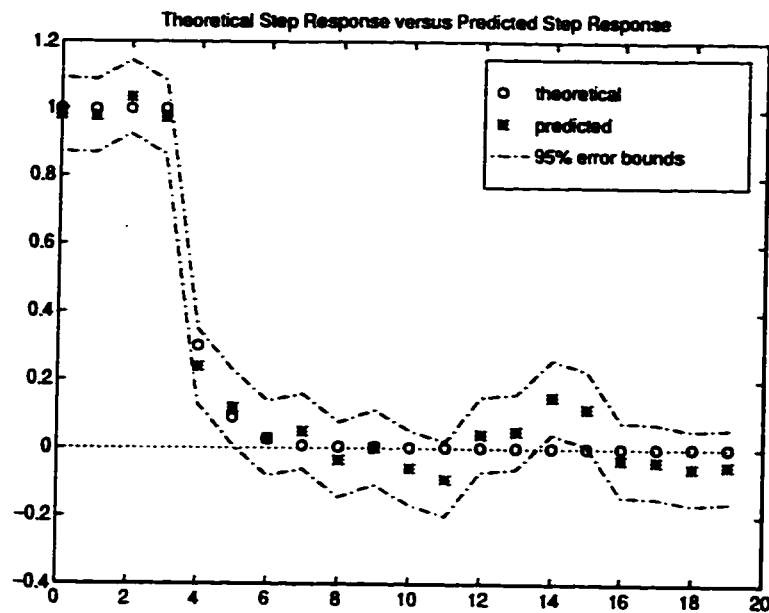


Figure 11.6: *Predicted output response to a step disturbance (Dahlin controller)*

This also agrees well with the previous analysis for the process with only stochastic disturbances in Section 11.4. Therefore, the simple P-controller has “optimal” performance for rejection of “routine” stochastic disturbances, but has very poor performance for rejection of step-type disturbances.

## 11.8 Conclusions

Feedback control loop performance assessment for regulating both stochastic and deterministic disturbances and/or setpoint tracking has been discussed in a unified manner under the  $H_2$  framework. It has been shown that performance assessment of deterministic disturbances and/or setpoint tracking can be treated in a very similar way as the treatment of the stochastic system. The proposed method has been evaluated by a simulated example.

## Chapter 12

# Performance Assessment: User-defined Benchmark

### 12.1 Introduction

Control loop performance assessment has been extended to many situations, and many approaches have been developed as discussed in the earlier chapters; e.g. performance assessment of: 1) SISO feedback control systems (Desborough and Harris, 1992; Stanfelj *et al.*, 1993; Kozub and Garcia, 1993; Lynch and Dumont, 1993; Tyler and Morari, 1995b), 2) feedback control of nonminimum phase SISO systems (Tyler and Morari, 1995a); and 3) MIMO feedback control systems (Huang *et al.*, 1995a; Huang *et al.*, 1996b; Harris *et al.*, 1995; Harris *et al.*, 1996). The portion of a process output that is feedback controller invariant determines the theoretically achievable minimum variance and characterizes the most fundamental performance limitation of a system due to existence of time-delays/infinite zeros. However, practically there are many other limitations on the achievable control loop performance. Existence of nonminimum phase or poorly damped zeros, sampling rate, amplitude and/or rate constraints on control action, robustness constraints etc. are examples of such limitations. Therefore, a feedback controller that

---

<sup>1</sup>A version of this chapter has been accepted for presentation at the 1997 IFAC Advanced Chemical Process Control Symposium.



indicates performance reasonably close to minimum variance control does not require further tuning (if the variance is of main interest). However, a feedback controller that indicates poor performance relative to minimum variance control is not necessarily a poor controller. Further analysis of performance limitations and comparisons with more realistic benchmarks is usually required. Performance assessment with minimum variance control as a benchmark requires minimum effort (routine operating data plus *a priori* knowledge of time-delays), and therefore serves as the most convenient first-level performance assessment test (if the variance is of main interest). Only those loops that indicate poor first-level performance need to be re-evaluated by higher-level performance assessment tests. A higher-level performance tests usually requires more *a priori* knowledge than just a knowledge of time-delays. This chapter addresses practical issues which are considered for such higher-level performance assessment test.

The main contribution of this chapter is to propose a technique of practical control loop performance assessment relative to a benchmark in terms of a user-specified closed-loop dynamics. All of these are discussed for SISO and MIMO systems. Normally, the MIMO case is general and includes the SISO system as a special case. However, the delay matrix (or the interactor matrix) of the MIMO system is not a simple extension to the time-delay term of the SISO system. Thus, the SISO case is first considered for clarity of presentation. This chapter is organized as follows. Performance assessment of minimum phase systems with desired closed-loop dynamics as a more practical benchmark is considered in Section 12.3, and the treatment of nonminimum phase systems is discussed in Section 12.4, followed by concluding remarks in Section 12.5.

## 12.2 Preliminaries

In Section 12.3, we will assume that the plant transfer function (matrix)  $T$  has no zeros or poles outside the unit circle except for the time-delays (infinite zeros). This condition will be relaxed in Section 12.4. The disturbance transfer function (matrix)  $N$  has no poles outside the unit circle, but can have zeros outside the unit circle. However, an all-pass factor  $N_p$ , which contains all zeros that are outside the unit circle including

the infinite zeros, can be factored out from  $N$ , such that  $N = \tilde{N}N_p$  and  $\tilde{N}$  is a minimum-phase transfer function (matrix). This factorization does not change the  $H_2$  norm of the closed-loop system, i.e.  $\|(I + TQ)^{-1}N\|_2^2 = \|(I + TQ)^{-1}\tilde{N}\|_2^2$ . The admissible minimum variance or optimal  $H_2$  control law does not depend on the all-pass term  $N_p$  (Astrom and Wittenmark, 1990; Morari and Zafiriou, 1989). Therefore, if there are unstable or infinite zeros in  $N$ , one simply needs to factorize an all-pass term from it. The remaining  $\tilde{N}$  term is then considered as the disturbance transfer function (matrix). This will not affect the  $H_2$  norm of the closed-loop system and its optimal control law. Time series analysis does automatically produce such minimum phase disturbance transfer function (matrix). Thus, we assume that the disturbance transfer function (matrix)  $N$  has no zeros outside the unit circle as well.

### 12.3 Performance assessment with desired closed-loop dynamics as the benchmark: minimum phase systems

#### 12.3.1 SISO case

The minimum variance or optimal  $H_2$  control law serves as a good global reference point to assess control loop performance. However, the minimum variance or optimal  $H_2$  control law may not be a desired one in practice. For example, if the process has a fast controller sampling rate, then minimum variance or minimum SSE control with such sampling rate usually requires excessive control actions. Therefore, in many practical circumstances, a more realistic user-specified benchmark control is desirable. For example, one may wish to consider desired closed-loop dynamics as a reference benchmark in terms of settling times, overshoot etc. Specifically it would be of interest to know if the actual closed-loop dynamics are close to or far away from the desired dynamics. Kozub and Garcia(1993) have suggested that one of the choices for the practical benchmark performance can be the minimum variance control response (finite moving-average term) filtered by a filter. Tyler and Morari(1995b) suggested using a generalized likelihood ratio to test if the actual performance (in the form of impulse response coefficients of the closed-loop transfer

function  $G_d = (I + TQ)^{-1}N$  is in the set of the desired performance. All of these are limited to SISO applications. However, since the actual performance (in the form of impulse response coefficients of  $G_d$ ) can be estimated from data using time series analysis or standard identification tools (Ljung, 1987), performance assessment can be directly computed by comparing the actual impulse response coefficients to the desired impulse response coefficients. Direct observation and analysis of the actual impulse response coefficients gives one significantly more information than a simple “yes or no” test, and can be easily extended to MIMO applications. For example, a maximum likelihood ratio test cannot tell whether the controller is over-tuned or under-tuned or how and in which way it is different from the desired performance. On the other hand, a cursory study of the impulse response coefficients may easily provide such tuning guidelines.

An important fact that has been ignored by other researchers is that the desired closed-loop dynamics ( $G_{des}$ ) cannot be arbitrarily specified. They need to consider the physical limitations. For example, closed-loop response within the time-delay period is feedback control invariant and cannot be specified by users. Nonminimum phase zeros cannot be cancelled by a stable controller and must affect the desired closed-loop dynamics as well. These limitations are considered in the present chapter when the desired closed-loop dynamics are specified.

The differences between optimal  $H_2$  control and the user specified benchmark control (desired closed-loop dynamics) can be clearly seen from equation (11.4). For optimal  $H_2$  control, the remaining terms after the first  $d$  terms should be zero. For user specified benchmark control, the first  $d$  terms should be the same as those under optimal  $H_2$  control, but the remaining terms are no longer zero. These remaining terms define the desired closed-loop dynamics. The closed-loop dynamics (e.g. for the SISO case) therefore have the following form<sup>2</sup>:

$$y_t|_{user} = \underbrace{(f_0 + f_1q^{-1} + \cdots + f_{d-2}q^{-d+2} + f_{d-1}q^{-d+1})}_F + q^{-d}G_R)a_t \quad (12.1)$$

where  $G_R$  is a stable and proper transfer function. There are many ways to specify the

---

<sup>2</sup>In this chapter, the subscript “user” stands for a user-specified benchmark control. For example,  $y_{user}$  represents the process output under the user-specified control.

term  $G_R$  based on information such as closed-loop settling time, time constant, decay ratio, desired variance, frequency domain characteristics, robust performance etc. If  $G_R$  is directly specified as desired closed-loop dynamics, i.e.  $G_R = G_{des}$ , then only *a priori* knowledge of time-delays is required for calculation of such benchmark performance. If the desired closed-loop response is specified by some other characteristic such as settling time, then  $G_R$  consists of a set of transfer functions, and no explicit expression for  $G_R$  is actually defined. One can simply test, for example, whether the actual closed-loop settling time is the same as the desired value. However, all these specifications of  $G_R$  are somehow arbitrary, and it is not clear how such specifications affect closed-loop dynamics, e.g. in terms of performance optimality and robustness properties. For example, in the specification of the settling time, there are infinite number of  $G_R$  that can be considered, and one does not know which one has the performance closest to optimal control. On the other hand, it is well-known that optimal  $H_2$  control augmented by a filter improves robust performance and provides good compromise between performance and robustness, and the closed-loop dynamics can be adjusted by the tuning of the filter parameters (Mohtadi, 1988; Morari and Zafiriou, 1989).

Consider the specification of  $G_R$  as

$$G_R = (1 - G_F)R \quad (12.2)$$

where  $G_F$  is a stable and proper filter and,  $R$  (a rational proper transfer function) is defined via the Diophantine identity:

$$N = F + q^{-d}R$$

Then equation (12.1) becomes

$$y_t|_{user} = (f_0 + f_1 q^{-1} + \dots + f_{d-1} q^{-d+1} + q^{-d}(1 - G_F)R)a_t \quad (12.3)$$

The filter  $G_F$  can be specified according to the desired closed-loop dynamics. It should be chosen in such a way that asymptotically  $(1 - G_F)R$  converges to zero, i.e. no offset occurs. For example, if  $R$  has a pole equal to 1 (e.g. step-type disturbances), then  $(1 - G_F)$  must have a zero equal to 1 in order to preserve the asymptotic property of the optimal  $H_2$

control law. If a commonly used first-order filter, which satisfies the asymptotic property for type 1 system, is specified as:

$$G_F = \frac{1 - \alpha}{1 - \alpha q^{-1}}$$

then  $\alpha$  can be calculated via the desired closed-loop settling time or time constant by

$$\alpha = \exp\left(-\frac{\Delta T}{\tau}\right)$$

where  $\Delta T$  is the sampling interval and  $\tau$  is the time constant of the closed-loop process. However, one should note that the closed-loop dynamics also depend on  $R$  in addition to the filter dynamics.

We shall show that the specification of the closed-loop system as in equation (12.1) is practically achievable for a minimum-phase system, and the specification in equation (12.2) is equivalent to the  $H_2$  optimal control law augmented by a filter.

Consider the controller specification in the IMC framework as shown in Figure 12.1. Write the plant transfer function as  $T = q^{-d}\tilde{T}$ , where  $\tilde{T}$  is the delay-free transfer function. Then by assuming  $\hat{T} = T$ , we have

$$\begin{aligned} y_t &= (1 - q^{-d}\tilde{T}Q^*)Na_t \\ &= Na_t - q^{-d}\tilde{T}Q^*Na_t \\ &= (F + q^{-d}R)a_t - q^{-d}\tilde{T}Q^*Na_t \\ &= Fa_t + q^{-d}(R - \tilde{T}Q^*N)a_t \end{aligned} \quad (12.4)$$

Equating equation (12.4) and equation (12.1) yields

$$R - \tilde{T}Q^*N = G_R$$

This results in

$$Q^* = \frac{R - G_R}{\tilde{T}N} \quad (12.5)$$

This IMC controller is proper and stable. Therefore the closed-loop response specified in equation (12.1) is achievable. For specification in equation (12.2), equation (12.5) becomes

$$Q^* = \frac{R - (1 - G_F)R}{\tilde{T}N} = \frac{G_F R}{\tilde{T}N} \quad (12.6)$$

If  $G_F = 0$ , then  $Q^* = 0$  and the controller is in open-loop mode. If  $G_F = 1$ , then according to equation (12.3),

$$y_t|_{user} = (f_0 + f_1 q^{-1} + \dots + f_{d-1} q^{-(d-1)}) a_t$$

This is the minimum variance control response or optimal  $H_2$  control response. Thus, the controller as specified in equation (12.6) is in fact an optimal  $H_2$  control law augmented by a filter  $G_F$  (Morari and Zafriou, 1989). The role of the filter is to adjust or tune the controller from the open-loop mode ( $G_F = 0$ ) to optimal  $H_2$  control mode ( $G_F = 1$ ).

However, the specification in equation (12.2) requires a knowledge of  $R$ . The term  $R$  must be calculated from the disturbance transfer function  $N$  via the Diophantine identity. Therefore, the disturbance transfer function should be known in order to apply such a specification. For most setpoint tracking problems and some regulatory problems, the dynamics of the setpoint are known as *a priori* knowledge. For example, if one is interested in the tracking or regulatory performance of step-type setpoint or disturbances, then the disturbance dynamics are simply  $N = 1/(1 - q^{-1})$ . If *a priori* knowledge of  $N$  is not available, it will be shown in Section 12.4 that the disturbance transfer function  $N$  can be conveniently estimated under closed-loop conditions with dither excitation.

Since complete dynamics of the user-specified closed-loop system are available, one can directly compare the current closed-loop dynamics with the user-specified closed-loop dynamics. For example, to calculate the performance index under the stochastic framework, the variance of the user-specified benchmark control can be calculated from equation (12.1) and is defined as  $\sigma_{user}^2$ . The performance index can then be calculated as the ratio:

$$\eta_{user} = \frac{\sigma_{user}^2}{\sigma_y^2}$$

**Example 11** Consider a first-order process with a time-delay and the transfer function given by:

$$T = \frac{(2 - q^{-1})q^{-2}}{1 - 0.8q^{-1}}$$

Let the disturbance transfer function be:

$$N = \frac{1}{1 - q^{-1}}$$

*The sampling interval  $\Delta T = 5$  sec. The main objective in this design is to regulate  $y_t$  in the presence of integrated white noise or random-walk type disturbances. The choice of the desired closed-loop time constant,  $0.5 \leq \tau \leq 1$  min, reflects this. If setpoint tracking performance was of interest, perhaps a smaller desired closed-loop time constant could have been specified.*

Since the time-delay  $d = 2$ ,  $N$  is expanded according to the Diophantine identity as

$$N = \underbrace{1 + q^{-1}}_F + q^{-2} \underbrace{\frac{1}{1 - q^{-1}}}_R$$

Therefore, the minimum variance is

$$\sigma_{mv}^2 = \text{Var}(Fa_t) = 2\sigma_a^2$$

Now consider a first-order filter:

$$f = \frac{1 - \alpha}{1 - \alpha q^{-1}}$$

To satisfy the desired closed-loop time constant  $0.5 \leq \tau \leq 1$  min with sampling interval  $\Delta T = 5$  sec, the parameter  $\alpha$  can be calculated from

$$\alpha = \exp\left(-\frac{\Delta T}{\tau}\right)$$

This results in  $0.85 \leq \alpha \leq 0.92$ . The desired closed-loop response can be calculated from equation (12.3) as

$$\begin{aligned} y_t|_{user} &= f_0 a_t + f_1 a_{t-1} + \left(1 - \frac{1 - \alpha}{1 - \alpha q^{-1}}\right) \frac{1}{1 - q^{-1}} a_{t-2} \\ &= a_t + a_{t-1} + \frac{\alpha}{1 - \alpha q^{-1}} a_{t-2} \end{aligned} \quad (12.7)$$

$$= \frac{1 + (1 - \alpha)q^{-1}}{1 - \alpha q^{-1}} a_t \quad (12.8)$$

where  $0.85 \leq \alpha \leq 0.92$ . This gives the achievable user-specified closed-loop response.

The variance of the desired closed-loop can also be calculated from equation (12.8) as

$$\sigma_{user}^2|_{\alpha=0.85} = \text{Var}(y_t)|_{\alpha=0.85} = 4.6036\sigma_a^2$$

and

$$\sigma_{user}^2|_{\alpha=0.92} = Var(y_t)|_{\alpha=0.92} = 7.5104\sigma_a^2$$

Therefore

$$4.6036\sigma_a^2 \leq \sigma_{user}^2 \leq 7.5104\sigma_a^2$$

Now consider the same process under integral control

$$Q = \frac{0.1}{1 - q^{-1}}$$

with  $Var(a_t) = 1$ . The closed-loop system was simulated and 5000 data points were recorded. A truncated moving-average model is obtained from time series analysis of  $y_t$ . The coefficients of this moving-average model correspond to the closed-loop impulse response coefficients. These coefficients together with their 95% bounds are plotted in Figure 12.2. The desired closed-loop dynamics have been shown in equation (12.8). Their corresponding impulse response coefficients are calculated and plotted together with the actual impulse response coefficients in Figure 12.2. Since the desired impulse response is not a single curve but a region (a region between the two solid lines), any actual impulse response which falls within this region is considered acceptable. However, the actual impulse response coefficients are estimated values. Therefore a statistical test should be used to determine whether or not the actual impulse response falls into the region. One can consider the desired performance region as if it constitutes a thick or 'fuzzy' desired impulse response curve: (1) For any particular actual impulse response coefficient, if its 95% confidence interval and the 'fuzzy' desired performance region do not intersect, then we may conclude that this particular coefficient does not fall in the desired region with 95% confidence; (2) If more than 5% of impulse response coefficients, over the time-period of interest, do not fall in the desired region as tested in the first step, then one may conclude that the actual performance does not lie in the set of the desired performance. The confidence bounds can always be narrowed by increasing the data sampling size, and hence the reliability of such test can be increased. This is a quantitative or 'yes' or 'no' decision criteria. However, a visual or qualitative analysis of the plot is more important and it is recommended that this be done. Figure 12.2 clearly shows unacceptable performance



of the integral controller. The actual closed-loop behaves as an underdamped system, and in fact the system appears to be over-tuned.

Now we add a second-order filter to the integral controller:

$$Q = \left( \frac{0.05 - 0.04q^{-1}}{2 - 0.9q^{-1} - 0.05q^{-2}} \right) \frac{1}{1 - q^{-1}}$$

The simulation result is shown in Figure 12.3. The actual closed-loop dynamics are slightly slower than the desired, and in fact are not in the desired set. The controller appears to be under-tuned. Finally a slightly aggressive controller

$$Q = \left( \frac{0.11 - 0.088q^{-1}}{2 - 0.78q^{-1} - 0.11q^{-2}} \right) \frac{1}{1 - q^{-1}}$$

is implemented. The result shown in Figure 12.4 indicates that the actual performance is now in the set of the desired performance.

Note that by using the same method, one can make many performance tests. For example, one can even specify the desired performance set in terms of the frequency domain specifications. Then the actual closed-loop dynamics together with their confidence intervals in the frequency domain can be calculated. The performance test can be made in the frequency domain. The significance of this method is that it can provide information including tuning guidelines, via observation of the patterns of the impulse response coefficients or the spectrum of the closed-loop systems.

### 12.3.2 MIMO case

Consider the MIMO system:

$$Y_t = TU_t + Na_t$$

where  $T$  is a process transfer function matrix,  $N$  is the disturbance transfer function matrix,  $Y_t$ ,  $U_t$  and  $a_t$  are output, input and disturbance with appropriate dimensions. A unitary interactor matrix  $D$  with  $D^T(q^{-1})D(q) = I$  can be factored from the transfer function matrix  $T$ , such that  $\tilde{T} = DT$  is a delay free transfer function matrix. Factorization of such a unitary interactor matrix does not change the  $H_2$  norm of the transfer function

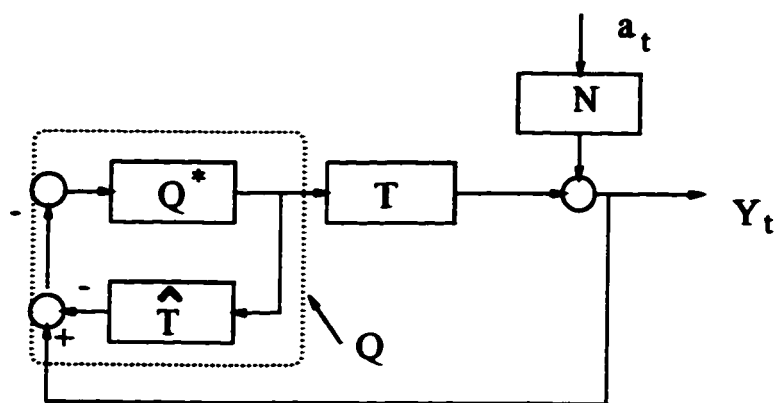


Figure 12.1: *Control loop configuration under IMC framework*

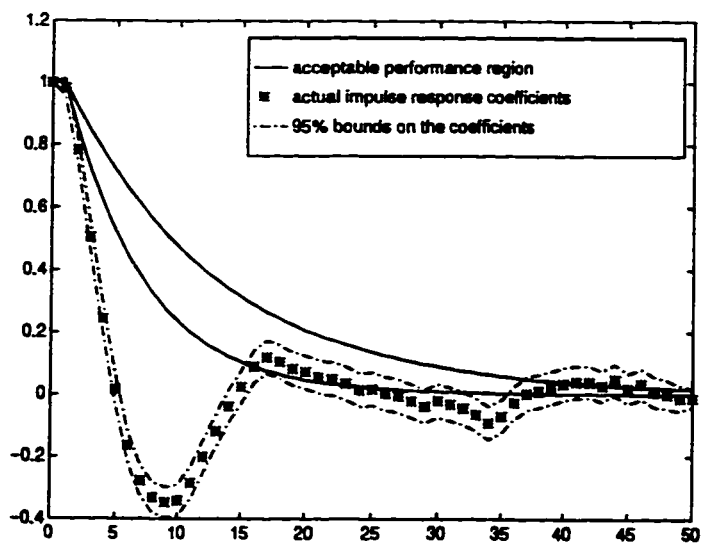


Figure 12.2: *Closed-loop impulse response coefficients for a simple integral controller.*

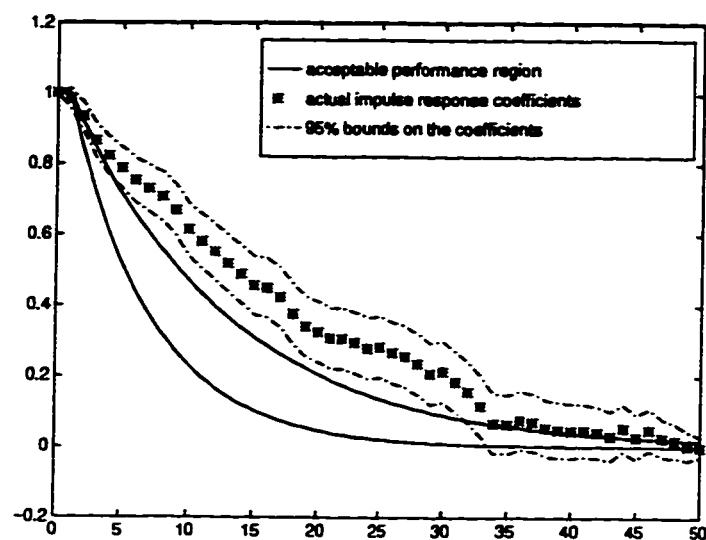


Figure 12.3: *Closed-loop impulse response coefficients for an integral plus filter controller.*

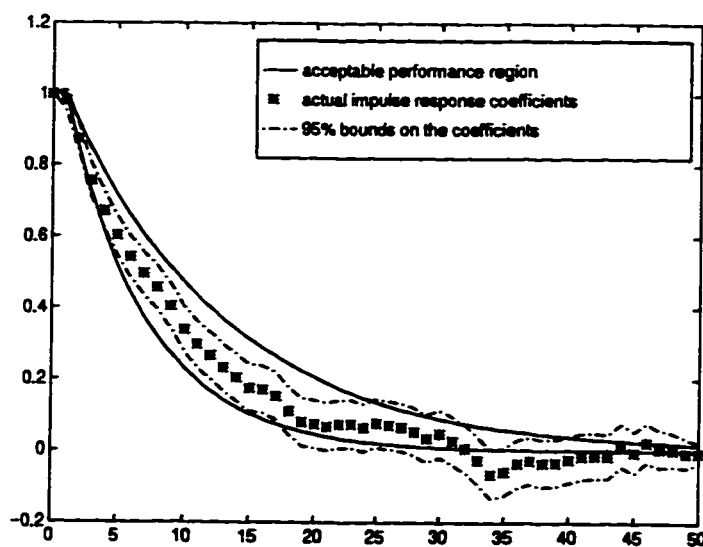


Figure 12.4: *Closed-loop impulse response coefficients for a detuned integral plus filter controller.*

matrix, i.e.  $\|\tilde{T}\|_2^2 = \|T\|_2^2$ . Using the Diophantine identity, the disturbance transfer function matrix  $N$  can be expanded as

$$q^{-d}DN = \underbrace{F_0 + F_1q^{-1} + \dots + F_{d-1}q^{-(d-1)}}_F + q^{-d}R$$

where  $F_i$  (for  $i = 1, \dots, d-1$ ) are constant coefficient matrices, and  $R$  is the remaining proper transfer function matrix after the expansion. In Chapter 8 the minimum variance or optimal  $H_2$  norm control response has been shown to be<sup>3</sup>:

$$Y_t|_{\min} = q^d D^{-1}(F_0 + F_1q^{-1} + \dots + F_{d-1}q^{-(d-1)})a_t \quad (12.9)$$

$$= (E_0 + E_1q^{-1} + \dots + E_{d-1}q^{-(d-1)})a_t \quad (12.10)$$

where  $E_i$  (for  $i = 1, \dots, d-1$ ) are constant coefficient matrices. It has also been shown in Chapter 8 that the minimum variance control response  $Y_t|_{\min}$  can be estimated from routine operating data with *a priori* knowledge of the unitary interactor matrix  $D$ .

For performance assessment with a reference benchmark different from minimum variance or optimal  $H_2$  norm control, a user specified transfer function matrix  $G_R$  should be augmented to equation (12.10) as

$$Y_t|_{\text{user}} = (E_0 + E_1q^{-1} + \dots + E_{d-1}q^{-(d-1)} + G_Rq^{-d})a_t \quad (12.11)$$

$G_R$  is a stable and proper transfer function matrix. In practice,  $G_R$  may be specified as a diagonal matrix. Then dynamics of each output correspond to the diagonal elements. Now we are in the position to show that the user-specified closed-loop response as shown in equation (12.11) is achievable.

Under the IMC framework, the closed-loop response can be written as

$$Y_t = (I - TQ^*)Na_t$$

Factor  $T$  as  $T = D^{-1}\tilde{T}$ , where  $\tilde{T}$  is the delay-free transfer function matrix. Then

$$\begin{aligned} Y_t &= (I - D^{-1}\tilde{T}Q^*)Na_t \\ &= q^d D^{-1}(q^{-d}DN - q^{-d}\tilde{T}Q^*N)a_t \end{aligned}$$

---

<sup>3</sup>In Chapter 8,  $Y_t|_{\min}$  represents the process output under minimum variance control. In this chapter, this output is changed to  $Y_t|_{\min}$  to reflect the minimum variance or equivalently optimal  $H_2$  control.

Using the Diophantine identity  $q^{-d}DN = F + q^{-d}R$ , we have

$$\begin{aligned} Y_t &= q^d D^{-1}(F + q^{-d}R - q^{-d}\tilde{T}Q^*N)a_t \\ &= q^d D^{-1}Fa_t + D^{-1}(R - \tilde{T}Q^*N)a_t \end{aligned} \quad (12.12)$$

As shown in Chapter 8, the first term on the right hand side of equation (12.12) is the minimum variance control response and can be written as

$$Y_t|_{min} = q^d D^{-1}Fa_t = (E_0 + \dots + E_{d-1}q^{-d+1})a_t \quad (12.13)$$

Substituting equation (12.13) into equation (12.12), and then equating the result to equation (12.11) yields

$$D^{-1}(R - \tilde{T}Q^*N) = G_R q^{-d}$$

This results in

$$q^d D^{-1}(R - \tilde{T}Q^*N) = G_R \quad (12.14)$$

Solving equation (12.14) yields

$$Q^* = \tilde{T}^{-1}(R - q^{-d}DG_R)N^{-1}$$

Again,  $Q^*$  is proper and stable, and therefore is a practically achievable controller.

As discussed in the SISO case, there are many ways to specify the transfer function matrix  $G_R$ . One may directly specify it as a desired transfer function matrix, i.e.  $G_R = G_{des}$ . Performance assessment with such specification requires only routine operating data plus *a priori* knowledge of the interactor matrix.

Alternatively, one may directly add a desired term into equation (12.9) such that

$$Y_t|_{min} = q^d D^{-1}(F_0 + F_1 q^{-1} + \dots + F_{d-1} q^{-(d-1)} + q^{-d}G_R)a_t$$

where  $G_R = I - G_F$ , and  $G_F$  is the user specified filter transfer function matrix according to the desired closed-loop dynamics. The filter serves as a tuning knob between optimal  $H_2$  control ( $G_F = I$ ) and open-loop performance ( $G_F = 0$ ).

**Example 12** Consider a process with the following transfer function matrices:

$$T = \begin{bmatrix} \frac{q^{-1}}{1-0.4q^{-1}} & \frac{q^{-2}}{1-0.1q^{-1}} \\ \frac{0.3q^{-1}}{1-0.1q^{-1}} & \frac{q^{-2}}{1-0.8q^{-1}} \end{bmatrix}$$

$$N = \begin{bmatrix} \frac{1}{1-0.5q^{-1}} & \frac{-0.6}{1-0.5q^{-1}} \\ \frac{0.5}{1-0.5q^{-1}} & \frac{1.0}{1-0.5q^{-1}} \end{bmatrix}$$

A unitary interactor matrix  $D$  can be factored out as:

$$D = \begin{bmatrix} -0.9578q & -0.2873q \\ -0.2873q^2 & 0.9578q^2 \end{bmatrix}$$

Then

$$q^{-d}DN = \underbrace{\begin{bmatrix} -1.1014q^{-1} & 0.2874q^{-1} \\ 0.1916 + 0.0958q^{-1} & 1.1302 + 0.5651q^{-1} \end{bmatrix}}_F + q^{-2} \underbrace{\begin{bmatrix} \frac{-0.5507}{1-0.5q^{-1}} & \frac{0.1437}{1-0.5q^{-1}} \\ \frac{0.0479}{1-0.5q^{-1}} & \frac{0.2826}{1-0.5q^{-1}} \end{bmatrix}}_R$$

The minimum variance term can be written as

$$e_t = Fa_t = \begin{bmatrix} -1.1014q^{-1} & 0.2874q^{-1} \\ 0.1916 + 0.0958q^{-1} & 1.1302 + 0.5651q^{-1} \end{bmatrix} a_t$$

Therefore

$$Y_{t|min} = q^d D^{-1} e_t$$

$$= \left( \underbrace{\begin{bmatrix} 1 & -0.6 \\ 0.5 & 1 \end{bmatrix}}_{E_0} + q^{-1} \underbrace{\begin{bmatrix} -0.0275 & -0.1624 \\ 0.0918 & 0.5413 \end{bmatrix}}_{E_1} \right) a_t$$

Note that this explicit expression for  $Y_{t|min}$  can always be estimated from routine operating data under any feedback control with *a priori* knowledge of the unitary interactor matrix.

If we assume  $\Sigma_a = Ea_t a_t^T = I$ , then the minimum variance can be calculated as

$$\Sigma_{min} = Var(Y_{t|min}) = \begin{bmatrix} 1.3871 & -0.1904 \\ -0.1904 & 1.5504 \end{bmatrix}$$

with the quadratic performance measure ( $H_2$  norm) as

$$E(Y_t^T Y_t)|_{min} = tr(\Sigma_{min}) = 2.9375$$

Now we assume that the controller sampling interval is  $\Delta T = 5$  sec, the desired response of output #1 is first-order with time constant  $\tau_1 = 1$  min, and the desired response of output #2 is also first-order but with time constant  $\tau_2 = 0.5$  min. If the desired closed-loop response is specified as

$$Y_t|_{user} = (E_0 + E_1 q^{-1} + \dots + G_F E_{d-1} q^{-(d-1)}) a_t \quad (12.15)$$

i.e. the closed-loop impulse response coefficient matrices decay steadily at the desired time constants starting from the last feedback control invariant term,  $E_{d-1}$ , then the filter transfer function matrix should be designed according to the desired dynamics as

$$G_F = \begin{bmatrix} \frac{1}{1-0.92q^{-1}} & 0 \\ 0 & \frac{1}{1-0.85q^{-1}} \end{bmatrix}$$

Equation (12.15) can be further written as

$$Y_t = (E_0 + E_1 q^{-1} + \dots + E_{d-1} q^{-(d-1)} + \underbrace{q(G_F - I)E_{d-1} q^{-d}}_{G_R}) a_t$$

Since  $G_F(q^{-1} = 0) = I$ ,  $G_R = q(G_F - I)E_{d-1}$  is proper. According to equation (12.11), this is an achievable closed-loop response. Substituting numerical values to equation (12.15) yields

$$Y_t|_{user} = \begin{bmatrix} \frac{1-0.9475q^{-1}}{1-0.92q^{-1}} & \frac{-0.6+0.3896q^{-1}}{1-0.92q^{-1}} \\ \frac{0.5-0.3332q^{-1}}{1-0.85q^{-1}} & \frac{1-0.3087q^{-1}}{1-0.85q^{-1}} \end{bmatrix} a_t$$

This achievable closed-loop response satisfies the user requirement, and can be estimated from routine operating data under any feedback control with *a priori* knowledge of the unitary interactor matrix. Its variance can be calculated as

$$\Sigma_{user} = Var(Y_t|_{user}) = \begin{bmatrix} 1.5366 & -0.5148 \\ -0.5148 & 2.3362 \end{bmatrix}$$

with the quadratic performance measure ( $H_2$  norm) as

$$E(Y_t^T Y_t)|_{user} = tr(\Sigma_{user}) = 3.8729$$

which is 1.3 times as large as  $E(Y_t^T Y_t)|_{min}$ .

## 12.4 Performance assessment with desired closed-loop dynamics as the benchmark: nonminimum phase systems

In this section, we relax the assumption of minimum-phase plants by assuming that the plant transfer function (matrix)  $T$  can have zeros outside the unit circle. The user-specified performance assessment of the MIMO process when the process has non-invertible zeros is discussed in this section.

Consider the MIMO system:

$$Y_t = TU_t + Na_t$$

Factor  $T$  as  $T = D_G^{-1}\tilde{T}$ , where  $D_G^{-1}$  is the all-pass factor or the generalized unitary interactor matrix as is discussed in Chapter 10, which contains both infinite and non-invertible zeros of  $T$ . The generalized unitary interactor matrix  $D_G^{-1}$  can also be regarded as an all-pass factor of  $T$ , and can be calculated via the Inner-Outer factorization (Chu, 1985) as well. A proper feedback controller cannot cancel time-delays. Time-delays are therefore constraints on the achievable performance. A stable controller cannot cancel non-invertible zeros. Non-invertible zeros also impose constraints on the achievable performance.

In Chapter 10, we have shown a procedure for performance assessment of nonminimum-phase MIMO processes. The procedure consists of the following steps:

1. Factor the generalized unitary interactor matrix from  $T$  as  $D_G$ ;
2. Fit routine operating data  $Y_t$  by a time series model,  $G_d$ ;
3. Multiply  $G_d$  by  $q^{-d}D_G$  to obtain  $G'_d = q^{-d}D_G G_d$ , where  $d$  is the order of the interactor matrix;
4. Expand  $G'_d$  into

$$G'_d = \underbrace{F_0 + F_1 q^{-1} + \dots + F_{d-1} q^{-(d-1)}}_F + q^{-d} \phi$$



where  $F_i$  for  $(i = 1, 2, \dots, d-1)$  are constant coefficient matrices, and  $\phi$  is the remaining (proper) term after the expansion;

5. Using partial fraction expansion,  $\phi$  can be expanded into

$$\phi = R_{nmp} + L$$

where all poles of  $R_{nmp}$  are unstable poles which are the non-invertible zeros of  $T$ , and  $L$  is the remaining term after the partial fraction expansion. Then the process under admissible minimum variance or optimal  $H_2$  control can be written as<sup>4</sup>

$$Y_t|_{admv} = q^d D_G^{-1} (F + q^{-d} R_{nmp}) a_t \quad (12.16)$$

This procedure will evaluate control performance with the admissible minimum variance or optimal  $H_2$  control as the benchmark. To assess control performance with the user specified benchmark as the desired closed-loop dynamics, a user specified transfer function matrix  $G_R$  should be augmented to equation (12.16) as

$$Y_t|_{user} = q^d D_G^{-1} (F + q^{-d} R_{nmp} + q^{-d} G_R) a_t \quad (12.17)$$

Note that the closed-loop dynamics also depend on the poles of  $D_G^{-1}$  (reciprocals of the non-invertible zeros) in addition to poles of  $G_R$ .

Now we show that the specification in equation (12.17) gives performance that is achievable. Under the IMC framework, closed-loop response can be written as

$$\begin{aligned} Y_t &= (I - TQ^*) N a_t \\ &= N a_t - TQ^* N a_t \end{aligned} \quad (12.18)$$

$$= (q^d D_G^{-1}) (q^{-d} D_G N) a_t - TQ^* N a_t \quad (12.19)$$

Using the Diophantine identity,  $q^{-d} D_G N$  can be expanded as

$$q^{-d} D_G N = \underbrace{F_0 + F_1 q^{-1} + \dots + F_{d-1} q^{-(d-1)}}_F + q^{-d} \underbrace{(R_{nmp} + R_{mp})}_R$$

---

<sup>4</sup>In this chapter, the subscript "admv" stands for "admissible minimum variance control". For example,  $Y_t|_{admv}$  represents the process output under the admissible minimum variance control.

where  $R_{nmp}$  contains all unstable poles of  $R$  after partial fraction expansion, while  $R_{mp}$  contains all stable poles after the partial fraction expansion. Using this identity, equation (12.19) can be written as

$$\begin{aligned} Y_t &= q^d D_G^{-1} (F + q^{-d} R_{nmp} + q^{-d} R_{mp}) a_t - T Q^* N a_t \\ &= q^d D_G^{-1} (F + q^{-d} R_{nmp}) a_t + [(q^d D_G^{-1}) R_{mp} q^{-d} - T Q^* N] a_t \end{aligned} \quad (12.20)$$

Equating equation (12.20) and equation (12.17) yields

$$(q^d D_G^{-1}) R_{mp} q^{-d} - T Q^* N = q^d D_G^{-1} G_R q^{-d}$$

This can be written as

$$(q^d D_G^{-1}) R_{mp} q^{-d} - D_G^{-1} \tilde{T} Q^* N = q^d D_G^{-1} G_R q^{-d} \quad (12.21)$$

Solving equation (12.21) yields

$$Q^* = \tilde{T}^{-1} (R_{mp} - G_R) N^{-1} \quad (12.22)$$

This is an achievable IMC control law.

As in the discussion for the minimum phase system, if one specifies  $G_R = (I - G_F) R_{mp}$ , where  $G_F$  is a filter transfer function matrix, then equation (12.22) becomes

$$Q^* = \tilde{T}^{-1} G_F R_{mp} N^{-1} \quad (12.23)$$

and equation (12.17) becomes

$$Y_t|_{user} = q^d D_G^{-1} (F + q^{-d} R_{nmp} + q^{-d} (I - G_F) R_{mp}) a_t \quad (12.24)$$

If  $G_F = 0$ , then the process is in the open-loop mode. If  $G_F = I$ , then equation (12.24) is the admissible minimum variance or optimal  $H_2$  control response. Therefore, the filter  $G_F$  adjusts the controller performance between open-loop mode and optimal  $H_2$  control.

Consider the closed-loop transfer function defined by

$$G_w = (I + TQ)^{-1} T$$

$G_w$  is the closed-loop transfer function from the dither signal  $w_t$  to the output  $Y_t$  (see Figure (12.5)). With dither signal excitation,  $G_w$  can be identified under closed-loop

conditions. Identification of the closed-loop transfer function matrix  $G_w$  under closed-loop conditions is equivalent to an open-loop identification problem.

Using routine operating data, the disturbance transfer function  $N$  can be identified via time series analysis of sensitivity-filtered data  $S^{-1}Y_t$ , i.e.

$$S^{-1}Y_t = (I + TQ)Y_t = Na_t$$

where the sensitivity  $S$  is defined by  $S = (I + TQ)^{-1}$ . Since  $G_w = (I + TQ)^{-1}T$ , we have

$$S = I - G_wQ$$

where  $Q$  is normally assumed to be known, but it can also be directly identified from closed-loop data. Therefore, the disturbance transfer function matrix can be estimated under closed-loop conditions. With the knowledge of  $D_G$ ,  $N$  and the user specified filter  $G_F$ , one can calculate the user specified benchmark performance via equation (12.24). The simplest form of  $G_R$  will be a diagonal matrix.

**Example 13** Consider the following system from Tsiliogiannis and Suvoronos(1989):

$$T = \begin{bmatrix} \frac{0.6q^{-1}}{1-0.4q^{-1}} & \frac{0.5q^{-1}}{1-0.5q^{-1}} \\ \frac{0.6q^{-1}}{1-0.5q^{-1}} & \frac{0.6q^{-1}}{1-0.4q^{-1}} \end{bmatrix}$$

Assume the disturbance transfer function matrix as

$$N = \begin{bmatrix} \frac{1}{1-0.5q^{-1}} & \frac{-0.6}{1-0.5q^{-1}} \\ \frac{0.5}{1-0.5q^{-1}} & \frac{1}{1-0.5q^{-1}} \end{bmatrix}$$

A generalized unitary interactor matrix can be factored as:

$$D_G = D_f D_{inf} = \begin{bmatrix} -0.6742q & -0.7385q \\ \frac{-0.7385(1-1.5477q)q}{q-1.5477} & \frac{0.6742(1-1.5477q)q}{q-1.5477} \end{bmatrix}$$

and the solution of the Diophantine identity yields

$$\begin{aligned} q^{-d}D_G N &= q^{-1}D_G N \\ &= \underbrace{\begin{bmatrix} -1.0434 & -0.3340 \\ \frac{0.6213-0.1340q^{-1}}{1-1.5477q^{-1}} & \frac{-1.7293+0.3731q^{-1}}{1-1.5477q^{-1}} \end{bmatrix}}_{F+q^{-d}R_{nmp}} + q^{-1} \underbrace{\begin{bmatrix} \frac{-0.5217}{1-0.5q^{-1}} & \frac{-0.1670}{1-0.5q^{-1}} \\ \frac{0.0433}{1-0.5q^{-1}} & \frac{-0.1205}{1-0.5q^{-1}} \end{bmatrix}}_{R_{mp}} \end{aligned}$$

The closed-loop response under admissible minimum variance control is therefore given by

$$q^{-d}D_G Y_t|_{admv} = (F + q^{-d}R_{nmp})a_t \quad (12.25)$$

Assume, for simplicity, that  $Var(a_t) = I$ , then the achievable minimum variance can be calculated from equation (12.25) as:

$$\Sigma_{admv} \triangleq Var(Y_t|_{admv}) = \begin{bmatrix} 1.6137 & -0.3521 \\ -0.3521 & 1.4988 \end{bmatrix} \quad (12.26)$$

and its quadratic measure ( $H_2$  norm)

$$E(Y_t^T Y_t)|_{admv} = tr(\Sigma_{admv}) = 3.1125$$

Suppose that the controller sampling interval is  $\Delta T = 5$  sec and a closed-loop response with time constant  $\tau = 1$  min is desired. According to this requirement, a filter can be designed as

$$G_F = \begin{bmatrix} \frac{0.08}{1-0.92q^{-1}} & 0 \\ 0 & \frac{0.08}{1-0.92q^{-1}} \end{bmatrix}$$

Since  $G_F(q^{-1} = 1) = I$ , this specification preserves the asymptotic property of the type 1 system. From equation (12.24), the user specified closed-loop response can be written as

$$q^{-d}D_G Y_t = (F + q^{-d}R_{nmp} + q^{-d}(I - G_F)R_{mp})a_t \quad (12.27)$$

Substituting numerical values into equation (12.27) and simplifying the results gives

$$\begin{aligned} & \begin{bmatrix} -0.674 + 0.957q^{-1} - 0.310q^{-2} & -0.738 + 1.048q^{-1} - 0.339q^{-2} \\ 1.143 - 2.361q^{-1} + 1.574q^{-2} - 0.339q^{-3} & -1.001 + 2.069q^{-1} - 1.379q^{-2} + 0.297q^{-3} \end{bmatrix} Y_t \\ &= \begin{bmatrix} -1.523 + 1.961q^{-1} - 0.48q^{-2} & -0.487 + 0.627q^{-1} - 0.153q^{-2} \\ 0.661 - 1.117q^{-1} + 0.537q^{-2} - 0.061q^{-3} & -1.840 + 3.111q^{-1} - 1.497q^{-2} + 0.171q^{-3} \end{bmatrix} a_t \end{aligned}$$

This is an achievable closed-loop response satisfying user's requirement. Its variance can be calculated as

$$\Sigma_{user} \triangleq Var(Y_t|_{user}) = \begin{bmatrix} 2.3131 & 0.3130 \\ 0.3130 & 2.3248 \end{bmatrix}$$

and its quadratic measure ( $H_2$  norm) as

$$E(Y_t^T Y_t)|_{user} = tr(\Sigma_{user}) = 4.6379$$

which is 50% larger than the achievable minimum variance. The performance indices are also adjusted accordingly. For example, the quadratic function based performance measure is adjusted according to

$$\eta_{user} = 1.5\eta_{admv}$$

where

$$\eta_{user} \triangleq \frac{tr(\Sigma_{user})}{tr(\Sigma_Y)}$$

## 12.5 Conclusions

Practical feedback control performance assessment has been discussed in this chapter. A filtered optimal  $H_2$  control law with desired closed-loop dynamics has been proposed as a practical benchmark to assess control loop performance. The proposed approach has taken into account both minimum phase and nonminimum phase systems. Simulated examples have illustrated application of the proposed methods.

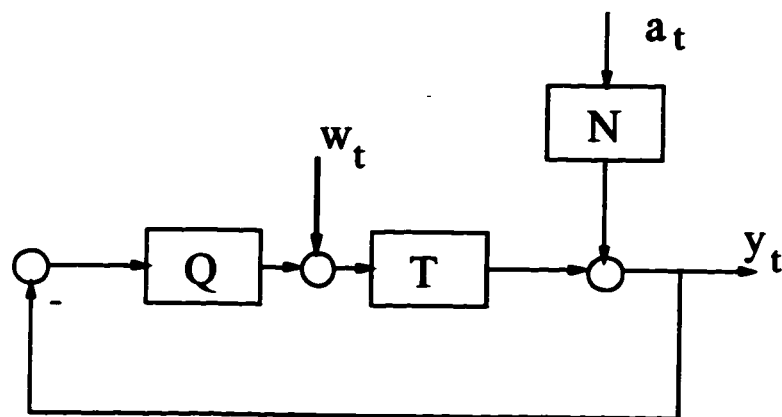


Figure 12.5: *Block diagram of the closed-loop system.*

## Chapter 13

# Performance Assessment: LQG Benchmark

### 13.1 Introduction

Many authors (Harris(1989), Desborough and Harris(1992) , Stanfelj *et al.*(1993) , Lynch and Dumont(1993) , Kozub and Garcia(1993) ) have reported the use of minimum variance control as a benchmark standard against which to assess control loop performance. This idea has been extended to MIMO processes in the previous chapters. However, these methods are concerned with performance assessment with minimum variance or optimal  $H_2$  norm control as the benchmark, a benchmark which does not explicitly take into account the control effort.

In any case, minimum variance control is usually not a desired control algorithm of choice in most practical situations due to its demand for excessive control action and poor robustness. However, performance assessment with minimum variance or optimal  $H_2$  norm control as the benchmark does provide us with such useful information as a global lower bound of process variance or the  $H_2$  norm measure. For example, if a controller indicates good performance relative to minimum variance control, then further tuning of the existing

---

<sup>1</sup> A version of this chapter has been presented at the 1996 AIChE Annual Meeting.

controller would be neither useful nor necessary. However, if a process indicates poor performance relative to minimum variance control, then there is a potential to improve its performance but no guarantee that the performance may be improved by retuning the existing controller. In such cases further analysis, such as performance evaluation with control action constraints taken into account, may be necessary. In general, tighter quality specifications result in smaller variation in the process output but typically requires more control effort. One may therefore be more interested in knowing how far away is the control performance from the “best” achievable performance with the same control effort, i.e. in mathematical form the resolution of the following problem may be of interest:

Given  $E[u_t^2] \leq \alpha$ , what is  $\min\{E[y_t^2]\}$ ?

The solution (achievable performance) is given by a tradeoff curve as shown in Figure 13.1. This curve can be obtained from solving the LQG problem (Kwakernaak and Sivan, 1972; Harris, 1985; Boyd and Barratt, 1991), where the LQG objective function is defined by

$$J(\lambda) = E[y_t^2] + \lambda E[u_t^2]$$

By varying  $\lambda$ , various optimal solutions of  $E[y_t^2]$  and  $E[u_t^2]$  can be calculated. Thus a curve with the optimal  $E[u_t^2]$  as the abscissa and  $E[y_t^2]$  as the ordinate is formed from these solutions. Boyd and Barratt (Boyd and Barratt, 1991) have also shown that a variety of constraints (e.g. hard constraints, robustness specification and etc.) can be formed as convex optimization problems and are readily solved via convex optimization tools. Any linear controller can only operate in the region above the tradeoff curve (Boyd and Barratt, 1991) shown in Figure 13.1. It is clear that given  $E[u_t^2] = \alpha$ , the minimum value (or the Pareto optimal value (Boyd and Barratt, 1991)) of  $E[y_t^2]$  can be found from this curve. This curve therefore represents the bound of performance and can be used for performance assessment purpose.



## 13.2 Performance assessment with control action taken into account

### 13.2.1 LQG solution via state space or input-output model

The theory in this section is well-known. Readers are referred to Kwakernaak and Sivan (1972) and Astrom and Wittenmark (1990). We will not discuss the theory but rather emphasize the LQG solution strategy via the Control Toolbox in Matlab in this section.

Consider a state space model as

$$\begin{aligned}x_{t+1} &= Ax_t + Bu_t + Gw_t \\ y_t &= Cx_t + Du_t + v_t\end{aligned}$$

where

$$E[w] = E[v] = 0, \quad E[ww^T] = Q, \quad E[vv^T] = R, \quad E[wv^T] = V$$

Then the Kalman filter can be written as

$$x_t^f = x_t^p + K^f(y_t - Cx_t^p - Du_t)$$

where  $x_t^p$  is the state prediction and can be written as

$$x_{t+1}^p = Ax_t^f + Bu_t$$

The steady state Kalman filter gain  $K^f$  can be solved via the Riccati equation (Kwakernaak and Sivan, 1972). The solution is readily available via a Matlab function such as *dlqe*. If the state transition matrix  $A$  is singular (e.g. due to time delays), then the function *dlqe2* in the Matlab based MPC toolbox can be used. This uses the iterative method to solve the Riccati equation.

The optimal state feedback gain  $L$  ( $u_t = -Lx_t^f$ ) is also solved via the Riccati equation (Kwakernaak and Sivan, 1972). The solution is readily available in the Matlab function *dlqr*. For a singular matrix  $A$ , one could use *dare* in the LMI/Matlab toolbox, which also uses an iterative method to solve the Riccati equation.

One can also solve the LQG problem with the input-output transfer function via Harris and MacGregor (1987) approach which uses the spectral factorization and the solution of the Diophantine identity. A special case (when the control weighting is zero) has been discussed in Chapter 4. For the general solution, readers are referred to Harris and MacGregor (1987).

### 13.2.2 LQG solution via GPC

Another way to solve this LQG problem is via the generalized predictive control (GPC) or model predictive control (MPC) approach (since the multivariate MPC/Matlab toolbox is available). Consider a cost function of the form (Clarke *et al.*, 1987):

$$J_{GPC} = E\left\{ \sum_{j=N_1}^{N_2} [y_{t+j} - r_{t+j}]^2 + \sum_{j=1}^{N_u} \lambda [\Delta u_{t+j-1}]^2 \right\}$$

GPC gives a control law which “minimizes” the above objective function. However, in order to achieve a time-invariant control law, only the first control action is actually implemented in GPC, i.e. it is a receding horizon control law. Therefore, the GPC control law does not truly minimize the above objective function. However for  $N_1 = 1$ ,  $N_u = N_2$ , and  $N_2 \rightarrow \infty$ , this objective function converges to the LQG objective function (Clarke *et al.*, 1987; Garcia *et al.*, 1989; Bitmead *et al.*, 1990), i.e.

$$\frac{1}{N_2} J_{GPC} \rightarrow J_{LQG} = E[y_t - r_t]^2 + \lambda E[\Delta u_t]^2$$

Minimization of this LQG objective function, as has been shown in Kwakernaak and Sivan (1972), yields a time-invariant optimal control law. Since the control law is time invariant for this special tuning, the GPC control law does truly optimize its objective function irrespective of the fact that only the first control move is actually implemented. Therefore, the LQG problem can be solved via the infinite GPC solution. But as  $N_2 \rightarrow \infty$ , GPC computation requires the solution of a large linear least squares problem, while LQG involves the solution of the recursive Riccati equation. Nevertheless, in practice, a finite value of  $N_2$  is usually enough to achieve the approximate infinite horizon LQG solution via the GPC approach. Thus, the MPC toolbox in Matlab provides a convenient approach to solve the LQG problem of MIMO processes.

### 13.2.3 The tradeoff curve

Once the problem is formulated as the LQG problem, the tradeoff curve can be calculated by varying the control weighting  $\lambda$ . For the SISO application, this is straightforward. To extend this result into MIMO systems, we need to further explore this idea. Suppose that the white noise sequence  $a_t$  satisfies  $Var(a_t) = 1$ . However if  $Var(a_t) = \sigma_a^2 \neq 1$ , one can always normalize it to achieve such a form. For example, in the ARMAX form

$$Ay_t = Bu_t + Ca_t$$

If  $Var(a_t) = \sigma_a^2 \neq 1$ , then multiply the polynomial  $C$  such that  $C' = C\sigma_a$ , and the new ARMAX model can be written as

$$Ay_t = Bu_t + C'a'_t$$

where the new white noise sequence  $a'_t = \sigma_a^{-1}a_t$  and therefore satisfies  $Var(a'_t) = 1$ . In the sequel, we therefore assume  $Var(a_t) = 1$  without loss of generality.

Suppose that a regulatory LQG control law is  $u_t = -\frac{E}{F}y_t$ , then

$$y_t = \frac{CF}{AF + BE}a_t \triangleq G_y a_t$$

and

$$u_t = -\frac{CE}{AF + BE}a_t \triangleq G_u a_t$$

where  $F$  and  $E$  are functions of  $\lambda$ . The variance can be expressed as

$$Var(y_t) = Var[G_y a_t] = \frac{1}{2\pi} \int_{-\pi}^{\pi} |G_y(e^{j\omega})|^2 \sigma_a^2 d\omega = \|G_y\|_2^2 \sigma_a^2 = \|G_y\|_2^2$$

where the second equality holds by applying Parseval's Theorem. Similarly,

$$Var(u_t) = \|G_u\|_2^2 \sigma_a^2 = \|G_u\|_2^2$$

Therefore,  $Var(y_t)$  and  $Var(u_t)$  are the  $H_2$  norms of the closed-loop transfer functions from disturbance  $a_t$  to  $y_t$  and  $u_t$  respectively. Thus, the “size” of the closed-loop transfer function of  $y_t$  or  $u_t$  is of main concern in the performance assessment, irrespective of the type of the disturbances  $a_t$ . In this way, the  $H_2$ -norm measure of  $y_t$  or  $u_t$  can

Table 13.1: The procedure for calculation of the LQG tradeoff curve

- 
- 
1. Formulate the problem in an appropriate LQG format.
  2. Choose appropriate output weighting  $W$  and control weighting  $R$ .
  3. By varying  $\lambda$ , a series of LQG control laws can be calculated. Using these LQG control laws, one can form the closed-loop transfer function from  $a_t$  to  $Y_t$  and  $U_t$  respectively.
  4. The  $H_2$  norms of the closed-loop transfer functions from  $a_t$  to  $Y_t$  and  $U_t$  respectively can then be calculated to provide a tradeoff curve.
- 
- 

also be applied to deterministic systems by replacing  $N$  to correspond to deterministic disturbances or a specific setpoint model. More importantly, this measure can be directly extended to the MIMO case, i.e.  $H_2$  norms of the closed-loop transfer function matrices from disturbance  $a_t$  to  $Y_t$  and  $U_t$  are used for the performance measure.

For the MIMO case, the objective function of LQG control is written as

$$J = E[Y_t^T W Y_t] + \lambda E[U_t^T R U_t]$$

where the output weighting  $W$  should be chosen in such a way that it reflects the relative importance of the individual outputs; the control weighting  $R$  is also chosen according to the relative cost of individual control moves. By varying  $\lambda$ , various LQG control law can be calculated. From the LQG control laws, one can calculate the closed-loop transfer function matrices from  $a_t$  to  $Y_t$  and  $U_t$  respectively as e.g.,  $G_Y$  and  $G_U$ . Then the  $H_2$  norm,  $\|G_Y\|_W^2 = \{E(Y_t^T W Y_t)\}$  and  $\|G_U\|_R^2 = \{E(U_t^T R U_t)\}$  can be used to plot the tradeoff curve. The procedure for constructing the tradeoff curve is summarized in Table 13.1

### 13.2.4 Performance assessment

Using LQG as the benchmark to assess control loop performance requires a complete knowledge of the plant model. An open or closed-loop identification effort is therefore required. Recent research on control relevant identification has shown that closed-loop identification is not necessarily poorer than open-loop identification if the objective of identification is for control (Bitmead, 1993; Gevers, 1993; Van den Hof and Schrama, 1995). For example, to design an LQG controller, the model is best identified under closed-loop condition with the desired LQG controller running in the loop (Zang *et al.*, 1995). Calculation of the tradeoff curve is similar to the design of a series of LQG controllers by identifying an appropriate plant model. In control relevant identification, the “best” model is identified by using an iterative method, i.e. identify a model; then re-design an LQG controller; re-identifying the model using data collected under the LQG control; then re-designing the LQG controller and so on. This approach is clearly not suitable for calculation of the tradeoff curve which requires a series of LQG designs. Identification of a “best” model for calculation of the LQG tradeoff curve thus remains an open problem for future research. In this section, the traditional identification methods are used to find the plant model instead. For example, we can identify the model under either closed-loop or open-loop conditions. Under closed-loop condition, we can use direct identification or the two-step identification as proposed in the next chapter.

The noise model is also important for the solution of the LQG problem. It may be jointly identified with the plant model using routine operating data with dither excitation, if regulation of these “routine” disturbances is of interest. The prediction error method (PEM) provides models of both plant and disturbances. On the other hand, one may want to assess control loop performance with hypothetical disturbances. For example, one may want to know how well a controller regulates step disturbances or tracks setpoints. In this case, the noise model (or setpoint dynamics) may simply be substituted by  $1/(1 - q^{-1})$ , if step-type disturbance regulation or tracking is of interest.

Once the tradeoff curve is calculated, the next step is to calculate the  $H_2$ -norm of  $Y_t$  and  $U_t$  under existing control in order to compare them with the tradeoff curve. Three

different situations need to be considered.

If “routine” disturbances are of interest, then the white noise sequence  $a_t$  can be estimated from identification of the plant and noise model, i.e.

$$\hat{a}_t = \hat{N}^{-1}(Y_t - \hat{T}U_t)$$

where  $\hat{T}$  is the estimate of  $T$  and  $\hat{N}$  is the estimate of  $N$ . With the estimate of the white noise sequence  $\hat{a}_t$ , the transfer functions from  $a_t$  to  $Y_t$  and  $U_t$  can be identified. Then the  $H_2$  norms of  $Y_t$  and  $U_t$  are calculated.

If other hypothetical disturbances are of interest, then one needs to identify the sensitivity function  $S$ . The closed-loop transfer functions from  $a_t$  to  $Y_t$  and  $U_t$  can then be written as

$$Y_t = SNa_t$$

and

$$U_t = -SQNa_t$$

where

$$S = (I + TQ)^{-1}$$

If hypothetical setpoint changes ( $r_t$ ) are of interest, then the tracking error  $E_t$  is considered. The closed-loop transfer functions from  $r_t$  to  $E_t$  and  $U_t$  can be identified and denoted as  $G_E$  and  $G_U$ . Then the  $H_2$  norms of  $E_t$  and  $U_t$  are  $\|G_EN\|_2^2$  and  $\|G_UN\|_2^2$  respectively, where  $N$  characterizes the hypothetical setpoint dynamics.

### 13.3 Pilot-scale experimental evaluation

**Example 14** *To evaluate the proposed algorithm on a pilot-scale process, performance assessment of multivariate control loops was conducted on a two-interacting tank process shown in Figure 13.2. The levels ( $h_1, h_2$ ) of the two tanks are the two controlled variables. The two inlet flow rates ( $u_1, u_2$ ) are the manipulated variables. The sampling interval is selected as  $T_s = 5\text{sec}$ . One step time delay (in addition to the delay due to the zero-order-hold) is introduced at the actuator of the control valve supplying water to Tank #2.*

Table 13.2: Controller tuning parameters

Controller	$N_2$	$N_u$	$\lambda_1$	$\lambda_2$
GPC #1	10	10	0.4	0.4
GPC #2	5	5	0.33	0.33
GPC #3	5	5	0.5	0.5

IMC and GPC (or MPC) controllers were implemented on this process. To implement the IMC and GPC controllers, an open-loop identification test was first conducted to estimate the plant model. Using the *pem* function in Matlab, the open-loop model was identified as

$$T = \begin{bmatrix} \frac{0.1963q^{-1}-0.1737q^{-2}-0.0112q^{-3}}{1-1.7208q^{-1}+0.7272q^{-2}} & \frac{0.0406q^{-7}-0.0113q^{-8}+0.0009q^{-9}}{1-0.6495q^{-1}+0.0482q^{-2}} \\ \frac{0.0147q^{-1}-0.0127q^{-2}+0.02q^{-3}}{1-1.3537q^{-1}+0.3707q^{-2}} & \frac{0.0406q^{-2}-0.0299q^{-3}-0.0047q^{-4}}{1-1.7849q^{-1}+0.7902q^{-2}} \end{bmatrix}$$

The time domain validation on a separate set of data is shown in Figure 13.3.

The hypothetical disturbances dynamics, in this example, is taken to be

$$N = \begin{bmatrix} \frac{1}{1-q^{-1}} & 0 \\ 0 & \frac{1}{1-q^{-1}} \end{bmatrix} \quad (13.1)$$

to represent step-type disturbances or setpoint changes. Based on the estimated plant model, three GPC controllers with different tuning parameters were implemented on this process. The tuning parameters are shown in Table 13.2: As  $N_u = N_2$  and  $N_2 \rightarrow \infty$ , GPC theoretically converges to LQG solution. In this example, GPC converges to the infinite horizon case as  $N_2 = N_u \geq 10$ . Therefore, controller # 1 should theoretically give LQG performance. But this may not be true due to possible model-plant mismatch. We will evaluate the performance of these controllers in this section.

A multivariate IMC controller was also implemented on this process. To design the IMC controller, a unitary interactor matrix has to be factored out from the plant transfer function matrix  $T$ . It is

$$D = \begin{bmatrix} -0.9972q & -0.0748q \\ 0.0748q^2 & -0.9972q^2 \end{bmatrix}$$

This unitary interactor matrix (an all-pass factor of the infinite zeros) represents time-delays in the MIMO system. The optimal IMC (Optimal  $H_2$ -norm) controller is the inverse of the delay-free transfer function matrix  $\tilde{T}$ , where

$$\tilde{T} = DT$$

To make the IMC controller implementable on this process, a filter

$$f = \begin{bmatrix} \frac{0.1}{1-0.9q^{-1}} & 0 \\ 0 & \frac{0.1}{1-0.9q^{-1}} \end{bmatrix}$$

has to be cascaded to the optimal IMC controller. The final IMC controller is

$$Q^* = \tilde{T}^{-1} f$$

where  $Q^*$  is the controller in the IMC framework (Morari and Zafiriou, 1989). This IMC controller is denoted as controller #4 in the following discussion.

Now we begin the evaluation of these four controllers using experimental data. Suppose we have no knowledge of the plant model and the controllers in this case. Closed-loop identification has to be used to identify this model in order to assess performance of the four controllers. A random binary dither signal was inserted in the setpoint. The closed-loop response (both  $Y_t$  and  $U_t$  of the four controllers are shown in Figures 13.4, 13.5, 13.6 and 13.7. One can roughly get an indication of the relative performance of the four controllers by inspecting these four figures, but it is difficult to see how good these four controllers are relative to the best achievable control with the same control efforts.

A direct closed-loop identification using the prediction error method (Ljung, 1987; Soderstrom and Stoica, 1989) was applied to the four sets of data to estimate the plant model. Since the step-type setpoint tracking performance is of interest in this example, the setpoint dynamics requires  $N$  to take the form as expressed in equation 13.1. The tradeoff curve can be calculated as shown in Figure 13.8. One can see difference in the curves from different sets of data. This difference is clearly not due to disturbances since the signal to noise ratio is fairly high in this experiment. It is mainly attributable to the bias error, i.e., the model sets does not contain the true dynamics of the plant. Thus an



“LQG relevant identification strategy” is highly desirable for such an application. The topic of control relevant identification is beyond the scope of this thesis. Interested readers are referred to Kosut et al.(1992), Shook et al.(1992), Bitmead (1993) , Gevers (1993) and Van den Hof and Schrama (1995) for interesting discussions on this topic.

Since controller #1 is the closest to LQG control, the tradeoff curve calculated from this data set is used as the benchmark in this example. By directly fitting the tracking error  $E_t$  and the controller output  $U_t$  to the setpoint dither excitation  $r_t$ , we can estimate the closed-loop transfer function matrices from  $r_t$  to  $E_t$  and  $U_t$  respectively. The fittings from  $r_t$  to  $E_t$  and from  $r_t$  to  $U_t$  are open-loop identification problems. Time domain validation (first 100 data points) for one of the experiments, controller #1, is shown in Figure 13.9. The upper two graphs represent time domain validation of the fitting from  $r_t(2 \times 1)$  to  $E_t(2 \times 1)$ . The lower two graphs represent time domain validation of the fitting from  $r_t(2 \times 1)$  to  $U_t(2 \times 1)$ . The other three sets of controllers show similar results and are not reproduced here. Using the setpoint dynamics as in equation (13.1), the  $H_2$  norm of  $E_t$  and  $U_t$  for the four sets of controllers can be calculated and is shown in Figure 13.10. From this graph, one can compare the performance of different controllers or just one controller with different tuning parameters. Among the three GPC controllers, controller #1 is the closest to LQG as it should be. The difference between controller #1 and LQG may be attributed to model-plant mismatch. Controller #2 has the same “size” of tracking error as controller #1, but requires a larger control effort. Controller #3 exhibits a control effort which is similar to the IMC controller, controller #4, but yields a much smaller tracking error. We do not intend to show the superiority of any one controller over the other. In fact, any of the controllers can be retuned by adjusting the tuning or the filter parameters such that it moves toward the tradeoff curve. From this curve, one can clearly see the potential for improving the performance of controllers #2, #3 and #4. This study also provides insight as to how the various GPC controllers may be tuned to give the desired performance.

### 13.4 Case study on an industrial process

**Example 15** *The proposed performance assessment method was applied to monitor control loop performance of an industrial cascade control loop shown in Figure 13.11. In this example, we are interested in control performance under a regulatory mode for rejecting routine disturbances at the outer loop.*

In Chapter 2. We have shown that the average performance index in the outer loop is approximately 0.15, indicating relatively poor control. Clearly this loop has the potential to provide better controller via retuning the existing controller or redesigning the control algorithm. However one may ask how good this controller is relative to the achievable optimal control with the same control effort.

An open-loop test was conducted on this process using PRBS excitation. Due to the strong signal-noise-ratio in the experiment, a reasonable open-loop model is expected from open-loop data (Miller, 1995). However, the estimated noise model from open-loop data may not be completely reliable, since the noise model may vary with the operating conditions. The routine closed-loop operation may also be different from open-loop operation, since a relative large dither signal excitation was injected to perform the open-loop tests. Consequently the noise model obtained from open-loop tests may not represent the true noise dynamics under routine closed-loop condition. For performance assessment purposes, a noise model which reasonably represents the noise dynamics under normal working condition is necessary.

One approach to bypass this problem is to use routine closed-loop operating data for estimation of the noise model. This can be done by 1) calculating the sensitivity function, *i.e.*  $S = 1/(1 + TQ)$ ; 2) collecting routine closed-loop operating data and filtering the closed-loop data by the inverse sensitivity function, *i.e.*  $y^f = y/S$ ; 3) fitting the filtered closed-loop data by a time series model. Then this time series model is the estimated noise model from closed-loop data. This procedure is based on the fact that routine closed-loop data  $y_t$  can be written as

$$y_t = \frac{N}{1 + TQ} a_t$$

where  $N$  is the noise model and  $a_t$  is the white-noise excitation. If  $y_t$  is filtered by  $1/S$ , then  $y_t^f = y(1 + TQ) = Na_t$ . Therefore  $N$  can be estimated from time series analysis of  $y_t^f$ .

With the plant model and the noise model, the tradeoff curve is obtained from the LQG solution as shown in Figure 13.12. The abscissa represents the control variance measured by the expectation of incremental control action, while the ordinate represents the variance of the temperature.

Using this graph, we can also assess the performance relative to minimum variance control. The graph indicates that the tradeoff curve converges (towards right) to 0.07 when there is no constraint on incremental control action  $\Delta u_t$ . Therefore the minimum variance (without incremental control action constraint) is  $\sigma_{mv}^2 = 0.07$ . With the actual temperature variance  $\sigma_y^2 = 0.38$ , the performance index  $\eta(d) = \sigma_{mv}^2/\sigma_y^2 = 0.18$ .

The current variance of incremental control action is about  $E[\Delta u_t]^2 = 0.68$ . Using this control action variance, the achievable temperature variance can be found from the curve which is about 0.1. Thus the achievable performance measure with LQG as the benchmark is  $0.1/0.38 = 0.26$ . This is a more realistic measure of current control performance if control action cannot be allowed to exceed the current level. This number indicates that there is significant potential to improve the feedback controller performance without increasing the control effort. If we draw a horizontal line along the actual working point, it intersects the tradeoff curve at the point where  $E[\Delta u_t]^2 \rightarrow 0$ . A significant reduction of the incremental control variance would be possible without increasing output variance if an advanced controller such as LQG or DMC is implemented.

## 13.5 Conclusions

A practical control benchmark has been proposed for assessment of control loop performance. This practical benchmark takes both the control effort and the output performance into account. Calculation of such a benchmark control requires process identification. LQG is one such practical benchmark and its tradeoff curve can be

obtained in terms of the  $H_2$  norm of the appropriate transfer function matrices. Other practical benchmarks, which usually yield a similar tradeoff curve (Boyd and Barratt, 1991) and require a numerical solution, may also be considered for further study of practical performance assessment.

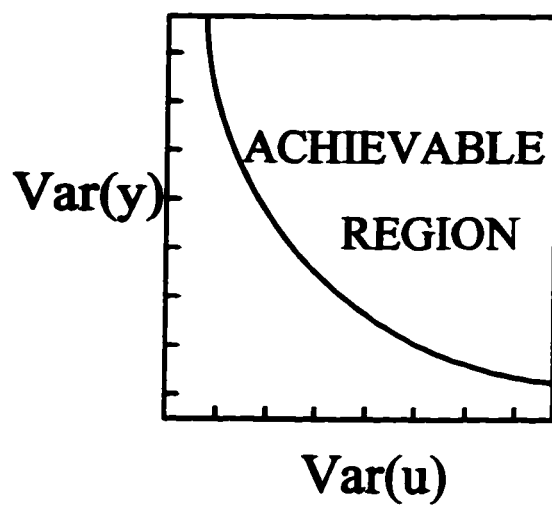


Figure 13.1: a typical tradeoff curve

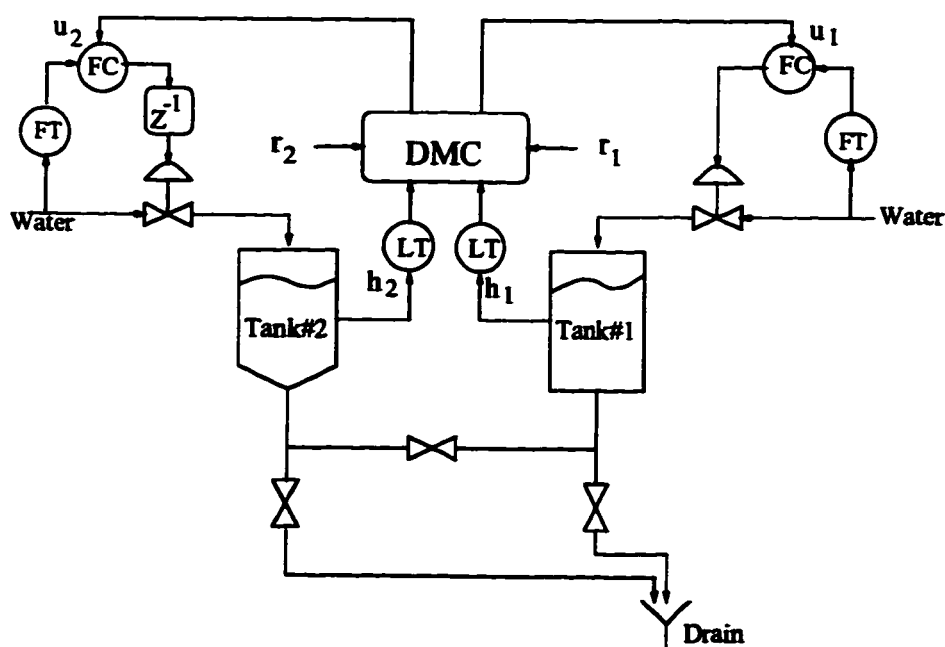


Figure 13.2: Schematic diagram of the pilot-scale process.

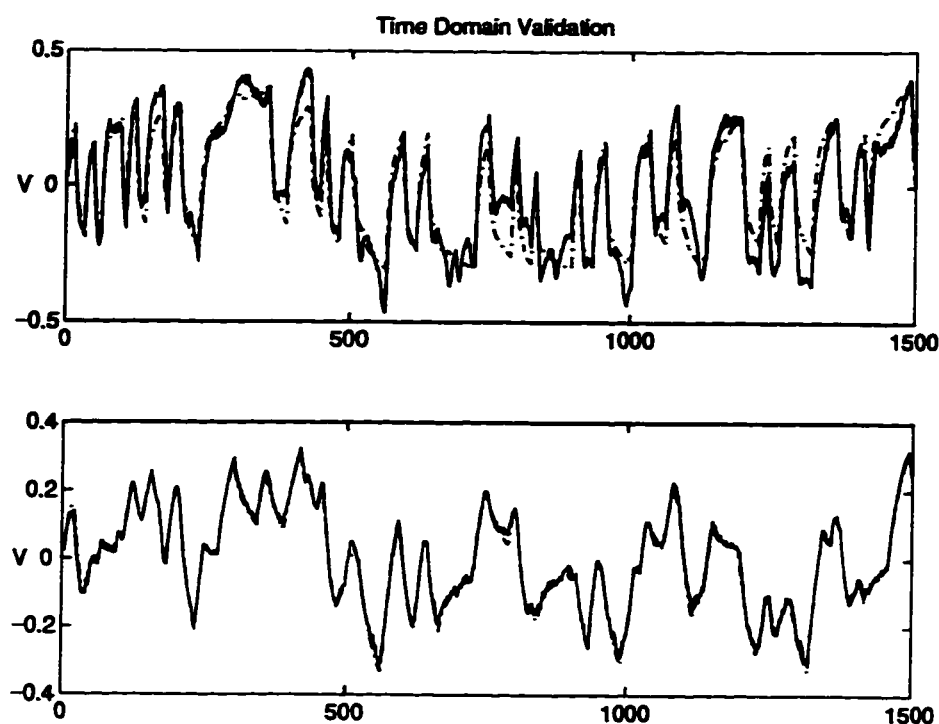


Figure 13.3: *Time domain validation of the open-loop model. The time scale is in terms of sampling intervals.*

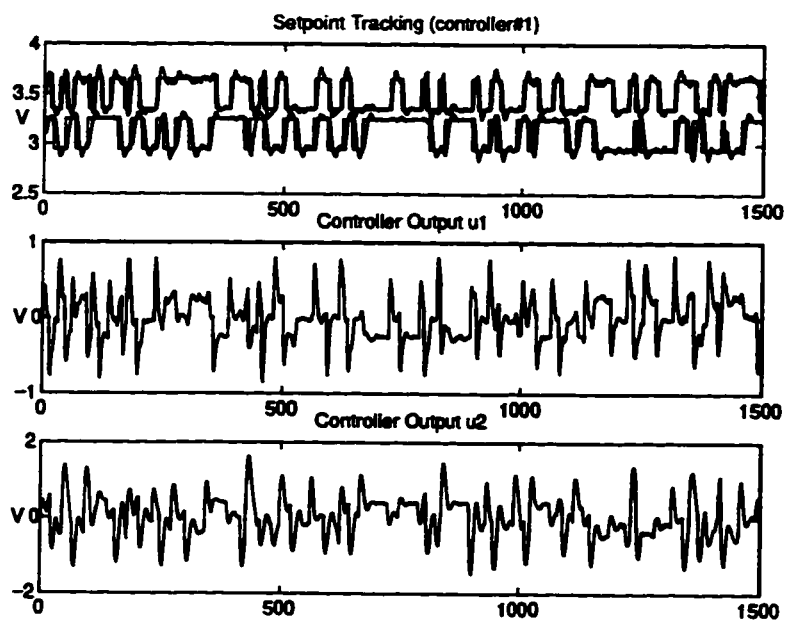


Figure 13.4: *Closed-loop test for controller #1. The time scale is in terms of sampling intervals.*

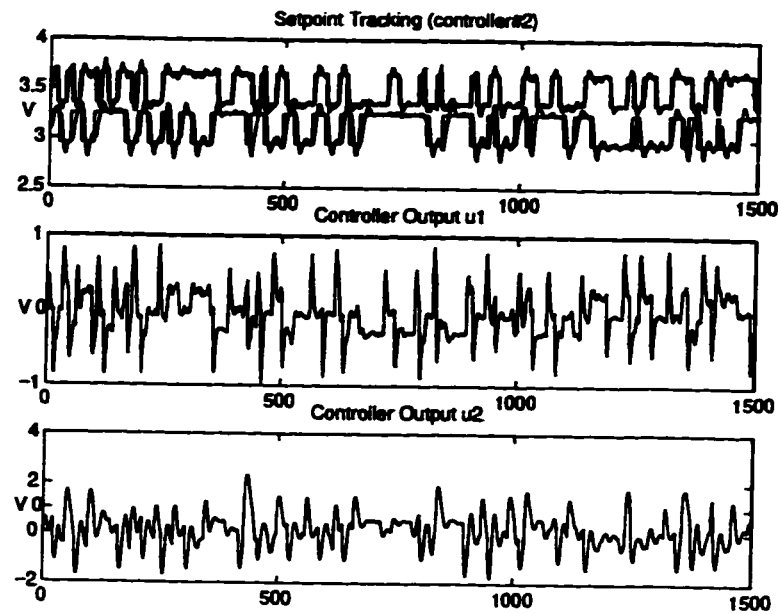


Figure 13.5: *Closed-loop test for controller #2. The time scale is in terms of sampling intervals.*

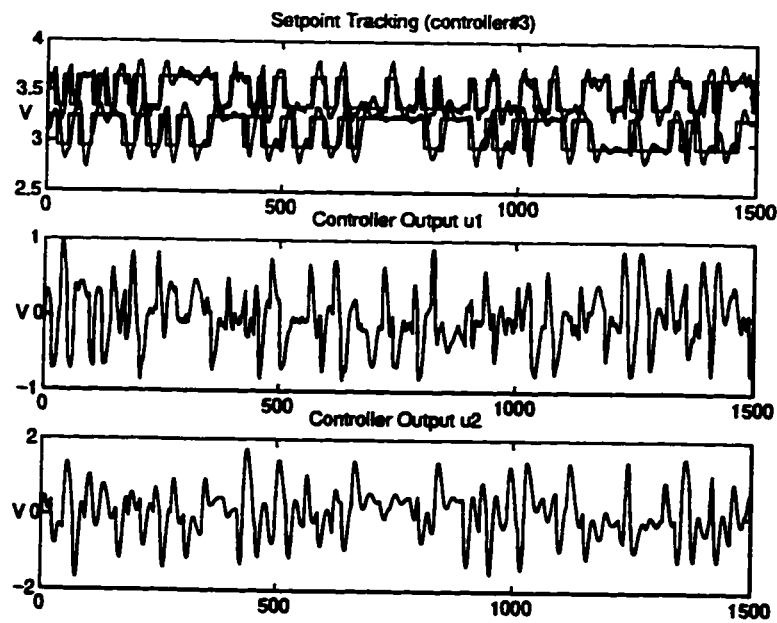


Figure 13.6: *Closed-loop test for controller #3. The time scale is in terms of sampling intervals.*

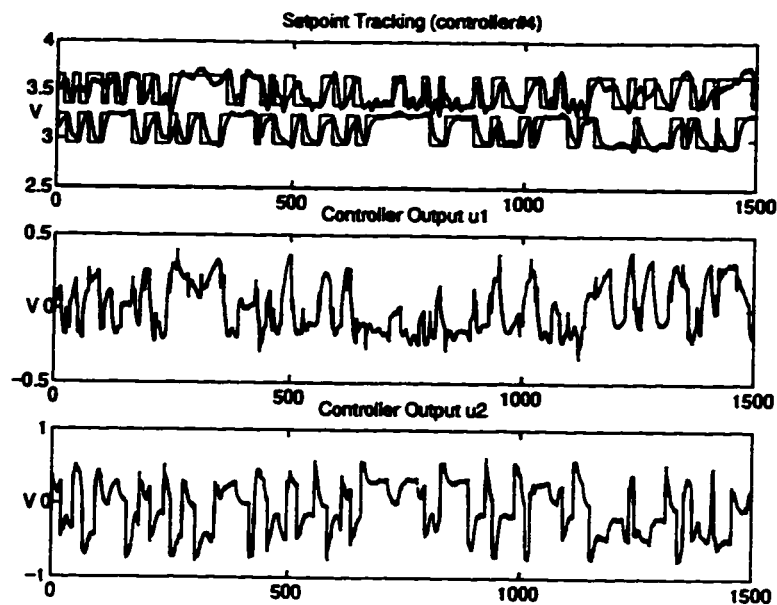


Figure 13.7: *Closed-loop test for controller #4. The time scale is in terms of sampling intervals.*

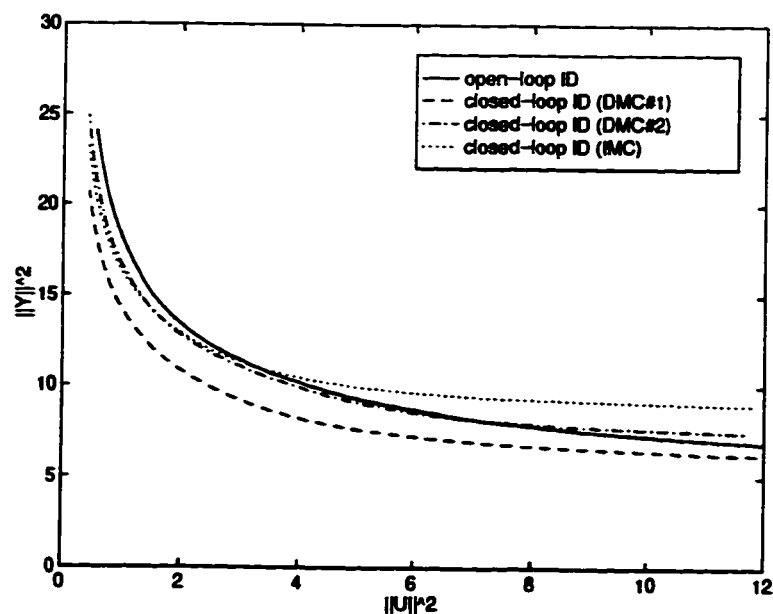


Figure 13.8: *Tradeoff curve estimated from different set of data. Controller #3 (DMC#3) is not shown in the graph for clarity of the graph.*



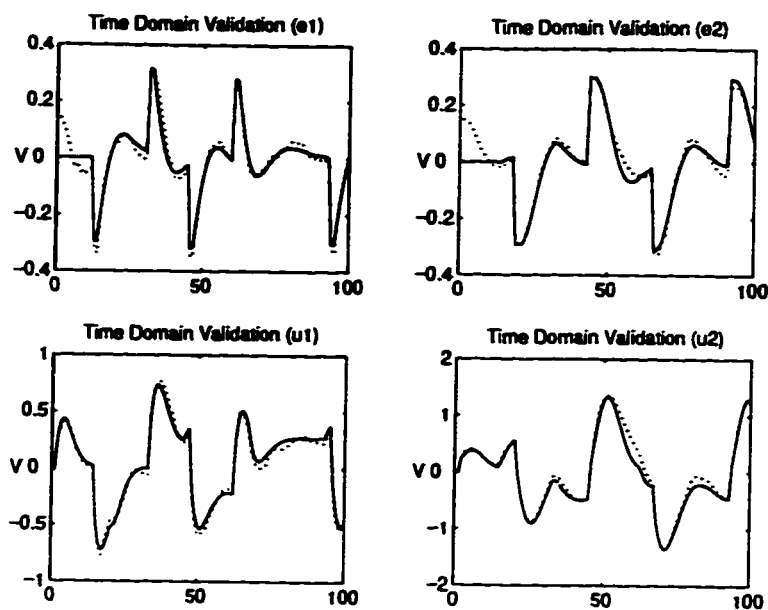


Figure 13.9: *Time domain validation for controller #1. The time scale is in terms of sampling intervals.*

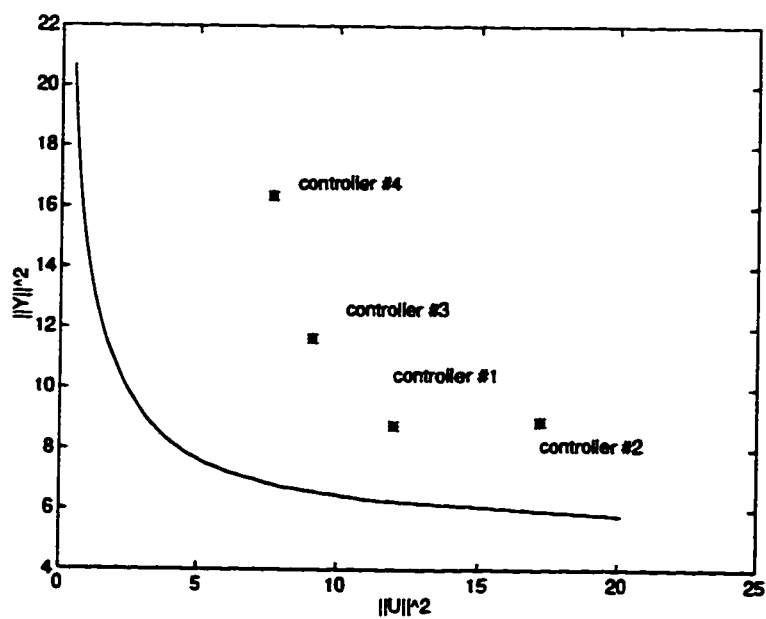


Figure 13.10: *Performance assessment of the four controllers.*

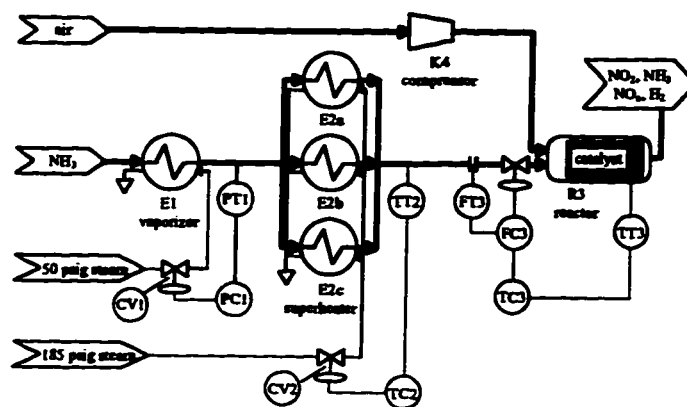


Figure 13.11: Schematic diagram of the industrial cascade reactor control loop

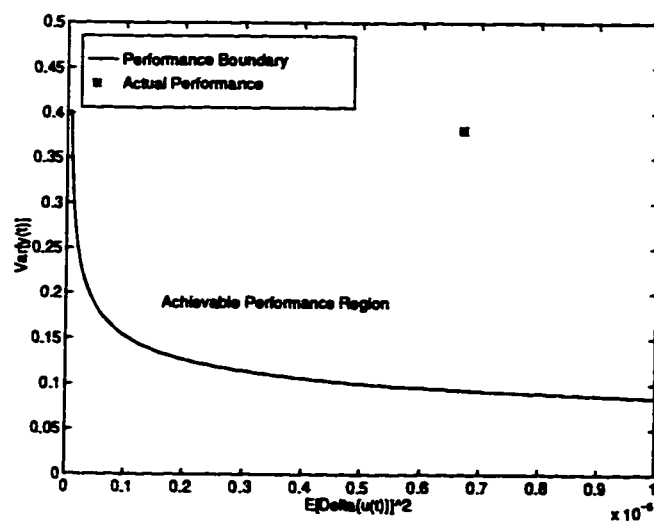


Figure 13.12: Performance assessment of the industrial cascade control loop (outer loop)

## Chapter 14

# Closed-loop Identification

### 14.1 Introduction

A necessary prerequisite for model-based control is a model of the process. Such certainty-equivalence, model-based control schemes rely on an off-line estimated model of the process, *i.e.* the process is “probed” or excited by a carefully designed input-signal under open-loop conditions and the input-output data are used to generate a suitable model of the process. In a majority of model-based control schemes used in the chemical process industry, the models are generated with little regard for their ultimate end-use, *e.g.* as in model-predictive control. Almost always in such cases, reduced-complexity models are generated to capture the most dominant dynamics of the process. Such batch or off-line identification methods represent a major effort and may require anywhere from several hours to several weeks of open-loop tests.

In contrast with this, the objective in closed-loop identification is to use routine operating data with dither signal excitation to develop a dynamic model of the process. It is practically a very appealing idea. In this mode, process identification can commence with the process in its natural closed-loop state. In some cases, the plant has to run under closed-loop conditions due to safety reasons. In other cases, if a linearized dynamic model

---

<sup>1</sup>A version of this chapter has been accepted for publication in the Journal of Process Control and has also been presented at the 1996 CShE Conference.

around a nominal operating point is desired, then this can be achieved by closed-loop identification, since otherwise under open-loop conditions the process variables may drift away from the nominal operating point.

The method of closed-loop identification has been in the development stage over the last 20 years. Important issues such as identifiability under closed-loop conditions have received attention from many researchers (Box and MacGregor, 1976; Goodwin and Payne, 1977; Gustavsson *et al.*, 1978; Soderstrom and Stoica, 1989). A number of identification strategies have been developed (Ljung, 1987; Soderstrom and Stoica, 1989). In traditional identification literature, the quality of identification and identifiability issues are mainly addressed under the assumption that the model set contains the plant i.e. the model can describe true process dynamics.

The more typical case is that of under-modelling or identification of reduced-complexity models when the plant is not in the model set. This is the focus of the present chapter and is a more realistic situation since a plant is generally of relatively high-order and the model structure used to approximate such process is almost always lower order. Stated simply, identification is an exercise in model-reduction. Under such circumstances, the model-plant error consists of two terms, the bias error (due to under-modelling) and the random error (or variance error) due to noise and disturbance effects. Several general expressions for the asymptotic variance and bias errors have been given by Ljung (Ljung, 1987). The relationship between the variance and bias errors has been recently addressed by Guo and Ljung (1994) and Ljung (1994). These general expressions for the bias distribution have also been extended to closed-loop identification (Bitmead *et al.*, 1990; Zhu and Backe, 1993; MacGregor and Fogal, 1995). It is well known that a data pre-filter can change the distribution of the bias error in the frequency range of interest (Ljung, 1987), and therefore plays a somehow similar role as the change in the frequency content of the dither signal. The choice of this pre-filter or alternatively the spectrum of the input signal is application dependent (Gevers and Ljung, 1986; Ljung, 1987; Rivera *et al.*, 1992).

Closed-loop identification has also attracted much interest due to the emerging research area of joint identification and control. The key idea in the joint identification and control

strategy (as opposed to a 'disjoint' or separate identification and control) is to identify *and* control with the objective of minimizing a joint global control performance criterion. This topic has received attention under such headings as: control-relevant identification, iterative identification and control *etc.* Readers are referred to Kosut *et al.*(1992), Shook *et al.*(1992), Bitmead (1993) , Gevers (1993) and Van den Hof and Schrama (1995) for detailed discussions on these topics. The study of control-relevant identification requires that the best identification strategy is to identify the process under feedback with the intended controller in use. For example, a model intended for the design of minimum variance control is best identified under minimum variance feedback control (Gevers and Ljung, 1986), and similarly for LQG control (Zang *et al.*, 1995; Hakvoort *et al.*, 1994), model reference control (Hjalmarsson *et al.*, 1994) *etc.*

The purpose of this chapter, however, is to focus attention *only* on the identification of the process model under closed-loop conditions. The estimated model is shown to have asymptotically identical expressions for the bias and variance terms regardless of how the identification run is conducted, *i.e.* irrespective of open-loop or closed-loop conditions. The estimated model can then be subsequently used for improving existing controller design, controller re-design, control-loop performance assessment, general analysis, *etc.* For example, a model obtained from closed-loop data under PID control may be used for the design of a DMC controller. Control loop performance assessment techniques as discussed in the previous chapters do not require an explicit process model when minimum variance control is used as a benchmark. However, if a more practical benchmark standard such as LQG is used for evaluating existing control loop performance, then more information about the process is required.

The main contribution of this chapter is the development of a two-step closed-loop identification algorithm which asymptotically yields the same expressions for both variance and bias errors as in open-loop identification. These results obviate the need to conduct expensive open-loop tests when simple closed-loop tests with dither signal excitation can suffice. This chapter illustrates the point that a suitable model of the process can be estimated from closed-loop data with appropriate filtering.

The chapter is organized as follows. Section 14.2 gives comparison between open-loop and closed-loop identification in terms of variance and bias errors. In Section 14.3, a two-step closed-loop identification scheme is proposed, which asymptotically yields the same expressions of variance and bias errors as open-loop identification. The proposed algorithm is evaluated on simulation examples in Section 14.5, and a computer-interfaced pilot-scale plant in Section 14.6.

## 14.2 Accuracy aspects of closed-loop identification

Consider a linear SISO plant, schematically illustrated in Figure 14.1, and described by

$$y = Tx + Na$$

where  $a$  is a white noise sequence,  $x$  is the input to the process,  $T$  is the process transfer function, and  $N$  is the noise transfer function. Let a model of the form

$$\hat{y} = \hat{T}x + \hat{N}a$$

be used to approximate the process dynamics. The prediction error is defined as

$$\hat{a} = \frac{1}{\hat{N}}(y - \hat{T}x)$$

The commonly used objective function for parameter identification is to minimize the sum of squares of the prediction error:

$$V = \frac{1}{M} \sum_{t=1}^M \hat{a}^2(t)$$

This method is denoted as the prediction error method or PEM (Ljung, 1987). The total error of the estimates can be attributed to variance and bias errors (Ljung, 1987) and may be conceptually written as a sum of the variance error and the bias error (Ljung, 1994):

$$V_T = V_V + V_B$$

In this section, we deal with both the bias and variance estimation errors and compare them between the open-loop and closed-loop cases. We show that the issue of variance and

bias error of the parameter estimates is common to both open and close-loop identification. The PEM is a general and efficient method for system identification. The variance of the PEM estimator asymptotically reaches the Cramer-Rao lower bound (Ljung, 1987). This asymptotic variance expressed in the frequency domain has been given by Ljung(1987).

**Theorem 11** (Ljung, 1987) *For input and output data  $x$  and  $y$  obtained from the process shown in Figure 14.1, where*

$$y = Tx + v = Tx + Na \quad (14.1)$$

*the following result holds for large sample size  $M$ , large model order  $n$  and small  $n/M$ :*

$$\text{Cov} \begin{bmatrix} \hat{T}(e^{j\omega}) \\ \hat{N}(e^{j\omega}) \end{bmatrix} \sim \frac{n}{M} \Phi_v(\omega) \Phi^{-1}(\omega) \quad (14.2)$$

where

$$\Phi(\omega) = \begin{bmatrix} \Phi_x(\omega) & \Phi_{xa}(\omega) \\ \Phi_{ax}(\omega) & \sigma_a^2 \end{bmatrix} \quad \text{and} \quad \Phi_v(\omega) = |N(e^{j\omega})|^2 \sigma_a^2$$

and where  $\Phi_*(\omega)$  denotes the spectrum of the corresponding signal  $*$ .

**Corollary 3** *For an open-loop system, with the input  $x = w$  ( $w$  is input excitation signal and is independent of noise  $a$ ), and output  $y$ , equation (14.1) can be written as*

$$y = Tw + v = Tw + Na \quad (14.3)$$

*The asymptotic variance of estimates using the PEM is given by*

$$\text{Var}[\hat{T}(e^{j\omega})] = \frac{n}{M} \frac{|N(e^{j\omega})|^2 \sigma_a^2}{\Phi_w(\omega)} = \frac{n}{M} \frac{\Phi_v(\omega)}{\Phi_w(\omega)} \quad (14.4)$$

$$\frac{\text{Var}\hat{N}(e^{j\omega})}{|N(e^{j\omega})|^2} = \frac{n}{M} \quad (14.5)$$

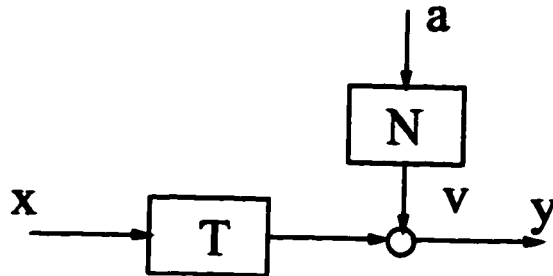


Figure 14.1: Process model block diagram

Proof follows directly from equation (14.2).

The results of Theorem 11 are more general than its statement may indicate. These results are also applicable to the closed-loop case (direct identification <sup>2</sup>) (Gevers and Ljung, 1986) since in this case the correlation between  $x$  and  $a$ ,  $\Phi_{xa}(\omega)$ , is considered in the expression for  $\Phi(\omega)$  (see equation(14.2)). In this way, Theorem 11 can also be extended to find the asymptotic variance of estimates  $\hat{T}$  (Zhu and Backe, 1993) and  $\hat{N}$  under closed-loop conditions, i.e.  $\Phi_{xa}(\omega) \neq 0$  (for the closed-loop case).

**Corollary 4** *Under closed-loop control, as illustrated in Figure 14.2, the asymptotic variance of the estimates is given by*

$$\text{Var}[\hat{T}(e^{j\omega})] = \frac{n}{M} \frac{\Phi_v(\omega)}{\Phi_w(\omega)} \frac{1}{|S(e^{j\omega})|^2} \quad (14.6)$$

$$\text{Var}[\hat{N}(e^{j\omega})] = \frac{n}{M} |N(e^{j\omega})|^2 (1 + |Q(e^{j\omega})|^2) \frac{\Phi_v(\omega)}{\Phi_w(\omega)} \quad (14.7)$$

where  $S = 1/(1+QT)$  is the sensitivity function;  $w$  is the dither signal and is independent of the noise sequence,  $a$ .

**Proof:** Under closed-loop conditions, the manipulated variable  $x$  can be written as

$$x = Sw - SQNa$$

Therefore

$$\Phi_x(\omega) = |S(e^{j\omega})|^2 \Phi_w(\omega) + |S(e^{j\omega})|^2 |Q(e^{j\omega})|^2 |N(e^{j\omega})|^2 \sigma_a^2 \quad (14.8)$$

$$\Phi_{xa}(\omega) = -S(e^{j\omega})Q(e^{j\omega})N(e^{j\omega})\sigma_a^2 \quad (14.9)$$

The corollary follows after substituting equation (14.8) and (14.9) into equation (14.2).

■

Thus the asymptotic variance of  $\hat{T}$  under closed-loop conditions depends on the sample size  $M$ , the signal to noise ratio (SNR),  $\Phi_w(\omega)/\Phi_v(\omega)$ , and the sensitivity function  $S(e^{j\omega})$ . Increasing sample size tends to improve the estimate. However, the sensitivity function

<sup>2</sup>Direct identification—identification of a plant model by directly using the input and output data regardless of the feedback effect.



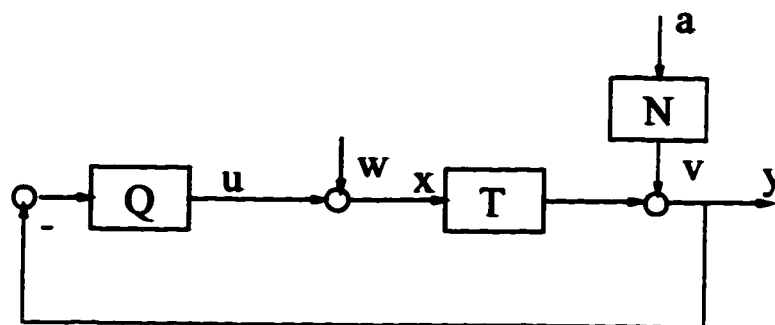


Figure 14.2: *Feedback control loop block diagram*

affects the accuracy inversely. In process control, the asymptotic regulatory property under closed-loop control is of main term of interest, i.e. it is desired to have asymptotic disturbance rejection or  $\lim_{\omega \rightarrow 0} S(e^{j\omega}) = 0$ . Typically the disturbances are step-type and therefore such asymptotic disturbance rejection (for step-type disturbances) is achieved by incorporating integral action. The estimate is consequently poor at these low frequencies if a white noise dither signal is used. However, one can also take advantage of the small value of the sensitivity at low frequency and use a dither signal which has more power at low frequency without upsetting the process. For other control strategies such as regulation of stochastic disturbances, the sensitivity function may have a small value in the middle or high frequency range, and therefore poor estimates in middle or high frequency range would be expected. The main difference in the asymptotic variance between open-loop and closed-loop identification, is the presence of the sensitivity function  $S$  (cf eqns (14.4) and (14.6)).

In addition to the variance of the estimates, another important measure of identification quality is the bias error. It exists whenever the process dynamics are not contained in the model set, as in reduced-complexity model identification. This in fact is almost always the case in practice. The distribution of bias errors in the frequency domain has been considered by Ljung (1987) through spectral characterization of the identification problem.

**Theorem 12** (Ljung, 1987) *For an open-loop process shown in equation(14.3), the estimation of model parameters in the limit is given by the following optimization problem:*

$$\theta_M \xrightarrow{M \rightarrow \infty} \arg \min \int_{-\pi}^{\pi} [|T(e^{j\omega}) - \hat{T}(e^{j\omega})|^2 \Phi_w(\omega) + \Phi_v(\omega)] \frac{1}{|\hat{N}(e^{j\omega})|^2} d\omega \quad (14.10)$$

where  $\theta_M$  is the estimated model parameters. If the noise model  $\hat{N}$  is chosen as being fixed such as  $\hat{N} = \bar{N}$ , then the second term on the right hand side of Equation (14.10) is constant, and the optimization problem simplifies to

$$\theta_M \xrightarrow{M \rightarrow \infty} \arg \min \int_{-\pi}^{\pi} |T(e^{j\omega}) - \hat{T}(e^{j\omega})|^2 \Phi_w(\omega) \frac{1}{|\bar{N}(e^{j\omega})|^2} d\omega \quad (14.11)$$

These results clearly indicate that the bias distribution of  $|T(e^{j\omega}) - \hat{T}(e^{j\omega})|$  in the frequency domain is weighted by the dither spectrum,  $\Phi_w(\omega)$ , and the inverse of the noise spectrum, i.e.  $1/|\hat{N}(e^{j\omega})|^2$  (also regarded as a noise filter), or simply the signal to noise ratio (SNR),  $\Phi_w(\omega)/|\hat{N}(e^{j\omega})|^2$ . If a unity noise model is considered, i.e.  $\bar{N} = 1$ , then the identification algorithm can be characterized as the output error method (OEM) (Ljung, 1987) which does not depend on the noise spectrum:

$$\theta_M \xrightarrow{M \rightarrow \infty} \arg \min \int_{-\pi}^{\pi} |T(e^{j\omega}) - \hat{T}(e^{j\omega})|^2 \Phi_w(\omega) d\omega \quad (14.12)$$

Theorem 12 can also be extended to the closed-loop case.

**Corollary 5** (MacGregor and Fogal, 1995) *For the closed-loop process shown in Figure 14.2, the estimation of model parameters in the limit is given by the following optimization problem:*

$$\theta_M \xrightarrow{M \rightarrow \infty} \arg \min \int_{-\pi}^{\pi} [|T(e^{j\omega}) - \hat{T}(e^{j\omega})|^2 \frac{|S(e^{j\omega})|^2}{|\hat{N}(e^{j\omega})|^2} \Phi_w(\omega) + \frac{|S(e^{j\omega})|^2}{|\hat{S}(e^{j\omega})|^2} \frac{|N(e^{j\omega})|^2}{|\hat{N}(e^{j\omega})|^2} \sigma_a^2] d\omega \quad (14.13)$$

where  $S$  is the sensitivity function and  $\hat{S} = \frac{1}{1+QT}$ .

**Proof:** See the proof in (MacGregor and Fogal, 1995). ■

If  $w$  is a sufficiently high order persistently exciting signal, and the set of  $\hat{T}$  contains  $T$ , the set of  $\hat{N}$  contains  $N$ , then both estimates are consistent by using the direct identification

Table 14.1: Expressions of the asymptotic variance and bias errors

	open-loop	closed-loop
Variance	$\frac{n}{M} \frac{\Phi_v(\omega)}{\Phi_w(\omega)}$	$\frac{n}{M} \frac{\Phi_v(\omega)}{\Phi_w(\omega)} \frac{1}{ S(e^{j\omega}) ^2}$
Bias distribution	$\int_{-\pi}^{\pi} [ T(e^{j\omega}) - \hat{T}(e^{j\omega}) ^2 \frac{\Phi_w(\omega)}{ N(e^{j\omega}) ^2} + \frac{\Phi_v(\omega)}{ N(e^{j\omega}) ^2}] d\omega$	$\int_{-\pi}^{\pi} [ T(e^{j\omega}) - \hat{T}(e^{j\omega}) ^2 \frac{ S(e^{j\omega}) ^2}{ N(e^{j\omega}) ^2} \Phi_w(\omega) + \frac{ S(e^{j\omega}) ^2}{ S(e^{j\omega}) ^2} \frac{ N(e^{j\omega}) ^2}{ N(e^{j\omega}) ^2} \sigma_a^2] d\omega$

method (Soderstrom and Stoica, 1989), *i.e.*,  $\hat{T} \xrightarrow{M \rightarrow \infty} T$  and  $\hat{N} \xrightarrow{M \rightarrow \infty} N$ . When the model set does not contain the process dynamics, which is generally the case and is of the interest in this chapter, a bias in estimation results, which is weighted once again not only by the SNR but also by the sensitivity function  $S$ . Thus the presence of the sensitivity function is the key difference between open-loop and closed-loop identification (cf Table 14.1). To summarize, the expressions for the asymptotic variance and bias errors under open-loop and closed-loop conditions are listed in Table 14.1.

**Remark 9** As pointed out by Schrama(1992) , Gevers(1993) and Hjalmarsson *et al.*(1994), the “best” model for the joint identification and control design is not necessarily the “best” open-loop model. In fact the “best” model for such design should have the bias error distribution weighted by the sensitivity function. But this sensitivity function is precisely the sensitivity function that one wishes to “design” through the choice of a suitable model-based controller once a suitable model is available. In terms of identification and control, this represents a “catch-22” situation, since an optimal controller cannot be designed if a control-compatible model is not available, and such a model cannot be estimated via closed-loop identification if its bias spectrum is not weighted by the appropriate sensitivity function. This is the main justification for iterative identification and control. However, in the majority of the design of model-based controllers, the estimation will not have the appropriate sensitivity function as a weighting term. Throughout this chapter, we do not assume that the feedback controller under which the closed-loop data are collected is the intended or the ideal controller of

choice. In such cases, the dependence on the sensitivity function in place, based on existing control, should be decoupled in the first place. Therefore one can decouple the effect of the current sensitivity function on the variance and bias errors and also shape the bias distribution through the choice of appropriate data filters and the spectrum of the signal (for closed-loop identification) or the input signal (for open-loop identification). In this way a model obtained via open or closed-loop identification can truly serve the purpose of improved control law design, analysis or control-loop performance assessment.

### 14.3 Two-step closed-loop identification

An effective way to reduce variance of estimates is to increase sample size, but this may not have the desired effect on the reduction of the bias error. Depending on the application, smaller errors in some frequency range, *e.g.* around the cross-over frequency may be desired, while larger errors at other frequencies may be tolerated. Data prefiltering can change the distribution of the bias error over the frequency range of interest (Ljung, 1987; Bitmead *et al.*, 1990). MacGregor and Fogal(1995) have also shown that data prefilters and the noise model have significant effect on the bias error and identifiability for closed-loop identification. Under closed-loop conditions, the design of data filter is complicated by the presence of the sensitivity function. In this section, we propose a two-step closed-loop identification method which can asymptotically decouple closed-loop parameter estimation from the effect of the undesired sensitivity function. In so doing, this work provides a closed-loop identification method which asymptotically retains the accuracy of open-loop identification. Thus many of the available open-loop experimental design techniques and data prefilters can be applied to closed-loop data. The most recent two-step identification algorithm proposed by Van den Hof and Schrama(1993), which has a similar procedure but has a different objective, is also summarized and compared with the two-step approach proposed here.

Table 14.2: Item to item correspondence between two equations

equation(14.3)	equation(14.15)
$y$	$x$
$w$	$w$
$T$	$S$
$N$	$-SQN$
$v$	$-SQNa$

### 14.3.1 Estimation of the sensitivity function—Step 1

For a closed-loop system shown in Figure 14.2, the closed-loop response can be written as

$$y = TS w + N S a \quad (14.14)$$

and

$$x = S w - SQ N a \quad (14.15)$$

The sensitivity function,  $S$ , can be estimated from equation (14.15), i.e. equation (14.15) presents a simple open-loop identification problem where the correlation between  $w$  and  $x$  yields  $\hat{S}$ . In order to apply Corollary 3 to analyze the variance error of the estimate,  $\hat{S}$ , the corresponding terms between equation(14.3) and equation(14.15) should be identified. The one-to-one correspondence between different terms in equations (14.3) and (14.15) is summarized in Table 14.2.

Using Table 14.2, the variance of the estimate of  $S$  can be found by applying Corollary 3 to equation (14.15) as

$$\text{Var}[\hat{S}(e^{j\omega})] = \frac{n}{M} \frac{\Phi_a(\omega) |N(e^{j\omega})|^2}{\Phi_w(\omega)} |S(e^{j\omega})|^2 |Q(e^{j\omega})|^2 = \frac{n}{M} \frac{\Phi_v(\omega)}{\Phi_w(\omega)} |S(e^{j\omega})|^2 |Q(e^{j\omega})|^2$$

and its relative variance as

$$\frac{\text{Var}[\hat{S}(e^{j\omega})]}{|S(e^{j\omega})|^2} = \frac{n}{M} \frac{\Phi_v(\omega)}{\Phi_w(\omega)} |Q(e^{j\omega})|^2 \quad (14.16)$$

which depends on controller dynamics  $Q$  in addition to the sample size, the model order and SNR. In subsequent applications we will show that only the relative accuracy of the sensitivity function is important.

Using Table 14.2, the bias distribution of the sensitivity function over the frequency range can be found by applying Theorem 12 to equation (14.15). This yields the bias distribution in the frequency domain as

$$\theta_{SM} \xrightarrow{M \rightarrow \infty} \arg \min \int_{-\pi}^{\pi} [|S(e^{j\omega}) - \hat{S}(e^{j\omega})|^2 \Phi_w(\omega) + |H(e^{j\omega})|^2 \sigma_a^2] \frac{1}{|\hat{H}(e^{j\omega})|^2} d\omega \quad (14.17)$$

where  $\hat{H}$  is the noise model with  $H = -SQN$ . Since the sensitivity function serves as the first or intermediate result for subsequent identification of the process dynamics, its order can be selected to be fairly large, *i.e.* the model set  $\hat{S}$ , should then be able to capture most of the dynamics of the actual sensitivity function,  $S$ . The total error (bias plus variance) would then be dominated by the variance error (Guo and Ljung, 1994). The variance error is then the main issue of concern here. To achieve this, PEM may be used for estimation of the sensitivity function, which has asymptotic minimum variance. However the distribution of the asymptotic minimum variance error over the frequency range cannot be controlled by pre-filtering of the input-output data since both the process model and the noise model (or filter), are jointly parametrized in the PEM algorithm to yield asymptotic minimum variance estimates (Ljung, 1987). Therefore the main “tuning knob” or “control parameter” to adjust the relative variance of the sensitivity function (see equation(14.16)) is the spectrum of the dither signal, which has to be designed carefully in order to control the variance error over the frequency range of interest. However, the variance error can also be reduced by increasing the number of data points. Since it is not difficult to collect a relatively large number of data points under closed-loop operation, a relatively accurate estimate of the sensitivity function can be expected. In the following discussion we therefore assume that  $\hat{S} \rightarrow S$ .

### 14.3.2 Estimation of the process model—step 2

Once the sensitivity function is available, the process dynamics can be estimated by filtering output data with the inverse of the sensitivity function.

**Proposition 1** *If one filters  $y$  by the inverse of the sensitivity function, and then applies PEM (joint parameterization of process and noise models) to equation (14.14), the asymptotic variance of the estimates is given by*

$$\text{Var}[\hat{T}(e^{j\omega})] = \frac{n}{M} \frac{\Phi_v(\omega)}{\Phi_w(\omega)} \quad (14.18)$$

and

$$\frac{\text{Var}[\hat{N}(e^{j\omega})]}{|N(e^{j\omega})|^2} = \frac{n}{M} \quad (14.19)$$

*Thus the variance of  $\hat{T}$  and  $\hat{N}/N$  is independent of closed-loop dynamics, i.e. both open-loop and closed-loop estimates have the same expression of accuracy with respect to variance (see Corollary 3).*

**Proof:** Using  $1/S$  to filter  $y$  yields the following relationship between  $y$  and  $w$  from equation (14.14):

$$y/S = y^f = Tw + Na \quad (14.20)$$

Identification of  $T$  from equation(14.20) is an open-loop problem. This equation has the same form as equation(14.3). Using  $w$  as input data and  $y^f$  as output data by applying corollary 3, the proposition follows. ■

The bias distribution of the estimate over frequency domain is also asymptotically independent of the closed-loop dynamics as shown in the following proposition.

**Proposition 2** *From equation(14.20), the asymptotic estimates of  $T$  and  $N$  by using the filtered data  $y^f$  and  $w$  are given by the following optimization problem:*

$$\theta_M \xrightarrow{M \rightarrow \infty} \underset{\theta}{\text{argmin}} \int_{-\pi}^{\pi} [|T(e^{j\omega}) - \hat{T}(e^{j\omega})|^2 \Phi_w(\omega) + \Phi_v(\omega)] \frac{1}{|\hat{N}(e^{j\omega})|^2} d\omega \quad (14.21)$$

*Again this yields the same bias distribution as under the open-loop condition (see Theorem 12). If both model sets, i.e. the process,  $\hat{T}$ , and the noise,  $\hat{N}$ , contain the true process dynamics, and  $w$  is a sufficiently high-order persistently exciting signal, then the parameter estimates as per equation (14.21) will converge to the true values.*

**Proof:** Follows by applying Theorem 12 to equation(14.20). ■

**Remark 10** *In the proof of proposition 1 and 2, it is assumed that the true sensitivity function  $S$  is used to filter  $y$ . If this sensitivity function is substituted by its estimate,  $\hat{S}$ , then equation(14.20) should be written as*

$$y/\hat{S} = y^f = \frac{S}{\hat{S}}Tw + \frac{S}{\hat{S}}Na$$

*The validity of Propositions 1 and 2 will then depend on the relative accuracy of the sensitivity function,  $S/\hat{S}$ . Therefore the relative accuracy of the estimated sensitivity is of main concern in the first step. However, provided that  $\hat{S}$  is sufficiently close to  $S$  (there is no model order or other structural limitations for the estimate of  $S$ ), this relative error of the estimate of  $S$  should have a negligible effect on the bias expression in the estimates of  $T$  and  $N$ , but the effect on the variance expression remains as a future research topic.*

If only the process model  $T$  is to be estimated, then the output error method can be applied in this two-step identification approach. Estimation of both, the sensitivity function,  $S$ , and the process model,  $T$ , are open-loop identification problems. The consistency of the estimates  $\hat{S}$  and  $\hat{T}$  is independent of the noise model, as long as the noise model is fixed (Ljung, 1987) as in the output error method.

Pre-filtering of data is important in identification. In particular, the choice of the data pre-filter can allow one to shape the spectral distribution or composition of the bias errors. The choice of the shaping filter should take into account the intended end-use of the model. This topic overlaps with the area of joint identification and control and has received much attention in the literature. The design and application of shaping filters for control-loop performance assessment is the subject of a future study. The point is that the sensitivity function decoupling filter provides a good or fair starting point for the design of the shaping filter under closed-loop conditions. In the following proposition, we show that the bias error under the two-step identification strategy can be freely shaped.

**Proposition 3 (Shaping Filter)** *For the two-step identification, based on the output error method, if output data  $y$  is filtered by  $F = G_f/S$ , and the input data  $w$  is filtered by  $G_f$  only, where  $G_f$  is a shaping filter, then the asymptotic bias distribution is given by*

$$\theta_M \xrightarrow{M \rightarrow \infty} \underset{\theta}{\operatorname{argmin}} \int_{-\pi}^{\pi} [|T(e^{j\omega}) - \hat{T}(e^{j\omega})|^2 \Phi_w(\omega) |G_f(e^{j\omega})|^2] d\omega$$



*Therefore the bias distribution in the limit is independent of the closed-loop sensitivity function and can be shaped by the free filter  $G_f$  to meet accuracy requirement over frequencies of interest.*

**Proof:** Using filter  $F = G_f/S$ , the relationship between  $y$  and  $w$  from equation (14.14) is now written as

$$y^f = Tw^f + G_f Na \quad (14.22)$$

where

$$\begin{aligned} y^f &= \frac{G_f}{S} y \\ w^f &= G_f w \end{aligned}$$

Therefore

$$\Phi_{w^f} = |G_f(e^{j\omega})|^2 \Phi_w(\omega) \quad (14.23)$$

By applying Theorem 12 with fixed noise model of unit value (i.e.  $\bar{N} = 1$ ) as in OEM yields

$$\theta_M \xrightarrow{M \rightarrow \infty} \arg \min \int_{-\pi}^{\pi} |T(e^{j\omega}) - \hat{T}(e^{j\omega})|^2 \Phi_{w^f}(\omega) d\omega \quad (14.24)$$

The proposition follows on substituting equation (14.23) into (14.24). ■

The significance of this result is that *the estimate obtained under closed-loop conditions can be shaped in the frequency domain if the model does not contain the true dynamics, while the estimator still maintains the property of consistency should the plant model ( $\hat{T}$  only) contain the true dynamics. The classic closed-loop direct identification does not have such a property.* All available methods for the design of the shaping filter for open-loop identification can therefore be applied in this closed-loop case. For example, Shook et al.(1992)'s open-loop long range predictive identification prefilter and Rivera et al.(1992)'s systematic design of the control-relevant shaping filter can be applied. The choice of the shaping filter is analogous to selecting frequency weighting of the bias error function. Tighter weighting at some frequencies would result in expected corresponding reduction in bias errors at these frequencies but at the cost of perhaps larger bias errors at other frequencies. The effect of the shaping filter will be briefly shown in the experimental study of a pilot-scale process.

Table 14.3: The procedure for two-step identification

- 
- 
1. Fit  $x$  to  $w$  by using the PEM or OEM, and obtain an estimate,  $\hat{S}$ , of the sensitivity function,  $S$ .
  2. Filter  $y$  by  $F = 1/\hat{S}$  and then fit  $y^f$  to  $w$  by applying the PEM. Then obtain estimates of  $T$  and  $N$  whose variance and bias expressions are asymptotically the same as open-loop identification.
- 
- 

The aforementioned two-step identification algorithm is summarized in Table 14.3 and Table 14.4:

**Remark 11** *If  $S$  contains non-minimum phase zeros, then  $1/S$  cannot be used as an unstable decoupling filter. In this case, factorize  $S$  as*

$$S = \frac{N^+ N^-}{D}$$

*where the polynomial  $N^+$  contains all non-minimum phase or unstable zeros. Let polynomial  $N^{+*}$  be the reciprocal polynomial of  $N^+$ . Then all roots of  $N^{+*}$  are inside the unit circle. Instead of using  $1/S$  as the sensitivity function decoupling filter,  $1/S'$  should be used as the decoupling filter to filter  $y_t$ , where  $S' = (N^{+*} N^-)/D$ . At the same time,  $w_t$  should be also filtered by  $N^+/N^{+*}$ . This will yield the same asymptotic properties (variance and bias) as using  $1/S$  to filter  $y_t$ . However, when  $S$  contains the unit-value zeros, the decoupling filter  $1/S$  will have an integral term which in some cases may cause numerical problems. In this case, the probing or excitation signal is preferably inserted at the setpoint as discussed in the following sections.*

Among many other two-step closed-loop indirect identification strategies (Caines and Chan, 1975; Phadke and Wu, 1974; Defalque *et al.*, 1976; Soderstrom and Stoica, 1989),

Table 14.4: The procedure for two-step identification plus shaping

- 
- 
1. Fit  $x$  to  $w$  by using the PEM or OEM, and obtain an estimate,  $\hat{S}$ , of the sensitivity function  $S$ .
  2. Filter  $y$  by  $F = G_f/\hat{S}$  and  $w$  by  $G_f$  and then fit  $y^f$  to  $w^f$  by using the OEM. Obtain an estimate of  $T$  whose bias is asymptotically independent of the closed-loop sensitivity function and is shaped by the filter  $G_f$ .
- 
- 

one of the most recent two-step identification strategies with a different objective has been proposed by Van den Hof and Schrama(1993) whose approach is summarized below.

**Lemma 7** *Assume that the consistent estimate of the sensitivity function,  $\hat{S} \rightarrow S$ , is obtained in the first step. If the input data  $w$  is filtered by  $S$ , i.e.  $w^f = Sw$ , before applying OEM, then  $\hat{T}$  can be directly estimated from the filtered data and is a consistent estimate.*

This is clearly seen from equation (14.14), where

$$y = TSw + NSa = Tw^f + NSa \quad (14.25)$$

whereas the approach proposed in this chapter considers filtering  $y$  by  $1/S$  as follows:

$$y/S = Tw + Na$$

which is

$$y^f = Tw + Na$$

For brevity, the approach proposed by Van den Hof and Schrama is denoted as  $w$ -filtering method, while the approach proposed in this chapter is denoted as  $y$ -filtering method. In Van den Hof and Schrama(1993), “*The sensitivity function is used to simulate*

*a noise free input signal for an open loop identification of the plant to be identified. Using the output error method, an explicit approximation criterion can be formulated, characterizing the bias of identified models in the case of undermodelling".*

**Lemma 8** *By using the OEM, the  $w$ -filter approach yields the asymptotic frequency bias distribution as*

$$\theta_M \xrightarrow{M \rightarrow \infty} \arg \min \int_{-\pi}^{\pi} [|T(e^{j\omega}) - \hat{T}(e^{j\omega})|^2 |S(e^{j\omega})|^2 \Phi_w(\omega) d\omega$$

*Thus the frequency weighting on the bias  $|T(e^{j\omega}) - \hat{T}(e^{j\omega})|^2$  depends on the sensitivity function,  $S$ . In the approach proposed in this chapter, the frequency weighting on the bias is independent of the sensitivity function.*

This can be proved by applying equation(14.12) in Theorem 12 to equation(14.25). It should be pointed out that, under the framework of joint identification and control, the dependency of the bias error on the sensitivity function is not undesired provided that the desired sensitivity function or the intended feedback controller is running during the data collection.

**Remark 12** *One of the main differences between the  $w$ -filtering approach and the  $y$ -filtering approach is whether  $w$  or  $y$  should be filtered by the sensitivity function or the inverse of the sensitivity function before carrying out the second step of identification. These two approaches result in different identification objectives. The  $y$ -filtering approach as proposed in this chapter aims at 1) achievement of the same "accuracy" expressions with respect to bias and variance errors under closed-loop and open-loop conditions (including consistency of the estimates if the model set contains the plant dynamics); this result is achieved by decoupling the closed-loop sensitivity function from closed-loop data, and 2) obtaining explicit expressions for both asymptotic variance and bias errors. This approach is obtained by comparison of the asymptotic variance and bias errors for open-loop and closed-loop conditions. The  $w$ -filtering approach as proposed by Van den Hof and Schrama provides 1) a consistent estimate of the input-output transfer function if the model contains the plant dynamics, and 2) an explicit expression for the asymptotic bias distribution*

*only. The following illustrations show that these have important implications in closed-loop identification.*

### 14.3.3 Other practical considerations

Until now we mainly consider the case where the dither signal is injected from  $w$  as shown in Figure 14.2. We will illustrate that the general result can be extended to the case where the dither signal is injected from any point, for example via the setpoint  $r$ . Figure 14.3 shows an equivalent transformation of the block diagrams. The closed-loop response is now written as

$$y = STQr + SNa$$

This can be transformed to

$$\frac{1}{SQ}y = Tr + \frac{N}{Q}a$$

Therefore if  $y$  is filtered by  $1/SQ$  before applying the PEM or OEM, the relationship between  $r$  and  $y^f$  is

$$y^f = Tr + \frac{N}{Q}a$$

It is clear that both variance and bias distribution of estimates by using the PEM or OEM will be independent of the sensitivity function. Since it is again an open-loop identification problem, a shaping filter  $G_f$  can also be cascaded to the decoupling filter to shape the bias distribution in the frequency domain as illustrated in the foregoing discussion.

In this case instead of estimating the sensitivity function  $S$  during the first step as in the foregoing section,  $QS$  should be estimated jointly. This can be obtained by noticing the following relationship between  $r$  and  $x$ :

$$x = QSr - NQSa$$

Identification of  $QS$  using data  $r$  and  $x$  is an open-loop identification problem. Therefore it can be shown that the relative accuracy of the estimate of  $QS$  is independent of the sensitivity function. *Since the inverse of  $QS$  does not contain the unit-value zeros introduced by integral control, it is the preferred sensitivity function decoupling filter when integral action exists in the controller.*

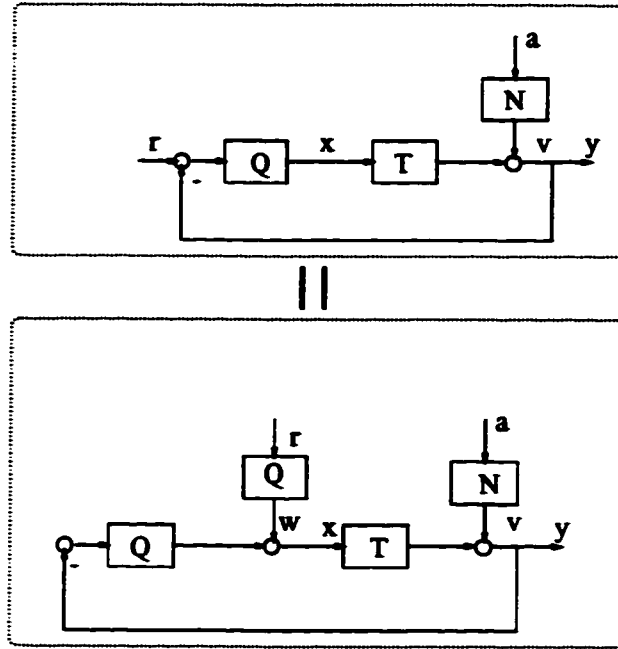


Figure 14.3: *Equivalent transformation of block diagrams.*

## 14.4 Extension to MIMO systems

The two-step closed-loop identification can be extended to MIMO systems.

**Proposition 4** *Under closed-loop condition, the transfer function matrix  $T$  can be estimated via two steps. The sensitivity function is estimated from closed-loop data in the first step. The transfer matrix  $T$  from the sensitivity-filtered closed-loop data is then estimated in the second step.*

**Proof:** From figure 14.2, we have

$$\begin{aligned} Y_t &= (I + TQ)^{-1}Tw_t + (I + TQ)^{-1}Na_t \\ &= STw_t + SNa_t \end{aligned} \tag{14.26}$$

where  $S = (I + TQ)^{-1}$  is defined as the sensitivity matrix. Filtering both sides of equation (14.26) by the inverse sensitivity matrix  $S^{-1} = (I + TQ)$  (or the return difference matrix (Bitmead *et al.*, 1990)) gives

$$Y_t^f = S^{-1}Y_t = Tw_t + Na_t \tag{14.27}$$

This is clearly an open-loop identification problem. We also have

$$\begin{aligned} x_t &= (I + QT)^{-1}w_t - (I + QT)^{-1}QN a_{2t} \\ &= S_x w_t - S_x Q N a_{2t} \end{aligned} \quad (14.28)$$

where  $S_x \triangleq (I + QT)^{-1}$ . The sensitivity function  $S$  can be written as

$$S = Q^{-1}(I + QT)^{-1}Q = Q^{-1}S_x Q \quad (14.29)$$

where the controller transfer function matrix  $Q$  either is known as *a priori* knowledge or can be identified from closed-loop data. Clearly, estimation of  $S_x$  via equation (14.28) is also an open-loop identification problem. Therefore the two-step identification can be achieved by 1) estimation of the sensitivity function  $S$  via equations (14.28) and (14.29), and 2) identification of the transfer function matrix  $T$  via equation (14.27). ■

## 14.5 Simulation

**Example 16** Consider a second order ARMAX model with the transfer function given by

$$(1 - 0.7859q^{-1} + 0.3679q^{-2})y_t = (0.3403 + 0.2417q^{-1})u_{t-1} + (1 - 0.8q^{-1} + 0.12q^{-2})a(t)$$

A unity feedback control law is implemented in this simulation. The proposed  $y$ -filtering approach is compared with the direct identification method. The white noise  $a_t$  and the white-noise dither signal  $w_t$  are independent with  $\text{Var}(a_t) = 2.25$  and  $\text{Var}(w_t) = 1$  respectively. The number of data points in the simulation is  $M = 5000$ .

In general, identifiability under direct closed-loop identification requires that both the plant and disturbance dynamics lie in the set of plant and disturbance models (Soderstrom and Stoica, 1989). However, the  $w$ -filtering and  $y$ -filtering approaches do not have such a restriction in the choice of the noise model. The difficulty with the direct identification method is the choice (or tradeoff) of the plant model and the noise model, i.e. the plant model and the noise model are strongly coupled. One may choose high order models for both the plant and the noise, but this may violate the parsimony principle and also increase

the variance error of the estimates as discussed in the previous sections. Therefore, an incorrect choice of the noise model may yield an erroneous plant model and vice versa. In this example, we show that a first-order model, that is identified using the direct identification method and passes all residual tests, gets deviates significantly from the true dynamics. On the other hand, the  $y$ -filtering approach transforms the closed-loop identification to an open-loop identification problem and successfully detects the lack of fit when the first-order plant model is used.

Both the direct identification and  $y$ -filtering methods begin with a model of the first-order plant and second-order disturbances. There is clearly a model-order mismatch for such a choice of plant model. We will see which identification method can detect such a mismatch. Both methods use the Box-Jenkins model structure, i.e.  $BJ$  function in the System Identification toolbox in Matlab. Residual tests for the models identified from both methods find the correlation between residuals and inputs and thus indicate a lack of fit or a model-plant mismatch. This indicates that one may either increase the order of the noise model or increase the order of the plant model for the next trial.

To see the effect of the noise model, the noise models are increased to order three. The residual test for the direct identification is shown in Figure 14.4. The upper part of the figure shows the autocorrelation of the residuals and clearly indicates “whiteness” of the residuals. The lower part of the figure is the cross correlation between residuals and past inputs, i.e.  $E[\hat{a}_t u_{t-\tau}] / \sigma_{\hat{a}} \sigma_u$  for  $\tau > 0$ , where  $\tau$  is the lag of the cross correlation function. This cross correlation test clearly indicates sufficiently good fit of the data, i.e. no regions outside the 99% confidence intervals. Therefore, the model obtained from direct identification passes the residual test, but the Bode diagram of the model shown in Figure 14.6 clearly demonstrates lack of fit. On the other hand, the residual test of the  $y$ -filtering identification is shown in Figure 14.5. The residuals also pass the “whiteness” test, but the cross correlation between the residuals and the inputs shows “spikes” outside the 99% confidence intervals and fails the test. Note that since the  $y$ -filtering approach transforms the closed-loop identification problem into the open-loop identification problem, the cross correlation test has to be carried out for both positive and negative lags (including the zero lag), i.e. the cross correlations between the residuals



and all inputs (both past and future inputs) (Ljung, 1987; Soderstrom and Stoica, 1989). Now we try to further increase the order of the noise model to a higher order (e.g. 5<sup>th</sup> order) for the  $y$ -filtering method while keeping the first-order plant model. The residual test is shown in Figure 14.7, and the model again fails the cross correlation test. This indicates that one has to increase the plant model order. Consequently, the plant model is increased to second order. The residual test is shown in Figure 14.8, and this model clearly passes the residual test. Therefore, the  $y$ -filtering method is able to find the correct model of the plant despite the error in the choice of the noise model and the Bode plot of the final estimate is shown in Figure 14.6.

The asymptotic variance of the estimate  $Var(\hat{T})$  using the  $y$ -filtering approach is given in equation (14.18). This equation is valid when the exact sensitivity function  $S$  is used as the decoupling filter,  $1/S$ , as shown in Proposition 1 and Remark 10. The predicted variance can be calculated from equation (14.18) and is denoted by the dotted lines in Figure 14.9. To test validity of this predicted variance, 50 Monte-Carlo simulation runs are performed for this example.  $\hat{T}$  is calculated from the two-step  $y$ -filtering approach using the exact sensitivity function as the decoupling filter. The variance of the estimate,  $\hat{T}$ , from 50 runs is calculated and also plotted in Figure 14.9 as the dash-dotted lines. Two cases with different data points for each simulation run are considered. The result for 512 data points is shown in the top part of the figure, and the result for 1024 data points is shown in the bottom part of the figure. The predicted  $1\sigma$  bounds of the Nyquist plot are shown in Figure 14.10. Note that  $Var(\hat{T})$  is defined by the variance of complex-valued random variables as (Ljung, 1987)

$$Var(\hat{T}) = E(\hat{T} - E\hat{T})(\hat{T} - E\hat{T})^*$$

where  $*$  means complex conjugate. From Figure 14.9, one can see that a good match in the low to medium frequency range is obtained in this example, but the mismatch in the high frequency range is relatively large. The reason could be: 1) the asymptotic variance as given by Ljung(1987) is an approximate expression, and should not be regarded as an exact expression; and 2) the spectrum of dither and disturbances in each Monte-Carlo simulation run is different and may not be flat (white) over the frequency range of interest.

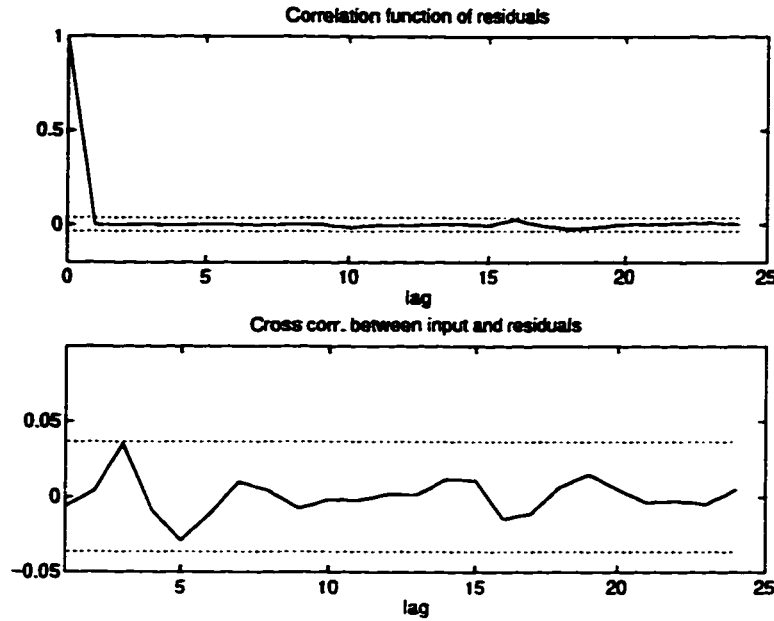


Figure 14.4: *Residual test for the model identified by using direct identification method (first-order plant and third-order noise).*

**Example 17** Consider an example in Schrama(1991). The plant under consideration consists of a transfer function, which is a discrete-time model of a laboratory set-up, and some artificial noise contribution. The plant transfer function is given by

$$T = \frac{10^{-3}(0.98q^{-1} + 12.99q^{-2} + 18.59q^{-3} + 3.30q^{-4} - 0.02q^{-5})}{1 - 4.40q^{-1} + 8.09q^{-2} - 7.83q^{-3} + 4.00q^{-4} - 0.86q^{-5}}$$

In order to state a non-trivial case-study, according to Schrama(1991), noise contributions are assumed to additively affect the input  $u$  and output  $y$ . The additive input noise is a white noise with variance  $1/9$ . The output noise is a white noise that is filtered by

$$N = \frac{0.01(2.89 + 11.13q^{-1} + 2.74q^{-2})}{1 - 2.70q^{-1} + 2.61q^{-2} - 0.90q^{-3}}$$

A control law

$$Q = \frac{0.61 - 2.03q^{-1} + 2.76q^{-2} - 1.83q^{-3} + 0.49q^{-4}}{1 - 2.65q^{-1} + 3.11q^{-2} - 1.75q^{-3} + 0.39q^{-4}}$$

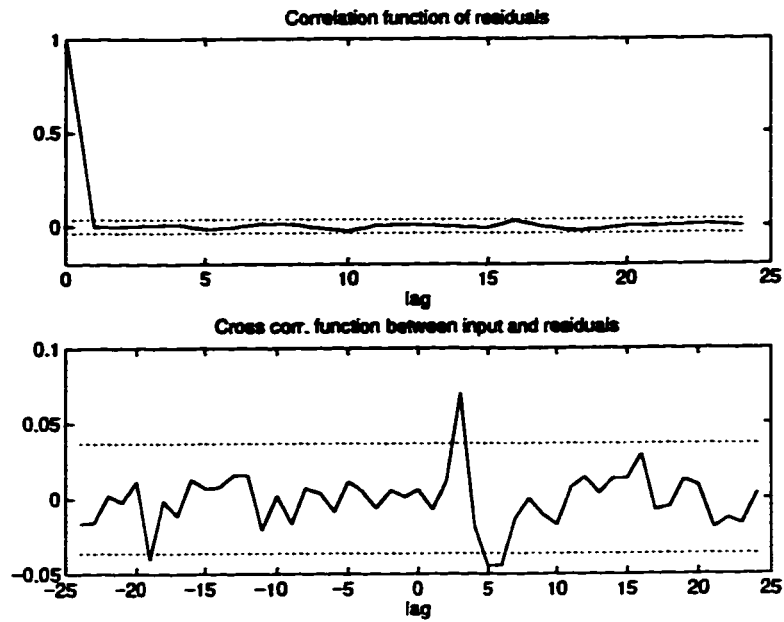


Figure 14.5: *Residual test for the model identified by using the y-filtering method (first-order plant and third-order noise).*

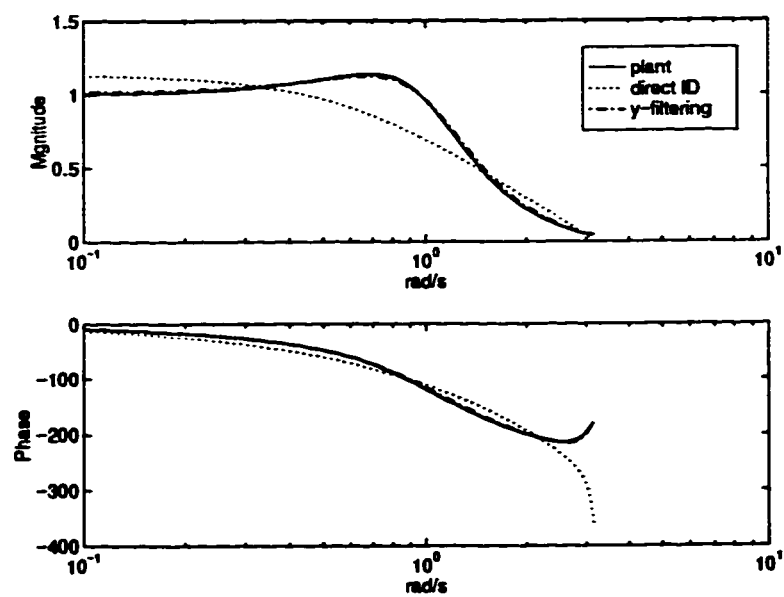


Figure 14.6: *Comparison between direct identification and the y-filtering methods.*

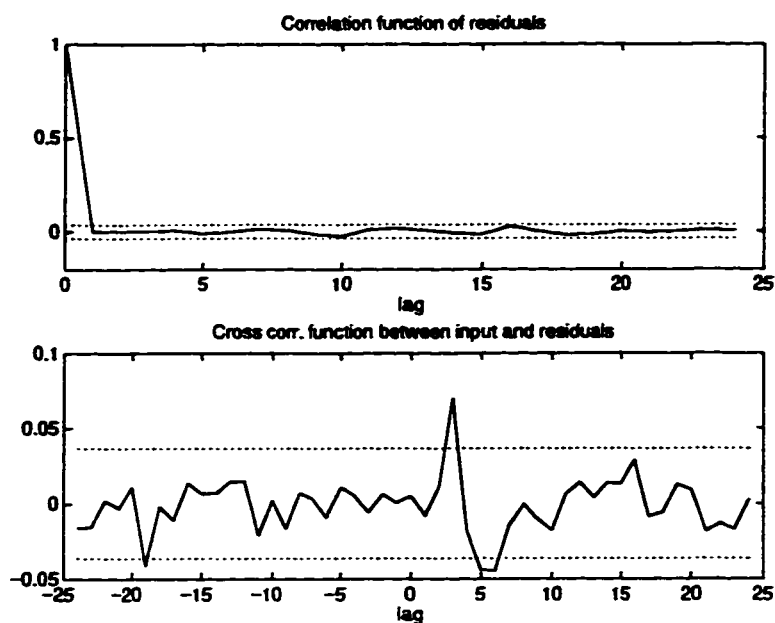


Figure 14.7: *Residual test for the model identified by using the  $y$ -filtering method (first-order plant and fifth-order noise).*

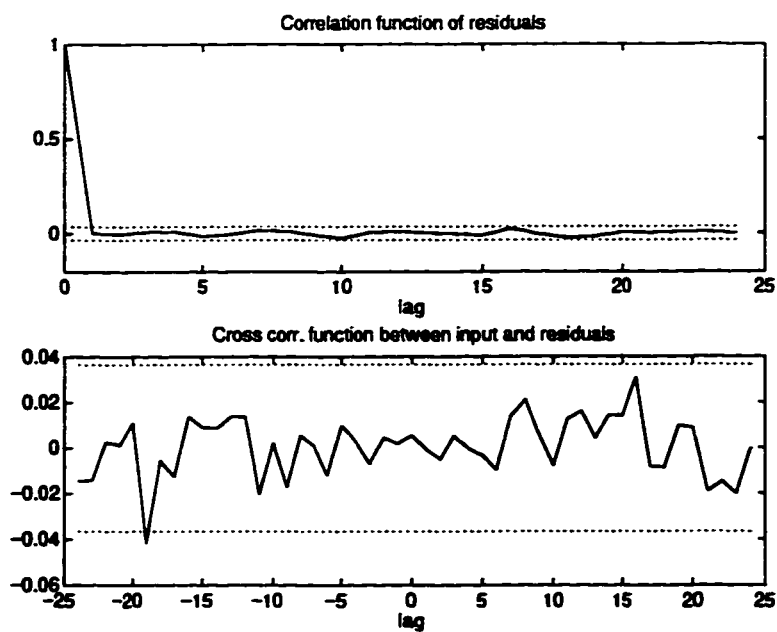


Figure 14.8: *Residual test for the model identified by using the  $y$ -filtering method (second-order plant and second-order noise).*

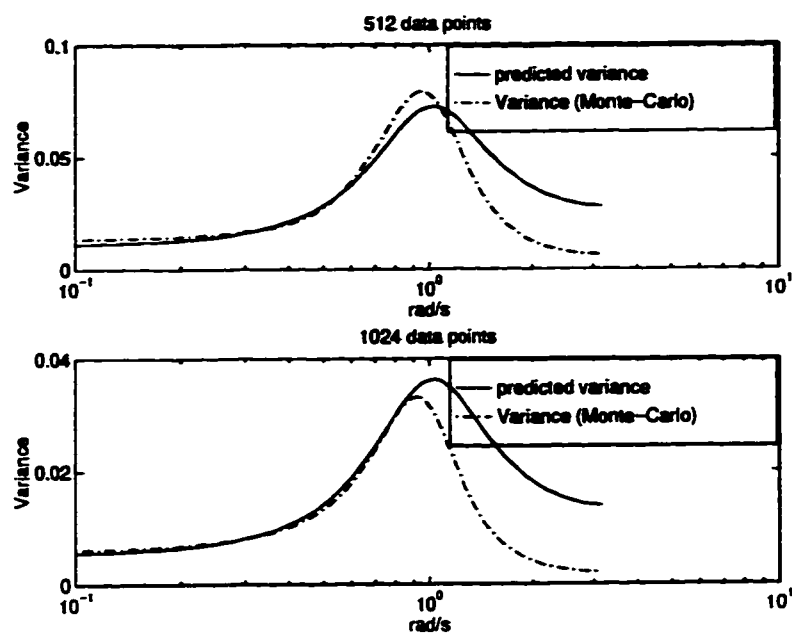


Figure 14.9: *Variance of the estimate calculated from Monte-Carlo simulation (second-order plant and second-order noise).*

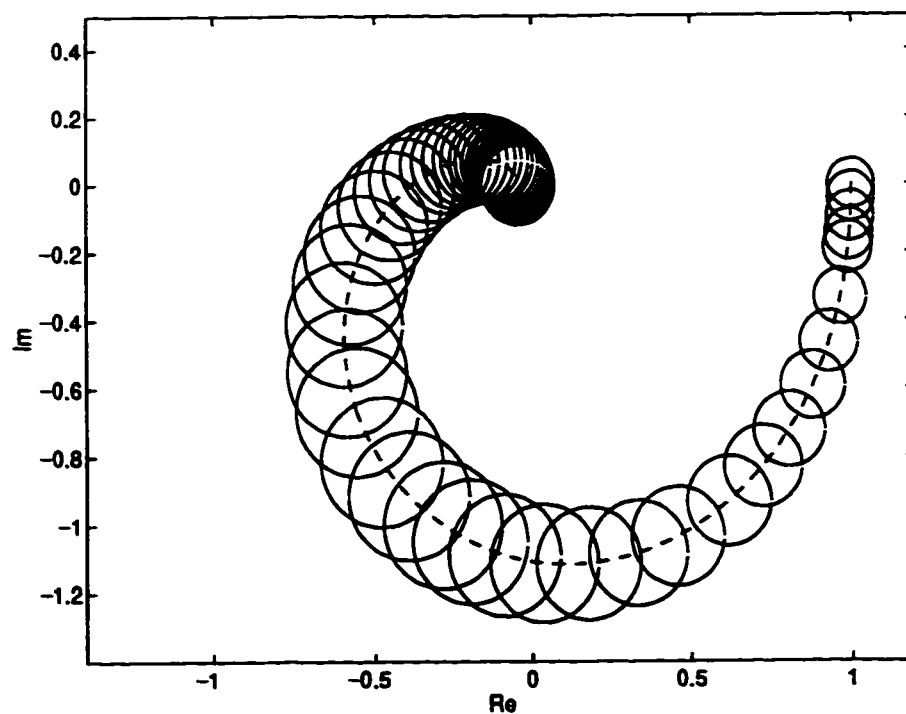


Figure 14.10: *Predicted  $1\sigma$  bound of the Nyquist plot (second-order plant and second-order noise).*

*is implemented in the plant. A dither signal with variance 1 is injected in the process in order to perform closed-loop identification. To demonstrate the effect of under-modeling, a 4<sup>th</sup>-order plant model (the original plant is 5<sup>th</sup>-order) is used for the identification.*

The  $w$ -filtering approach and  $y$ -filtering approach are applied to the process and the results presented in the Bode diagrams shown in Figure 14.11. Since the interest in this example is the plant model and the output error method is used for parameter estimation, the most relevant model validation is the cross-correlation test between residuals and inputs (Ljung, 1987). The cross-correlation tests are performed with results shown in Figure 14.12 and 14.13. Since both  $w$ -filtering and  $y$ -filtering transform the closed-loop identification to open-loop identification, the cross-correlation test should be conducted over the whole graph (i.e. including both negative and positive legs). Clearly, the models obtained under  $w$ -filtering and  $y$ -filtering both pass the residual test.

Although both models have passed the time-domain test, the qualities of the models are significantly different in the frequency domain. If we look at the estimated sensitivity function shown in Figure 14.14, we can see the smaller magnitude of the sensitivity function in the medium frequency range with the minimum occurring around the frequency  $\omega = 0.17\text{rad/s}$ . This shape of the sensitivity function is expected to affect the identification result. This is confirmed in Figure 14.11. The  $w$ -filtering approach gives a poor match in the medium frequency range including the cross-over frequency, particularly around the frequency  $\omega = 0.17\text{rad/s}$ . The  $y$ -filtering, on the other hand, matches the true plant relatively well in the medium frequency range including the cross-over frequency, although this improvement is at the cost of the high frequency mismatch.

**Example 18** *The example used by Van den Hof and Schrama(1993) is considered in this Monte Carlo simulation for comparison of different approaches. The discrete plant (casual but not strictly causal) is represented by transfer functions*

$$T = \frac{1}{1 - 1.6q^{-1} + 0.89q^{-2}}$$

$$Q = q^{-1} - 0.8q^{-2}$$

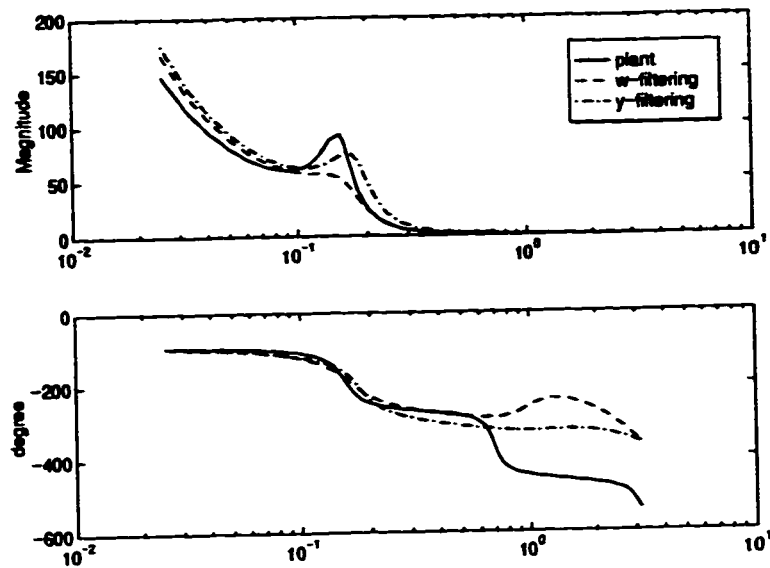


Figure 14.11: Comparison between  $y$ -filtering and  $w$ -filtering approaches.

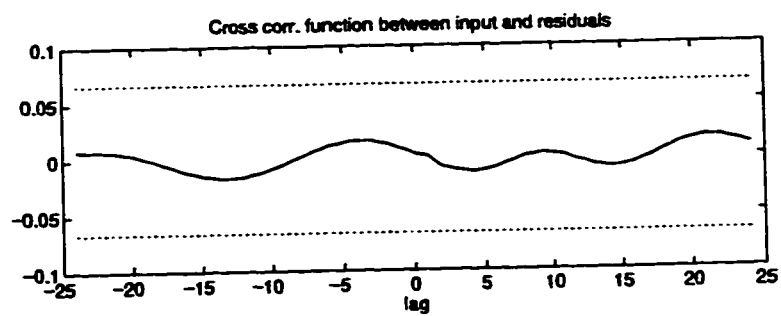


Figure 14.12: Cross-correlation test for  $w$ -filtering.

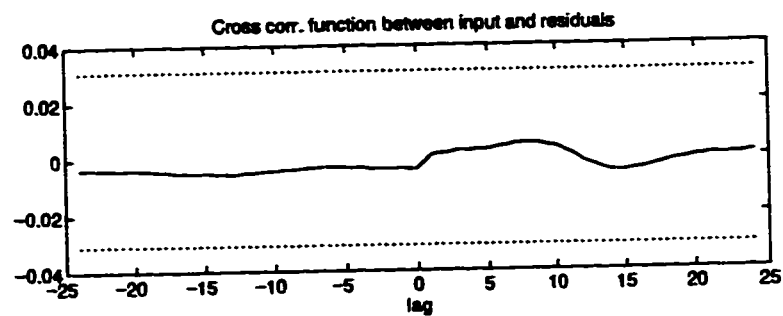


Figure 14.13: Cross-correlation test for  $y$ -filtering.

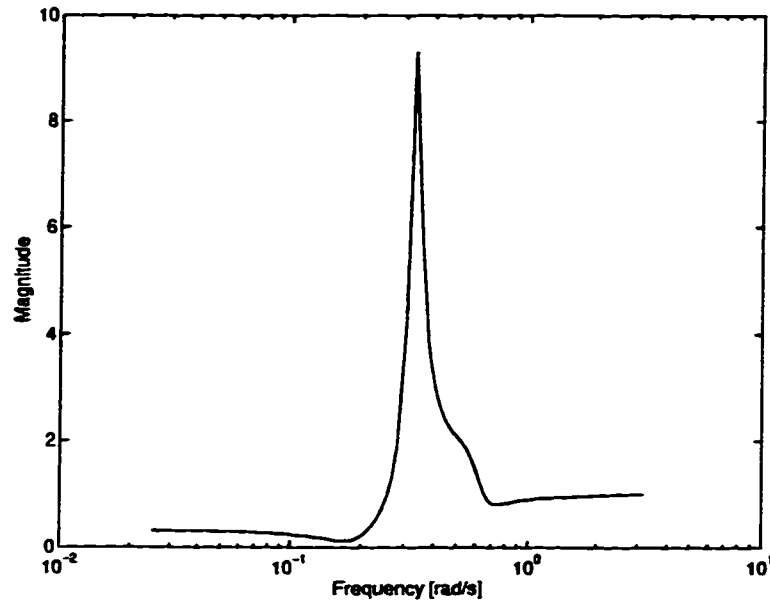


Figure 14.14: *Estimate of the sensitivity function*

$$N = \frac{1 - 1.56q^{-1} + 1.045q^{-2} - 0.3338q^{-3}}{1 - 2.35q^{-1} + 2.09q^{-2} - 0.6675q^{-3}}$$

The noise signal  $a$  and the dither signal  $w$  are independent unit variance zero mean random signals. The number of data points for each run is chosen as  $M = 2048$  in accordance with Van den Hof and Schrama(1993) and the simulation was run 50 times with different random seeds. Although this is an unrealistic plant (without any time-delay), mathematically this is a good simulation example to compare the sensitivity to the model structure mismatch for different identification schemes.

To compare sensitivity of the  $w$ -filtering,  $y$ -filtering and the direct PEM closed-loop identification to model-plant mismatch, one step time-delay is considered in the model. Without model-plant mismatch, all of these three methods should give consistent estimates as discussed in the previous sections. A model of the following form is therefore assumed

$$\hat{T} = \frac{(b_1 + b_2q^{-1})q^{-1}}{1 + a_1q^{-1} + aq^{-2}}$$

The estimated sensitivity function is shown in Figure 14.15. The sensitivity at lower frequency is smaller than at higher frequency. There is a valley with a minimum magnitude



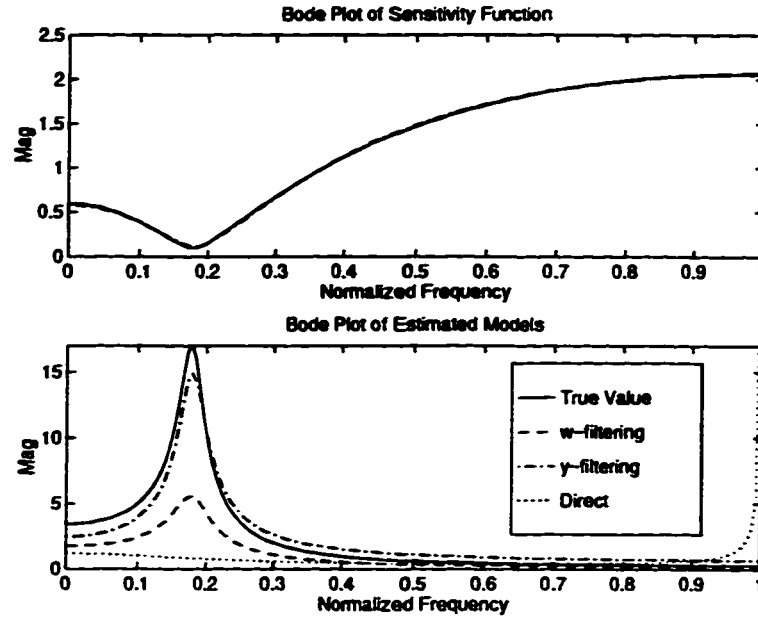


Figure 14.15: *The upper plot is the sensitivity function. The lower plot is the averaged Bode magnitude graph of  $\hat{T}$  over 50 runs.*

at the frequency of 0.18. This shape of the sensitivity function reduces the accuracy at lower frequency, and one would expect relatively large estimation errors around the frequency of 0.18, if the  $w$ -filtering approach is used (see Lemma 8). The lower portion of Figure 14.15 confirms this. Compared to the  $w$ -filtering approach, the  $y$ -filtering method clearly avoids the peak error with a slightly larger mismatch at high frequencies. The direct closed-loop identification does not work in this example due to the structure mismatch. The comparison of the three approaches can also be clearly seen from the averaged Nyquist plot shown in Figure 14.16.

## 14.6 Experimental evaluation on a pilot-scale process

In real practical situations, it is difficult to validate the model,  $\hat{T}$ , estimated under closed-loop conditions with the real process,  $T$ , since the latter is unknown. For the purpose of practical evaluation, in the following experimental study, separate identification tests under open-loop and closed-loop conditions are performed. The model estimated

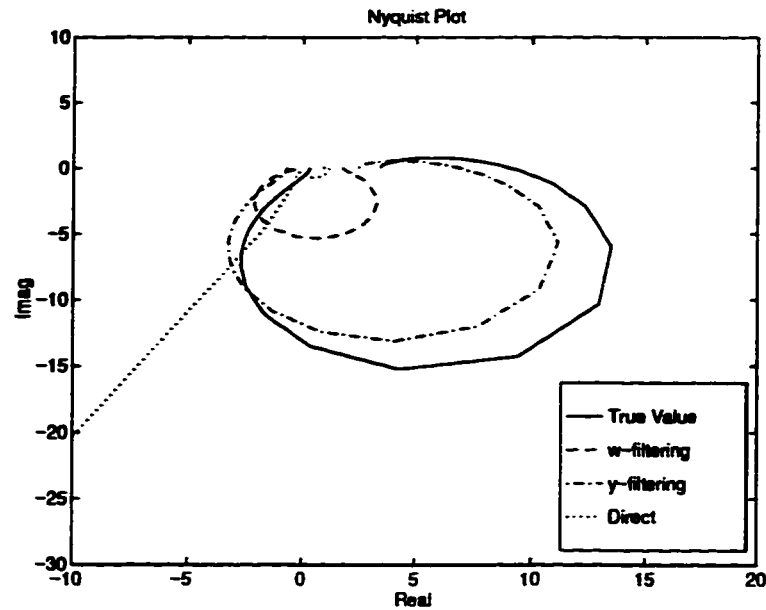


Figure 14.16: *The averaged Nyquist plot of the estimate over 50 runs*

under closed-loop condition can be considered a suitably adequate and validated model if it matches the model estimated under carefully designed open-loop conditions.

**Example 19** *The proposed algorithm is evaluated on a pilot-scale process shown in figure 14.17. Each tank is a double-walled glass tank 50 cm high with an inside diameter of 14.5 cm. The level of the second tank is the output or controlled variable. The water flow to the first tank is manipulated in order to control the level of the second tank. A PID controller (with  $T_s = 1\text{sec}$ ) is implemented on the inner loop (flow loop). An IMC controller ( $T_s = 5\text{sec}$ ) is implemented on the outer loop (level loop). The block diagram of the real-time Simulink Workshop implementation of the IMC controller is shown in Figure 14.18. A second-order model was obtained from open-loop test. This model was validated by checking it with a separate input-output data set. Closed-loop tests were then conducted. Using the proposed method and other closed-loop identification methods, several process models were obtained. These models were compared with the model obtained from the open-loop test.*

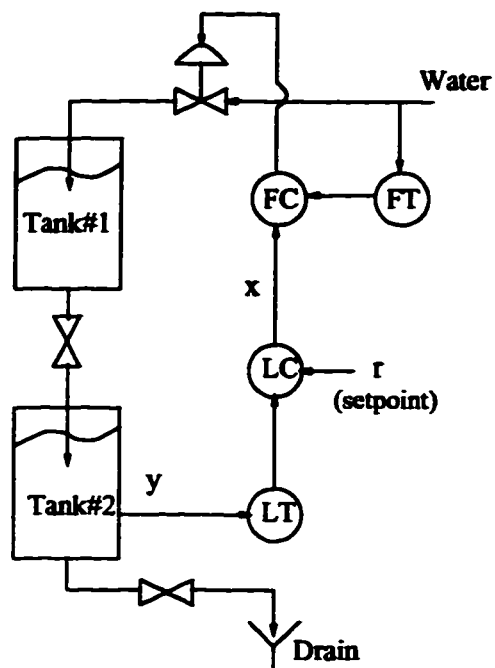


Figure 14.17: Schematic of the computer-interfaced pilot-scale process.

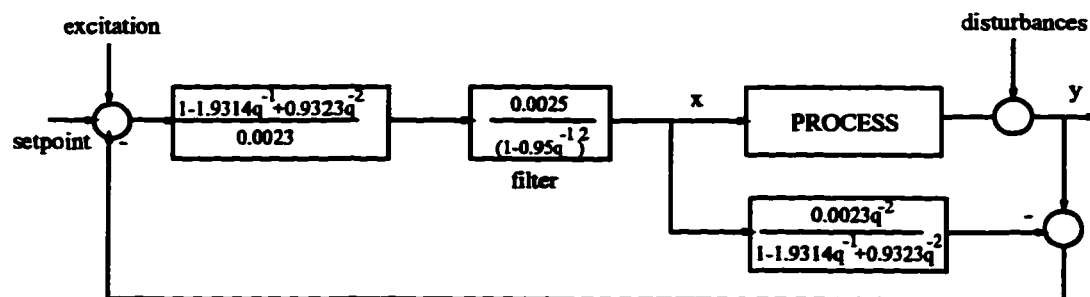


Figure 14.18: Block diagram for implementation of IMC control using the real-time Simulink Workshop.

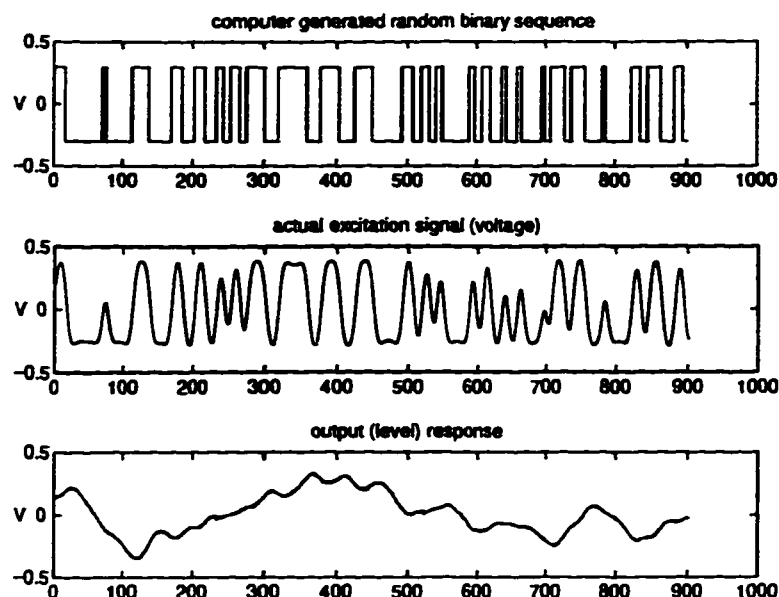


Figure 14.19: *Excitation signal and response. The physical units are voltage in the plot where  $-2V$  to  $+2V$  correspond to 0% to 100%. The time scale is in terms of sampling intervals.*

Figure 14.19 shows the computer-generated random binary sequence as used in the open-loop test. The step-type random binary sequence was smoothed by a second order Butterworth filter with the cutoff frequency significantly larger than the bandwidth of the process. The bandwidth of the process was estimated from previous open-loop tests. A second-order model was estimated by using the prediction error method and found to be

$$\hat{T} = \frac{0.0023q^{-2}}{1 - 1.9314q^{-1} + 0.9323q^{-2}}$$

where the two-step time delay is due to a zero order hold and an additional artificially introduced unit-step time delay. The predicted versus actual data (using a separate validation or test data with different setpoint excitation inputs) are shown in Figure 14.20. Clearly the open-loop model is a good representation of the real process.

Since there is integral action in the IMC control, it is preferable to insert an excitation signal via the setpoint to avoid a pole on the unit circle in the sensitivity function decoupling filter. Figure 14.21 shows the excitation signal and the output under the closed-loop test. The y-filtering, w-filtering and direct closed-loop identification methods

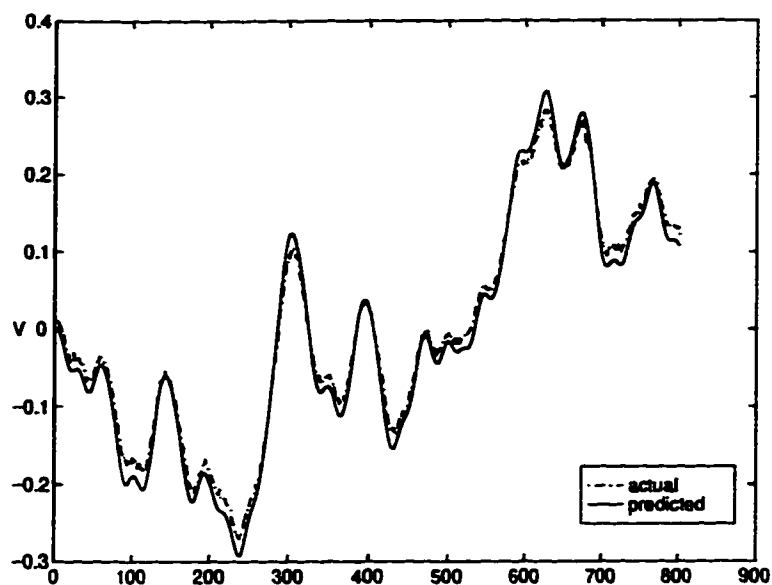


Figure 14.20: *Predicted versus actual data from another open-loop test. The time scale is the sampling intervals.*

were used to estimate the process model. Second order models are identified and the resulting Nyquist plots are shown in Figure 14.22. If there is no model-plant mismatch, all the Nyquist plots should converge to one plot when the sample size increases.

If a first order process model is assumed, then a model-plant mismatch is indeed present. A larger bias error would be expected at lower frequencies if  $w$ -filtering or direct closed-loop identification is used. Nyquist plots of the identified models shown in Figure 14.23 confirm this. Since this is a over-damped second order plant, the model-plant mismatch by using a first order to represent a second-order over-damped plant is not severe. The direct identification does not fail in this example. The effect of the shaping filter on the identification is illustrated by using a 4<sup>th</sup> order low-pass Butterworth filter cascaded to the decoupling filter. As shown by the results displayed in Figure 14.24. Clear improvement of the estimate at low to middle frequencies is obtained by cascading the shaping filter to the decoupling filter. Depending on the application, different shaping filters at different frequencies can be designed for the control algorithm of choice.

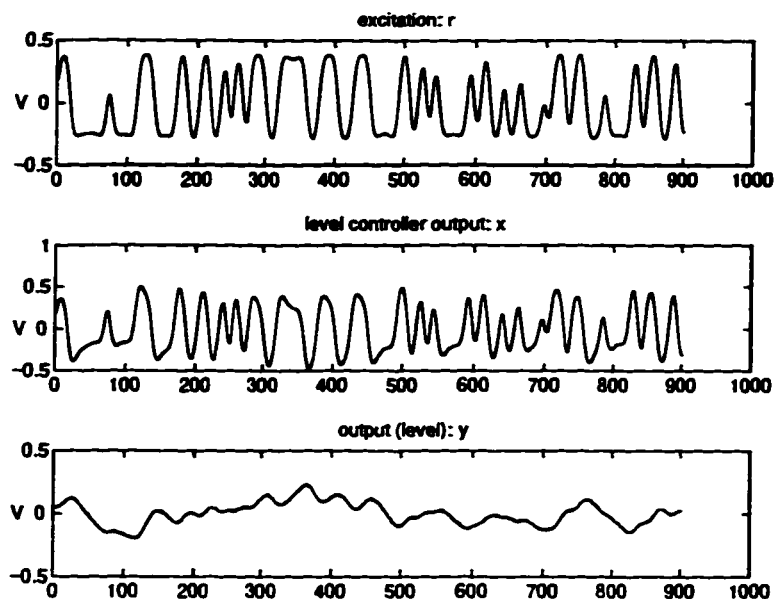


Figure 14.21: *Excitation signal and response under the closed-loop condition. All physical units are voltage in the plot where  $-2V$  to  $+2V$  correspond to 0% to 100%. The time scale is in terms of sampling intervals.*

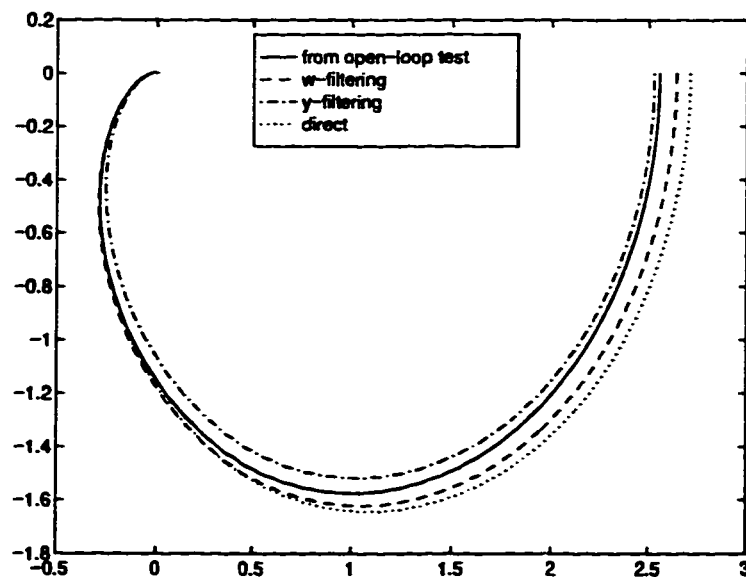


Figure 14.22: *Comparison of the identified process models using different methods when a second-order model is used.*

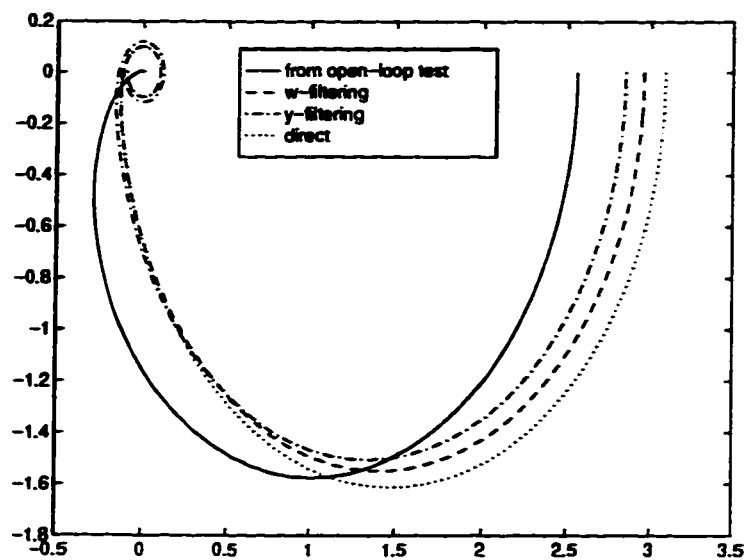


Figure 14.23: *Comparison of the identified process models using different methods when a first-order model is used.*

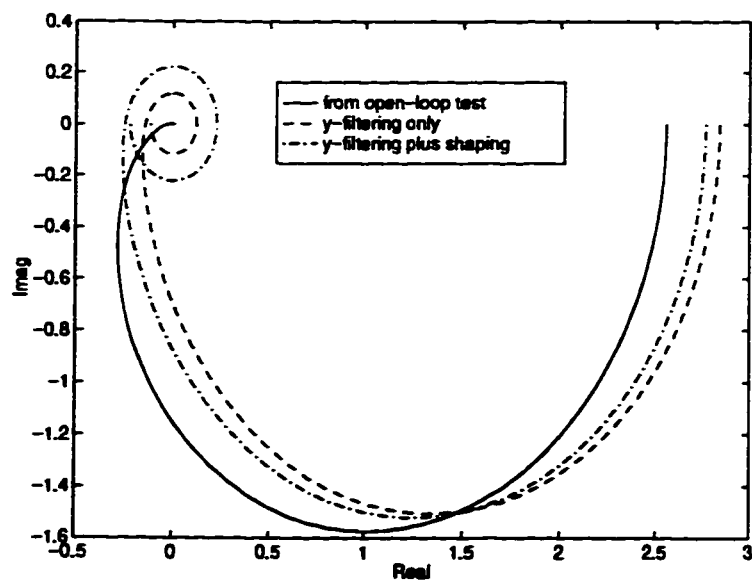


Figure 14.24: *Effect of the shaping filter for the first-order model.*

## 14.7 Conclusions

The accuracy aspects of closed-loop identification have been discussed. It has been shown that the key difference between closed-loop and open-loop identification is the sensitivity function. The sensitivity function inversely affects the variance and bias errors of the estimate under closed-loop conditions. A two-step closed-loop identification has been proposed, which yields identical asymptotic properties as under open-loop identification. The proposed algorithm has been evaluated by simulated examples as well as by pilot-scale experiments. These results affirm the strategy, that a suitable model commensurate with its intended end use can always be identified under closed-loop conditions through the choice of appropriate data prefilters.



## **Chapter 15**

# **Conclusions and Recommendations**

### **15.1 Concluding remarks**

The main contributions of this thesis are development of the theory and computational algorithms for control loop performance assessment using multivariate statistical methods, and experimental evaluation of these techniques on computer-interfaced pilot-scale processes and actual industrial processes. Specific theoretical and computational contributions include:

1. Extension of the unitary interactor matrix into the weighted/generalized unitary interactor matrices.
2. Application of the unitary, weighted unitary and generalized unitary interactor matrices to solve multivariable minimum variance control problem, the benchmark for multivariate control loop performance assessment.
3. Proof of the equivalence of the minimum variance control law (Goodwin and Sin, 1984) and the singular LQ control law (a special solution in Harris and MacGregor(1987)) by using the weighted unitary interactor matrix.

4. Development of an algorithm for estimation of the unitary interactor matrix under both open-loop and closed-loop conditions.
5. Derivation of the explicit expression for the feedback control invariant portion of process variance.
6. Development of an efficient algorithm for performance assessment of multivariable processes, which is denoted as the FCOR algorithm (for Filtering and CORrelation analysis).
7. Development of the multivariate feedforward & feedback control loop performance assessment technique.
8. Development of the technique for feedback control performance assessment of nonminimum-phase multivariate systems.
9. Proposal of a unified approach for performance assessment of both regulatory control and setpoint tracking for both stochastic and deterministic systems under the  $H_2$  framework.
10. Development of performance assessment schemes with practical considerations such as a user-defined benchmark.
11. Development of a performance assessment scheme which takes control effect into account.
12. Development of a two-step closed-loop identification scheme, which asymptotically yields the same variance and bias expressions as open-loop identification.
13. Evaluation of the proposed algorithms using simulated, pilot-scale processes and actual industrial processes.

Computer code for simulations, pilot-scale experiments and industrial applications in this thesis was written using Matlab and real-time Matlab/Simulink.

## 15.2 Recommendations for future work

Control loop performance assessment is a relatively new and active area of research. The results presented in this thesis address some of the fundamental issues in this theory. As stated in this thesis, there are many limitations on the achievable control performance. Higher level assessment generally requires more *a priori* knowledge of the processes which is typically unavailable in industry. This in itself poses a stumbling block in the application of these ideas in industry. The emphasis in new and ongoing research must be to develop tests, tools and techniques that are plant-friendly and conceptually simple to understand and apply. Future development in this and related areas should therefore dwell on these issues and consider the following class of problems:

1. LQG is a good benchmark for performance assessment of DMC controllers. To obtain such a benchmark, a suitable model should be identified under closed-loop conditions. Although it cannot be directly applied, the control relevant identification technique is recommended for such a solution.
2. The confidence intervals for performance assessment results are desired for on-line performance monitoring, since the number of data points in such an environment is often limited and the uncertainty can be severe. This typically requires analysis based on asymptotic statistical theory and is a challenging theoretical problem.
3. Robustness performance should be taken into account in higher-level control loop performance assessment. This could require frequency domain analysis of the sensitivity or complementary sensitivity functions.
4. Hard constraints should also be taken into account in practical control loop performance assessment. This would require an optimization procedure. The convex optimization is one possible technique in the resolution of this problem.
5. Control loop performance assessment of a linear plant with a non-linear controller such as constrained DMC or adaptive controller is worthy of further investigation. The solution to this problem would have great industrial appeal.

6. Control loop performance assessment with recommendation for controller tuning. Ideally, the solution to this problem should be obtained by using routine operating data only. The recommended tool for such a solution could be spectral analysis of both input and output data.
7. Multivariate statistical analysis should be further explored in control loop performance assessment. ANOVA analysis can give insight into the internal relationship of different control loops. Hypothesis tests can tell whether the monitored process variables deviate from the target values.
8. Control loop performance assessment is naturally related to process fault detection, another important research area yet to be explored.
9. Control loop performance assessment can be integrated with quality control, loop maintenance, and fault detection to form a highly integrated expert system.
10. It is of interest to generalize all Matlab codes in this thesis to form a toolbox for control loop performance assessment.

# References

- AOKI, M. 1987. *State Space Modeling of Time Series*. Berlin Heidelberg: Springer-Verlag.
- ASTROM, K.J. 1967. Computer Control of a Paper Machine - an Application of Linear Stochastic Control Theory. *IBM J.*, 11, 389-405.
- ASTROM, K.J. 1970. *Introduction to Stochastic Control Theory*. New York: Academic Press.
- ASTROM, K.J., AND WITTENMARK, B. 1990. *Computer-Controlled Systems, Theory and Design*. Second edn. Prentice-Hall.
- BITMEAD, R.R. 1993. Iterative Control Design Approaches. *Pages 381-384 of: Proceedings of the 12th IFAC World Congress*, vol. 9.
- BITMEAD, R.R., GEVERS, M., AND WERTZ, V. 1990. *Adaptive Optimal Control*. Prentice Hall.
- BITTANTI, S., COLANERI, P., AND MONGIOVI, M.F. 1994 (December). The Spectral Interactor Matrix for the Singular Riccati Equation. *Pages 2165-2169 of: Proceedings of the 33rd CDC*.
- BORISON, U. 1979. Self-tuning Regulators for a Class of Multivariable Systems. *Automatica*, 15, 209-215.
- BOX, G.E.P., AND JENKINS, G.M. 1976. *Time Series Analysis Forecasting and Control*. Holden-Day.

- BOX, G.E.P., AND MACGREGOR, J.F. 1974. the Analysis of Closed-loop Dynamic Stochastic Systems. *Technometrics*, **18**, 371–380.
- BOX, G.E.P., AND MACGREGOR, J.F. 1976. Parameter Estimation with Closed-loop Operating Data. *Technometrics*, **18**, 371 – 380.
- BOYD, S.P., AND BARRATT, C.H. 1991. *Linear Control Design*. Prentice Hall.
- CAINES, P.E., AND CHAN, C.W. 1975. Feedback between Stationary Stochastic Processes. *IEEE Trans AC*, **20**, 498–508.
- CHU, C.C. 1985.  *$H_{\infty}$ -Optimization and Robust Multivariable Control*. Ph.D. thesis, University of Minnesota, Minneapolis, MN.
- CLARKE, D.W., MOHTADI, C., AND TUFFS, P.S. 1987. Generalized Predictive Control - Part 2. Extensions and Interpretations. *Automatica*, **23**(2), 149–160.
- DAHLEH, M.A., AND DIAZ-BOBILLO, I.J. 1995. *Control of Uncertain Systems—a Linear Programming Approach*. Englewood Cliffs, New Jersey: Prentice Hall.
- DEFALQUE, B., GEVERS, M., AND INSTALLE, M. 1976. Combined Identification of the Input-output and Noise Dynamics of a Closed-loop Controlled Linear System. *Int. J. Control*, **24**, 345–360.
- DESBOROUGH, L., AND HARRIS, T. 1992. Performance Assessment Measure for Univariate Feedback Control. *Can. J. Chem. Eng.*, **70**, 1186–1197.
- DESBOROUGH, L., AND HARRIS, T.J. 1993. Performance Assessment Measures for Univariate Feedforward/Feedback Control. *Can. J. Chem. Eng.*, **71**, 605–616.
- DEVRIES, W.R., AND WU, S.M. 1978. Evaluation of Process Control Effectiveness and Diagnosis of Variation in Paper Basis Weight via Multivariate Time Series Analysis. *IEEE Trans. on AC*, **AC-23**, No 4(August).
- DUGARD, L., GOODWIN, G.C., AND XIANYA, X. 1984. The Role of the Interactor Matrix in Multivariable Stochastic Adaptive Control. *Automatica*, **20**(5), 701–709.

- ERIKSSON, P.G., AND ISAKSSON, A.J. 1994. Some Aspects of Control Performance Monitoring. *Pages 1029–1034 of: Proc. 3rd IEEE conf. Control Applications.*
- GARCIA, C.E., PRETT, D.M., AND MORARI, M. 1989. Model Predictive Control: Theory and Practice - a Survey. *Automatica*, **25**(3), 335–348.
- GEVERS, M. 1993 (June). Towards a Joint Design of Identification and Control. *Presented at 2nd European Control Conference.*
- GEVERS, M., AND LJUNG, L. 1986. Optimal Experiment Designs with Respect to the Intended Model Application. *Automatica*, **22** No 5, 543 – 554.
- GOLUB, G.H., AND LOAN, C.F. VAN. 1989. *Matrix Computations*. Second edn. The Johns Hopkins University Press.
- GOODWIN, G.C., AND PAYNE, R.L. 1977. *Dynamic System Identification: Experiment Design and Data Analysis*. New York: Academic Press.
- GOODWIN, G.C., AND SIN, K.S. 1984. *Adaptive Filtering Prediction and Control*. Englewood Cliffs: Prentice-Hall.
- GUO, L., AND LJUNG, L. 1994. The Role of Model Validation for Assessing the Size of the Unmodelled Dynamics. *In: Proceedings of CDC.*
- GUSTAVSSON, I., LJUNG, L., AND SODERSTROM, T. 1978. Identification of Processes in Closed Loop — Identifiability and Accuracy Aspects. *Identification and System Parameter Estimation*, 41–77.
- HAKVOORT, R.G., SCHRAMA, R.J.P., AND VAN DEN HOF, P.M.J. 1994. Approximate Identification with Closed-loop Performance Criterion and Application to LQG Feedback Design. *Automatica*, **30**(4), 679–690.
- HARRIS, T. 1989. Assessment of Closed Loop Performance. *Can. J. Chem. Eng.*, **67**, 856–861.
- HARRIS, T.J. 1985. A comparative study of model based control strategies. *In: Proceedings of ACC.*

- HARRIS, T.J., AND MACGREGOR, J.F. 1987. Design of Multivariable Linear Quadratic Controllers Using Transfer Functions. *AIChE J.*, **33**, 1481–1495.
- HARRIS, T.J., BOUDREAU, F., AND MACGREGOR, J.F. 1995. Performance Assessment of Multivariable Feedback Controllers. *In: 1995 AIChE Annual Meeting (also in Personal Communication).*
- HARRIS, T.J., BOUDREAU, F., AND MACGREGOR, J.F. 1996. *Performance Assessment of Multivariable Feedback Controllers.* To appear in *Automatica*.
- HJALMARSSON, H., GEVERS, M., BRUYNE, F.D., AND LEBLOND, J. 1994 (December). Identification for Control: Closing the Loop Gives More Accurate Controllers. *Pages 4150–4155 of: Proceedings of 1994 CDC.*
- HUANG, B., AND SHAH, S.L. 1996a. *Closed-loop Identification: a Two-step Approach.* To appear in *Journal of Process Control*.
- HUANG, B., AND SHAH, S.L. 1996b (November). Limits of Control Loop Performance: Practical Measures of Control Loop Performance Assessment. 1996 AIChE Annual Meeting, Chicago.
- HUANG, B., AND SHAH, S.L. 1996c. *The Role of the Unitary Interactor Matrix in the Explicit Solution of the Singular LQ Output Feedback Control Problem.* Submitted to *Automatica*.
- HUANG, B., SHAH, S.L., AND KWOK, K.Y. 1995a (June). On-line Control Performance Monitoring of MIMO Processes. *Pages 1250–1254 of: Proc. American Control Conference.* American Control Conference, Seattle, Washington.
- HUANG, B., SHAH, S.L., AND KWOK, K.Y. 1995b (November). Performance assessment and diagnosis of multivariable processes. 1995 AIChE Annual Meeting, Miami, USA.
- HUANG, B., SHAH, S.L., AND KWOK, K.Y. 1996a. *Good, Bad or Optimal? Performance Assessment of MIMO Processes.* To appear in *Automatica*.



- HUANG, B., SHAH, S.L., AND KWOK, K.Y. 1996b (July). How Good Is Your Controller? Application of Control Loop Performance Assessment Techniques to MIMO Processes. *Pages 229-234 of: Proc. 13th IFAC World Congress*, vol. M.
- HUANG, B., SHAH, S.L., AND FUJII, H. 1996c (July). Identification of the Time Delay/Interactor Matrix for MIMO Systems Using Closed-loop Data. *Pages 355-360 of: Proc. 13th IFAC World Congress*, vol. M.
- HUANG, B., SHAH, S.L., KWOK, E.K., AND JIM, J. 1996d. *Performance Assessment of Multivariate Control Loops on a Paper Machine Headbox*. To appear in Canadian Journal of Chemical Engineering, February, 1997.
- HUANG, B., SHAH, S.L., AND FUJII, H. 1996e. *The Unitary Interactor Matrix and Its Estimation using closed-loop data*. To appear in Journal of Process Control.
- KEVICZKY, L., AND HETTHESSY, J. 1977. Self-tuning Minimum Variance Control of MIMO Discrete Time Systems. *Control Theory and Applications*, 5(1).
- KOSUT, R.L., GOODWIN, G.C., AND POLIS, M.P. 1992. Special Issue on System Identification for Robust Control Design. *IEEE Trans Automatica Control*, 37.
- KOZUB, D.J., AND GARCIA, C.E. 1993 (Nov. 9). *Monitoring and Diagnosis of Automated Controllers in the Chemical Process Industries*. Presented at AIChE Annual Meeting.
- KWAKERNAAK, H., AND SIVAN, R. 1972. *Linear Optimal Control System*. John Wiley and Sons.
- LJUNG, L. 1987. *System Identification*. Prentice-Hall.
- LJUNG, L. 1994. System Identification in a MIC perspective. *Modeling, Identification and Control*, 15(3), 153 - 159.
- LYNCH, C.B., AND DUMONT, G.A. 1993 (Sept.13-16). Closed Loop Performance Monitoring. *In: Proc. 2nd IEEE Conf. Control Applications*.
- MACGREGOR, J.F. 1976. Optimal Choice of the Sampling Interval for Discrete Process Control. *Technometrics*, 18(2), 151-160.

- MACGREGOR, J.F., AND FOGAL, D.T. 1995. Closed-loop Identification: The Role of the Noise Model and Prefilters. *Journal of process control*, 5(3), 163–171.
- MACGREGOR, J.F., HARRIS, T.J., AND WRIGHT, J.D. 1984. Duality between the control of processes subject to randomly occurring deterministic disturbances and ARIMA stochastic disturbances. *Technometrics*, 26.
- MIAO, T., AND SEBORG, D.E. 1995 (June). A Monitoring Strategy for Flow and Pressure Control Loops. In: *The 2nd Asia-Pacific Conf. on Control and Measurement*.
- MILLER, R. 1995. *Stochastic Predictive Control*. M.Phil. thesis, University of Alberta.
- MOHTADI, C. 1988. On the Role of Prefiltering in Parameter Estimation and Control. Pages 121 – 138 of: S.L., SHAH, AND DUMONT, G. (eds), *Adaptive Control Strategies for Industrial Use*. Springer-Verlag.
- MORARI, M., AND ZAFIRIOU, E. 1989. *Robust Process Control*. Prentice Hall.
- MUTOH, Y., AND ORTEGA, R. 1993. Interactor Structure Estimation for Adaptive Control of Discrete-time Multivariable Nondecouplable Systems. *Automatica*, 29(3), 635–647.
- NEWCOMBE, D.P. 1991. Roll headboxes and their approach flow. *Pulp and Paper Manufacture*, 7, 97–116.
- NORDSTROM, B., AND NORMAN, B. 1994. Influence of Headbox Nozzle Contraction Ratio on Sheet Formation and Anisotropy. Pages 225–228 of: *Proceedings of the 1994 Engineering Conference*.
- PAIGE, C.C. 1981. Properties of Numerical Algorithms Related to Computing Controllability. *IEEE Trans. Aut. Control*, AC-26, 130–138.
- PAPLINSKI, A.P., AND ROGOZINSKI, M.W. 1990. Right Nilpotent Interactor Matrix and its Application to Multivariable Stochastic Control. Pages 494–495 of: *Proceedings of ACC*, vol. 1.

- PENG, Y., AND KINNAERT, M. 1992. Explicit Solution to the Singular LQ regulation Problem. *IEEE Trans AC*, 37(May), 633–636.
- PHADKE, M.S., AND WU, S.M. 1974. Identification of multi-input-multi-output Transfer Function and Noise Model of a Blast Furnace from Closed-loop Data. *IEEE Trans AC*, 19, 944–951.
- PIERCE, D.A. 1975. Forecasting in Dynamic Models with Stochastic Regressors. *Journal of Econometrics*, 3, 349–374.
- REINSEL, G.C. 1993. *Elements of Multivariate Time Series Analysis*. New York: Springer-Verlag.
- RHINEHART. 1995. A Watch Dog for Controller Performance Monitoring. *Pages 2239 – 2240 of: Proceedings of the 1995 American Control Conference*.
- RICE, J.S. 1972 (November 21). *U.S. Patent 3,703,436*. Noyes Data Corporation. Park Ridge New Jersey.
- RIVERA, D.E., POLLARD, J.F., AND GARCIA, C.E. 1992. Control-Relevant Prefiltering: A Systematic Design Approach and Case Study. *IEEE Tran AC*, 37(7), 964–974.
- ROGOZINSKI, M.W., PAPLINSKI, A.P., AND GIBBARD, M.J. 1987. An Algorithm for Calculation of a Nilpotent Interactor Matrix for Linear Multivariable Systems. *IEEE Trans. AC*, 32(3), 234–237.
- SCHRAMA, R. 1992. *Approximate Identification and Control Design*. Ph.D. thesis, Delft University of Technology.
- SCHRAMA, R.J.P. 1991. An open-loop solution to the approximate closed-loop approximation problem. *Pages 761–766 of: Proceedings of IFAC identification and system parameter estimation*.
- SHAH, S.L., MOHTADI, C., AND CLARKE, D.W. 1987. Multivariable Adaptive Control without a prior Knowledge of the Delay Matrix. *Systems and Control Letters*, 295–306.

- SHOOK, D.S., MOHTADI, C., AND SHAH, S.L. 1992. A Control-Relevant Identification Strategy for GPC. *IEEE Trans. AC*, **37**(7), 975–980.
- SODERSTROM, T., AND STOICA, P. 1989. *System Identification*. UK: Prentice Hall International.
- SRIPADA, N.R. 1988. *Multi-step Adaptive Predictive Control with Disturbance Modeling*. Ph.D. thesis, Department of Chemical Engineering, University of Alberta, Edmonton, Alberta, Canada.
- STANFELJ, N., MARLIN, T.E., AND MACGREGOR, J.F. 1993. Monitoring and Diagnosing Process Control Performance: the Single-loop Case. *Ind. Eng. Chem. Res.*, **32**.
- STERNAD, M., AND SODERSTROM, T. 1988. LQG-optimal Feedforward Regulators. *Automatica*, **24**(4), 557–561.
- TIAO, G.C., AND BOX, G.E.P. 1981. Modeling Multiple Time Series with Application. *JASA*, **76**, 802–816.
- TSILIGIANNIS, C.A., AND SVORONOS, S.A. 1988. Dynamic Interactors in Multivariable Process Control-1, the General Time Delay Case. *Chemical Engineering Science*, **43**(2), 339–347.
- TSILIGIANNIS, C.A., AND SVORONOS, S.A. 1989. Dynamic interactors in multivariable process control-2, time delays and zeros outside the unit circle. *Chemical Engineering Science*, **44**(9), 2041–2047.
- TYLER, M.L., AND MORARI, M. 1995a. *Performance assessment for unstable and nonminimum-phase systems*. Tech. rept. IfA-Report No 95-03. California Institute of Technology.
- TYLER, M.L., AND MORARI, M. 1995b. Performance Monitoring of Control Systems Using Likelihood Methods. *Pages 1245 – 1249 of: Proceedings of the American Control Conference*.

- VAN DEN HOF, P.M.J., AND SCHRAMA, R.J.P. 1993. An Indirect Method for Transfer Function Estimation from Closed Loop Data. *Automatica*, **29**(6), 1523–1527.
- VAN DEN HOF, P.M.J., AND SCHRAMA, R.J.P. 1995. Identification and Control—Closed-loop Issues. *Automatica*, **31**(12), 1751–1770.
- WALGAMA, K.S. 1986. *Multivariable Adaptive Predictive Control for Stochastic Systems with Time Delays*. M.Phil. thesis, University of Alberta.
- WIENER, N. 1949. *Extrapolation, Interpolation and Smoothing of Stationary Time Series*. Cambridge, Mass.: MIT Press.
- WOLOVICH, W.A., AND ELLIOTT, H. 1983. Discrete Models for Linear Multivariable Systems. *Int. J. Control*, **38**(2), 337–357.
- WOLOVICH, W.A., AND FALB, P.L. 1976. Invariants and Canonical Forms under Dynamic Compensation. *SIAM J. Control*, **14**, 996–1008.
- YOULA, D.C., AND BONGIORNO, J.J. 1985. A feedback Theory of two-degree-of-freedom optimal Wiener-Hopf Design. *IEEE on AC*, **30**.
- ZANG, Z., BITMEAD, R.R., AND GEVERS, M. 1995. Iterative Weighted Least-Squares Identification and Weighted LQG Control Design. *Automatica*, **31**(11), 1577–1594.
- ZHU, Y., AND BACKE, T. 1993. *Identification of Multivariable Industrial Processes*. Springer-Verlag.

## Appendix A

# The algorithm for the calculation of a unitary interactor matrix

The following algorithm is from Rogozinski et al. (Rogozinski *et al.*, 1987) and Peng and Kinnaert (Peng and Kinnaert, 1992).

**Definition 4** The  $n \times n$  first degree polynomial matrix  $U(q)$  will be called a row shift polynomial matrix (r.s.p.m) of order  $k_i$ , where

$$U(q) = U_0q + U_1 = \begin{bmatrix} 0 & I_r \\ qI_{k_i} & 0 \end{bmatrix}$$

The matrices  $U_0$  and  $U_1$  are defined through the matrix of coefficients

$$U = \begin{bmatrix} U_0 \\ U_1 \end{bmatrix} = \begin{bmatrix} 0_r \\ I_n \\ 0_{k_i} \end{bmatrix}, \quad n = r + k_i$$

in which  $U_0, U_1$  are of dimension  $n \times n$ ,  $I_n$  is the  $n \times n$  identity matrix, and  $0_r$  is a  $r$ -row matrix of zeros.

From RMF (right matrix fraction) description of  $T(q^{-1}) = N(q)R^{-1}(q)$ , where

$$N(q) = N_0q^p + N_1q^{p-1} + \dots + N_p \quad (\text{A.1})$$

a block matrix of coefficients is formed as

$$\Lambda = \begin{bmatrix} N_0 \\ \vdots \\ N_p \end{bmatrix}$$

The unitary interactor matrix  $D(q)$  can be factored out from equation (A.1) (or the block matrix of coefficients) by the following theorem.

**Theorem 13** (Rogozinski et al., 1987) *For a transfer matrix  $T(q)$  satisfying Assumption (1) and (2) there exists a unitary interactor matrix consisting of finite ( $t$ ) factors:*

$$D(q) = S^{(t)}(q)S^{(t-1)}(q)\dots S^{(1)}(q) \quad (\text{A.2})$$

where

$$S^{(i)}(q) = U^{(i)}(q)Q^{(i)} \quad (\text{A.3})$$

and  $U^{(i)}(q)$  is a r.s.p.m. of order  $k_i$  and  $Q^{(i)}$  is a non-singular  $n \times n$  real matrix (an orthogonal matrix for the factorization of the unitary interactor).

The algorithm is as follows:

Set  $i = 0$ ,  $N^{(0)}(q) = N(q)$ ,  $\Lambda^{(0)} = \Lambda$ , and  $D^{(0)} = I_n$  to start the algorithm. Consider the  $i^{\text{th}}$  iteration in the evaluation of  $D(q)$

**Step 1:**

If  $r_i = \text{rank}(N_0^{(i-1)}) = \min(n, m)$ , the algorithm terminates and the unitary interactor matrix is  $D(q) = D^{(i-1)}(q)$ , set  $t = i - 1$ ;

If  $r_i < \min(n, m)$ , factorize  $N_0^{(i-1)}$  by QR factorization into

$$N_0^{(i-1)} = (Q^{(i)})^{-1} \begin{bmatrix} 0_i \\ N_{0D}^{(i)} \end{bmatrix}, \quad \text{i.e.,} \quad Q^{(i)} N_0^{(i-1)} = \begin{bmatrix} 0_i \\ N_{0D}^{(i)} \end{bmatrix} \quad (\text{A.4})$$

where  $Q^{(i)}$  is an  $n \times n$  unitary (orthogonal) real matrix,  $k_i = n - r_i$  and  $0_i$  is a  $k_i$ -row zero matrix.

**Step 2:**

Pre-multiplying  $N^{(i-1)}(q)$  by matrix  $Q^{(i)}$

$$\bar{N}(q) = Q^{(i)} N^{(i-1)}(q) \quad (\text{A.5})$$

[the leading coefficient of  $\bar{N}(q)$  is now equal to the right-hand side of (A.4)].

**Step 3:**

Pre-multiplying  $\bar{N}(q)$  by the r.s.p.m. of order  $k_i$

$$N^{(i)}(q) = U^{(i)}(q) \bar{N}(q) \quad (\text{A.6})$$

[this multiplication shifts the matrix of coefficients of  $\bar{N}(q)$ ,  $\Lambda^{(i)}$ , upwards by  $k_i$  rows of zeros. Update the matrix

$$D^{(i)}(q) = S^{(i)}(q) D^{(i-1)}(q) \quad (\text{A.7})$$

This ends the  $i^{th}$  iteration. Combining equations (A.4) to (A.7), the  $i$ th iteration of the algorithm results in

$$N^{(i)}(q) = U^{(i)}(q) Q^{(i)} N^{(i-1)}(q) = S^{(i)}(q) N^{(i-1)}(q) = D^{(i)}(q) N(q)$$

where  $S^{(i)}(q)$  and  $D^{(i)}(q)$  are defined by equations (A.3) and (A.7).

The final iteration ( $t = i - 1$ ) yields

$$N^{(t)}(q) = D(q) N(q) \quad (\text{A.8})$$

where  $D(q) = D^{(t)}(q)$  is the unitary interactor matrix.



## Appendix B

# Examples of the diagonal/general interactor matrices

The diagonal interactor matrix is relatively easy to obtain. For processes with diagonal interactor matrices, the smallest delay in each row is associated with the diagonal element of the matrix, *i.e.*, each element,  $d_i$ , of the diagonal interactor matrix,  $D = \text{diag}\{q^{d_1}, \dots, q^{d_n}\}$ , is actually the minimum delay in the  $i^{\text{th}}$  row of the transfer function matrix. In other words, the diagonal interactor matrix solely depends on the minimum delay of each row of the transfer function matrix. Most interactor matrices of the *actual* multivariable process are either diagonal or general matrices (Goodwin and Sin, 1984; Walgama, 1986; Wolovich and Elliott, 1983). The non-diagonal interactor matrix occurs when certain linear dependencies exist among the rows of the transfer function matrix (as  $q^{-1} \rightarrow 0$ ) after the minimum delay of each row is factored out. For example, consider a  $2 \times 2$  process

$$T = \begin{bmatrix} \frac{0.5q^{-2}}{1-0.7q^{-1}} & \frac{q^{-4}(1.4-0.9q^{-1})}{1-0.3q^{-1}} \\ \frac{1.23q^{-3}}{1-0.5q^{-1}} & \frac{4.7q^{-3}}{1-0.7q^{-1}} \end{bmatrix} \quad (\text{B.1})$$

The minimum time delay of the first row is  $q^{-2}$ , and the second row  $q^{-3}$ . After factoring out these minimum time delays from each row ( this is equivalent to pre-multiplying  $T$  by

a diagonal matrix  $\text{diag}(q^2, q^3)$ , we have the transfer function matrix

$$\tilde{T} = \begin{bmatrix} \frac{0.5}{1-0.7q^{-1}} & \frac{q^{-2}(1.4-0.9q^{-1})}{1-0.3q^{-1}} \\ \frac{1.23}{1-0.5q^{-1}} & \frac{4.7}{1-0.7q^{-1}} \end{bmatrix}$$

Thus

$$\lim_{q^{-1} \rightarrow 0} \tilde{T} = \begin{bmatrix} 0.5 & 0 \\ 1.23 & 4.7 \end{bmatrix}$$

which is of full rank. Therefore the interactor matrix is a diagonal matrix, i.e.,  $D = \text{diag}(q^2, q^3)$ . However, if the element  $T_{1,2}$  of the transfer function matrix in equation (B.1) happens to be  $\frac{q^{-2}(1.91-0.9q^{-1})}{1-0.3q^{-1}}$ , then using the same diagonal factorization yields

$$\lim_{q^{-1} \rightarrow 0} \tilde{T} = \begin{bmatrix} 0.5 & 1.91 \\ 1.23 & 4.7 \end{bmatrix}$$

which is rank defective, and a non-diagonal interactor matrix is then expected. In real processes, the exact linear dependency as in this illustration rarely occurs. Another special case happens when the time delays associated with a particular input are larger than delays associated with other inputs. For example, if the transfer function of equation (B.1) is changed to

$$T = \begin{bmatrix} \frac{0.5q^{-2}}{1-0.7q^{-1}} & \frac{(1.4-0.9q^{-1})q^{-4}}{1-0.3q^{-1}} \\ \frac{1.23q^{-3}}{1-0.5q^{-1}} & \frac{4.7q^{-5}}{1-0.7q^{-1}} \end{bmatrix}$$

then the delays associated with second input are larger than the delays associated with the first input. Thus using only the diagonal factorization will yield

$$\lim_{q^{-1} \rightarrow 0} \tilde{T} = \begin{bmatrix} 0.5 & 0 \\ 1.23 & 0 \end{bmatrix}$$

which is rank defective, and a non-diagonal interactor matrix is therefore expected. The existence of a general (non-diagonal) interactor matrix is generally due to this latter case.

In many multivariable processes under multiloop control, it is implicitly assumed that the input-output pairing is such that the diagonal elements have smaller delays. This leads to the observations that the occurrence of a diagonal interactor matrix is not rare. More generally, even if a multivariable process has the minimum-delay pairing structure but is not paired in such a way in the actual multiloop design, the interactor matrix is still diagonal.